

## INFORMATION TO USERS

This manuscript has been reproduced from the microfilm master. UMI films the text directly from the original or copy submitted. Thus, some thesis and dissertation copies are in typewriter face, while others may be from any type of computer printer.

**The quality of this reproduction is dependent upon the quality of the copy submitted.** Broken or indistinct print, colored or poor quality illustrations and photographs, print bleedthrough, substandard margins, and improper alignment can adversely affect reproduction.

In the unlikely event that the author did not send UMI a complete manuscript and there are missing pages, these will be noted. Also, if unauthorized copyright material had to be removed, a note will indicate the deletion.

Oversize materials (e.g., maps, drawings, charts) are reproduced by sectioning the original, beginning at the upper left-hand corner and continuing from left to right in equal sections with small overlaps. Each original is also photographed in one exposure and is included in reduced form at the back of the book.

Photographs included in the original manuscript have been reproduced xerographically in this copy. Higher quality 6" x 9" black and white photographic prints are available for any photographs or illustrations appearing in this copy for an additional charge. Contact UMI directly to order.

# UMI

A Bell & Howell Information Company  
300 North Zeeb Road, Ann Arbor MI 48106-1346 USA  
313/761-4700 800/521-0600



University of Alberta

Numerical simulation of sedimentation and consolidation of fine tailings

by

Srboljub Masala



A thesis submitted to the Faculty of Graduate Studies and Research in partial fulfilment

of the

requirements for the degree of Master of Science

in

Geotechnical Engineering

Department of Civil and Environmental Engineering

Edmonton, Alberta

Fall 1998



**National Library  
of Canada**

**Acquisitions and  
Bibliographic Services**

**395 Wellington Street  
Ottawa ON K1A 0N4  
Canada**

**Bibliothèque nationale  
du Canada**

**Acquisitions et  
services bibliographiques**

**395, rue Wellington  
Ottawa ON K1A 0N4  
Canada**

*Your file Votre référence*

*Our file Notre référence*

The author has granted a non-exclusive licence allowing the National Library of Canada to reproduce, loan, distribute or sell copies of this thesis in microform, paper or electronic formats.

The author retains ownership of the copyright in this thesis. Neither the thesis nor substantial extracts from it may be printed or otherwise reproduced without the author's permission.

L'auteur a accordé une licence non exclusive permettant à la Bibliothèque nationale du Canada de reproduire, prêter, distribuer ou vendre des copies de cette thèse sous la forme de microfiche/film, de reproduction sur papier ou sur format électronique.

L'auteur conserve la propriété du droit d'auteur qui protège cette thèse. Ni la thèse ni des extraits substantiels de celle-ci ne doivent être imprimés ou autrement reproduits sans son autorisation.

0-612-34390-1


**Canada**



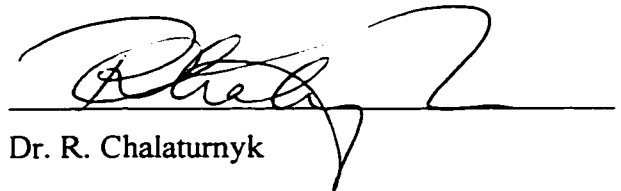
University of Alberta

Faculty of Graduate Studies and Research

The undersigned certify that they have read, and recommend to the Faculty of Graduate Studies and Research for acceptance, a thesis entitled "Numerical Simulation of Sedimentation and Consolidation of Fine Tailings" submitted by Srbojub Masala in partial fulfillment of the requirements for the degree of Master of Science in Geotechnical Engineering.



Dr. D. Chan  
(Supervisor)



Dr. R. Chalaturnyk



Dr. C. Mendoza

June 22, 1998

## ABSTRACT

This thesis is concerned with numerical aspects of the simulation of the process of simultaneous sedimentation and consolidation of suspended soils, with particular reference to oil sands fine tailings.

Two models were developed. The first is a sedimentation model based on a modification of Kynch's theory. It assumes time-dependent concentration in the suspension zone and neglects consolidation effects in the sediment layer. The second model unifies sedimentation and consolidation through the concept of permeability, which is assumed to be continuously valid in both the suspended and solid states of a soil. The main novelty of both models is in their consistent treatment of the suspension zone as a liquid, with zero effective stresses, contrary to the current geotechnical practice of treating a suspension as a consolidating soil.

Applied to large-scale sedimentation tests on oil sands fine tailings, both models show significantly improved agreement with experimental observations.

*To my family*

## **Acknowledgement**

I would like to thank my mentor Dr. D. H-K. Chan for his guidance and support during the course of my studies, as well as the faculty and the staff of the Geotechnical Engineering Group of the Department of Civil and Environmental Engineering for providing pleasant and friendly surroundings which stimulated my studies and research.

## **TABLE OF CONTENTS**

<b>Chapter 1</b>	<b>INTRODUCTION</b>	<b>1</b>
1.1	STATEMENT OF THE PROBLEM	1
1.2	OVERVIEW OF PREVIOUS STUDIES	2
1.2.1	Phenomenology	2
1.2.2	Modelling	2
1.3	OBJECTIVES AND SCOPE OF THE THESIS	3
1.4	ORGANIZATION OF THE THESIS	4
 <b>Chapter 2</b>	 <b>LITERATURE REVIEW</b>	 <b>6</b>
2.1	ELEMENTS OF THE COLLOID CHEMISTRY OF CLAY SYSTEMS	6
2.2	ELEMENTS OF PHASE INTERACTION IN A SOLID-LIQUID DISPERSION	8
2.2.1	Physical properties of the fluid phase	8
2.2.2	Fluid-particle interaction	9
2.2.3	Particle interaction	10
2.2.3.1	Electrostatic forces	11
2.2.3.2	Inertial forces	13
2.2.3.3	Indirect particle-particle interaction	13
2.2.4	Particle structure development in clay suspensions	14
2.2.4.1	Particle structure in oil sands fine tailings	16
2.3	SEDIMENTATION	19
2.3.1	Phenomenology	19
2.3.1.1	Coe and Clevenger (1916)	19
2.3.1.2	Tiller and Khatib (1984)	20
2.3.1.3	Tailings settling in a pond (Yong 1984)	22
2.3.1.4	Experimental settling of a dredge spoil (Lin and Lohnes 1984)	24
2.3.1.5	Sedimentation and fluizidation	27

2.3.1.6	Been and Sills' experiments (1981)	28
2.3.1.7	Large scale sedimentation tests on oil sands tailings at the University of Alberta	35
2.3.2	Modelling	39
2.3.2.1	Stokes' equation	39
2.3.2.2	"Stokes + concentration" approach	40
2.3.2.3	Kynch's theory (1952)	41
2.3.2.4	Tiller (1981)	45
2.3.2.5	Auzerais, Jackson and Russel (1988)	46
2.3.2.6	Diplas and Papanicolaou (1997)	51
2.3.2.7	Eckert et al. (1996)	53
2.4	SELF-WEIGHT CONSOLIDATION	56
2.4.1	Phenomenology of self-weight consolidation	56
2.4.1.1	Sediments of colloidal suspensions (van Olphen 1977)	56
2.4.1.2	Sediment fabric and initial concentration in clayey sediments	56
2.4.1.3	Volume changes and the influential factors	57
2.4.1.4	Compressibility and permeability testing of the oil sands fine tailings	58
2.4.2	Modelling of self-weight consolidation	65
2.4.2.1	Terzaghi's theory	65
2.4.2.2	Gibson's theory	66
2.4.2.3	Lee and Sills (1979)	70
2.4.2.4	Linked sedimentation and consolidation (Pane and Schiffman, 1985)	71
2.4.2.5	Linked sedimentation and consolidation (Shodja and Feldkamp, 1993)	73
2.4.2.6	Discrete element method in consolidation (Anandarajah 1994)	75
2.5	SUMMARY OF LITERATURE REVIEW	77
2.5.1	Sedimentation phenomenology	77
2.5.2	Sedimentation modelling	79
2.5.3	Phenomenology of self-weight consolidation	80

	2.5.4 Modelling of self-weight consolidation	80
<b>Chapter 3</b>	<b>FORMULATION OF A TIME-DEPENDENT SEDIMENTATION MODEL</b>	<b>82</b>
3.1	MATHEMATICAL DERIVATION OF THE MODEL	82
3.1.1	Introduction	82
3.1.2	Assumptions of the model	84
3.1.3	Mathematical derivation of the model	85
3.1.3.1	Empirical procedure	87
3.1.3.2	Alternative method with elements of suspension micromechanics	88
3.2	SOLVED EXAMPLES	92
3.2.1	Checking the method - simplification to Kynch theory	92
3.2.1.1	Toorman (1998)	92
3.2.2	University of Alberta large scale sedimentation tests on oil sands fine tailings	94
3.2.2.1	Material properties and behaviour	94
3.2.2.2	Possibilities of presently used methods of analysis	98
3.2.2.3	Comparison of the results for the 10 m standpipe test with the consolidation theory	98
3.2.2.4	Simulation of the 2 m standpipe test	116
<b>Chapter 4</b>	<b>A MODEL FOR COUPLED SEDIMENTATION AND CONSOLIDATION</b>	<b>124</b>
4.1	A MODEL FOR SEDIMENTATION	124
4.1.1	Introduction	124
4.1.2	Derivation	125
4.1.2.1	Conservation of mass (continuity) equation	125
4.1.2.2	Equilibrium equation	128
4.1.2.3	Connecting continuity and equilibrium	129
4.1.2.4	Differential governing equation for sedimentation	131
4.2	A MODEL FOR CONSOLIDATION	134
4.2.1	Introduction	134

4.2.2	Derivation	135
4.2.2.1	Equilibrium equation	135
4.2.2.2	Continuity equation	135
4.2.2.3	Connection between continuity and equilibrium	136
4.2.2.4	Differential governing equation for consolidation	136
4.3	SOLUTION	139
4.3.1	Introduction	139
4.3.2	Mathematical aspects	140
4.3.3	Description of the solution method	143
4.4	EXAMPLE	147
4.4.1	Result of simulation of 10 m standpipe test	147
4.4.1.1	Checking parameters from the sedimentation analysis in Chapter 3	147
4.4.1.2	Best-fit permeability function for this model	149
4.4.1.3	Sensitivity analysis of the model	151
4.5	CONCLUSIONS	161
<b>Chapter 5</b>	<b>CONCLUSIONS AND RECOMMENDATIONS</b>	<b>163</b>
5.1	CONCLUSIONS	163
5.1.1	Phenomenology of sedimentation and consolidation	163
5.1.2	Modelling sedimentation and consolidation	165
5.2	RECOMMENDATIONS	168
	<b>BIBLIOGRAPHY</b>	<b>169</b>
<b>Appendix 1</b>	<b>VOLUMETRIC AND WEIGHT RELATIONS</b>	<b>173</b>
A.1.1	Notation	173
A.1.2	Basic definitions	174
A.1.3	Mutual relations	175



<b>Appendix 2</b>	<b>ELEMENTS OF THE THEORY OF HYPERBOLIC AND PARABOLIC PARTIAL DIFFERENTIAL EQUATIONS AND FINITE DIFFERENCE METHODS FOR SOLVING THESE EQUATIONS</b>	<b>177</b>
A.2.1	Elements of the theory of hyperbolic and parabolic partial differential equations	177
A.2.1.1	Auxiliary conditions and well-posed problems	177
A.2.1.2	Characteristics	178
A.2.1.3	Qualitative behaviour of solutions of hyperbolic and parabolic equations - peculiarities of time evolution processes defined by them	180
A.2.1.4	Illustrative examples of hyperbolic differential equations and influence of boundary conditions	181
A.2.1.4.1	Travelling wave equation	181
A.2.1.4.2	Nonlinear “conservation law” equation	182
A.2.1.4.3	Boundary conditions	182
A.2.2	Finite difference schemes for hyperbolic PDE	184
A.2.2.1	Introduction	184
A.2.2.2	Basic concepts	184
A.2.2.3	Review of the schemes investigated	185
A.2.2.3.1	Upwind differencing scheme	186
A.2.2.3.2	Lax-Wendroff explicit scheme	187
A.2.2.3.3	MacCormack’s scheme	187
A.2.2.3.4	Chakravarthy and Osher	188
A.2.2.4	Author’s experience	188

## **LIST OF TABLES**

Table 3.1	Governing equations for the sedimentation model with time-dependent density in suspension	91
-----------	--	----

## LIST OF FIGURES

Figure 2.1	Energies of repulsion, attraction and net interaction curve for parallel flat plates (Mitchell 1976)	12
Figure 2.2	Various modes of particle association in clay suspensions (Mitchell 1976)	15
Figure 2.3	Research of solids structure of the mature fine tailings (MFT) using electron scanning microscope (Tang et al. 1997)	17
Figure 2.4	Settling behaviour of an attapulgitic slurry (Tiller and Khatib, 1984)	21
Figure 2.5	Solids concentration profile of a tailings slurry in a containment pond after several years (Yong 1984)	23
Figure 2.6	Settling behaviour of a slurry at different initial concentrations (Lin and Lohnes, 1984)	26
Figure 2.7	Settling behaviour of three clay slurries with identified flocculation, settling and consolidation periods (Li and Mehta, 1998)	26
Figure 2.8	Sedimentation and fluidization (Pane and Schiffmann, 1997)	28
Figure 2.9	Been and Sills' (1981) experimental setup	29
Figure 2.10	Been and Sills (1981), experiment 7	30
Figure 2.11	Been and Sills (1981), experiments 11 and 15 - density profiles and pore pressures	32
Figure 2.12	Been and Sills (1981), experiments 7 and 8 - particle grain size distributions at different heights in the sediment	34
Figure 2.13	University of Alberta 10 m standpipe tests on oil sand fine tailings	37
Figure 2.14	Kynch's method (1952), the height of suspension surface versus time	44
Figure 2.15	Three types of settling behaviour, depending on the shape of the flux curve and the initial solids concentration (Auzerais et al. 1998)	44
Figure 2.16	Three periods of a batch settling process after Tiller (1981)	45
Figure 2.17	Complete solution for an initially uniform suspension using Kynch theory and shock conditions (Auzerais et al. 1998)	47
Figure 2.18	Concentration profiles for stable suspensions (Auzerais et al. 1998)	50
Figure 2.19	Concentration profiles for flocculated suspensions (Auzerais et al. 1998)	50

Figure 2.20	Coupled sedimentation and consolidation analysis after Diplas and Papanicolaou (1997)	52
Figure 2.21	Coupled sedimentation and consolidation after Eckert et al. (1996)	54
Figure 2.22	Coupled sedimentation and consolidation after Eckert et al. (1996) - simulation of Been and Sills' experiment No. 15	55
Figure 2.23	Sediments of colloidal suspensions (van Olphen 1997)	57
Figure 2.24	Slurry consolidometer at the University of Alberta (Suthaker 1995)	59
Figure 2.25	Compressibility of oil sand fine tailings for various solids contents (Suthaker 1995)	61
Figure 2.26	Variation of flow velocity with time in the permeability testing (Suthaker 1995)	61
Figure 2.27	Permeability of oil sand fine tailings	63
Figure 2.28	Compressibility of oil sand fine tailings	64
Figure 2.29	Eulerian and Lagrangian coordinates in consolidation (Schiffman, Vick and Gibson, 1984)	68
Figure 2.30	Eulerian and Lagrangian coordinates in consolidation - pore pressure measurement (Schiffman, Vick and Gibson, 1985)	68
Figure 2.31	Modified effective stress principle after Pane and Schiffman (1985) - interaction coefficient $\beta$ as a function of void ratio	72
Figure 2.32	Linked sedimentation and consolidation after Shodja and Feldkamp (1993) - threshold function $\Phi(e)$	74
Figure 2.33	Distinct element method in consolidation (Anandarajah 1994) - distinct element assembly at two stages during one-dimensional compression	76
Figure 2.34	Distinct element method in consolidation (Anandarajah 1994) - histograms of particle orientation	76
Figure 3.1	Sedimentation modelling - the initial, the final and intermediate states	83
Figure 3.2	Sedimentation modelling - a general layout of the model and boundary conditions for the suspension layer	90
Figure 3.3	Test example - simulation of glass beads settling (Toorman 1998)	93
Figure 3.4	10 m and 2 m standpipe test setups	95
Figure 3.5	Grain size distribution and plasticity diagram of the 10 m standpipe test material	96
Figure 3.6	Material properties and grain size distribution of the 2 m standpipe test material	97

Figure 3.7	10 m standpipe test - the input data sheet for linear settling velocity function	100
Figure 3.8	10 m standpipe test - excess pore pressure and solids content distributions after 31 days	101
Figure 3.9	10 m standpipe test - excess pore pressure and solids content distributions after 681 days	102
Figure 3.10	10 m standpipe test - excess pore pressure and solids content distributions after 870 and 850 days, respectively	103
Figure 3.11	10 m standpipe test - excess pore pressure and solids content distributions after 1659 days	104
Figure 3.12	10 m standpipe test - excess pore pressure and solids content distributions after 2316 days	105
Figure 3.13	10 m standpipe test - excess pore pressure and solids content distributions after 3567 days	106
Figure 3.14	10 m standpipe test - excess pore pressure and solids content distributions after 5230 days	107
Figure 3.15	10 m standpipe test - comparison of various mathematical forms of the settling velocity function	109
Figure 3.16	The settling velocity as a function of the permeability	111
Figure 3.17	Sensitivity analysis of the proposed sedimentation model; the critical solids content variation	113
Figure 3.18	Sensitivity analysis of the proposed sedimentation model; the initial solids content variation	113
Figure 3.19	Sensitivity analysis of the proposed sedimentation model; the linear settling velocity - variation of the parameters A and B	114
Figure 3.20	Sensitivity analysis of the proposed sedimentation model; the settling velocity as a function of the permeability - variation of the parameters A and B	115
Figure 3.21	Summary of input data for analysis of 2 m standpipe tests using nonlinear large strain self-weight consolidation model (Suthaker 1995)	117
Figure 3.22	2 m standpipe test A	118
Figure 3.23	2 m standpipe test 1	119
Figure 3.24	2 m standpipe test 2	120
Figure 3.25	2 m standpipe test 3	121
Figure 3.26	2 m standpipe test 4	122

Figure 3.27	2 m standpipe test 5	123
Figure 4.1	The mass balance principle for a solid-liquid mixture	126
Figure 4.2	The equilibrium of an elemental volume	128
Figure 4.3	Numerical dispersion in the solution of a “travelling wave” equation (Ganzha and Vorozhtsov, 1996)	142
Figure 4.4	Numerical dissipation in the solution of a “travelling wave” equation (Ganzha and Vorozhtsov, 1996)	142
Figure 4.5	Numerical scheme in coupled sedimentation and consolidation analysis	144
Figure 4.6	10 m standpipe test - motion of internal interfaces in time for various permeability laws in the power function form	148
Figure 4.7	10 m standpipe test - motion of internal interfaces in time for various permeability laws in the power function form; enlarged view of the initial portion of settlement curves	148
Figure 4.8	10 m standpipe test - best-fit power law permeability function	150
Figure 4.9	10 m standpipe test - the three power law permeability functions used in the analysis presented in Figures 4.6 - 4.8	150
Figure 4.10	10 m standpipe test - sensitivity analysis of the proposed model; variation of the permeability parameter A	152
Figure 4.11	10 m standpipe test - sensitivity analysis of the proposed model; variation of the permeability parameter B	152
Figure 4.12	10 m standpipe test - sensitivity analysis of the proposed model; variation of the critical concentration $c_{cr}$	153
Figure 4.13	10 m standpipe test - sensitivity analysis of the proposed model; variation of the initial concentration $c_0$	153
Figure 4.14	10 m standpipe test - sensitivity analysis of the proposed model; variation of the compressibility parameter C	156
Figure 4.15	10 m standpipe test - sensitivity analysis of the proposed model; variation of the compressibility parameter D	156
Figure 4.16	10 m standpipe test - sensitivity analysis of the proposed model; solids content profiles after 14.33 years for various critical concentrations $c_{cr}$	157
Figure 4.17	10 m standpipe test - sensitivity analysis of the proposed model; solids content profiles after 14.33 years for various initial concentrations $c_0$	157

Figure 4.18	10 m standpipe test - sensitivity analysis of the proposed model; solids content profiles after 14.33 years for various compressibility parameters C from Figure 4.14	158
Figure 4.19	10 m standpipe test - sensitivity analysis of the proposed model; solids content profiles after 14.33 years for various compressibility parameters D from Figure 4.15	158
Figure 4.20	10 m standpipe test - sensitivity analysis of the proposed model; various initial concentration profiles	159
Figure 4.21	10 m standpipe test - sensitivity analysis of the proposed model; measured solids content profiles	159
Figure 4.22	10 m standpipe test - sensitivity analysis of the proposed model; solids content profiles for initially uniform suspension	160
Figure 4.23	10 m standpipe test - sensitivity analysis of the proposed model; solids content profiles for the initial profile with concentration increasing with depth	160
Figure A.1.1	Weights and volumes	174
Figure A.2.1	Travelling wave in 1-D	181
Figure A.2.2	Characteristics for the travelling wave equation with $a > 0$	183
Figure A.2.3	Testing FD schemes using the travelling wave equation - upwind differencing scheme	190
Figure A.2.4	Testing FD schemes using the travelling wave equation - Lax-Wendroff explicit scheme	190
Figure A.2.5	Testing FD schemes using the travelling wave equation - MacCormack scheme	191
Figure A.2.6	Testing FD schemes using the travelling wave equation - Chakravarthy and Osher scheme	191

## ***Chapter 1***

### ***INTRODUCTION***

#### **1.1 STATEMENT OF THE PROBLEM**

Sedimentation is the process of settling of solid particles dispersed in a liquid. The process is driven by gravity and is caused by the inability of a fluid to sustain long-term shear stresses. During sedimentation the solid particles gradually form a sediment, a saturated soil layer, at the bottom of the suspension column. Consolidation is the time-dependent compaction of the soil skeleton in a sedimented bed as a result of a load: its own weight and possibly other loads exerted on it. Both processes are of theoretical and practical interest in diverse scientific and technological fields, from chemistry and material engineering to geology and geotechnical engineering.

Historically, two major theories describing these processes have emerged independently: sedimentation has been a concern of chemists, while consolidation has traditionally remained a geotechnical subject. And, at a first sight, they really do seem completely different. It is apparent from a vast amount of available literature that there are differences in terminology, notation and manner of description which may lead an unfamiliar reader to utter confusion. It is not surprising, therefore, that until recently there have been no attempts to converge the different views and integrate the separately developed models into one unifying theory.

Sedimentation became a geotechnical concern in recent times when modern industries began to produce enormous quantities of waste material in a form of a slurry, whose deposition and maintenance naturally fell into the geotechnical field. These slurries, or tailings, have a high proportion of fine particles of colloidal size and exhibit exceptionally small rates of sedimentation; therefore, the sedimentation from the suspension and the consolidation of the sedimented material occur simultaneously.

In geotechnical engineering, sedimentation has often been treated as the consolidation of very loose soils, making use of non-linear finite strain consolidation theories. However, significant differences are encountered when the results of such analyses are compared with the observed or experimental responses as they happen, for example, with the oil sands fine tailings from Alberta. The need has thus arisen for a method that will be able to simulate and successfully predict the essential elements of the sedimentation and consolidation behaviour of these type of materials.



## **1.2 OVERVIEW OF PREVIOUS STUDIES**

### **1.2.1 Phenomenology**

Extensive experimental work on this subject has clarified the basics of a continuous process of sedimentation and consolidation of solid particles from an initially suspended state.

Three modes, or regimes, of settling behaviour were identified: free settling in dilute suspensions, hindered settling in concentrated suspensions and self-weight consolidation. The latter two are of importance in the analysis of stable colloidal suspensions (such as fine tailings). Among these three modes, the hindered settling phenomenon is relatively unfamiliar to a geotechnical engineer: it is characterized by the sedimentation of a suspension as a whole, as if the particles were in a spatial network, but without stable direct contacts and measurable effective stresses.

Zoning occurs in a suspension over time. Three principal zones are distinguished: almost clear water at the top, a suspension in the middle and sediment at the bottom. The settling behaviour of these zones in general corresponds to the above three settling regimes.

The settling velocity of the particles is found to be dependent on the concentration as the main variable. Based on the similarity between sedimentation and fluidization, permeability has become a customary measure of fluid-particle (hydrodynamic) interaction, although neither a physical process nor an exact theory for permeability measurements in suspensions has been developed. Similar comments, although to a lesser extent, may be made regarding the consolidation testing of very soft soils.

Some specific properties of oil sands fine tailings behaviour are: the time dependent increase of solids content in the suspension zone; the development of solids structure in the suspension and thixotropic strength gain in this zone; a relatively high creep in the sedimented material; difficulties in determining reliable parameters for mathematical modelling using laboratory methods; the presence of residual bitumen and its influence on the mechanical properties of the suspension; and the appearance of an odd "perched consolidation zone" near the top of the suspension, with increased concentration probably caused by microbial activity and gas production.

### **1.2.2 Modelling**

The Kynch theory of hindered sedimentation, with numerous modifications and derivatives, has been commonly applied in chemical engineering. Essentially, it is based on the assumption that the velocity of a particle settling in a fluid is the sole function of the concentration of the solids. In its usual simplified form, this theory postulates a constant rate of settling and a constant concentration in the suspension during the whole process of sedimentation. As such, it is not directly applicable to the fine tailings problem because it directly contradicts observation.

Gibson's nonlinear finite strain theory has been applied to the consolidation of sedimented beds both in geomechanics and in chemistry. It is even extended (unjustifiably from a physical point of view) to the whole settling system - the suspension zone is also treated as a soil, often resulting in a discrepancy with the measured data.

It may be noticed in recent reference texts that there is a tendency to converge the various traditional approaches to sedimentation and consolidation in chemical and geotechnical engineering: many texts attempt to unify the two processes under one theory, or at least suggest a computational scheme capable of tackling both processes.

There are examples in the literature of a coupled analysis at the level of a numerical scheme which uses existing sedimentation and consolidation theories (mainly Kynch's and Gibson's models, respectively). These analyses inherit all the limitations of the corporate models.

Few attempts at the theoretical unification of sedimentation and consolidation gather around permeability as the property that may integrate the processes. Actually, the permeability concept extends from the consolidation stage to the sedimentation stage. Although the direct physical meaning of permeability is less clear for a suspension, this property may be used as a link between the continuity and the force balance requirements, thus making the system of governing equations complete.

Despite a huge number of investigations on phase interaction in suspensions (and soils) at a detailed microscopic level, the engineering (continuum) approach dominates the theory and practical applications. This dominance is due to its simplicity (a minimum number of empirical parameters), easy calibration, sufficient accuracy and cost-effectiveness.

Computational problems are numerous in sedimentation analysis because of the appearance of discontinuities—sudden changes of variables—in the solution. These difficulties are even greater in coupled analyses. There is a wide variety of methods and procedures in the available literature, but no definite conclusions and guidelines are offered. It may be said that the mathematical aspects could be the main obstacles for further development.

### **1.3 OBJECTIVES AND SCOPE OF THE THESIS**

The objective of this research is to develop a theoretical approach and an analytical model which can capture the essential characteristics of the sedimentation and consolidation behaviour of fine tailings as a typical stable colloidal suspension. The model should be realistic in the sense that: (a) it has to be consistent with the physical nature of its constituents and (b) it has to be able to successfully simulate the actual behaviour with the parameters varying within the ranges of experimentally determined or reasonably estimated values.

The present study is focused on the mechanical aspects of the behaviour, so chemical processes are outside the scope of this study.

The basic approach consists of the following.

Firstly, the experimental results and observational data on sedimentation and consolidation are to be extensively and systematically reviewed and discussed, with particular attention to the behaviour of the oil sands fine tailings and the tests that have been performed on this material at the University of Alberta during the last 15 years. The same process should be conducted upon published papers on the modelling of these processes.

Secondly, the physical and numerical issues which are relevant for the theory and development of an efficient computational model have to be recognized and selected. Modelling should follow an engineering approach, starting from a basic level with the minimum number of variables sufficient for successful prediction of general trends in actual processes, followed by a gradual elaboration and improvement in order to achieve better quantitative agreement with chosen characteristic examples.

Finally, the model will be implemented in an efficient numerical scheme and tested on selected case histories. The principal parameters in a newly developed model have to be identified and the nature and extent of their influence compared to the effects of their physical counterparts.

## **1.4 ORGANIZATION OF THE THESIS**

The thesis is organized into five chapters.

A literature review on the sedimentation and consolidation is presented in Chapter 2. It begins with the pertinent elements of colloidal chemistry and a detailed discussion of the properties and mutual interaction of the phases in a solid-liquid dispersion. The review continues with a summary of sedimentation phenomenology as observed in experiments and monitored *in situ*. Modelling approaches in sedimentation are examined next, with a focus on chemical theories relatively unknown in geotechnical engineering. The chapter concludes with a very brief reconsideration of the well-known phenomenological facts and analytical aspects of self-weight consolidation.

A sedimentation model with time-dependent density is proposed in Chapter 3. It is based on an extension of Kynch's theory of sedimentation that allows for variation of solids concentration in a suspension. This is a model for "pure" sedimentation, so it neglects the deformation of the sedimented bed. From a geotechnical point of view, the novelty consists in its consistent treatment of the suspension as a fluid.

The model is used to analyze the small- and large-scale laboratory tests on oil sands fine tailings. The results indicate that this model is capable of capturing the variation of solids concentration with time, which results in improved agreement with experimental observations.

A model for simultaneous sedimentation and consolidation is presented in Chapter 4. It further develops the sedimentation model in Chapter 3 by including the consolidation of the sediment. The model is developed by extending the concept of permeability to a suspended state of solids, thus following the recent trends in this field. The computational procedure is based on the finite differences in Lagrangian coordinates. In its present form, it is capable of simulating "closed systems" without percolation of the

fluid through the spatial domain.

The proposed model was applied to a 10 m standpipe sedimentation test. The results show that it is possible to obtain a good match with the settlement observations and reasonable agreement with the concentration distributions (excluding the zone of “perched consolidation”) using the input data values only from the measured ranges, without any artificial adjustment of the model parameters.

The calculated behaviour of the simulated system highly resembles the general experimental and observational data in the reviewed literature, although the desired level of accuracy could not be achieved with a manual optimization procedure. Sensitivity analysis of the model shows that the two principal parameters for settlement behaviour are permeability and the initial concentration, while compressibility and the critical concentration of solids are of dominant importance only in the sediment.

Conclusions and recommendations for further research are presented in Chapter 5.

## ***Chapter 2***

### ***LITERATURE REVIEW***

This chapter begins with a brief review of the basic definitions and classifications of clay-water systems used in colloid chemistry, followed by a more detailed presentation of the properties of the two phases and their mutual interaction in a solid-liquid dispersion. The review continues with a summary of the sedimentation process as observed in laboratory experiments and field monitoring, limiting the discussion to only the most pertinent examples from the abundant literature on this topic. The subject of sedimentation modelling will be focused on chemical theories which are relatively less known in geotechnical engineering. The chapter concludes with a very brief reconsideration of consolidation, limiting itself to the well-known phenomenological facts and analytical aspects of this traditionally geotechnical field.

#### **2.1 ELEMENTS OF THE COLLOID CHEMISTRY OF CLAY SYSTEMS**

In almost every approach to the study of sedimentation and consolidation, one has to deal with dispersions of clay in water or another fluid. Such dispersions, characterized by the large interfacial area between the extremely small particles and the surrounding liquid, are colloidal systems (van Olphen, 1977).

Colloid chemistry, which deals with materials such as the above-mentioned, is a specialized field of physical chemistry. Although many branches in technology frequently use the terminology and methods of the colloid chemistry, a significant difference usually exists between chemistry and engineering points of view. The colloid chemist looks primarily at a system on a microscopic scale, while the engineer is mainly interested in the bulk physical and mechanical properties of the system in obtaining a solution for the engineering problem.

The bulk properties of clay systems depend on: (a) the type of clay and its concentration and (b) the composition of the fluid phase. The latter is sometimes even more important than the former.

A *colloidal dispersion* is defined as a system in which particles of colloidal dimensions, roughly between  $10^{-9}$  and  $10^{-6}$  m in at least one direction, are dispersed in a continuous phase of different composition (van Olphen, 1977). Both the dispersed

particles and the dispersing phase may be a solid, a liquid, or a gas. The present review is confined to the dispersed solid particles in a liquid phase.

The two major classes of hydrous colloidal systems are *hydrophobic* and the *hydrophilic colloids* (earlier called suspensions and emulsions). These terms were historically introduced to distinguish those colloids which exhibit a high affinity for water and spontaneously form a solution when they are contacted with it (hydrophilic) from those which do not readily form solutions (hydrophobic). Actually, the particles in a hydrophobic colloid are not hydrophobic at all: they have a layer of strongly adsorbed water on the particle surface. An essential difference between hydrophilic and hydrophobic colloids is in their sensitivity to the electrolyte concentration in dispersion or, in simple words, in their behaviour to the addition of salt to the solution. The hydrophobic colloids flocculate in the presence of relatively small amounts of salt, while the hydrophilic ones are almost insensitive to it.

Clay suspensions are most suitably treated as a class of hydrophobic colloids because their behavior is in most respects similar. Hydrophobic colloids may basically be defined as liquid dispersions of small crystalline solid particles and considered as two-phase systems with a large total interfacial area. Consequently, the properties of the particle surfaces play a dominant part in such systems.

A colloidally stable hydrophobic suspension in which individual particles are homogeneously dispersed in the liquid may remain virtually unchanged for a long time. Nevertheless, the system is only apparently stable and, while changes do occur, their rate is very slow. Two general processes, sedimentation and aging, may occur in a suspension. These processes may be distinguished as follows (van Olphen 1977):

(1) *Sedimentation* occurs because the particles are heavier than the liquid. As a result, the initial homogeneity of the suspension is disturbed. The rate of settling depends on the size and shape of the particles and on the difference between their density and that of the liquid. If particles are very fine settling may be counteracted by diffusion forces. This will be discussed in more detail at a later point.

(2) *Aging* is the name given to processes of spontaneous slow changes of the particles by their association in certain structures within the suspension. This gives some rigidity and strength to the system. Although the aging process is reversible to some extent, the agglomeration of particles in sedimentation is irreversible since the particles are unable to separate spontaneously faster than they associate. For this reason, colloidal chemistry refers to hydrophobic dispersion as an irreversible system.

In colloidal chemistry, the above-mentioned processes in solid-liquid dispersions are considered at a basically descriptive level. On the other hand, an engineering analysis requires a more quantitative approach and a more detailed consideration of the physical and mechanical relationships between the two phases.

## **2.2 ELEMENTS OF PHASE INTERACTION IN A SOLID-LIQUID DISPERSION**

The motion of particles in a two-phase system such as a solid-liquid dispersion is governed by the forces exerted by the fluid and by the particles themselves. In origins and effects, these forces are actually the result of very complicated mechanisms of mutual physical and chemical interactions between the two phases. A very simplified review of the interactions as suffices for the purposes of an engineering analysis is given below.

### **2.2.1 Physical properties of the fluid phase**

It is apparent that viscosity and density are the most important physical properties of the liquid phase in the sedimentation process. The relative density between the solid and the liquid provides the buoyancy on the particles. On the other hand, viscosity directly influences the frictional forces between solid particles and a liquid when they move relatively to each other. Viscosity depends mainly on temperature and influences permeability as another important property of a solid-fluid mixture.

Although this chapter presents a general review of colloidal systems, the focus of the present discussion will be mainly on water as the liquid phase in a suspension. Though the structure and properties of both “free” water and water bonded to the soil grains are not known in detail, their physical properties appear insignificant in comparison to their role as a medium for chemical reactions (for example ion transfer, electrokinetic phenomena, etc.). The latter is particularly important for clay-water mixtures with an enormous interfacial area (i.e. the grain surfaces area to mass ratio). This issue will be discussed in more detail in the chapter on interparticle forces and only several interesting details from the literature will be mentioned here.

One topic deserves attention when discussing about the liquid, “free” water. The structure of liquid water is not known exactly, except that some hydrogen bonding and regular structure existing in ice remain in the liquid state after melting. Otherwise, each water molecule would have twice its present number of neighbouring molecules, a specific density of 1.84 and, probably, completely different properties and behaviour (Mitchell 1976). The distorted hydrogen bond model and its extension, the random network model, are among various proposed theoretical models that have recently gained wide acceptance. Briefly, these two models state that water molecules are associated in an irregularly fluctuating network of rings rather than in an ordered lattice as in ice. Five molecules in a ring appear to be the rule, although rings may contain six, seven and more molecules. But, since this five-fold arrangement cannot form a regular, repeating pattern, liquid water cannot exist in a crystalline state. The importance of this lies not so much in the sedimentation problem itself but in a general conclusion that Mitchell stated, namely that “the liquid state could be explained precisely because of this, and solids and liquids can be distinguished as coherent materials with and without regular structure, respectively”. More precisely, the difference lies in the stability of the structure and permanency of the links between particles under external agents. So-called “immobilized pore water” (Toorman 1996) must also be considered. This is not only water adsorbed to the mineral particles but also the water that is caught within the open spaces of the floc

during aggregation. While the former is strongly bonded and makes an integral part of the aggregate, the latter may be released when the floc breaks up. This immobilized pore water determines the floc density and thus its actual settling velocity.

A question is raised here about the volumetric concentration of the solid particles as the proper parameter for determining the density of a suspension in general. Some authors (Parker, 1986, cited by Toorman, 1996) propose the effective volume concentration as a better density measure and define it as “the fraction of the volume occupied by aggregates and occluded water”. Toorman correctly comments on the difficulties in the measurement of this parameter.

This seemingly theoretical question has an immediate bearing on sedimentation modelling and the derivation of governing equations: that is, the mass balance principle usually applies in derivations in a form which assumes that no mass exchange occurs between the phases (continuity equations are written separately for the solid particles and the water in a suspension). This is not the case for the water in diffuse layers around the grains and within the flocs. Therefore, equations of conservation of mass which exclude the description of mass exchange implicitly assume a permanent proportion of the “free” and the bound pore liquid. Assessment suggests that this should not present a problem in the sedimentation analysis of clay-water mixtures as stable suspensions.

### **2.2.2 Fluid - particle interaction**

One source of fluid action on the particles is the thermal motion of water molecules surrounding the particles - *Brownian motion*. This causes apparently irregular vivid movements of a particle in all directions. Since the average velocity of a particle decreases with increasing mass, the Brownian motion becomes less lively with increasing particle size.

The particle size in natural clay dispersions usually varies widely and covers a range of both colloidal and non-colloidal particles. The Brownian motion may thus become effective in special cases only, for example, when a suspension is very diluted and the particles do not flocculate or form a solid net structure. Modelling this influence is possible as a diffusive mechanism and requires stochastic considerations.

Other forces exerted by the fluid on a particle are:

- *buoyancy* (submergence effect); and
- *hydrodynamic forces*, when there is relative motion between particles and the liquid phase.

The latter are the result of viscous effects, i.e. friction at the surface of a particle moving relative to the surrounding fluid, and can be subdivided into *lift* and *drag forces*, after Toorman (1996).

The *lift force* acts perpendicularly to the flow direction. It plays a major role in sediment transport, when there are significant gradients in the fluid velocity field and particles make spinning movements. This force then re-enters particles from the sediment



into the water and keeps them in suspension. It can be assumed that the lift force effect in sedimentation problems is negligible.

The *drag force* is the resisting force on the particle acting in the direction of the flow. Based on experimental data (Roberson and Crowe, 1990, cited by Toorman, 1996) its general form (on a single particle) is:

$$F_D = \frac{1}{2} C_D' \cdot A \cdot \rho \cdot (v_w - v_s)^2 \quad [2.1]$$

where:  $(v_w - v_s)$  is fluid velocity relative to the particle;  $A$  is the particle cross-sectional area perpendicular to the direction of flow;  $\rho$  is fluid density;  $C_D'$  is the drag coefficient and a function of the particle Reynolds number

$$Re = (v_w - v_s) \frac{d}{\nu} \quad [2.2]$$

where  $d$  is the representative particle diameter and  $\nu$  is the kinetic viscosity of the fluid.

The vertical force balance equation for a single particle falling in a column of still water is expressed for the combined effect of the buoyancy and the drag force (which is produced by relative motion of the particle and the local flow of displaced fluid). Its mathematical form is the well-known Stokes law, but it seems different from the one above: without Reynolds' number and the  $(v_w - v_s)$  term. It is, however, very easy to obtain the Stokes law from the equations shown above by simple substitution  $C_D' = 24 / Re$ , which is valid for small Reynolds numbers  $Re \leq 5$ , and putting the velocity of water  $v_w = 0$ .

With regard to that, it is pointed out that particle motion (actually, its very existence in the liquid) has certain return effect on fluid flow: it disturbs the flow regime (streamlines) in its neighbourhood. If different scales and particle size variability are borne in mind, it is obvious that a small particle in a dilute dispersion will have (and it is usually postulated so) no noticeable effect on the flow regime (except in the very vicinity of the particle) and thus the global pressure distribution within the suspension (Toorman 1996).

### **2.2.3 Particle interaction**

In a highly schematic way, the forces that exist between two adjacent clay particles originate either from direct mineral contact or from the electrical charge on the particles. In the case of clay dispersions, the latter becomes more important than the former since the influence of the electrical charge is directly related to the particle surface area relative to the volume (i.e. mass forces - the weight of the particle).

The effects of surface load interactions and small particle size are manifested by a variety of interparticle attractive and repulsive forces.

### 2.2.3.1 Electrostatic forces

The *attractive force* between dispersed particles is attributed to the general van der Waals attraction forces between all the atoms of one particle and all the atoms of another particle. The magnitude of the resultant attractive force depends on the size and shape of the particle and to some extent on the dispersion liquid (its dielectric constant) and temperature. Since the state variables do not change significantly in normal conditions and particles do not re-crystallize to change size and shape, attractive forces are generally of constant magnitude under stable conditions.

The *repulsive forces* arise in the clay-water-electrolyte system due to the surface activity of clay particles and resulting cation and anion distributions adjacent to the particle. The negative surface charge and the distributed positive charge in the surrounding fluid are together termed the diffuse double layer (Mitchell 1976). Among several theories that have been proposed for the description of ion distributions near charged surfaces in colloids, the Guoy-Chapman theory has received the greatest attention. Although this theory is of little quantitative help in the present study, it is of great help in understanding the fundamental behaviour of the surface forces.

According to this theory, the repulsion force is sensitive to changes in electrolytic concentration, cation valence, dielectric constant and pH. In normal situations, the principal parameter is the electrolyte concentration. In dilute electrolyte solutions, the extent of the double layer is of the order of magnitude of the particle dimensions. In concentrated solutions, the double layer is compressed toward the particle surface and its thickness is considerably reduced.

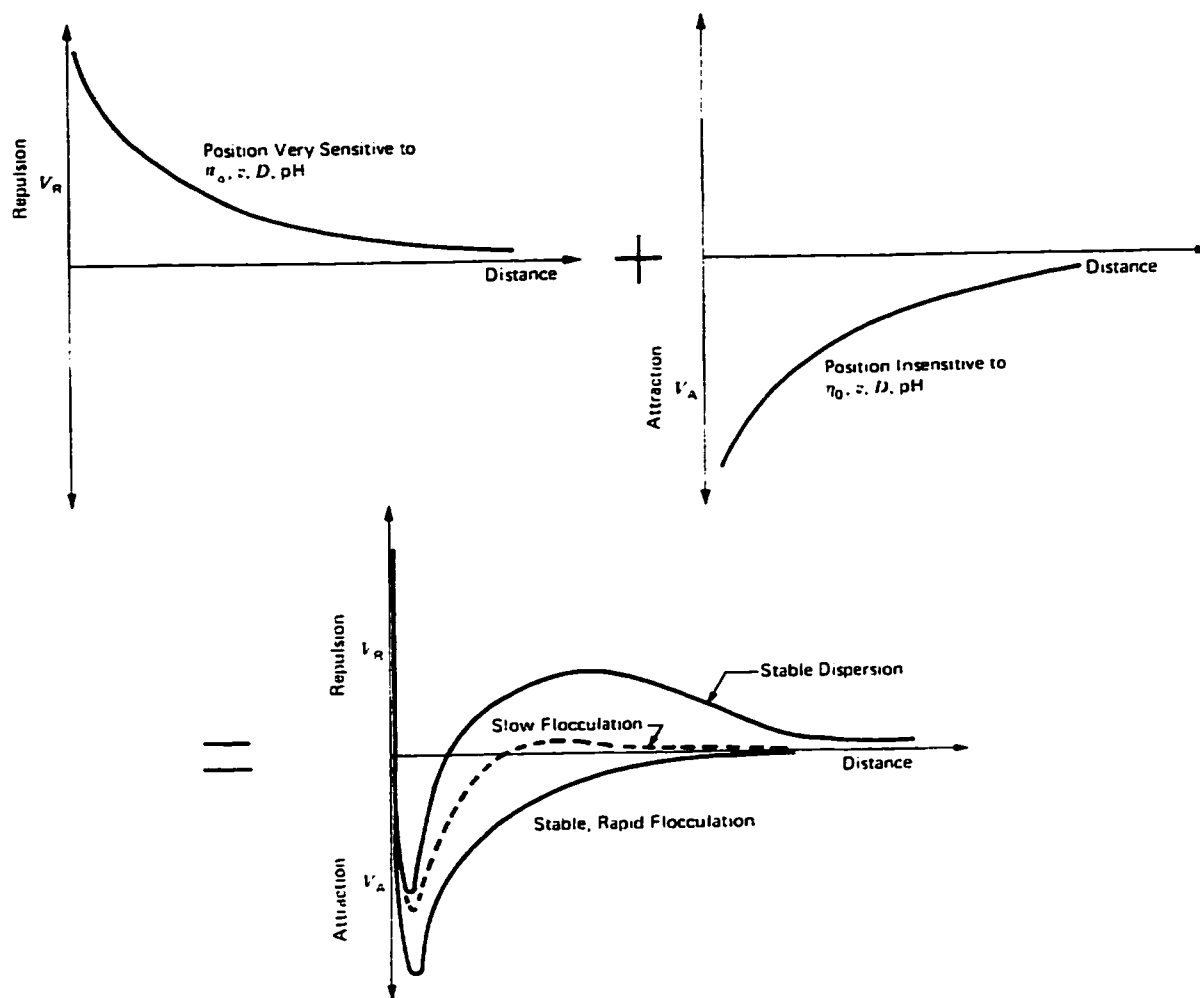
Quantitatively, the repulsion force is roughly exponentially increased with decreasing particle distance. On the other side, the van der Waals force for two large particles is inversely proportional to the third power of the distance between the surfaces. The net potential curve of particle interaction may be constructed simply by adding the attractive and the repulsive potential at each particle distance, as shown on Figure 2.1 (Mitchell 1976, for parallel flat plates).

The *net interaction curves* for a low and a medium electrolytic concentration (upper and middle curve) show a minimum with predominant attraction at close distances and a maximum with predominant repulsion at greater distances. There is no such maximum for the curve with high electrolytic concentration (lower curve) and attraction predominates at any particle distance.

Applied to the problem of stability (sedimentation) of colloidal suspensions, the following interpretation is plausible in terms of the shapes of the curves in Figure 2.1:

(a) At a high electrolyte concentration, where the repulsive forces vanish, if two particles approach each other owing to gravity and Brownian motion, they will attract each other and agglomerate, producing a floc unit. The rate of flocculation is maximal in this case, and the process is called rapid coagulation. The process is described by the diffusion equation.

(b) If repulsion prevails during the mutual approach of the particles (medium and low electrolyte concentration) gravity and Brownian motion are counteracted by the net repulsive force; not every collision of particles will produce a floc, and the coagulation



Energies of repulsion, attraction, and net curves of interaction for parallel flat plates.

Figure 2.1 Energies of repulsion, attraction and net interaction curve for parallel flat plates (after Mitchell, 1976)

process is slowed down: i.e., slow coagulation takes place. At very low electrolyte concentrations, the process is retarded to such an extent that “it may take weeks and months for coagulation to become perceptible. For all practical purposes the suspension is called ‘stable’ under these conditions” (van Olphen 1977). It is obvious from this description that the oil sands fine tailings, which are taken as the benchmark example in this study, belong to “stable” colloidal suspensions.

According to the above, an important conclusion may be deducted, namely that the stability of a dispersion is not an absolute; it is a matter of smaller or greater coagulation velocities. Furthermore, if physico-chemical parameters of the system are kept constant, i.e. chemical reactions are excluded and temperature, etc. does not change, the behaviour will uniformly depend on the concentration of particles (i.e. their distance) and the initial state parameters. The disadvantage is that the laws that govern the process are too complicated for any quantitative analysis.

The above conclusion is very important for modelling the sedimentation process since it justifies a common assumption of the settling velocity of particles as a unique function of their concentration.

#### **2.2.3.2 Inertial forces**

Traditionally, sedimentation analysis usually neglects the inertial forces on particles. It is assumed that the acceleration of a particle is very soon balanced by the drag force, an equilibrium state is reached and a constant terminal settling velocity is achieved. Harr (1977) gives a good illustration in support of this assumption by calculating the time required for a spherical particle 0.2 mm in diameter, with the specific gravity of 2.7, falling through water. A terminal velocity of 0.1 second is obtained, which is almost instantaneously for all practical purposes. For much smaller clay particles, this time is reduced to thousandths of a second.

There are, however, situations where inertia plays a significant role, for example across density discontinuities or “shocks”, such as a sediment-suspension interface (Auzerais et al. 1988). This important question will be discussed in Chapter 2.3.2.5.

Toorman (1996) explains the delay at the beginning of sedimentation, commonly observable in diagrams of settling of the suspension surface, by the acceleration stage of the particles. This is hard to accept for periods lasting months in cases of tailings sedimentation experiments. A more plausible explanation lies in the flocculation time (the rate of floc aggregation due to interparticle collision is high and the rate of fall, measured by settlement of the suspension surface, is small) or particle segregation and lifting up the small particles by the upward flowing water, displaced from the bottom by sedimenting coarser particles.

#### **2.2.3.3 Indirect particle - particle interaction**

In a suspension with higher solids concentration, i.e. with many settling particles, the upward flowing water, displaced from the bottom, increases the drag on the particles (by

increasing the difference of the water and the solids' velocity ( $v_w - v_s$ ), see Chapter 2.2.2). Smaller particles may be even driven upward into the clear water above the suspension interface, as when a blurring of the suspension surface is sometimes seen in sedimentation experiments as (e.g. Been and Sills 1981, Yong 1984).

In cases of suspensions with concentrations over a critical level for the “hindered settling” (when solid particles do not settle individually, but fall together as if they were in some kind of a spatial network), there is no segregation of particles but the whole solids column is subjected to fluid drag. This results in increasing resisting forces to the gravity and decreasing downward solids flux, and actually explains the occurrence of hindered settling.

#### **2.2.4 Particle structure development in clay suspensions**

Particle association in clay suspensions can be described as follows (van Olphen 1977):

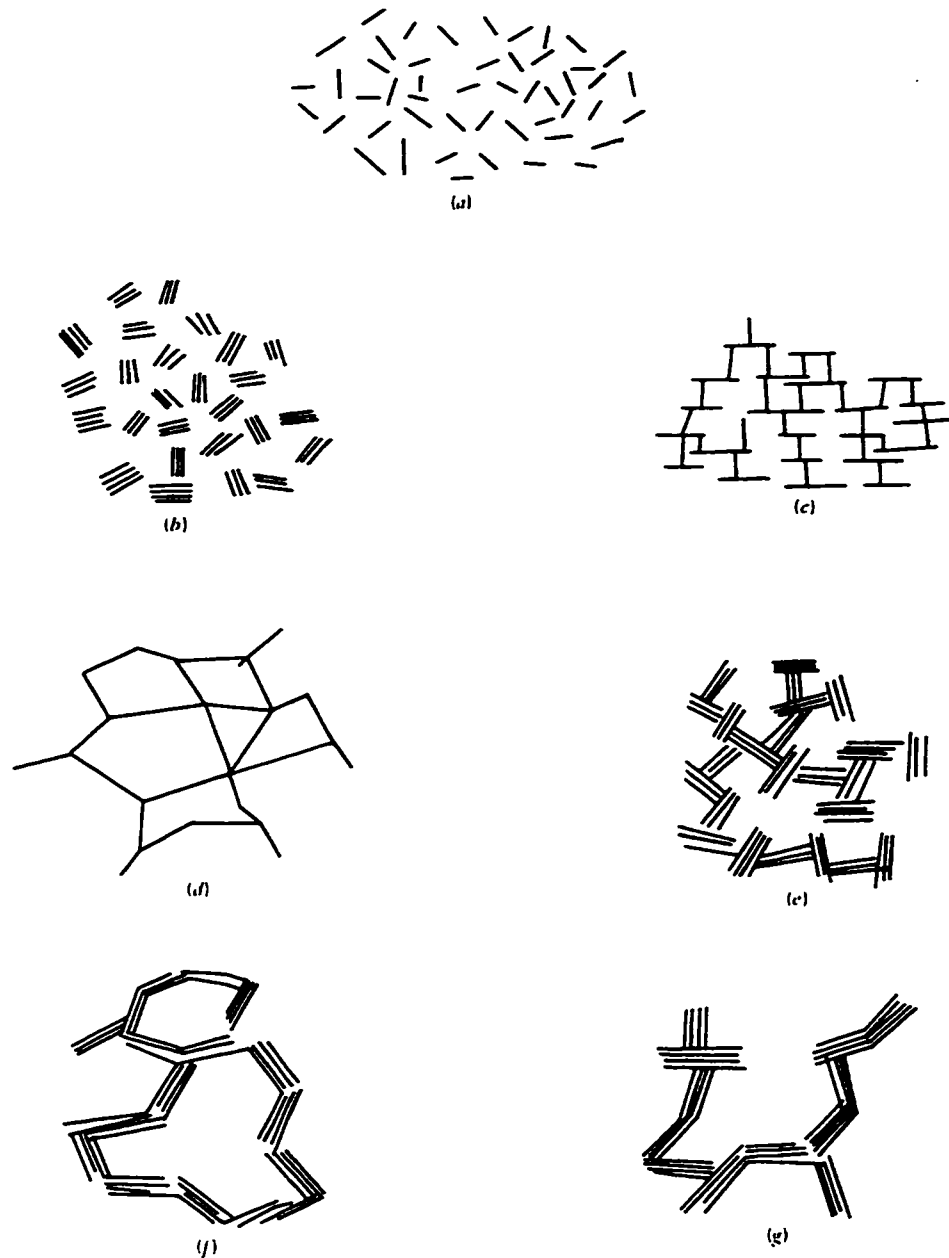
- *dispersed* - no face-to-face (FF) association;
- *aggregated* - face-to-face (FF) association of several particles;
- *flocculated* - edge-to-edge (EE) and edge-to-face (EF) association of aggregates;
- *deflocculated* - no association among aggregates.

Various modes of association are shown in Figure 2.2 (Mitchell 1976). The variety of arrangements results from the various combinations (FF, EF and EE) of possible interactions between the face double layer, negatively charged, and the edge double layer, positively charged.

The net potential curves of interaction for the three modes of association are different. Consequently, these three types of association will not occur simultaneously or to the same extent when the flocculation of suspension begins. The FF association obviously leads to thicker and larger flakes, while EF and EE associations produce continuous three-dimensional card-house structures that extend throughout the available volume. The resulting system is called *gel* (van Olphen 1977).

The consequences of various particle associations are quite different from the engineering point of view. In colloidal chemistry the flow behaviour (“rheological” behaviour) is adopted as a direct criterion for particle interaction (the viscometer test). It may be summarized briefly as follows: when flocs are formed by EE and EF associations (card house structure), the viscosity increases. The suspension behaves as a “Bingham system” with a characteristic “Bingham yield stress”. When particles associate according to the FF type, the number of links in the structure decreases, as well as the viscosity and the Bingham yield stress.

The card house structure is characteristic of low electrolytic concentrations and dilute suspensions, where well developed double layers are sufficient to prevent particle association by a van der Waals attraction (van Olphen 1977). The particles are then associated by EF type, in a double T fashion, in which the EF attraction prevails over the FF repulsion. The balance of forces is probably very slightly in favour of the attraction.



Modes of particle association in clay suspensions (After van Olphen, 1963). (a) Dispersed and deflocculated. (b) Aggregated but deflocculated. (c) Edge-to-face flocculated but dispersed. (d) Edge-to-edge flocculated but dispersed. (e) Edge-to-face flocculated and aggregated. (f) Edge-to-edge flocculated and aggregated. (g) Edge-to-face and edge-to-edge flocculated and aggregated.

Figure 2.2 Various modes of particle association in clay suspensions (Mitchell 1976)

If the card-house structure is idealized as an EF cubic network of plate particles with known dimensions, then it is possible to calculate the minimum volume of solids needed to create such a structure (the “gelating concentration”). For a certain type of sodium montmorillonite, van Olphen (1977) states that a minimum concentration of 2 % by volume was computed. For kaolinite type clays, the concentration should be accordingly higher, having in mind the corresponding particle sizes. But it is probable to expect that particle interaction affects the viscosity and other physical properties of suspensions at considerably lower volumetric concentrations than the gelating concentration.

The existence of a structure in suspension will thus cause a delay in sedimentation. Nevertheless, the question of the stability of this structure could not be clarified from the available literature. It is obvious that such agglomerations in dilute suspensions are very light and therefore prone to breakage under the influence of gravity or even Brownian motion. The repulsion between the face surfaces will most probably assist in the dispersion of broken particles and retain the stability of colloidal suspension. Hydrodynamic convection forces on very large plates (e.g. in montmorillonite) may have an additional dispersive effect in preventing particles from fast settling after the links are broken.

#### **2.2.4.1 Particle structures in oil sands fine tailings**

A slurry of oil sand fine tailings has particles mostly of colloidal size (clay and very fine silt) that segregate from the sand when the matter is discharged into a containment pond as a waste after the bitumen has been extracted from the oil sands. The bitumen separation involves the addition of caustic soda and hot water (the Clark Hot Water Extraction Process). The clays are predominantly kaolinite (60 % to 80 %) and illite (15 % to 25 %). The organic matter in the MFT is divided into three categories: residual bitumen, soluble compounds and mineral adhered compounds.

After several years, when the tailings achieve a void ratio of about 6, the settling process slows down considerably. The material is referred to then as mature fine tailings (MFT). The fluid-like nature of MFT can be explained by its unique clay structure - a gel, card house structure (Scott et al 1986). This structure is not characteristic of kaolinite slurries, which usually agglomerate in large flocs and settle relatively fast, but was shown to be a function of the total mineral grain surface and the pore water chemistry.

The clay structure of the mature fine tailings was examined using a scanning electron microscope, with the objective of identifying and examining the effect of the organic and inorganic compounds in the pore water on the structure of MFT (Tang 1997). A simplified clay-water model of MFT (kaolinite slurry) was created and tested under the influence of various chemical environments.

A typical MFT structure is reproduced in Figure 2.3.a (Tang et al., 1997). For comparison, the structure of kaolinite slurry with deionized water - a typical flocculated structure - is shown in Figure 2.3.b.

The results showed that the bicarbonate and the NaOH in the tailings water are the dominant agents in creating the card-house structure. High temperature in the extraction process enhances this. The bitumen and organic matter strongly bound to the mineral

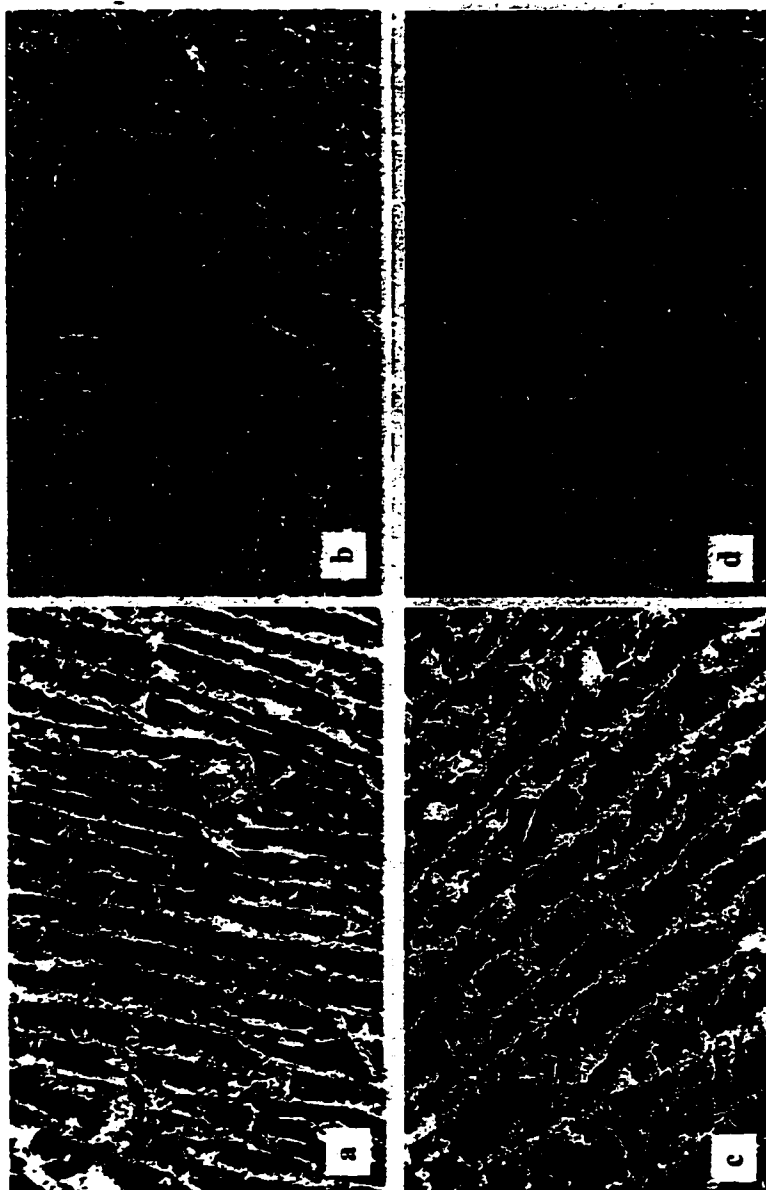


Figure 2.3

Research on solids structure of the mature fine tailings (MFT) and its simplified model in the form of a kaolinite slurry, using electron scanning microscope (Tang et al. 1997)

(a) MFT structure; (b) kaolinite slurry with deionized water (typical flocculated structure); (c) effect of bitumen and organic matter on the kaolinite slurry structure; (d) effect of gypsum on the MFT structure



grains also have a positive effect on the formation of a card house structure (Figure 2.3.c). The addition of gypsum to MFT did not change the structure but made it finer and much stronger (Figure 2.3.d).

In conclusion, different chemical additives in the extraction process result in different gel structures and further control important technological properties of the tailings (permeability, compressibility, etc.) and directly affect the observed mechanical behaviour during sedimentation and self weight consolidation.

## **2.3 SEDIMENTATION**

### **2.3.1 Phenomenology**

The phenomenon of settling of suspended solids is common to many natural processes (e.g. soil sedimentation as the initial stage in formation of sedimentary soils) and industrial processes (gravity thickening as a process for solid-liquid separation in chemical industry, management of tailings in mineral resource industries, etc.). Many experimental and observational programmes have been performed involving both natural and man-made sedimentation processes. Although each of them has had its own goals and aspects of interest, the general phenomenology is converging. A few examples were chosen from abundant literature on this subject. References from chemical engineering field are discussed first because they are historically earlier and, particularly, because they accentuate the phenomenology. These are followed by the references from geotechnical engineering which put more emphasis on quantification of the process and are a good introduction to the sedimentation modelling in the next chapter.

The terminology used in the original papers cited is mainly retained in this review, with necessary explanation when the terms significantly differ from those commonly used in geotechnics.

#### **2.3.1.1 Coe & Clevenger (1916)**

This is considered a classical account of the settling of metallurgical slimes and is cited in almost every paper in the available chemical literature. Coe and Clevenger's work provided the first rational basis for the design of continuous thickeners in the chemical industry. The description cited here is based on the compilation by Auzerais et al. (1988).

Clevenger and Coe recognized that the colloidal particles quite rapidly aggregate into flocs which subsequently separate from the liquid by gravity settling. For batch settling<sup>1</sup> they identified four zones:

- an upper layer of clear liquid separated from the suspension by a sharp interface,
- a layer of flocculated suspension of uniform density settling at a uniform rate,
- a layer within which the density increases continuously with depth and, finally,
- a layer containing flocs in contact supported by the forces transmitted through the contact points.

In the upper layer they imagined the flocs to move essentially only under the influence of gravity and hydrodynamic drag forces, although they realized, observing the interlocking structure of the flocs, that there are points of contact between the flocs even in this zone.

Coe and Clevenger distinguished two types of settling behaviour:

---

<sup>1</sup> The batch, hindered and zone settling are equivalent terms that are interchangeably used in this text.

- type 1, with the thickness of the third layer (the one with continuous increase in density) is small, and
- type 2, where this zone is a significant part of the total depth of the suspension.

### **2.3.1.2 Tiller and Khatib (1984)**

This paper has been chosen from the abundance of published work in chemical engineering not because it presents new details or different approaches but because it documents the known phenomenology in a concise and precise way. The facts in the following description are common experience from work in the chemical field. The description given here is the compilation by Diplas and Papanicolaou (1997).

Batch settling tests are typically used in the chemical industry to determine the settling characteristics of a slurry. This work focused on the slurries that exhibit zone settling behaviour when “the particles lose their individual identity and settle ‘en masse’”. The two interfaces that typically appear, plotted with respect to time, are called, respectively, the batch settling (interface between the supernatant liquid and the suspended solids) and the L-curve (interface between the settled solids and the suspension).

The settling behaviour of the attapulgite slurry tested by Tiller and Khatib is shown in Figure 2.4. The solids concentration is approximately uniform at the beginning. It is assumed that no induction period occurs (i.e. there is no flocculation which delays settling; this can be recognized by the absence of the initial convex upward portion of the batch settling curve).

As the test progresses, three different settling regions are identified in the batch settling diagram in Figure 2.4:

- the constant rate region OABO, where the suspension maintains the initial concentration and the particles fall with a nearly constant velocity;
- the first falling region OBCO, where the suspension has varying concentration (increasing toward the sediment layer) and the velocity of the falling particles decreases as they approach the sediment layer; and
- the second falling rate region OCEGKO (which is not explained in more detail by Tiller and Khatib).

The settling of solids within the suspension zone OACGKO is dominated by hydrodynamic forces. However, “within the sediment layer OKGDO the normal stress (also known as effective stress) controls the solids settling, due to the contact among the solid particles”, and that is termed self-weight compression. More detail is provided in the following description: “The buoyant weight of the solids in the sediment layer causes the gradual compression of the solids skeleton, which in turn results in the release and upward movement of the fluid trapped in its interstices.” (This is the primary consolidation in geotechnical terms.)

A description that follows in the original paper is more an attempt to make a proper basis for a proposed theoretical model since it does not deal with the phenomenology but

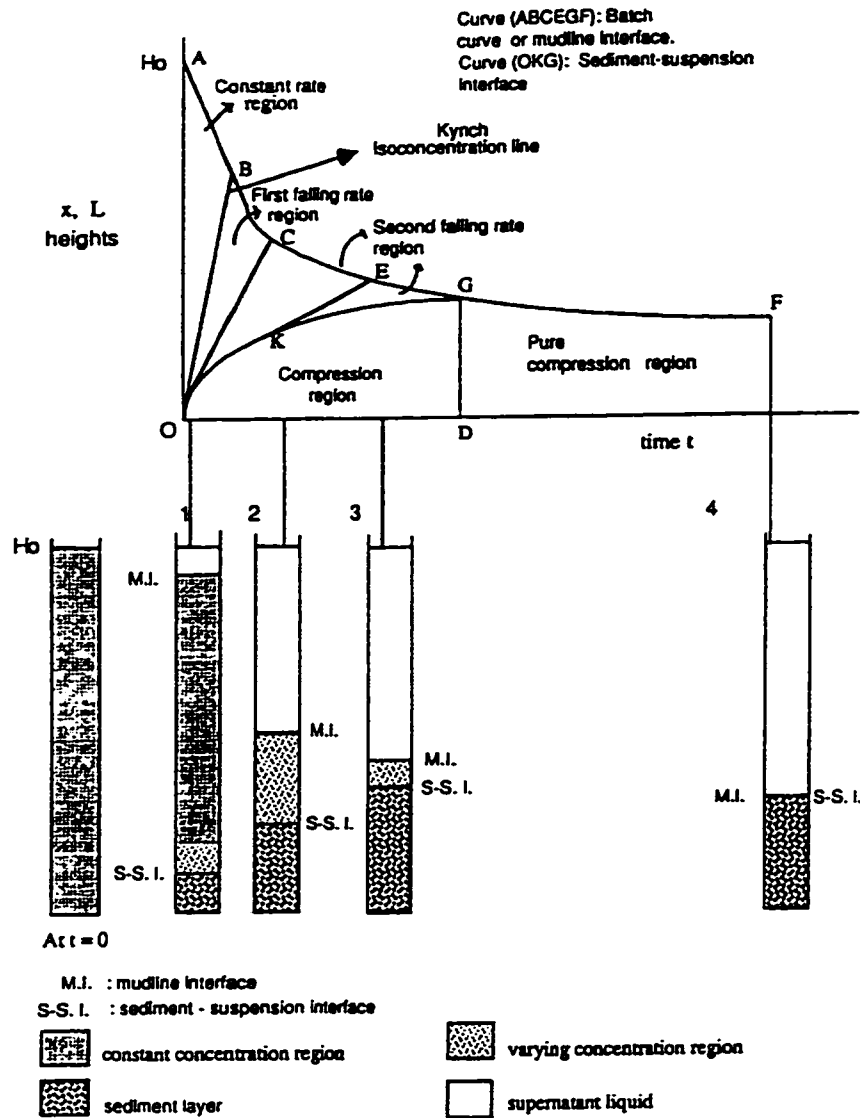


Figure 2.4 Settling behaviour of an attapulgite slurry (Tiller and Khatib, 1984)

explains it. “An effect of the upward fluid movement is the formation of varying concentration layers within the suspension region OACGKO. The propagation of these layers in the suspension region is typically depicted with straight lines, known as isoconcentration lines. These lines propagate through the suspension with a constant velocity known as propagation velocity (Kynch 1952). The isoconcentration lines that propagate through the first falling rate region OBCO originate from the bottom of the cylinder, while in the second falling rate region OCEGKO, they emanate tangentially (e.g. line KE in Figure 2.4) from the sediment-suspension interface”. The basic phenomena can actually be explained as follows:

A disturbance in the suspension travels with a finite velocity. In the constant rate region OABO, the velocity of the falling particle is constant (within the experimental error) and hence equal to the one in an infinitely long column - the upper portion of the suspension does not “feel” the bottom of the container yet. When the first sediment layer forms, the “information” in the form of a density wave OB in Figure 2.4 spans the suspension to the surface. This density wave “announces” all the other changes correlated with density: permeability, hydrodynamic resistive force on the particles, etc., and the suspension begins to behave in a non-linear manner. In the lower portion of Figure 2.4 this is shown in Column 1 as the varying concentration region at the bottom of the suspension zone. In the batch settling diagram in Figure 2.4, this action is indicated in portion BG.

At this moment another phenomenon has been observed in some tests. A zone of relatively short channels appears and moves upward until it meets with the suspension surface. This meeting “triggers an increase in settling velocity of the suspension surface” (Vesilind and Jones, 1993), but that increase is not shown in Figure 2.4. This phenomenon is known as channelling and typically occurs between the first and the second falling rate region (therefore, the line OC). “The existence and degree of channelling influence depend on the type of slurry, the initial solids concentration, the height of the column, and possibly other factors. A general quantitative model predicting the onset of channelling and its effect of solids settling is lacking.” Depending on the occurrence of channelling, the portion CEG in a batch settling curve is more or less pronounced, as can be observed in published data. This effect is usually neglected in sedimentation modelling.

An important observation, reported in almost all other papers (e.g. Been and Sills, 1981) is that the solids concentration at the sediment-suspension interface increases steadily, although the effective stress remains negligible.

### **2.3.1.3 Tailings settling in a pond (Yong 1984)**

Yong (1984) gives a description of the total sedimentation and consolidation process by tracing the “life” of the tailings slurry in a containment pond. He first recognizes that a simple Stokesian model may sometimes predict initial settling but is invalid for further analyses. Figure 2.5 presents the solids concentration profile of an initially dilute suspension after several years.

Zone A is supernatant water, almost free of solid particles. Below it, the solids concentration gradually increases in zone B and reaches an almost constant value in zone C (actually, the rate of solids concentration increase is remarkably low in comparison

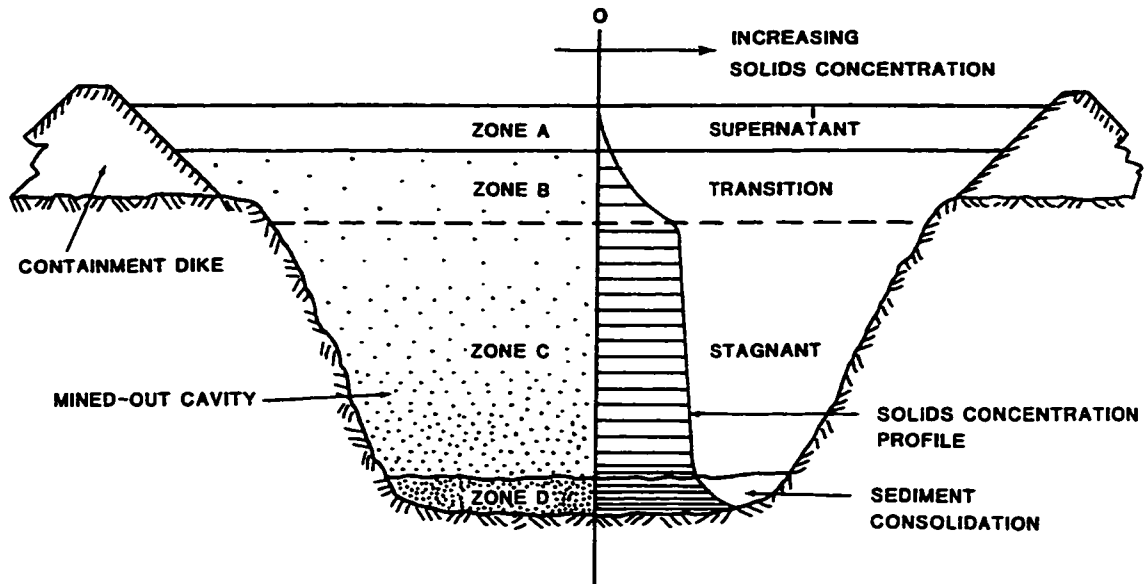


Figure 2.5 Solids concentration profile of a tailings slurry in a containment pond after several years (Yong, 1984)

with that in zone B). Zone D represents the sediment where consolidation occurs. The lines that separate the zones should be understood as transitions of variable thickness.

A difference from Coe and Clevenger's observations may be noticed: there is no sharp interface between supernatant water and suspension in Yong's description. It may be a consequence of particle segregation, due to wide grain size distribution ranges in real materials, and perhaps of a shorter duration of monitoring (fines remained in suspension longer than they were observed).

It is also worth mentioning that a kind of combination of zones A and B with a suddenly decreasing concentration appears in the experimental results of Been and Sills (1981); see Chapter 2.3.1.6. This zone is in the form of a thin layer atop the suspension and the authors do not pay particular attention to it, probably considering that it is a natural transition in density from water to suspension.

Zone A is described as a very dilute suspension (actually the initial state of suspension) where there is no particle interaction. Zone B represents the stage of interference of neighbouring solids exhibiting hindered settling characteristics. Zone C is said to be the region where, even though no direct physical contact between particles is

established (void ratios of about 4 to 6) there is “a physical evidence that some excess pore pressure can be measured” and “a form of compressive settling of the solids occurs”. When further settling causes adjacent solids to make physical contact in zone D, consolidation becomes the dominant mechanism. In zones A and B there are no measurable pore pressures, whereas in zone C they are detectable; in zone D, however, fully developed pore pressures and effective stresses exist. These statements are not quite clear, particularly for treatment of zone C.

The author then comments on representative analytical models. “Total” (coupled) analysis of the problem is not possible and separate treatment of each zone must be done. In zones A and B, sedimentation theories are applicable and Yong lists a number of allowable settling velocity functions. Zone D can be analyzed using finite strain consolidation theories, but the problems arise with zone C.

There is apparent inconsistency, say the authors, between high void ratios which show that there is no solid to solid contact, which is necessary for transfer of intergranular stresses, and “the satisfactory use of the models relying on pore pressure development,” i.e. consolidation models, “as demonstrated in practice.” The question is actually in “the point at which effective stresses are considered to be operative, i.e. when pore pressures are measurable in a solids suspension”. But, nevertheless, the author thinks that large strain consolidation theories are applicable, with non-linear relationships (for permeability and compressibility) and accounting for self-weight.

There is actually a certain ambiguity with regard to the treatment of zone C because the author concludes that there are “two theories capable of handling the settling problem over its entire range (of concentration): the convection-diffusion model can encompass solids settling performance in zones B and C, and large strain consolidation can encompass the lower part of zone C and all of zone D”. Therefore, zone C undergoes both sedimentation and consolidation, according to the author. This is not clear from the modelling point of view.

The transition point from suspension to soil is further calculated as the equilibrium suspension concentration which balances internal and external energy in the system, i.e. from the maximum volume of water that can be held by a particle at zero osmotic pressure (zero mid-plane potential) for various possible arrangements of the particles. It is interesting to mention the value obtained for “the sludge obtained from processing of tar sands in the Western Canada” - the solids content  $s$  (by weight) at about 42 %, with remarkably good matching between calculated and measured values.

#### **2.3.1.4 Experimental settling of a dredge spoil (Lin and Lohnes 1984)**

The settling behaviour of a lake bottom sediment was studied by a series of settling tests in a 140 mm inside diameter and 1.83 m high column. The material was 63 % silt and 37 % clay, with 5.6 % of organic matter by weight. Natural water content was 79 %, specific gravity 2.74, soil classification MH.

The preparation procedure included supply of the air from the bottom of the column to prevent the settlement of coarser material during the filling.

The laboratory observational procedure was as follows: When a sharp interface between the suspension and supernatant water forms, its height was recorded (the height of suspension, actually). After that, the interface height was observed at regular intervals and the diagram was plotted. The procedure was repeated for slurries of different initial concentrations. A series of tests was also performed with sample withdrawals through sample ports (using hypodermic needles) in order to obtain the concentration profiles at different times. Pore pressures were not measured during the testing.

In this description a vague point is the appearance of the “sharp interface”. The authors did not precisely explain whether this moment marked the end of turbulent motions caused by the filling procedure or, perhaps, a certain initial part of sedimentation was included. But, as it can be concluded according to the further description, the appearance of this “sharp interface” was really the moment when all the coarse particles had settled down.

The authors’ first observation at the beginning of the test was that the upper portion of the suspension became less concentrated than the initial concentration. The supernatant water above the suspension was turbid “partly because of finer particles still suspended and partly because of the upward moving particle flux”. The importance of this finding is in the presence of segregation while the suspension is still dilute (the phenomenon that regularly appears in all the examples cited in this chapter) and in confirmation of indirect particle-particle interaction described in Chapter 2.2.3 (in this case, the settling of coarse particles causes the upward flux of displaced water, which returns finer particles into the supernatant water).

Later on, the supernatant water cleared up and a sharp interface was formed. From that moment on “all the particles appear to be locked into a three-dimensional lattice and settle as a mass and consolidation begins.”

In Figure 2.6 one of the authors’ diagrams for the tests without sampling is presented. Lin and Lohnes comment “that the lower the initial concentration, the faster the settling rate. In a test with high initial concentration, for example N-5, the interface immediately forms, and the settling curve shows an early convex upward portion. In the test with low initial concentration the early convex portion is flattened.” There is no explanation for this in the paper. The authors further state that “after the interface has formed, the system is in self-weight consolidation”. The end of interface forming is obviously the end of the initial convex upward portion of the settlement curve. The linear portion is already showing a consolidation process. There is no explanation for the following concave upward portion although it should be a secondary consolidation stage, judging from the common shapes of the consolidation curves. It was remarked at the end that the shapes of the experimental curves resembled the theoretical self-weight consolidation curves obtained using the approximate method of Been and Sills (1981). The authors probably did not have sedimentation curves on hand whose shapes also resembled their experimental data.

The authors also find that the critical initial concentration is about 148 g/l (volumetric concentration roughly 0.15) and that it depends on the nature of the material and the settling environment, especially its electrolyte concentration. The critical concentration is



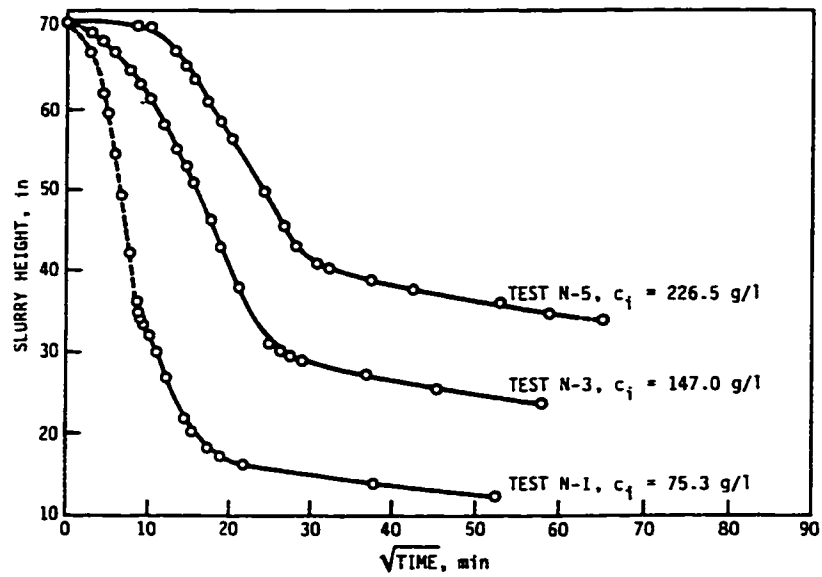


Figure 2.6 Settling behaviour of a slurry at different initial concentrations (Lin and Lohnes, 1984)

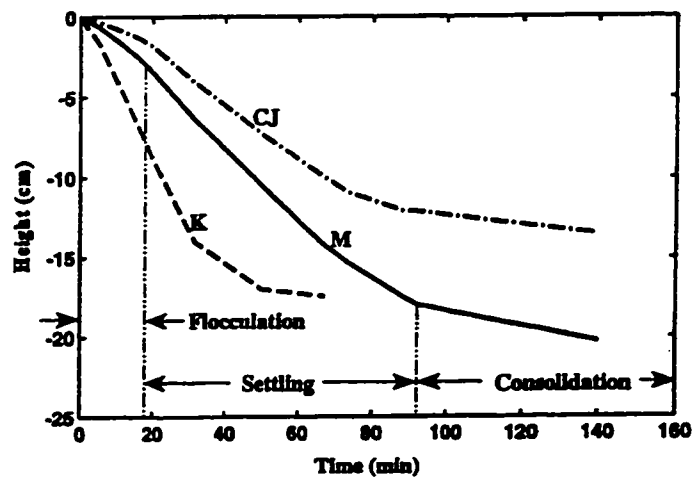


Figure 2.7 Settling behaviour of three clay slurries with identified flocculation, settling and consolidation periods (Li and Mehta, 1998)

the lowest in the slurry at which the interface forms immediately. Here this means that soil is formed from a slurry.

The “three-dimensional lattice” in which the solids are caught and undergo further “mass settling” is interpreted by Lin and Lohnes as the beginning of consolidation. The lattice structure further implied the existence of effective stresses between the solid particles, and Lin and Lohnes concluded that “the zone settling could be described and analyzed according to self weight consolidation theory”. The same data interpreted by a chemical engineer would most probably suggests that the initial convex upward portion of the settling curve is the flocculation stage, the linear portion that follows the hindered settling and the flat end of the curve consolidation of sedimented material. This is therefore an example of how different interpretations of the same data set lead to different conclusion. If pore pressure had been measured, they would have been decisive in explaining the phenomenon.

An example of a very similar diagram to the one presented by Lin and Lohnes, but interpreted in a completely opposite way - the way of a chemical engineer, as referred to in the previous paragraph - is shown in Figure 2.7 (from Li and Mehta, 1998).

### 2.3.1.5 Sedimentation and fluidization

Fluidization is a process in which a fluid is forced upward through a bed of solid particles. It has a variety of applications in modern industrial processes. By gradually increasing the flow rate, and thus the fluid velocity, the particles tend to reorient themselves to the loosest possible arrangement. At a certain “fluidization velocity,” the particles are kept in suspension by upward fluid flow, the solids bed remains at constant porosity, and the solid particles do not change their position with time.

The early experiments on fluidization revealed that the fluidization and sedimentation velocities of a given system at a given porosity were practically coincident. A rational explanation for this phenomenon was given by Richardson and Zaki (1954). Their analysis may be summarized in two fundamental statements (see Figure 2.8, taken from Pane and Schiffman, 1997).

“(a) The fluidization velocity necessary to maintain a uniform system at a given porosity is equal and opposite to the settling velocity of the same system at the same porosity.

(b) For a given system, the velocities of fluidization and sedimentation depend only on the system porosity:

$$v_s = -v_f = v_{Stokes} \cdot f(n) \quad [2.3]$$

where  $n$  is the porosity. This equation holds for inert spherical particles with predominant drag forces (viscous fluid friction).

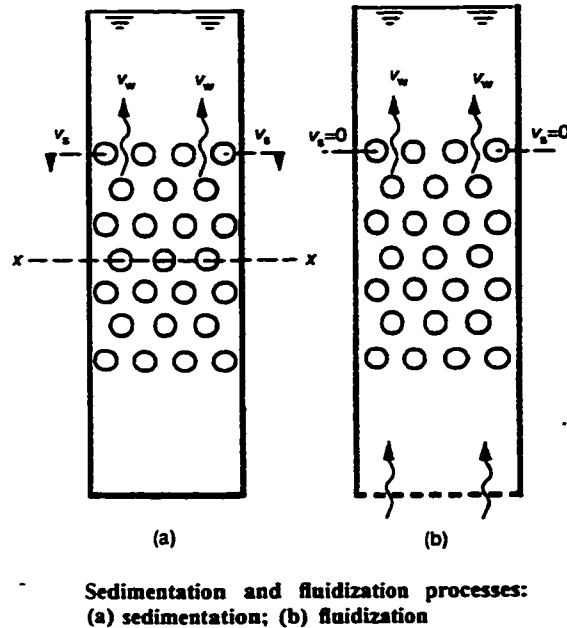


Figure 2.8 Sedimentation and fluidization (Pane and Schiffmann, 1997)

#### 2.3.1.6 Been and Sills' experiments (1981)

The results of Been and Sills laboratory experiments were published in 1981. The objective of the experiment was to measure the behaviour of real soil settling in idealized, controlled conditions. An estuarine mud was chosen, consisting of a uniformly graded silt passing through a  $75 \mu\text{m}$  sieve, with 30 % of clay. A precise routine of preparation and stirring was followed. A 2 m high and 102 mm in diameter settling column was used, as shown in Figure 2.9.

Density was measured throughout the column using a non-destructive X-ray technique, giving continuous profiles with an overall accuracy of  $\pm 0.1 \text{ kN/m}^3$  and vertical spatial resolution of the order of 10 mm.

A total vertical stress profile was obtained by integrating the density profile. A check of the accuracy of such a calculation was the value of the total stress at the bottom of the column that never varied more than a few percent. Another check was the measurement of the total stress at the base of the column with an accuracy of  $\pm 0.1 \text{ kN/m}^3$  or  $\pm 2 \text{ mm}$  head of water.

Pore pressures were measured at various points on the wall of the settling column. The transducers had an accuracy of  $\pm 0.03 \text{ kN/m}^3$  or  $\pm 2 \text{ mm}$  head of water.

Typical settling behaviour, as chosen by the authors and reproduced here in Figure 2.10, was exhibited in experiment 7. The initial density of the suspension was  $10.7 \text{ kN/m}^3$  with a corresponding solids content (concentration of solids by weight, see Appendix 1)  $s = 0.13$ .

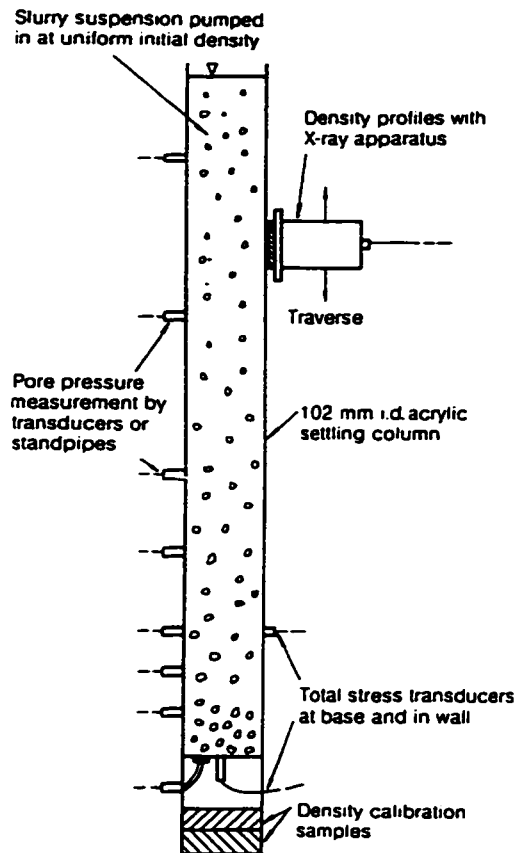


Figure 2.9 Been & Sills (1981) experimental setup

In the density profile diagram (Figure 2.10.a) the suspension is, according to the authors, “initially almost uniform” (after 20 minutes), although the difference between the top and the bottom is about  $0.2 \text{ kN/m}^3$  which is more than the measurement error. The equivalent change in solids content  $s$  is almost 0.03 and the change in concentration  $c$  (solids by volume) is about 0.01. This slight increase of density with depth is a repeating pattern in all the experiments. The question about the influence of this density trend in initial conditions on further behaviour of soil settling is neglected by the authors. Probably, the authors assume that only the beginning of the settling process is influenced and after some time this effect should gradually vanish.

It is interesting to remark that there was no discussion on the sensitivity of the sedimentation process toward the initial conditions in a suspension in the available literature. This lack of discussion probably suggests the difficulties in obtaining ideal uniform suspension conditions in the experimental work and, accordingly, an absence of the “right” data for checking the existing sedimentation models.

Subsequent density profiles show fast initial accumulation of sediment at the base with a high increase in density. This was partly attributed to settling of the coarser particles

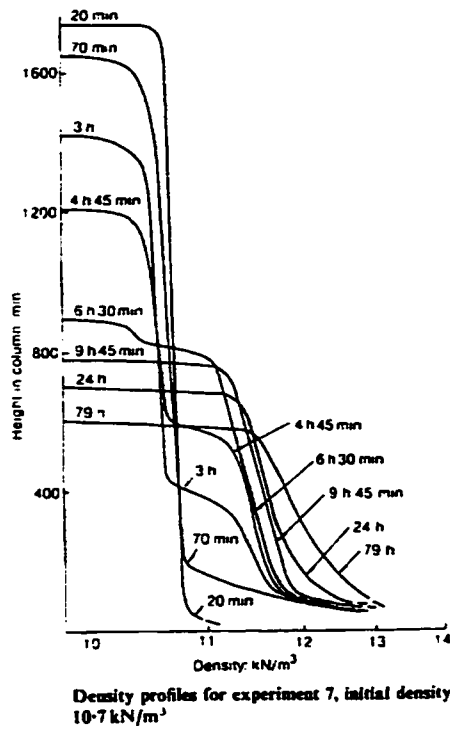


Fig. 2.10 a

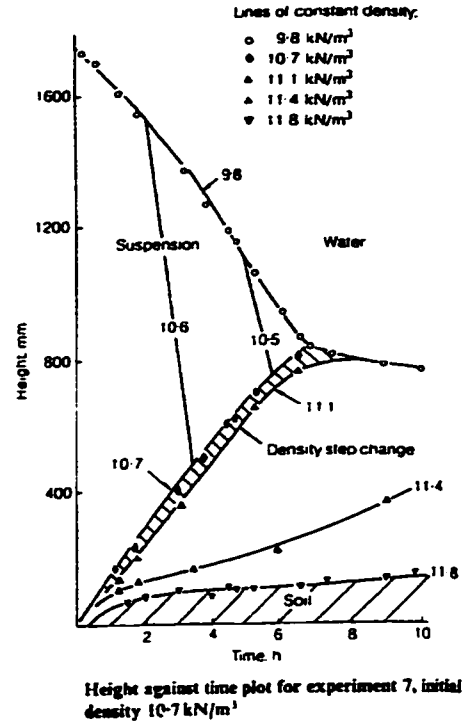


Fig. 2.10 b

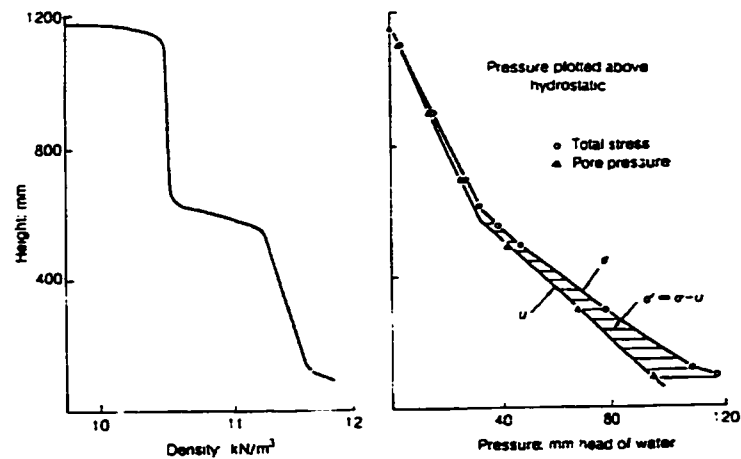


Fig. 2.10 c Density and stress distribution at 4 h 45 min, experiment 7, initial density  $10.7 \text{ kN/m}^3$

Figure 2.10 Been and Sills (1981), experiment 7

(a) density profiles; (b) heights of the interfaces in time; (c) density profile, and total and effective stress and pore pressure distribution after 4 h 45 min

before full flocculation, thus indicating certain segregation and a relatively dilute suspension.

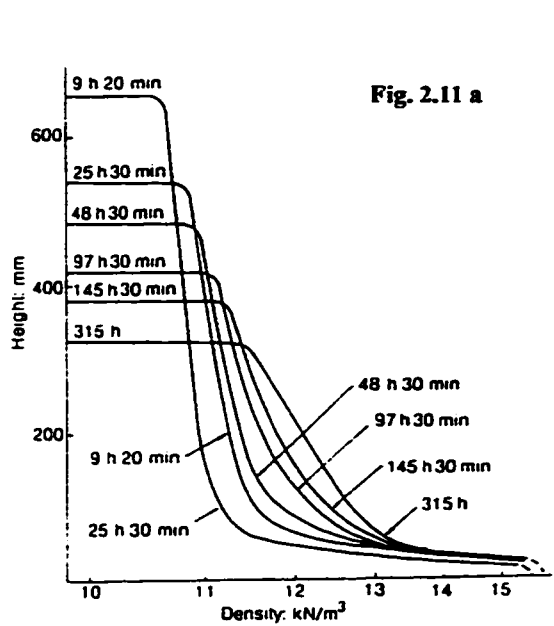
A region of intermediate density gradually develops above the sediment, with a distinct step toward the suspension above it. The suspension itself remains almost uniform, with the mentioned linear trend toward the bottom and the average density slightly decreasing in this experiment. It is not clear whether this was a rule or an exception. In Figures 2.11.a and 2.11.b the density profiles for experiments 11 and 15, respectively, are shown. Both reveal an increase in density in the suspension. The initial density in experiment 11 is less than in experiment 7, but the data are shown from after 9 hours on, meaning perhaps that the sedimentation stage for experiment 11 was already completed. There is no observable sedimentation stage in experiment 15, with a density of  $11.2 \text{ kN/m}^3$  and  $s = 0.20$ . The authors interpret this as a result of high concentration - the suspension does not actually exist in the beginning of this experiment.

Despite that, initial pore pressures in experiments 11 and 15 were very close to the total stress (Figures 2.11.c and 2.11.d), suggesting again that the effective stress may be close to zero. This thus raises certain doubts about the authors' opinion on the initial state of the system as a "soil".

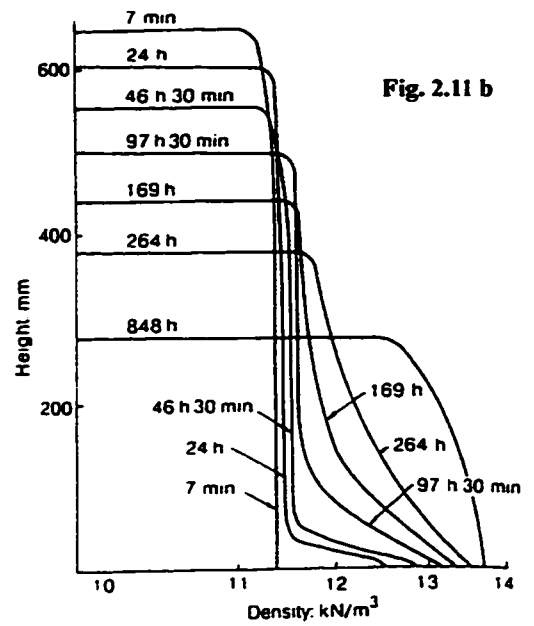
In Figure 2.10.b the settlement against time is plotted for the sedimentation stage, with the additional information in the density isolines. Sudden changes in density clearly show motions of the two interfaces (water-suspension and suspension-sediment). There is also a marked change of settling rate after about 7 hours, when the suspension no longer exists. It is, however, interesting to notice that there is also a pronounced density change within the sediment. The hashed zone marked as "soil" which develops at the very beginning of the experiment remains at almost the same density and thickness throughout the sedimentation stage. This confirms the above stated opinion that this zone is a product of an initial segregation of the coarse particles. Strictly speaking, it may probably be considered as an experimental "bias". The "real" sediment is the zone above it, with gradual change of density from  $11.1 \text{ kN/m}^3$  to  $11.8 \text{ kN/m}^3$  as a result of consolidation under the self-weight.

Figure 2.10.c shows a typical density profile which does not show anything new. In Figure 2.10.d the stress distribution after 4 hours 45 minutes is presented. The total stress is obtained by integrating the density profile, and the pore pressures are measured. Within the experimental error, this diagram clearly shows that the effective stress exists only in the sediment layer below the step change in density. In the suspension there is no discernible difference between the total stress and the pore water pressure; therefore the suspension behaves as a fluid.

The last fact is very important for sedimentation modelling, at least in engineering applications. *The suspension should be treated as a fluid*, actually a heavy fluid with its own density and viscosity, etc. and other properties which characterize a fluid. The stress distribution in the suspension should be described by the linear fluid pressure only, which is equal to the total stress, as in any fluid. It is possible to have a "structured, deformable" fluid, with layers of different densities and other properties (reflecting actual processes



Density profiles for experiment 11, initial density  $10.3 \text{ kN/m}^3$



Density profiles for experiment 15, initial density  $11.2 \text{ kN/m}^3$

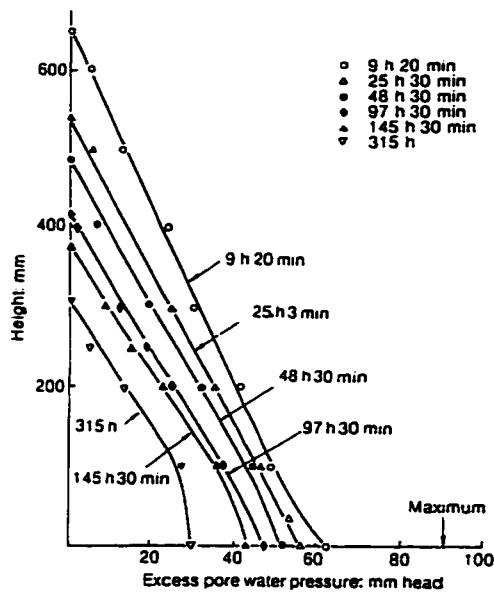


Fig. 2.11 c

Excess pore water pressure for experiment 11, initial density  $10.3 \text{ kN/m}^3$

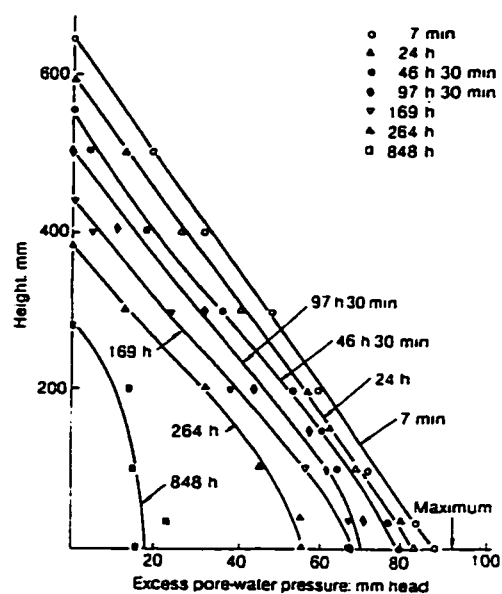


Fig. 2.11 d

Excess pore water pressure for experiment 15, initial density  $11.2 \text{ kN/m}^3$

Figure 2.11 Been & Sills (1981), experiments 11 and 15; (a) and (b) density profiles in experiments 11 and 15, respectively; (c) and (d) excess pore pressure profiles in experiment 11 and 15, respectively

of particles motion in sedimentation), but the external behaviour of such a system will still be governed by the laws which commonly apply to fluids.

The last comment that can be made is that this generalization strictly applies to the class of materials being tested in these experiments, but it does not seem that these material are particularly different from many common soils.

Inspection of Figures 2.11.a and 2.11.b leads the authors to remark that “the density and void ratio at the surface (or as near the surface as may be measured) increase steadily although the effective stress there remains negligible.” They then conclude that there is apparently no unique void ratio corresponding to zero effective stress. In other words, the compressibility curve for soils will be “undetermined” at very small stresses; i.e. will depend on the stress history of a soil while it was in a suspended state. They further conclude, based on data of experiment 15 in Figure 2.11.b, that the “stress history effect is small for very soft soils with concentration slightly over some threshold value marking transition from suspension to soil.” (This was later confirmed by the compressibility tests on oil sands fine tailings conducted by Pollock (1988) and Suthaker (1995), who obtained different compressibility curves for materials with solids contents varying from 20 % to 30 % and attributed that to the effect of aging, i.e. developed microstructure of solid particles in the tailings. They further suggested that a time-dependent factor into the effective stress - void ratio relationship should be introduced.)

The above considerations may be expanded by inspection of Figures 2.10.a and 2.10.b, in which we can see that the density and concentration of the suspension change while the effective stress remains negligible in the whole suspension zone. With respect to application of consolidation theories to sedimentation problems, this raises the question of a compressibility law that has to be applied and an experimental procedure by which these parameters are to be determined.

Another significant insight into the phenomenology of sedimentation comes from the analysis of segregation by particle grain size distribution measurement at different heights in the settled mud. The data were presented for experiments 7 (initial density  $10.7 \text{ kN/m}^3$ ), 8 ( $12.0 \text{ kN/m}^3$ ) and 9 ( $10.2 \text{ kN/m}^3$ ). Here only the data for experiments 7 and 8 are reproduced in Figure 2.7, because in experiment 9 a dispersing agent was added and the conditions were not the same.

It is apparent from Figure 2.12.a that the particle size distribution consistently changes throughout the sediment in experiment 7. A significant proportion of the coarse silt particles settled to the base at the beginning of the experiment, leaving the top layer with a high percentage of finer material. Highly contrasting is the picture in experiment 8, shown in Figure 2.12.b, where all three samples have the same grain size distribution. Therefore, the authors conclude that at higher initial stresses “when a suspension does not occur,” there is negligible particle size segregation. They also point out the importance of flocculation for the homogeneity of the settled bed and the suspension behaviour.

Putting aside the comment on the suspension, this finding is in complete agreement with what was concluded in chemical experiments. In dilute suspensions there is a tendency to segregation because of large distances among particles and weak particle interaction. Each particle behaves almost as if it is a lonely Stokesian sphere - large heavy grains suffer proportionally lower resistive force and fall faster. With increasing



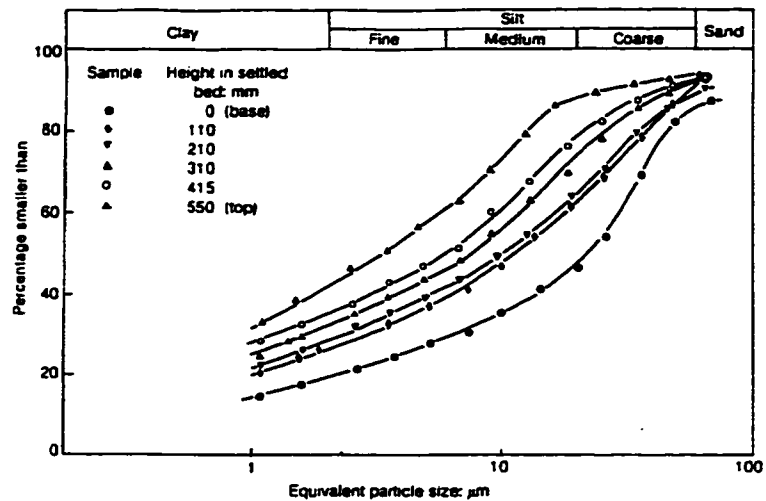


Fig. Particle size distribution at end of experiment 7, initial density  $10.7 \text{ kN/m}^3$ , no additive (hydrometer method)

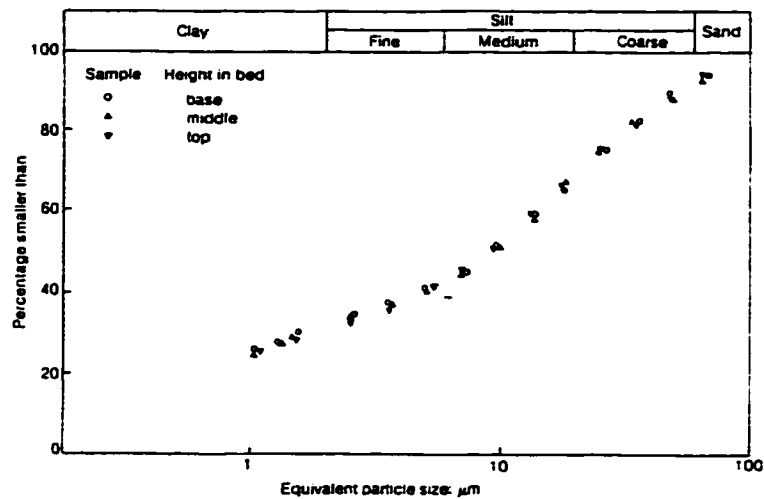


Fig. Particle size distribution at end of experiment 8, initial density  $12.0 \text{ kN/m}^3$ , no additive (hydrometer method)

Figure 2.12 Been & Sills (1981), experiments 7 and 8  
Particle grain size distributions at different heights in the sediment

concentration, the scene becomes crowded and, even if there is no direct particle interaction by electrostatic forces, there is less space for displaced water to flow through and the whole assembly of grains “feels” increased drag forces which slow down their fall through the column. From the point of view of a large grain, the medium consisting of water and fine particles becomes more viscous with progressing sedimentation.

The above formulation is practically the description of what is understood under the term “hindered settling” in the chemical engineering theories of sedimentation. There is some concentration (or, more accurately, a range) which designates the boundary between the state of “free” settling of individual particles (and segregation) and the hindered settling state when the whole assembly of particles behaves like a unit.

The authors further determine the permeability from the experimental data, using Darcy’s law and the mass continuity condition. The results, although somewhat scattered, show that the logarithm of permeability is approximately proportional to the void ratio.

The authors also derived the compressibility from experimental data. They found a large scattering of data for small effective stresses (less than  $0.15 \text{ kN/m}^3$ ) and attributed that to creep and viscous flow. Total stress measurements at the column base suggested small side (wall) friction indicating the existence of extremely low shear stress at these void ratios. Although statistical dispersion in material properties, the magnitude of experimental errors, etc. were verbally commented upon as small (but not shown in numbers), it is hard to accept the importance of creep with stresses of the order of magnitude  $0.1 \text{ kN/m}^3$ , particularly at void ratios from 5 to 12, as shown in their Figure 2.14 in the paper, when there is almost no contact between particles and therefore no effective stress. Creep itself is defined as a property of deformations of direct grain contacts and thus assumes the existence of measurable effective stresses.

In connection with this, a transition criterion from suspension to soil was considered by the authors as a “certain density at which a slurry can no longer exist in an effective stress free condition”. Values of this density vary for different soils, pore waters and many other factors. In these experiments, those values were roughly estimated as void ratios of about 6. Furthermore, the suspension-soil criterion was (intuitively) understood as an intermediate phase rather than a sudden change, a process where flocs in suspension come into contact and start breaking up. The chief significance of this transition was found to be in the absence of a unique zero effective stress void ratio for a cohesive soil.

The following section will describe how this idea of gradual transition from liquid to solid state was numerically exploited by Pane and Schiffman (1985) to propose a modification of the effective stress principle in solving the sedimentation / consolidation problem.

#### **2.3.1.7 Large scale sedimentation tests on oil sands tailings at the University of Alberta**

A self weight consolidation test in a 10 m high standpipe was commenced in 1982 to evaluate the behaviour of the oil sands fine tailings (Scott et al. 1986). The standpipe is equipped with pore pressure and sampling ports at 1 m intervals. Measurements have been regularly taken to obtain pore pressure and density profiles with time. This test was

taken as the benchmark for the modelling method developed here and will be described in more detail in the following sections. Only the most important facts of its behaviour will be given here; refer to Suthaker et al. (1997) for more details.

Figure 2.13.a shows the settlement of suspension with time. The behaviour is non-linear almost from the very beginning: i.e. there is no linear portion of the settlement curve. In this scale it is not visible, but the initial portion of the curve shows a characteristic convex upward shape. The estimated flocculation period is about 120 days.

Excess pore pressures, obtained as a difference between measured pore pressures and calculated hydrostatic ones, are shown in Figure 2.13.b. A linear trend dominates even after 14.4 years and the consolidation zone is of the order of 1-2 m in thickness.

The solids content in Figure 2.13.c is the most intriguing data. There is no gradual increase towards the bottom, as many other tests demonstrate and as the consolidation theory predicts. It seems that the whole suspension zone keeps a constant density over the height which homogeneously increases with time. The sediment at the bottom is not formed by the coarse fraction settling at the beginning of the test since the grain size analysis reveals a more or less uniform proportion of fines of about 90 % over the column height.

There is considerable variation in the solids content profile over time, a finding not shown in the Figure 2.13.c. but later presented in Chapter 3.2.2. It may be seen that there is a zone of higher concentration just below the suspension surface, which has not been noticed in other references on sedimentation. There is no explanation for this provided by the authors but a possible cause was indicated by others (Skopek and McRoberts, 1997) in microbial activity and gas (methane) production within the suspension layer.

At the end of a most recent paper (Suthaker et al. 1997), the authors point out the importance of the thixotropy of the fine tailings and its considerable creep properties (the consequences of a developed structural network of solids in the suspension, Tang et al. 1997), and the effect of residual bitumen on the hydraulic property (Suthaker and Scott, 1995).

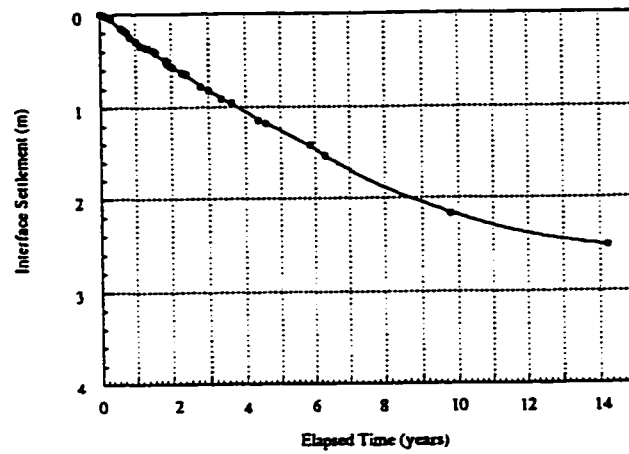


Figure 2.13.a University of Alberta 10 m standpipe tests on oil sand fine tailings  
Suspension settlement with time

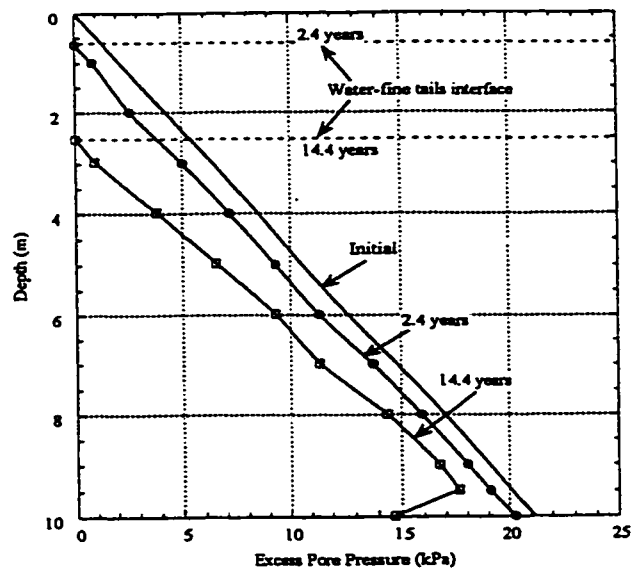


Figure 2.13.b University of Alberta 10 m standpipe tests on oil sand fine tailings  
Excess pore pressure distributions in time

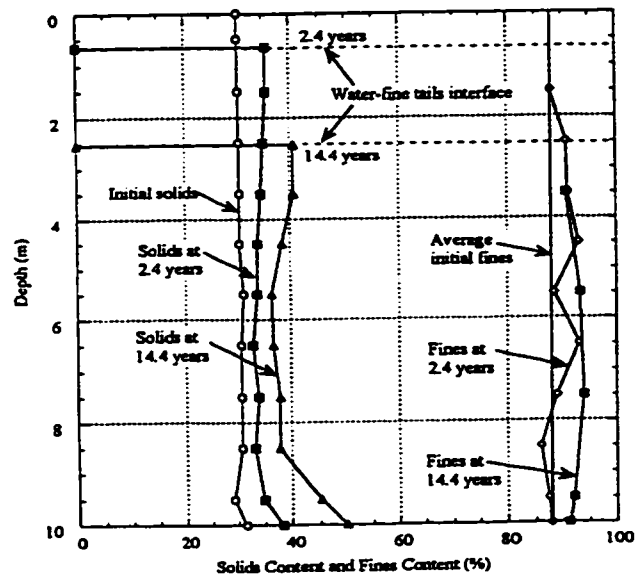


Figure 2.13.c University of Alberta 10 m standpipe tests on oil sand fine tailings  
Solids content profiles

## 2.3.2 Modelling

### 2.3.2.1 Stokes' equation

The first model to be considered is the Stokes' sphere (1851), falling steadily under gravity in a viscous fluid. Based on dynamic similarity, the total force of resistance to motion is found to be proportional to the product of viscosity  $\mu$ , velocity  $v$  and diameter  $d$ . Stokes' solution gives a force of resistance  $F$  as:

$$F = 3\pi \cdot \mu \cdot v \cdot d \quad [2.4]$$

The force  $F$  must be in equilibrium with the buoyant weight of the sphere, so that:

$$3\pi \cdot \mu \cdot v \cdot d = \frac{\pi}{6} \cdot (G_s - 1) \cdot \gamma_w \cdot d^3 \quad [2.5]$$

where  $\gamma_s = G_s \gamma_w$  is the weight of a unit volume of the solid material of the sphere and  $\gamma_w$  is the weight of a unit volume of the water. The free-fall velocity of a single spherical particle in an infinite fluid is thus:

$$v_{Stokes} = \frac{(\gamma_s - \gamma_w) \cdot d^2}{18\mu} = \frac{(G_s - 1)\gamma_w d^2}{18\mu} \quad [2.6]$$

Stokes' velocity is dependent on the specific gravity and the size of the particle and the viscosity of the liquid. For a given material and a fluid, however, it depends only on the size of the particle and is constant with time.

This calculation is only appropriate for small Reynolds' numbers (laminar flow) with the limiting value commonly adopted as  $Re \leq 1$ . According to Krumbein and Pettitjohn (Schofield and Wroth, 1968) the calculation gives close estimates for spherical quartz particles settling in water provided the particle diameters are less than 0.05 mm. Krumbein and Pettitjohn also suggest that the calculation continues to hold until particle diameters become less than 0.0001 mm (0.1  $\mu\text{m}$ ), despite the effect of Brownian motion at that diameter.

The Stokes' model finds its application in the sedimentary analysis. The range of applicability for grains between 0.05 mm and 0.0001 mm in diameter makes the sedimentary analysis technique particularly useful in sorting the particles of silt and clay sizes. The suspensions used in the sedimentary analysis are very dilute: solids content  $s$  (concentration by weight) is generally about 0.02, i.e. void ratio  $e$  is about 100.

In the sedimentary analysis the suspension becomes thinner with time due to segregation, and the settlement of suspension (i.e., the suspension-water interface<sup>\*</sup>) is governed by the smallest particles. Since it is usually difficult to identify this interface

---

<sup>\*</sup> The "settlement of the suspension" and the "settlement of the suspension-water interface" are used as equivalent terms in this text.

visually, the main property of a suspension is its density which is measured by a hydrometer in regular intervals.

Typical particles of silt and clay are not smooth and spherical in shape, nor does each separate particle have the same value of the specific density  $G_s$  as determined from the aggregated particles in bulk.

The above-mentioned are all limitations to the use of Stokes' formula in the analysis of a real sedimentation problem. Nevertheless, early work on the sedimentation of concentrated suspensions, undergoing hindered settling, was based on empirical and theoretical equations which relate the settling velocity  $v_s$  of the suspension to the Stokes velocity of a single particle having some "representative" diameter and to the system porosity  $n$ . This may be briefly described as the "Stokes + concentration" approach.

### 2.3.2.2 "Stokes + concentration" approach

The earliest published works date back to the beginning of the century: Einstein (1911), Smoluchowski and others (cited by Kynch, 1952). They derived formulas for the sedimentation velocity when the density of a suspension is very small and the distance of particles is much greater than their size (dilute suspensions).

A typical formula for a dilute suspension states that the speed of particle fall is:

$$v = u(1 - \alpha \cdot c) \quad [2.7]$$

where  $\alpha = 2.5$  for hard spheres,  $u$  is the Stokes velocity, and  $c$  is the volume concentration.

The coefficient  $\alpha$  should be greater than 2.5 for irregular particles (normal soils) because the settling speed of these particles is less than for spheres.

This formula sets up the upper limit to the volumetric concentration  $c$  and for spherical particles it is :

$$c_{\max} = \frac{1}{\alpha} = \frac{1}{2.5} = 0.4 \quad [2.8]$$

while for non-spherical particles (real soils)  $c_{\max}$  should be less than 0.4. This limiting concentration generally applies to a non-colloidal suspension of inert particles.

In early investigations of mixtures of inert particles (non-colloidal particles, i.e. no particle surface activity) a fair fit with experimental data was provided by a power function of the porosity  $n$ :

$$v = v_{Stokes} n^{\alpha} = v_{Stokes} (1 - c)^{\alpha} \quad [2.9]$$

Using dimensional analysis Richardson and Zaki (1954) suggested that  $\alpha$  depends on the Reynolds' number:

$$R = \frac{v_{Stokes} \cdot d}{\mu} \quad [2.10]$$

where  $d$  is the diameter of the particles and  $\mu$  is the kinematic viscosity of the fluid. Based on extensive experimental work on the sedimentation and fluidization the authors found that for low Reynolds numbers  $Re \leq 1$  the value of  $\alpha$  may be taken as  $\alpha = 4.65$ . However, the exponent  $\alpha$  in the above equation varies noticeably for various mixtures, as many researchers found it. For example, McRoberts and Nixon (1976) observed that for sedimentation of natural silty materials, the exponent  $\alpha$  ranged from 5 to 30 in their experiments.

It should be remarked that the Richardson and Zaki's formula may be used in a reverse manner as a best fit equation in an optimization procedure. It may be introduced in any convenient model as a settling velocity function for solid particles and the parameters,  $v_{Stokes}$  and  $\alpha$ , may be varied until the best matching with measured (experimental or observational) data is obtained. In such a case,  $v_{Stokes}$  is simply an optimization variable and there is no need to try to link it to any property of real solid grains. All the relevant properties that actually determine the value of  $v_{Stokes}$  are already encompassed in the optimization procedure.

### 2.3.2.3 Kynch's theory (1952)

This theory is the first attempt to solve a sedimentation problem when the density of particles in a suspension is great. It is based on the single main assumption that at any point in a dispersion the velocity of fall of a particle depends only on the local concentration of particles (Kynch, 1952). The settling process is then determined entirely from a continuity equation, without knowing the details of the forces acting on the particles, as a difference from the Stokes equation and its modifications.

The only equation in Kynch's theory is the continuity condition for solid particles:

$$\frac{\partial \rho}{\partial t} = -\frac{\partial S}{\partial x} = -\frac{\partial(\rho v)}{\partial x} \quad [2.11]$$

where:  $\rho$  is the volumetric concentration of solids,  $v$  is the velocity of fall of solid particles, and  $S = \rho v$  is the volumetric flux of solids. Kynch actually defines  $\rho$  as the number of particles per unit volume of the suspension which, since the particles are assumed all with the same size and shape, is equivalent to their volume fraction.

Introducing now the assumption that the velocity of a falling particle is a unique function of the concentration:

$$v = v(\rho) \quad \Rightarrow \quad S = S(\rho) \quad [2.12]$$

Kynch obtained a first order partial differential equation describing the settling behaviour of the particles:

$$\frac{\partial \rho}{\partial t} + \frac{\partial(\rho v)}{\partial x} = \frac{\partial \rho}{\partial t} + \frac{d(\rho v)}{d\rho} \cdot \frac{\partial \rho}{\partial x} = \frac{\partial \rho}{\partial t} + V(\rho) \cdot \frac{\partial \rho}{\partial x} = 0 \quad [2.13]$$

The properties of this equation are determined by  $V(\rho)$ , i.e. the form of the sedimentation flux curve  $S(\rho) = \rho v$ . The solution of this equation, using the method of



characteristics for hyperbolic partial differential equations, is some function of  $(x - V t)$  or:

$$\rho = f(x - V t) \quad [2.14]$$

where  $V(\rho)$  is some decreasing function of the concentration. When  $V$  is constant,  $(x - V t)$  is constant and  $\rho$  is constant in turn. Therefore, a characteristic line on which

$$x = V t + x_0 \quad [2.15]$$

is a straight line in the  $(x, t)$ -plane. Both the concentration and the flux rate are constant along a characteristic. Kynch shows how a solution to the sedimentation problem may be obtained using the net of characteristic lines in the  $(x, t)$ -plane, as illustrated in Figure 2.14.

Characteristics do not intersect in the regions where density continuously changes. However, in a case of singularity in the initial or boundary data the characteristic passing through such a point is a discontinuity and there is a sudden finite change of concentration across the characteristic. Kynch calls this “a discontinuity of the first kind”. There are at least two such discontinuities in his solution: the clear fluid - suspension interface (line ABCD in Figure 2.14) and the sediment - suspension interface (line OC). The differential continuity equation no longer applies along them. It has to be replaced by a so called “jump condition” which is actually an algebraic continuity condition across a discontinuity.

In deriving his theory Kynch did not consider the sediment: all his characteristics in the second falling rate zone (the one in which the influence of sediment layer appears - the non-linear portion BC in Figure 2.14) start from the origin. The sediment layer is regarded as incompressible with the density fixed at  $\rho_m$ : from OC to the right in Figure 2.14 all the characteristics are parallel with the same slope  $\rho = \rho_m$ .

Kynch has shown that his theory can predict the variation of the velocity of fall of the particles with the density of a particular dispersion using only the data on the motion of the suspension surface and the initial distribution of the particles. In simple words, one common sedimentation test is sufficient for predicting the behaviour of the same dispersion having an arbitrary concentration. The settling velocity against concentration curve deduced by this theory from a single experiment is a property of that particular dispersion. This is significant advantage over Coe and Clevenger's method, which require a series of sedimentation tests.

Despite the apparent simplicity of this theory, a variety of behaviour (modes of sedimentation) is possible depending entirely on the form of a solids flux curve, and an initial spatial distribution of the density. Figure 2.15 is reproduced from Auzerais et al. (1988) and shows a usual shape of a solids flux curve.

Three essentially different types of behaviour may be identified. In the first region of low initial concentration ( $0 < \phi_0 < \phi_a$ ) the suspension of constant concentration falls with constant speed to meet with the rising sediment and a discontinuity forms at their interface. In the second region in Figure 2.15 ( $\phi_a < \phi < \phi_b$ ) a zone of continuously varying concentration appears between the uniform suspension and the sediment. The

speed of fall of this zone decreases with time. A discontinuity is again formed between this zone and the sediment. The third region of high initial concentration ( $\phi_b < \phi < \phi_m$ ) resembles the second, only a discontinuity develops between the zone of varying concentration and the uniform suspension above it. The distinction between the first type of behaviour and the other two, as remarked by Auzerais et al. (1988) is analogous to Coe and Clevenger's distinction between the two types of settling (Chapter 2.3.1.1).

Kynch was a mathematician and he was aware of the difficulties in solving his equation in general terms; he did not even try to solve it numerically as well (although one must admit that it might not be possible at all at that time, without digital computing machines). For example, neglecting the sediment in his analysis actually means neglecting the boundary conditions on one side of the spatial domain in solving a partial differential equation in one dimension. Since the boundary conditions on the other side (the suspension surface) have already been accounted for, that would lead to a redundancy in boundary conditions and the solution would not be unique, if attainable at all.

Kynch tried to obtain an engineering solution, applicable in practice. Actually, he simplified it to a graphical method and the use of only one graph - the settlement versus time diagram. His derivation is sometimes vague and abundant in convenient assumptions. Some of them are listed in his conclusions:

- the initial concentration increases toward the bottom of the suspension,
- the settling velocity is a unique function of the local particle density,
- the settling velocity  $v$  tends to zero as  $\rho$  tends to the sediment density  $\rho_m$ ,
- the particles are of the same size and shape, etc.

and gives very correct comments on: their influence on the solution, the possibilities to overcome them in real analyses and likely ways to remove them in further research.

Because of neglecting the effect of sediment in the analysis, Kynch's method is applicable only in the first, linear settling region and, possibly, as an approximation in the initial part of the second, non-linear settling region.

According to the method of characteristics, taking the suspension settlement as linear means assuming the concentration jump constant across the water-suspension interface. Since the concentration in the clear water is constant (zero), that further implies that the concentration in the suspension is constant throughout the sedimentation. This was later adopted as the main characteristic of this method, even though the author himself has shown wider capabilities of the theory.

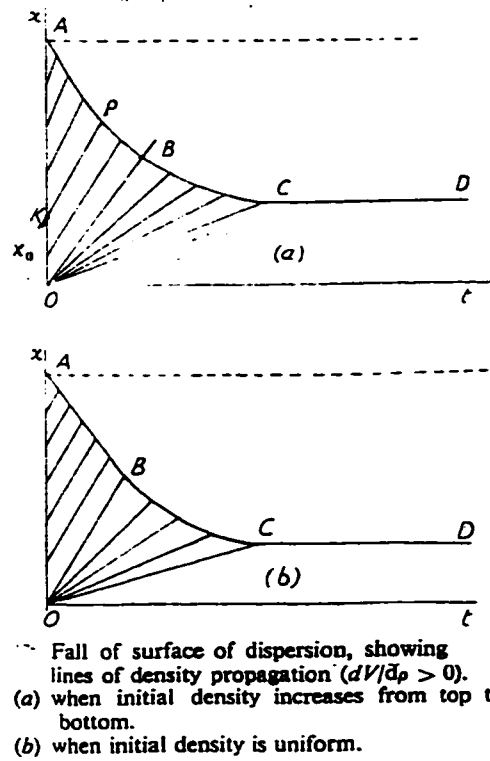


Figure 2.14 Kynch method (1952), the height of suspension surface versus time diagram

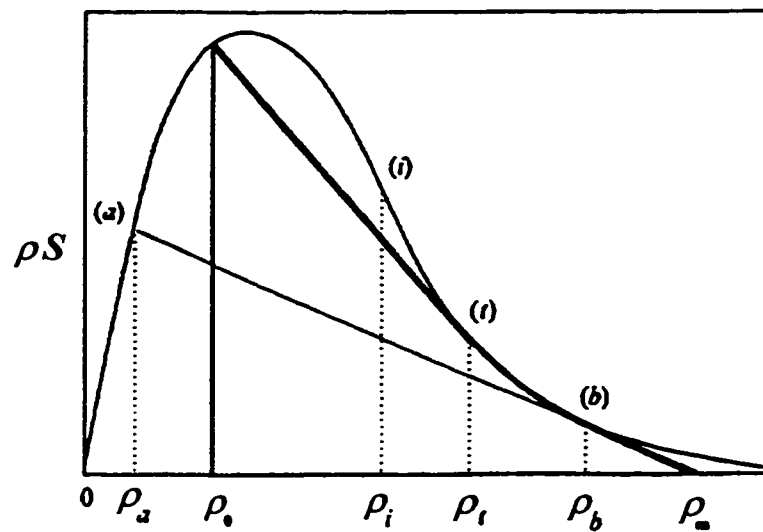


Figure 2.15 Three types of settling behaviour, depending on the shape of the flux curve and the initial solids concentration (Auzerais et al. 1988)

### 2.3.2.4 Tiller (1981)

Tiller's critics of Kynch's theory is based on the omission of the rising sediment effect on the settling behaviour of the suspension.

Tiller starts by dividing a typical batch sedimentation process, shown in Figure 2.16, into three periods, depending upon the positions of the upper and lower phase boundaries. He calls these periods: the constant rate, the first and the second falling rate period. The constant rate period ends when the upper phase boundary ceases to fall linearly (portion  $H_0A$  in Figure 2.16). Point A marks the intersection of the upper phase boundary and the characteristic emanating from the bottom of the container. The first falling rate period AB ends when the upper and lower phase boundaries merge and, at that moment, all the particles are incorporated in the sediment. This is actually the end of sedimentation. The second falling rate period "involves squeezing of liquid out of the sediment under the force of the buoyed weight of solids", i.e. that is already a consolidation in geotechnical terms. "When the cake structure carries the entire weight of particulates, liquid pressure gradients attain a null state and no further compression occurs." This is just the geotechnical explanation of the primary consolidation.

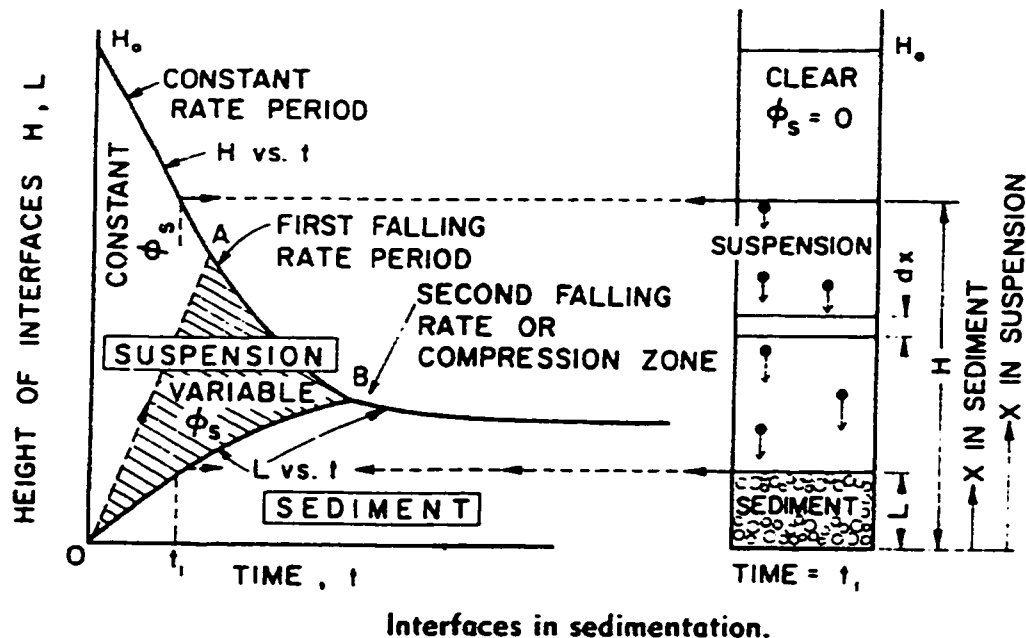


Figure 2.16 Three periods of a batch settling process after Tiller (1981)

The Kynch procedure involves fundamental errors as it does not take the rising sediment into proper account, says Tiller. Kynch assumed that the characteristics ( $x - Vt$ ) emanated from the origin of coordinates (the bottom of the column in Figure 2.16) during the first falling rate period. They actually originate at the surface of the rising sediment where the upward liquid velocity affects the rate of fall of the particles. Without going

into details of his derivation, Tiller obtained his solution based on the assumption that the characteristics emanate from the surface of the rising sediment. For the sediment, he used the continuity conditions both for the solids and the water phase, and “the equation of motion neglecting inertial effects” (i.e. the equilibrium equation) in which he balanced the effective pressure with the buoyant weight and the “upward friction due to the liquid flow” (i.e. the drag force of the fluid). The latter was expressed as related to the Darcy’s law, i.e. the permeability. Solving a non-linear partial differential equation of the second order that he obtained required the constitutive relations relating the porosity and permeability to the effective stress. In the first falling rate period, the sediment equation was coupled with the suspension equation using boundary conditions at the surface of the sediment, i.e. equating solids fluxes at the two sides.

Tiller’s procedure assumes that the positions of both phase boundaries are known functions of time. His equations can be solved in an implicit way only, following a graphical procedure similar to the one by Kynch, but it does not provide straightforward way to obtain flux curves from the data as in Kynch’s procedure. And finally, if the sediment height is assumed to be zero (which is equivalent to adopting infinite sediment density) the procedure proposed by Tiller reduces to the Kynch method.

#### **2.3.2.5 Auzerai, Jackson and Russel (1988)**

Since its publication there was a much discussion about Kynch’s ideas of selecting the physically correct solution in cases when there is more than one formal solution of the mathematical problem, namely when discontinuities or “shocks” appear. The main question was the conditions that have to be satisfied for a discontinuity to emerge within the suspension zone. Dixon (1977) was the first to point out the importance of inertial effects which, although commonly omitted in derivation, must not be neglected across the true discontinuity. “There the jump in momentum flux, which accompanies the jump in concentration, must be balanced by a corresponding jump in stress transmitted through the particle phase” (i.e. the effective stress). Dixon’s conclusion was that a shock can never separate two regions of free settling, which makes some of Kynch’s solutions inadmissible (for example, the one in which a discontinuity appears between the region of constant concentration and the region of varying concentration in the suspension). This treatise then raised the question of consistency of a range of systems and initial conditions encountered in practice. Auzerai, Jackson and Russel discussed this problem and resolved the conditions for appearance of discontinuities and the influence of compressible sediments in the settling process.

This derivation is rather lengthy and only important details will be presented here. The treatment starts with the complete equations of motion for both fluid and solid phases, including all the active forces, i.e. beside gravity, viscous (hydrodynamic) forces and interparticle stress, there are inertial forces too. The drag force exerted on solids by the fluid motion is assumed to be dependent on the solid concentration and the relative velocity between the phases. After specializing the equations for the sedimentation problem (the total average flux in the system vanishes) the authors obtained a theory of sedimentation comprising continuity and momentum balance equations. Next they examined the conditions for existence of shocks. They derived the so called “inner

solutions” for the regions of rapid variation of the parameters and related them to the “outer solutions”, valid for the regions of slow variation of the parameters, to obtain the jump conditions across the shocks. Beside the two usual discontinuities at the phase boundaries they found out that shocks within the suspension are possible: a compression shock, when concentration increases on moving down through the shock, and a rarefaction shock, when concentration decreases downward. These discontinuities depend on the shape of the settling velocity curve and the initial concentration.

The complete solution of the sedimentation problem for an initially uniform suspension of any concentration, making use of Kynch’s theory and shock conditions, is presented as an example in Figure 2.17. The suspension concentration is designated as  $\phi$  and the particle velocity as  $U$ . The transition from a suspension to a sediment (namely, the initial sediment concentration) is  $\phi_m$ . The point of inflexion of the flux curve is at  $\phi_i$ . The tangent from  $\phi_m$  touches the flux curve at  $\phi_b$ .

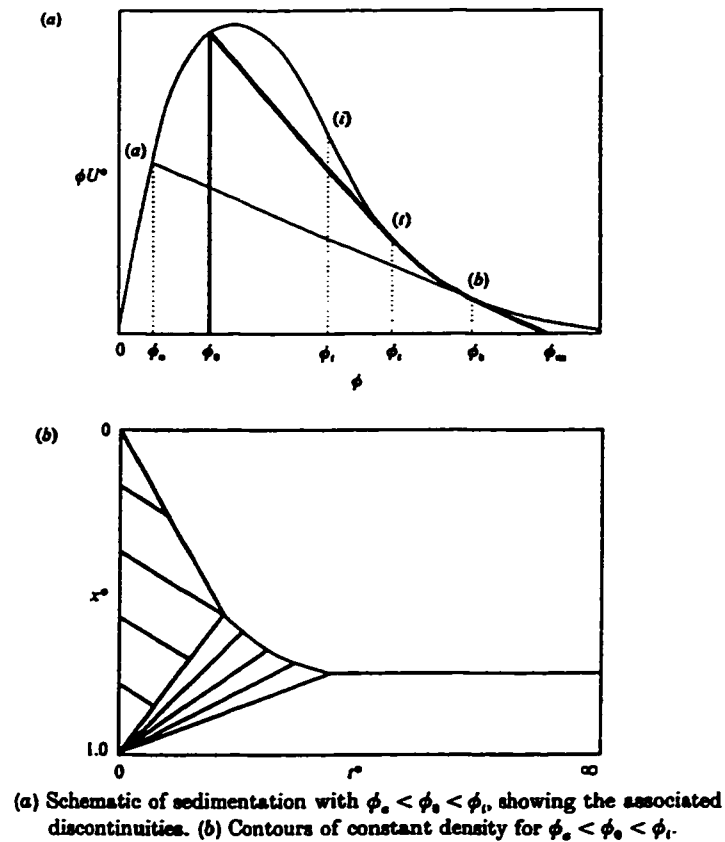


Figure 2.17 Complete solution for an initially uniform suspension using Kynch theory and shock conditions (Auzerais et al. 1988)

If the initial concentration  $\phi_0$  falls within the regions  $0 < \phi_0 < \phi_a$  and  $\phi_b < \phi_0 < \phi_m$  a direct jump from the concentration  $\phi_0$  to the concentration  $\phi_m$  is possible, the sediment surface is the only shock and the rate of suspension settlement is constant and equal to  $U(\phi_0)$ .

When  $\phi_i < \phi_0 < \phi_b$  there is a zone of varying concentration between the sediment and the suspension with constant concentration  $\phi_0$  and shock at the sediment surface is not permitted. In the zone of varying concentration  $\phi$  goes from  $\phi_0$  to  $\phi_b$  and then suddenly jumps to  $\phi_m$  in the sediment. The velocity of the suspension settlement slows down before all the particles settle and it is referred to as a “falling rate sedimentation” (the first falling rate region in Tiller’s method).

When  $\phi_a < \phi_0 < \phi_i$  the situation is similar to the previous one. The solution is to construct a compression shock from  $\phi_0$  to  $\phi_t$  (a point within  $\phi_i < \phi < \phi_b$  region) within the suspension and then a varying concentration zone from  $\phi_t$  to  $\phi_b$  which contacts the sediment, so that again one has a jump at the sediment surface (and another one in the suspension) and a varying concentration zone. Contours of constant density are shown in Figure 2.17.b. The authors remark that this case corresponds to what Been and Sills (1981) called a transition zone between dispersion and sediment.

The authors then presented a numerical scheme that applies only when there are no recognizable shocks. Two characteristic examples were modelled: a stable colloidal dispersion (hard spheres particles) and a flocculated suspension. These examples required specifying forms for the constitutive functions: the particle velocity  $U(\phi)$  and the compressibility  $\sigma(\phi)$ .

For the stable dispersion the authors adopted a linear  $U(\phi) = 1 - A\phi$  (Einstein, 1911) or a power law function  $U(\phi) = (1 - \phi)^p$  (Richardson and Zaki, 1954). For the compressibility in a sediment a rational function  $\sigma(\phi) = A \frac{\phi}{\phi_m - \phi}$  was chosen.

For the flocculated suspension, where a gelation phenomenon occurs at higher concentrations, the settling velocity  $U(\phi) = A\phi\kappa$  was related to the permeability  $\kappa$  which itself was defined as a rather peculiar rational function of  $\phi$  (after Brinkman’s model of porous medium as a network of spherical particles). The compressibility function was adopted similar to the previous one:  $\sigma(\phi) = \sigma_0 \frac{\phi^n}{\phi_m - \phi}$

It is interesting to cite here a few sentences from this paper which clearly illustrate rather confusing differences between the terminology used in the chemical engineering and the one used in the geotechnics, although both express the same phenomena (this was also noticed by Skopek and McRoberts, 1997).

The authors first talk about the gel structure: “The stress  $\sigma$  within a flocculated network cannot exceed the compressive yield stress. Otherwise the network collapses to a higher volume fraction capable of bearing the load.” The “compressive yield stress” should correspond to the effective stress and the “network collapse” to a deformation (void ratio change) caused by the effective stress. This should be a description of the

transition from an overconsolidated to a normally consolidated state of a soil in geotechnics. The authors then discuss the compressibility law: “This pseudo static form (the equation for  $\sigma$  cited above) for  $\sigma$  implies that the rate of consolidation is limited by the resistance to moving fluid through the network and not by the resistance to moving particles relative to each other.” The “rate of consolidation” is actually the settling velocity of particles  $U(\phi)$  which accounts for permeability changes in the suspension but not for interparticle forces since the effective stress in the suspension is zero. The second statement seems in contradiction with the first one: if there is no “the resistance of moving particles to each other” (i.e. the effective stress) then there should not be any “network collapse” (i.e. a deformation). It is not clear from the text how the authors actually calculate the “compressive yield stress”.

Several illustrations of the method are given. Figure 2.18.a presents concentration profiles for a stable suspension without shocks, Figure 2.18.b the same but for conditions with shocks. Both suspensions had initial concentration  $\phi_0 = 0.1$  chosen so that  $\phi_a < \phi_0 < \phi_i$  (the most complex case). The same is shown in Figure 2.19.a and 19.b for flocculated suspensions. The difference between cases (a) and (b) is in the ratio of gravitational forces to the compressibility (it is higher in the case *b*).

This method seems attractive from the point of view of a geotechnical user, beside the disadvantages in assumed constant concentration in the suspension and unusual constitutive laws for the permeability and compressibility versus concentration relationships. Substituting these relationships by the more common laws in the geotechnics would probably require deriving the equations from the very beginning. A comprehensive testing of presented numerical method for a stiff PDE system, which uses the second-order finite difference approximation and adjustment of the temporal step size during the calculation, would probably be required too.



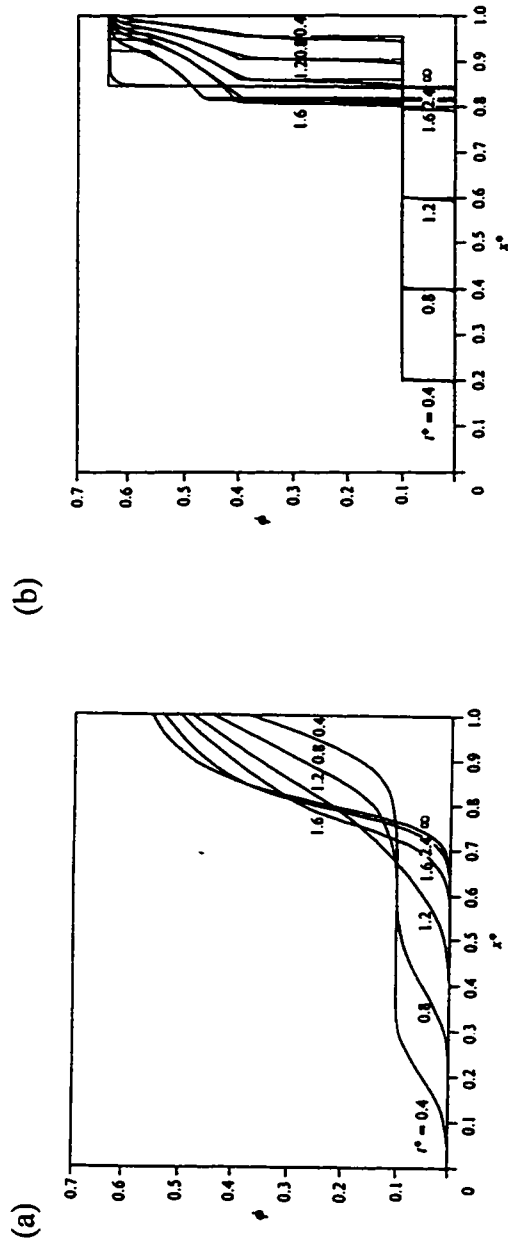


Figure 2.18 Concentration profiles for stable suspension: (a) without and (b) with shocks; initial concentration  $\phi_0 = 0.1$  chosen so that  $\phi_a < \phi_0 < \phi_i$

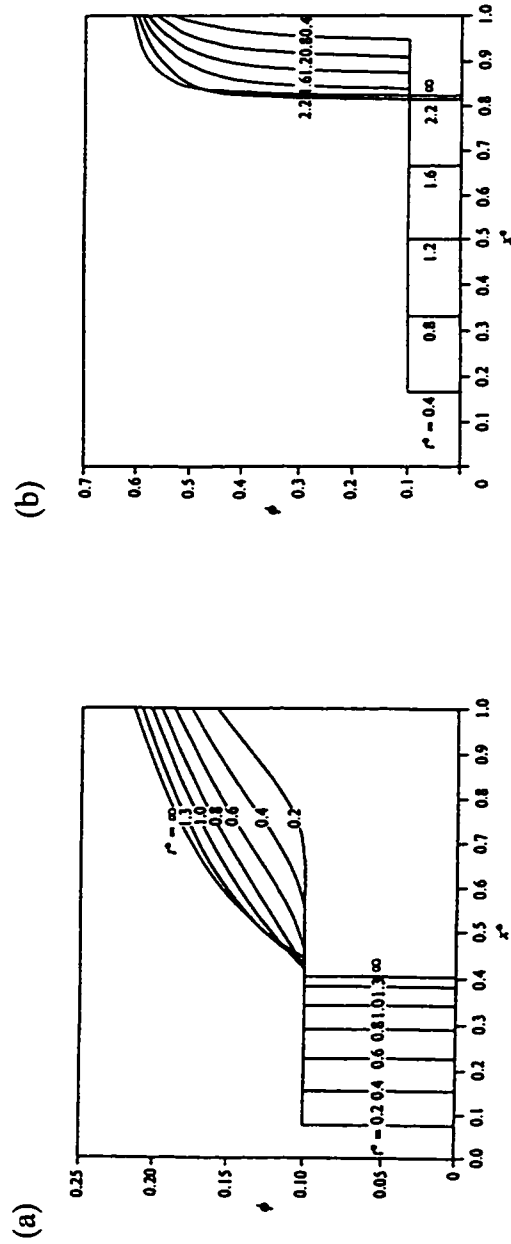


Figure 2.19 Concentration profiles for flocculated suspension: (a) without and (b) with shocks; initial concentration  $\phi_0 = 0.1$  chosen so that  $\phi_a < \phi_0 < \phi_i$

### 2.3.2.6 Diplas and Papanicolaou (1997)

This model has certain similarities with the previous ones. It integrates the two components of the zone settling behaviour, the sedimentation of solids in the suspension region and the compression of the settled material. The former is modelled by the Kynch theory, while the sediment compression is represented by a non-linear finite strain model of self weight consolidation.

A graphical procedure (similar to the one used by Tiller, described earlier in Chapter 2.3.2.4) is used to calculate the flux of solids on the top of the sediment. The governing equation for consolidation zone is a non-linear PDE of the parabolic type. The permeability of sediment is defined as a power function of effective stress (but not void ratio, as usual) after Tiller and Khatib (1984). Obtained governing equation for compression is defined in terms of effective stress as the dependent variable. It is solved using the finite element method (the weighted residual method of Petrov - Galerkin) in the spatial domain, and a finite difference scheme in the time domain. The validity of the model was checked on the attapulgate slurry problem from Tiller and Khatib (1984). Their results are presented in Figure 2.20. It can be seen from Figure 2.20.a that the method allows for increase in the suspension concentration with time.

The limitations of the model are encompassed by the assumptions:

- the settling velocity of particles in the suspension is a function of the concentration alone (Kynch),
- the isoconcentration lines are straight (Kynch),
- the inertial forces are neglected (according to Auzeais et al. (1988) the shocks are smeared),
- the flocculation period is neglected,
- the solids concentration in the suspension at the sediment surface level is not constant, but varies linearly with time; therefore, the null stress volume concentration (the transition point from suspension to soil) is not a unique value.

Although the last assumption seems a little arbitrary it agrees well with the experimental evidence; the authors refer to Been and Sills experiments (1981). A problem might rise with the parameters that define the time change of the compressibility and permeability at the sediment-suspension interface: they have to be determined from experiments.

The only input needed to use the program is a particle flux curve. It does not require prior knowledge of the interface heights, therefore it may be applied for preliminary design predictions.

(a)

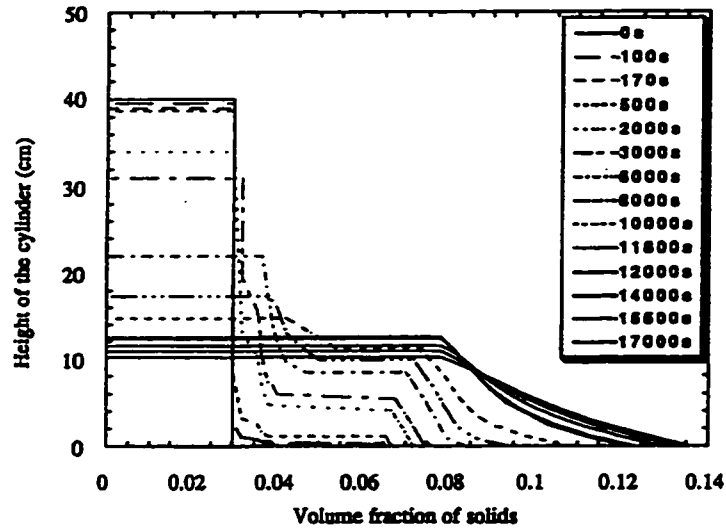


FIG. Volume Fraction of Solids Profiles throughout Cylinder Height at Several Time Instants

(b)

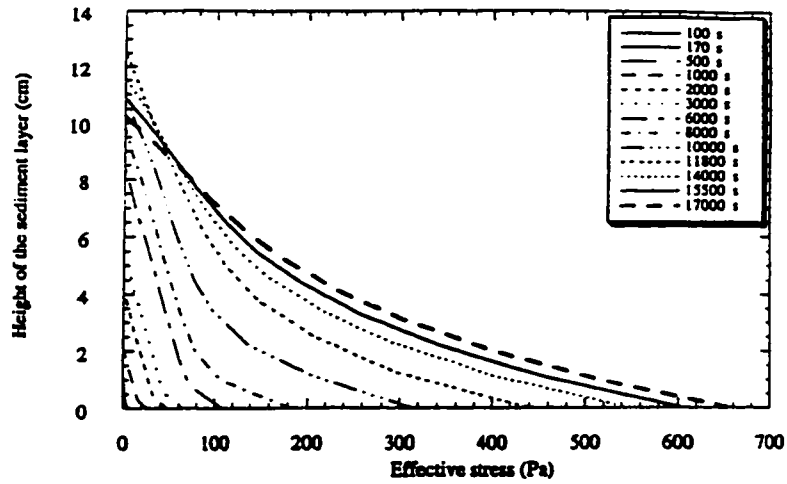


FIG. Effective Stress Distributions within Sediment Layer at Various Time Instants

Figure 2.20 Coupled sedimentation and consolidation analysis after Diplas and Papanicolaou (1997): (a) solids concentration and (b) effective stress distribution

### **2.3.2.7 Eckert et al. (1996)**

This method is another variation in coupling sedimentation and consolidation in the batch settling analysis. The theoretical basis is the method of Auzerais et al (1988). It is coupled with a centrifugation technique of Buscal and White (1987) for evaluating the parameters of the settling velocity function and the compressibility of sediment.

Skopek and McRoberts (1997) classify this method in the Fluid Dynamics Concept (FDC) models, to accentuate a difference in the approach compared with the geotechnical engineering which focuses on the bearing capability of sediments. Indeed, there is seemingly a significant difference in terminology, mentioned in the chapter on Auzerais et al. (1988) method, which can cause misunderstanding of a geotechnically trained reader. Fortunately, the authors give in the very beginning a glossary of parallel FDC and geotechnical terms and, later on, they sometimes explain the derivation using both approaches. Furthermore, they show that Gibson's Lagrangian formulation of large strain consolidation theory may be transformed into the FDC notation and, in such a case, becomes the same as the governing equation of consolidation developed by Auzerais et al. (1988). The authors also show how a permeability - void ratio relationship from the soil mechanics can be transformed to a particle settling velocity - volumetric concentration relationship used in the fluid dynamics.

The authors consider the main achievement of their method the possibility to derive the parameters of the compressibility law for sediment from a centrifuge testing, since the gravity sedimentation tests on certain materials may take many years. The centrifuge is also used for determination of the settling velocity function.

The following examples were presented to evaluate the method.

Two tests on whole and bitumen-free oil sand fine tailings were performed and later simulated by the model. The centrifuge test on bitumen-free tailings gave excellent agreement with numerical predictions (see Figure 2.21.a), while the settling tube test on whole tailings was less successfully calculated (Figure 2.21.b) probably because of the wall friction effect since the diameter of the tube was only 1 inch.

Further examples are a phosphatic clay and a copper fine tails settling experiments, taken from published literature, showing again very good agreement with the results of the numerical modelling.

The last example was Been and Sills' experiment 15 (1981), shown in Figure 2.22. A good matching with the interface boundaries motion was obtained, but the model failed to predict the increase of concentration in the suspension. This is because of the assumption of constant concentration in the suspension, made in the theory of Auzerais et al. which serves as the theoretical basis for the method. The authors theorize that a creep mechanism may be the cause of this densification of the suspension.

Assumed constancy of the suspension density is the main disadvantage of this method. It is not clear from the presented data (Figure 2.22) whether the possibility to account for shocks, elaborated by Auzerais et al. (1988), is incorporated in the model. Anyway, the limitations of the method are the same or more severe than those for the original method by Auzerais et al.

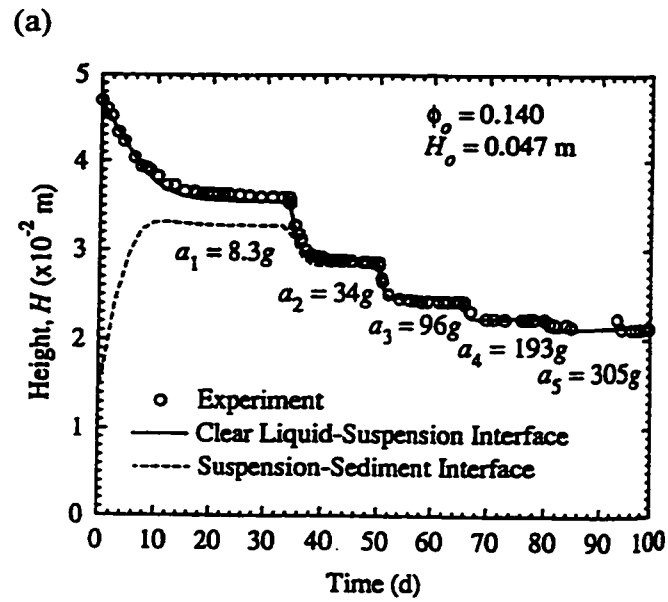


Figure . Measured suspension heights in a centrifuge vs. numerical prediction of both suspension and sediment layer heights for sample I of bitumen-free tails.

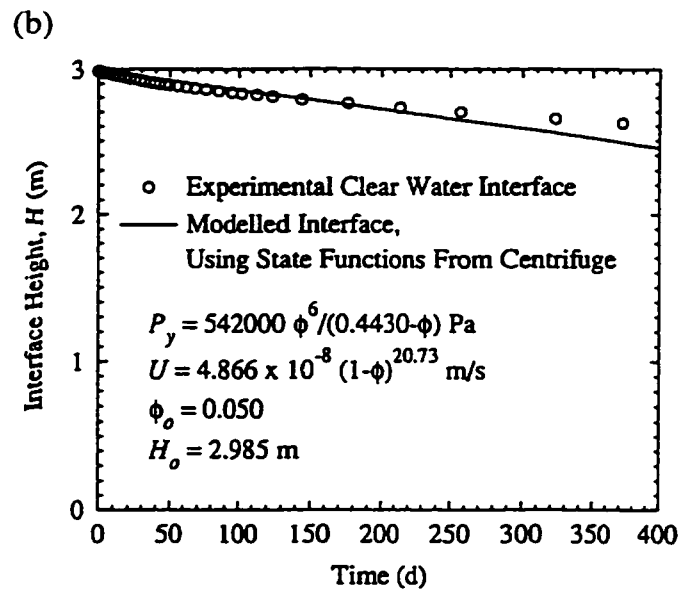
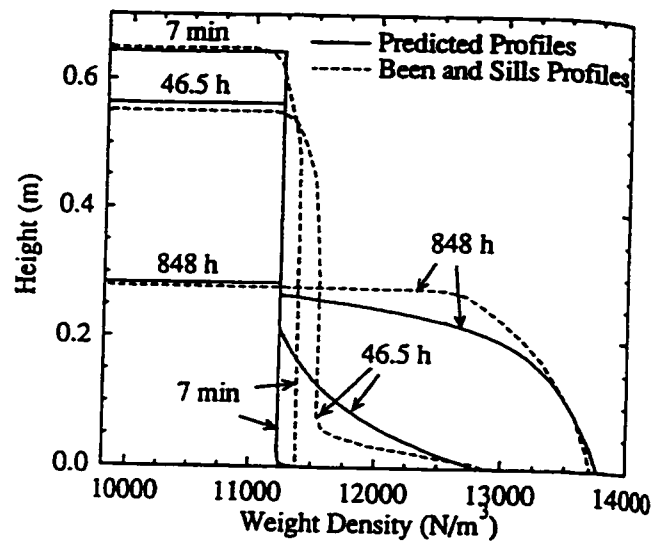


Figure . Measured height of interface in a settling tube vs. modeled height for whole fine tails.

Figure 2.21 Coupled sedimentation and consolidation after Eckert et al. (1996)  
(a) bitumen free tailings, centrifuge test  
(b) whole tailings, settling tube test



**Figure . Density profiles for a suspension of clay in water: our prediction vs. those measured in experiment #15 by Been and Sills (1981).**

**Figure 2.22 Coupled sedimentation and consolidation after Eckert et al. (1996)**

## **2.4 SELF-WEIGHT CONSOLIDATION**

### **2.4.1 Phenomenology of self-weight consolidation**

#### **2.4.1.1 Sediments of colloidal suspensions (van Olphen 1977)**

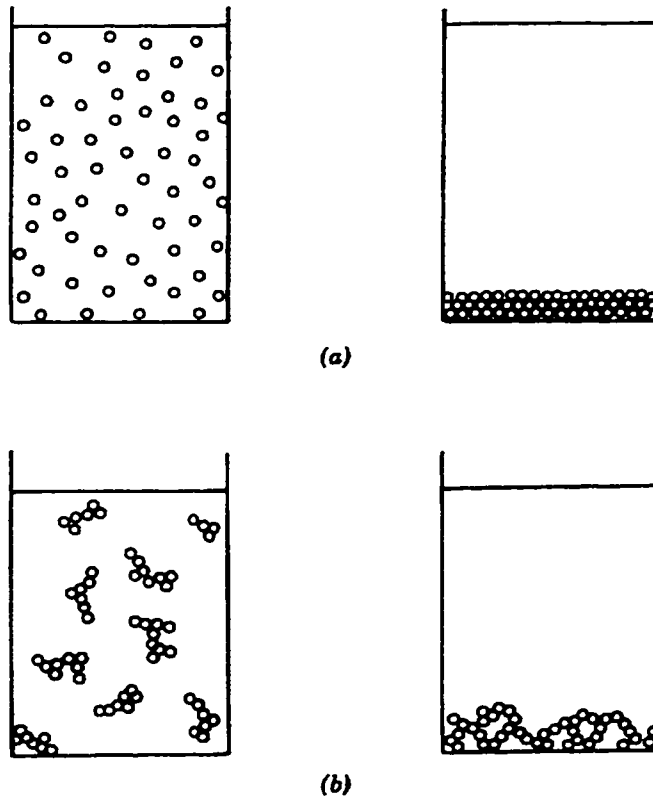
The character of the net interaction curve and the particles structure in a suspension is of major influence on the particle arrangements in the sedimented deposits. Of great importance is the difference between the structure of sediments of a flocculated and a stable suspensions. With the same initial concentration, the sediments of flocculated suspensions are usually much more voluminous than those of stable suspensions (van Olphen 1977). This somewhat paradoxical observation (having in mind that a flocculated suspension settle faster than a stable one) is easily explained.

“Individual particles of a stable suspension, when they settle at the bottom of a container, may slide and roll over each other until they reach the lowest possible position because the repulsive force prevents them from coming into direct, actual contact. On the other side, particles of a flocculated suspension, where the attractive force is dominant, ‘stick’ to each other and pile up to form a sediment with large void spaces both within and among the aggregates” (van Olphen 1977). This is illustrated in Figure 2.23. When gravity forces break the links in a settled floc some additional volume decrease will occur and this is called consolidation in the geomechanics.

#### **2.4.1.2 Sediment fabric and initial concentration in clayey sediments**

The term “fabric” refers to the arrangements of particles, particle groups and pore spaces in a soil. Particle associations in clay suspensions were discussed in Chapter 2.2.4 and the particle structures which develop in the oil sands fine tailings, particularly, in Chapter 2.2.4.1. Since it is not the intention to go into an explicit analysis of the soil fabric, only certain details that may be of interest in the consolidation modelling will be mentioned here.

Glass balls allowed to fall freely form an anisotropic assembly, with balls tending to arrange in chains. Packing arrangements of equal-sized spheres may vary in porosity from about 25 % to about 48 %, and the range of void ratios is from 0.34 to 0.91 (Mitchell 1977). The pyramidal and the tetrahedral arrangement, which appear as “natural arrangements” for stable suspensions according to van Olphen’s description in the previous chapter, are the tightest packings with the porosity of about 25 - 26 % and the void ratio of 0.34, i.e. the volumetric concentration of about 0.75. In the example in Chapter 3.2.1 a suspension of spherical glass beads of uniform size ( $67\ \mu\text{m}$  in diameter) formed a practically rigid sediment with the concentration  $c = 0.64$ , which seems a reasonable value within the above mentioned range.



Sedimentation in a peptized and in a flocculated suspension. (a) Peptized suspension; dense, close-packed sediment. (b) Flocculated suspension; loose, voluminous sediment.

Figure 2.23 Sediments of colloidal suspensions (after van Olphen, 1977)

A distribution of particle sizes will produce a tighter packing, the more so with the greater range of particle sizes. It can thus be expected that the above limits will be shifted to lower porosities (higher concentrations). This is valid for spherical particles. For natural soils (sands), however, the grain size distribution effect will be counteracted by irregular grain shapes which will increase porosity.

Clay plates and rods will make a “house of cards” type sediment. Van Olphen found that certain types of a montmorillonite can make a solids structure in suspensions with volumetric concentration as low as 2 %. Thus, transitional concentrations from suspended to sedimented state, namely initial sediment concentrations, may be very low in clays.

#### 2.4.1.3 Volume changes and the influential factors

Changes in sediment volumes may result from changes in stresses, temperature and chemical environment (Mitchell 1976). If we restrict our interest to the compression behaviour of a soil under the self weight, many of these factors will be eliminated:



- post depositional processes of physical, chemical and biological nature, such as cementation, leaching, desiccation, etc.,
- stress history effects, because of monotonic loading (the normal consolidation only ),
- partial saturation (always fully saturated),
- temperature, as changes are usually negligible in underwater conditions,
- pore water chemistry, etc.

We will also assume that the secondary compression, which involves a time-dependent adjustment of the soil structure and may be actually considered as a creep deformation of interparticle contacts, is not of sufficient importance in the self weight consolidation due to a relatively small contribution to the total settlement of the suspension. Therefore, self weight consolidation is treated as primary consolidation only.

In this way, the effect of stress, or the compressibility, remains as a main factor. Since the primary consolidation is controlled by the rate of dissipation of excess pore water pressure, the permeability appears as another important influence.

Quantification of compressibility and permeability laws for soft soils with high void ratios and in the range of very low effective stresses is a very difficult experimental task. The problems, solutions and results will be illustrated by the example of the oil sand fine tailings testing.

#### **2.4.1.4 Compressibility and permeability testing of the oil sands fine tailings**

The standard oedometer test is developed for small-strain consolidation problems common in the foundation engineering. In this test, constant load increments are applied to the sample and the settlement is observed in time. Terzaghi's small strain theory of consolidation is generally adopted as the interpretation tool for this test. The relationship between effective stress and void ratio is obtained as a direct result of the testing and then, using the theory and the coefficient of consolidation, the permeability may be determined in an indirect way.

A necessary assumption for application of Terzaghi's theory and its derivatives is the constancy of these parameters during the load increment. It is not the case with highly compressible soils which undergo large deformations during consolidation.

The permeability-void ratio relationship may be obtained by a direct laboratory measurement using several methods, see for example Suthaker (1995). In the case of a highly compressible material, they all suffer from the problem of a large variation of effective stress within the sample, resulting volume changes and varying permeability in turn. Decreasing hydraulic gradient or controlling fluid flow requires very accurate measurements, very sophisticated equipment and very long duration of the testing. Several procedures have been developed in an attempt to avoid or reduce the problems associated with the above factors, involving as a rule an inversion of a complex finite strain consolidation theory. The usefulness of these procedures is therefore dependent on the assumptions used in their derivation. Many authors still prefer to obtain the coefficient of permeability in a direct manner.

### *Slurry consolidometer*

Two significant experimental difficulties thus appear in the case of fine tailings: the large strain and the seepage forces. The slurry consolidometer has been developed to allow for large deformations during consolidation and to allow a direct permeability test to be performed on the sample at different void ratios during the consolidation. The instrument which is in use at the University of Alberta is shown in Figure 2.24 (from Suthaker, 1995). Its advantages are: the simplicity in testing procedure, apparatus and evaluation of the test data. The disadvantage is in the long duration of the test.

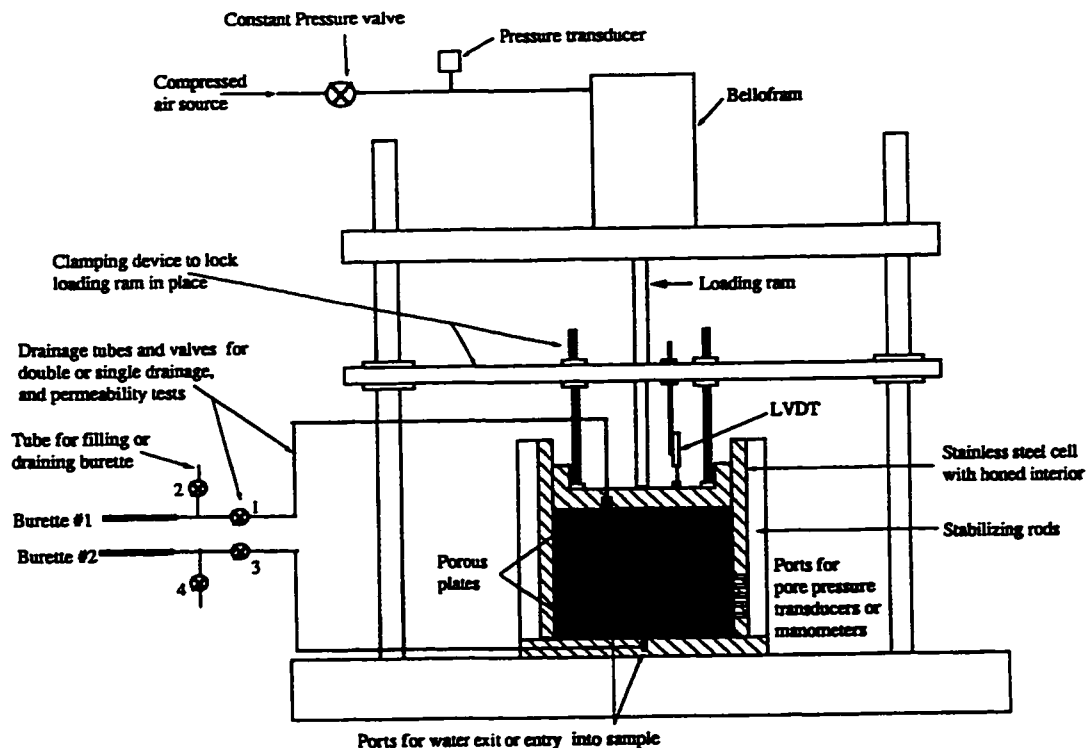


Figure 2.24 Slurry consolidometer at the University of Alberta (Suthaker 1995)

A step loading procedure similar to a standard oedometer test is employed in the compressibility portion of the test. For permeability testing, a constant head technique is employed because it allows extremely small gradients during the test and the monitoring of flow rate with time. The danger of additional consolidation of a slurry appears when the seepage forces during the permeability testing causes the effective stress which are greater than the stress under which the sample was previously consolidated. This problem is overcome by a clamping system which prevents any change of the sample volume during the permeability testing. The upward hydraulic gradient is applied to the sample, up to a value where the induced seepage stress is equivalent to the previously applied consolidation pressure.

Oil sand fine tailings with three different initial solids contents - 20%, 25% and 30% - were tested, see Pollock (1988) and Suthaker (1995). Liquid and plastic limits were approximately 59% and 23%, respectively, and the bitumen content by mass 3% of the mineral solids. Other properties are presented in more detail in Chapter 3.2.2.2. The applied stress increments during the consolidation were equal to the previously applied stress. Both consolidation and permeability test lasted for 2 years.

### *Test results*

Figure 2.25 shows the compressibility of the fine tailings (Suthaker 1995). It is obvious from this figure that the effect of initial void ratio is substantial in the low effective stress range up to about 100 kPa where the three distinct curves merge. The usual interpretation of the obtained compressibility curves in the soil mechanics would appeal to the overconsolidation: in the recompression range overconsolidated soils follow different void ratio-effective stress relationships until they reach the virgin compression line. Since the fine tailings are underconsolidated all the time, they should follow the virgin compression line irrespective of the initial void ratio. Therefore, concludes Suthaker, aging changes the microstructure of the tailings and, so, a time-dependent factor has to be taken into account which connect the individual void ratio-effective stress relationships. This "time dependent factor" has not been further elaborated, although it may be thought of as the thixotropic strength gain, with further testing being reported by the author.

The measured flow velocities during the permeability testing were not constant, but decreased with time. A typical flow velocity diagram with time is shown in Figure 2.26.

The time to reach the steady state varied between 30 minutes and 15 hours, increasing with the void ratio and decreasing with the hydraulic gradient. The ratio of an initial flow velocity to a steady state velocity varied between 400 and 20 for void ratios from around 6 to about 1.5, respectively. The repeatability of this behaviour was excellent and it only took 5 to 10 minutes for the tested material to return to the original state. The explanation given by Suthaker seems correct and finds the main cause in the internal mobility of fines (and the time dependent deformation of the residual bitumen too, but to a lesser extent). Since the upward seepage stress was much less than the downward gravity stress, it took a long time for the particles to move upward under the seepage stress and much less to return to their original position under gravity.

Suthaker also found that the permeability of fine tailings depends on the hydraulic gradient, as opposed to Darcy's law. As the gradient increases, the permeability of the fine tailings decreases at any given void ratio. This effect was found small for void ratios less than 1. Also, when tested under hydraulic gradients less than 0.2, all the samples gave similar values for the permeability. The fact that hydraulic conductivity at low gradients was the same before and after higher gradients were applied to the sample indicated a recoverable mechanism and eliminated the mobility of fines as a possible cause. The deformation of residual bitumen was therefore directly related to the applied hydraulic gradient. This was checked by testing the samples of tailings with the bitumen removed. The results showed that the permeability of bitumen-free samples was an upper bound for the permeability of the tailings and that it was independent of the hydraulic gradient.

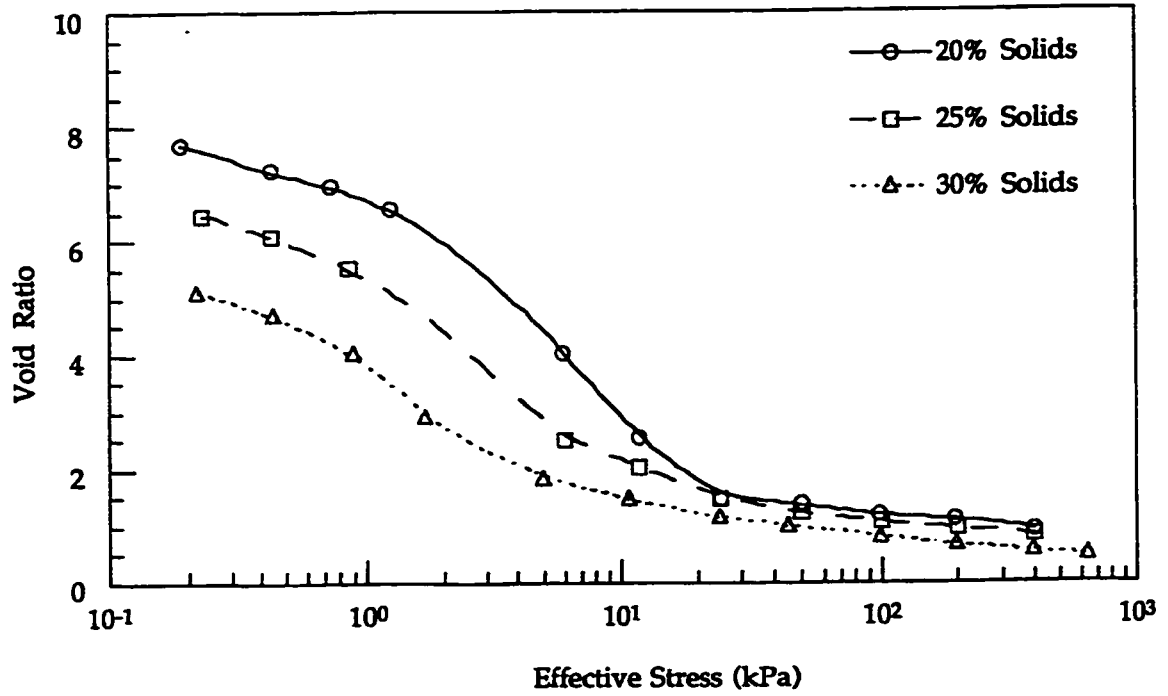


Figure 2.25 Compressibility of oil sand fine tailings for various solids contents (Suthaker 1995)

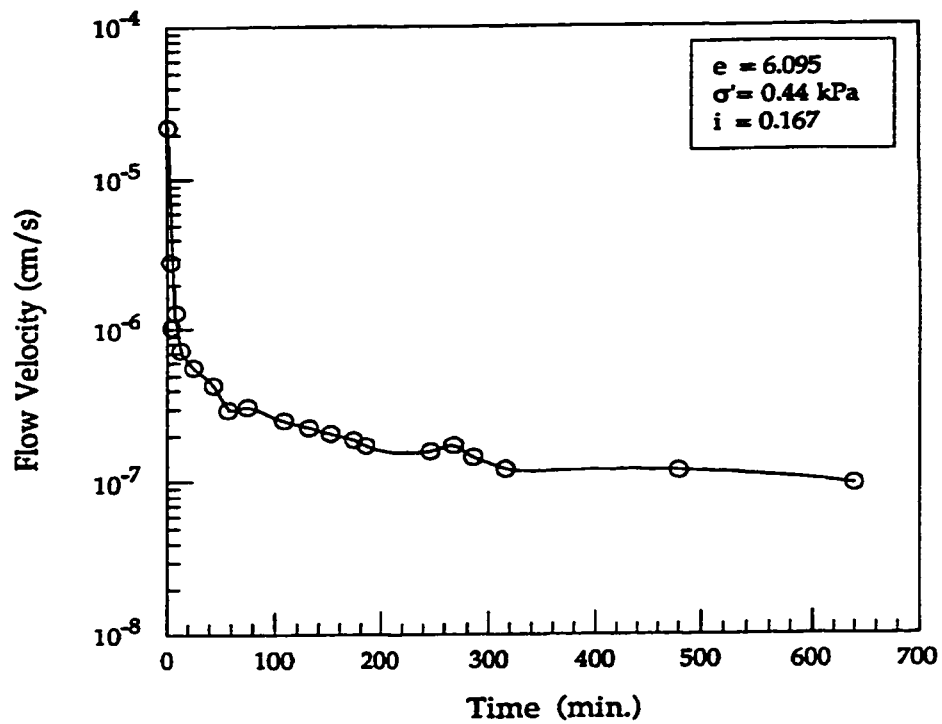


Figure 2.26 Variation of flow velocity with time in the permeability testing (Suthaker 1995)

It was also found by Suthaker that, unlike the compressibility, the permeability does not appear to be influenced by the initial void ratio. It was then suggested, without more precise indications, that “different micropore structures control the permeability and the compressibility of fine tailings”.

Suthaker then uses her tests and the results of Pollock (1988) and Bromwell Engineering Inc. (1983) to express the permeability as a power function of the void ratio. Her best-fit function (see Figure 2.27.a) is determined as:

$$k(e) = 6.16 \cdot 10^{-9} e^{4.468} \left[ \frac{cm}{s} \right] \quad [2.15]$$

Pollock’s best fitting function for the fine tailings with 30% of solids content differs, however, from Suthaker data (see Figure 2.27.b):

$$k(e) = 7.425 \cdot 10^{-9} e^{3.847} \left[ \frac{cm}{s} \right] \quad [2.16]$$

The compressibility function for tailings is defined again in a power law form. However, since it is dependent on the initial concentration, separate functions have to be defined for each initial solids content (Figure 2.28.a). The best fit function for the material with 30% solids content was determined by Pollock (1988), see Figure 2.28.b:

$$e = 29.04 \sigma'^{-0.3118} \left[ Pa^{-1} \right] \quad [2.17]$$

It was remarked by Suthaker that the above model does not incorporate the thixotropic behaviour (Suthaker and Scott, 1995) or the creep behaviour of tailings (Suthaker and Scott, 1995).

These properties were also investigated by Suthaker (1995). Very briefly, the following conclusions were derived by the author.

Long term strength in slurries can originate either from thixotropy\* or consolidation. The oil sands fine tailings exhibits higher thixotropic gain in strength than typical clays. It increases quadratically with age. The thixotropy is highly dependent on the water content: the lower the water content, the higher the thixotropic strength (in absolute value). But the thixotropic strength ratio (as a relative measure) increases with an increase in water content. The thixotropic strength may be affected by self weight consolidation, because the particle shearing resulting from consolidation reduces the bonding produced by thixotropy. In general, the higher the rate of consolidation, the smaller the thixotropic strength gain.

---

\* The “thixotropy” is the phenomenon of isothermal reversible gel-sol (solid-liquid) transformation in colloidal suspensions due to mechanical agitation. In geotechnics, it is defined as a process of softening caused by remoulding, followed by a time-dependent return to the original harder state at a constant water content and a constant porosity.

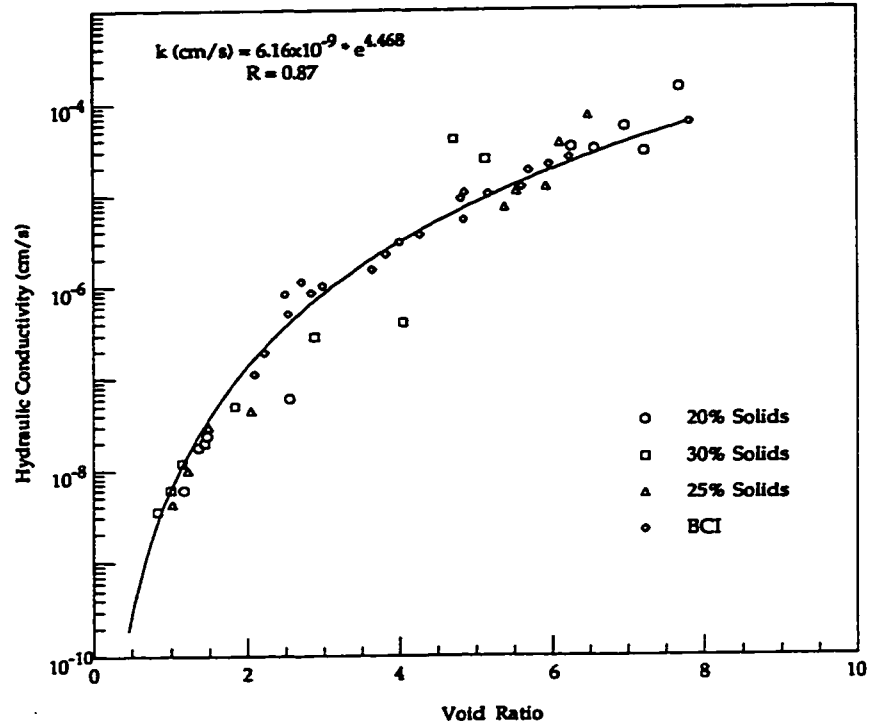


Figure 2.27.a Permeability of oil sand fine tailings - Suthaker's best-fit function (Suthaker 1995)

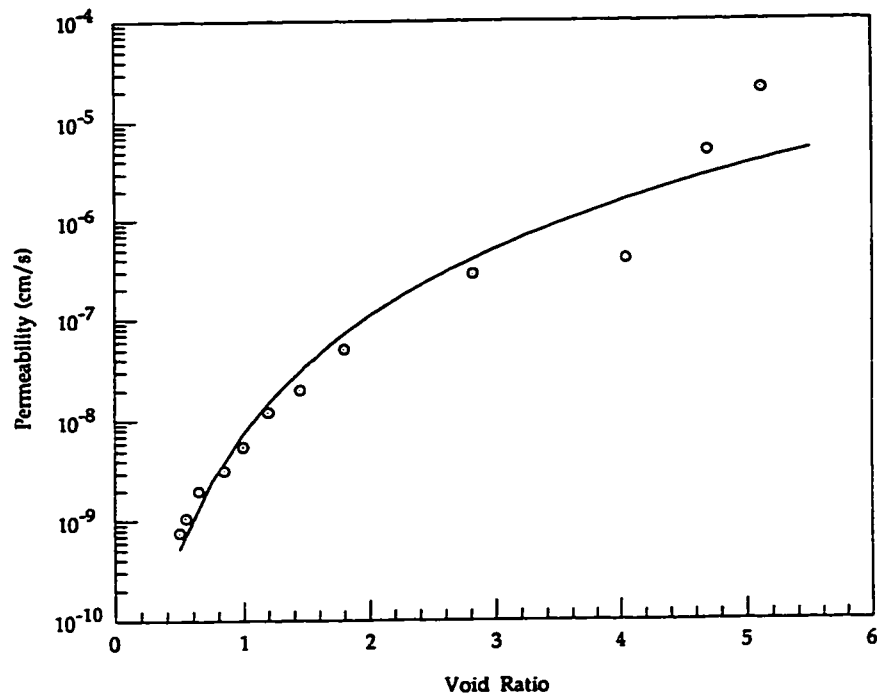


Figure 2.27.b Permeability of oil sand fine tailings - Pollock's best-fit function (Pollock 1988)

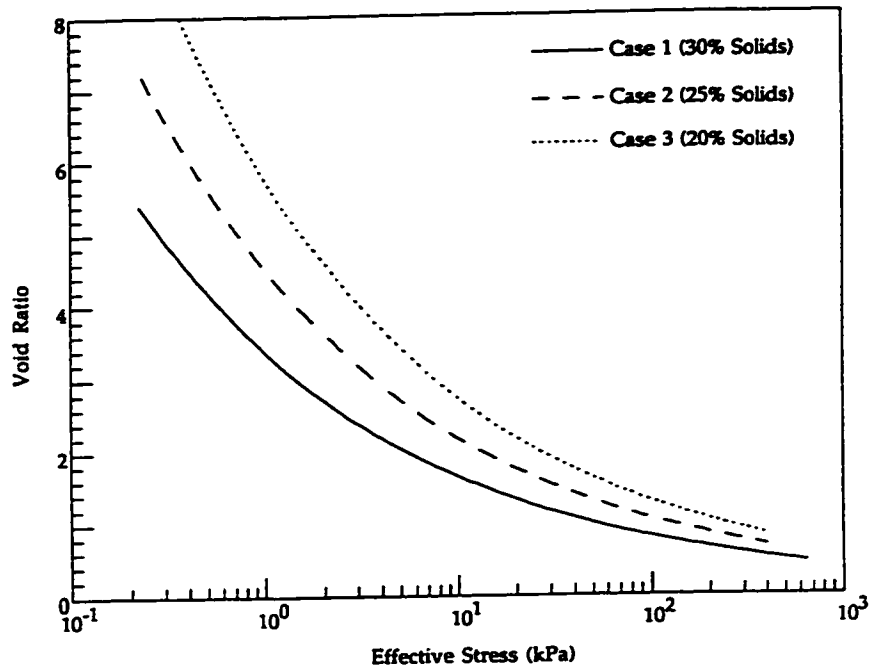


Figure 2.28.a Compressibility of oil sand fine tailings for various initial solids contents (Suthaker 1995)

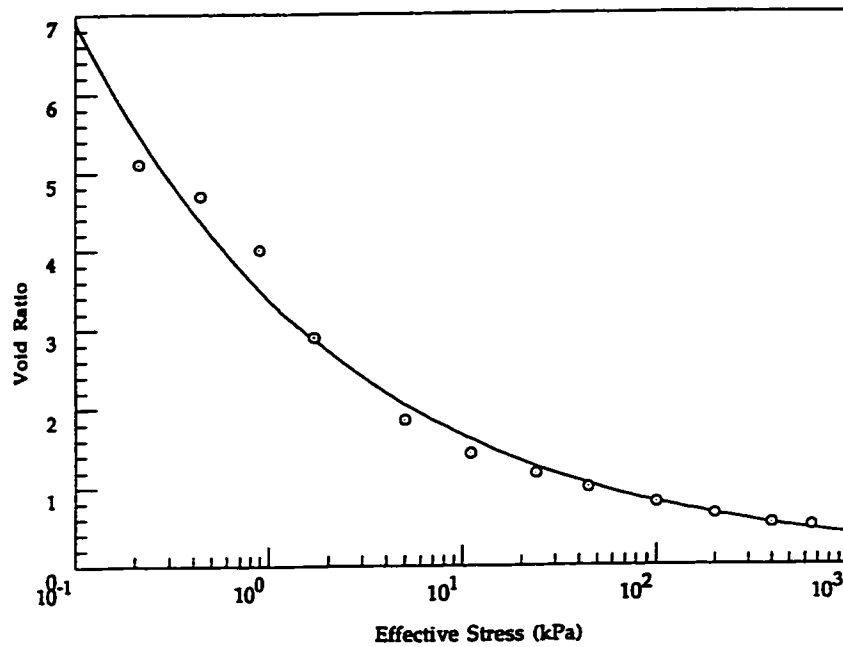


Figure 2.28.b Compressibility of oil sand fine tailings for the solids content of 30 % (Pollock 1988)

Fine tailings has a large creep index when compared to other clayey soils. The creep rate increases linearly with void ratio (as with other soils). The creep index  $C_\alpha$  is linearly proportional to the compression index  $C_c$  and their ratio is found to be 0.085 which is high and similar to that of organic soils. The cause for such a behaviour is found in the organic matter (hydrocarbons - bitumen).

One question has been left open after these tests. A slurry with 30%, 20% and even 10% of solid particles by weight has been investigated for compressibility, thixotropy and creep which all are properties of a solid body. This means that the transitional concentration from suspended to soil state has to be at least less than 10%. On the other side, a large scale self weight consolidation test with the same slurry having about 31% of solids shows that such a material remains in a liquid state for much longer periods than the test duration. This raises the problem of the boundary between a liquid and a solid: whether this is only a matter of concentration or there should be something more - a structure, etc.; whether the boundary is distinctive or gradual; the uniqueness of such a boundary for suspensions with different concentrations but the same composition, and the factors that determine that boundary. These questions have been asked earlier by many authors, see Chapter 2.3. The answers offered reflect wide differences in approaches and points of view.

## **2.4.2 Modelling of self weight consolidation**

### **2.4.2.1 Terzaghi's theory**

Terzaghi's theory is found to be inadequate for the self weight consolidation problem. It is presented here from historical reasons, as the origin of other models.

Terzaghi's theory is founded on the following basic assumptions (Burland and Roscoe, 1969):

- (a) The clay is saturated and homogeneous.
- (b) The pore water and soil grains are incompressible.
- (c) The average flow and compression are one-dimensional.
- (d) All stresses are uniformly distributed over any horizontal cross section.
- (e) The soil obeys Darcy's law of permeability in which the average velocity of the fluid is related to the excess pore pressure gradient.
- (f) The coefficient of permeability  $k$  is a constant during consolidation over a given stress increment.
- (g) The void ratio  $e$  is a unique function of the vertical effective stress  $\sigma_v'$  and is independent of time.



(h) The coefficient of compressibility  $a_v = -\frac{de}{d\sigma'_v}$  is a constant during consolidation under a given stress increment.

(i) The vertical displacements are small in comparison with the thickness of the soil layer.

Terzaghi's equation of one-dimensional small strain consolidation uses pore pressure as the dependent variable:

$$\frac{\partial u}{\partial t} = c_v \frac{\partial^2 u}{\partial t^2} \quad [2.18]$$

where:  $c_v = \frac{k}{m_v \gamma_w} = \frac{k(1+e_0)}{a_v \gamma_w}$  is the coefficient of consolidation,

$e_0$  the initial void ratio,

$k$  the coefficient of permeability,

$m_v = \frac{a_v}{1+e_0}$  the coefficient of volume change,

$a_v$  the coefficient of compressibility,

$\gamma_w$  the unit weight of water,

$t$  the time from the beginning of consolidation, and

$z$  the spatial coordinate, i.e. the vertical distance from the nearest horizontal drainage boundary to the point under consideration.

#### 2.4.2.2 Gibson's theory

This is a general theory of one-dimensional consolidation of saturated clays for which the limitations of assumptions

(f) - small strains,

(g) - linear relationship  $e / \sigma'_v$ , and

(i) - constant  $k$

in Terzaghi's theory are not imposed. Darcy's law - assumption (e) - is recast in a form in which the relative velocity of the soil skeleton and the pore fluid is related to the excess pore pressure gradient. The time-dependent effects (the soil skeleton creep) are excluded from this theory.

Although the governing equation in this theory is unique, two versions were published: the first one (Gibson, England and Hussey, 1967) dealing with a thin soil layer, and the second (Gibson, Schiffman and Cargill, 1981) for a thick layer, thus accounting for the self-weight.

The governing equation is derived using basic principles of the continuum mechanics: the continuity conditions, the equilibrium conditions (i.e. the equation of motion with the inertial forces neglected) and Darcy's law in a form which allows for motion of both phases. The governing equation is expressed with the void ratio as the dependent variable:

$$\left(\frac{\rho_s}{\rho_f} - 1\right) \cdot \frac{d}{de} \left(\frac{k(e)}{1+e}\right) \cdot \frac{\partial e}{\partial z} + \frac{\partial}{\partial z} \left[ \frac{k(e)}{\rho_f(1+e)} \frac{d\sigma'}{de} \frac{\partial e}{\partial z} \right] + \frac{\partial e}{\partial t} = 0 \quad [2.19]$$

where:  $\rho_s$  and  $\rho_f$  are densities of solids and water, respectively,

$z(a) = \int_0^a [1 - n(a', 0)] da'$  is the material (reduced) coordinate, i.e. the label of a grain in the solid skeleton,

$a$  is the Lagrangian coordinate in the initial state, and other symbols are the same as in Chapter 2.4.2.1.

The main novelty in this theory was the use of material or Lagrangian coordinates which greatly simplified the mathematical treatment of the problem, particularly the analytical one in the first paper from 1967. This is illustrated in Figures 2.29.a and 2.29.b, taken from Schiffman, Vick and Gibson (1984).

Figure 2.29.a shows an Eulerian system in which the referential element is a fixed box in the space through which both solids and fluid flow. In Figure 2.29.b an elementary box in Lagrangian system is shown which always contains the same solid particles. If an Eulerian system is adopted to describe the process of consolidation, the variables are expressed as functions of time  $t$  and spatial coordinate  $x$ . In the case of a Lagrangian system the variables are given in terms of  $t$  and either the initial coordinate  $a$  or the material coordinate  $z$  which is actually a function of  $a$ .

Figures 2.30.a and 2.30.b illustrate behaviours of the two systems by piezometers which are either fixed in space (Eulerian) or embedded in a moving elementary box (Lagrangian). The points A, B, C and D in Figure 2.30.a are labeled points in space, while P, Q, R and S are labelled grains in the skeleton. A piezometer in the Eulerian system measures pore pressure changes in a fixed point in space, while a piezometer in the Lagrangian system moves, always surrounded by the same solids, and measures pore pressures at different locations at different times.

Each system has its own advantages and disadvantages. When deformations are small Eulerian system is conveniently used since there is no change in geometry. In the case of large strains, however, the Lagrangian system is preferred: it labels the solid particles and actually moves with them. Therefore, the geometry of a consolidating layer remains unchanged in Lagrangian coordinates although it changes in an Eulerian system. This is very convenient from the mathematical point of view (simplified formulas, fixed boundary conditions, etc.). Nevertheless, at the end Lagrangian coordinates have to be converted to the Eulerian ones because the spatial positions of points is what one needs in the physical world.

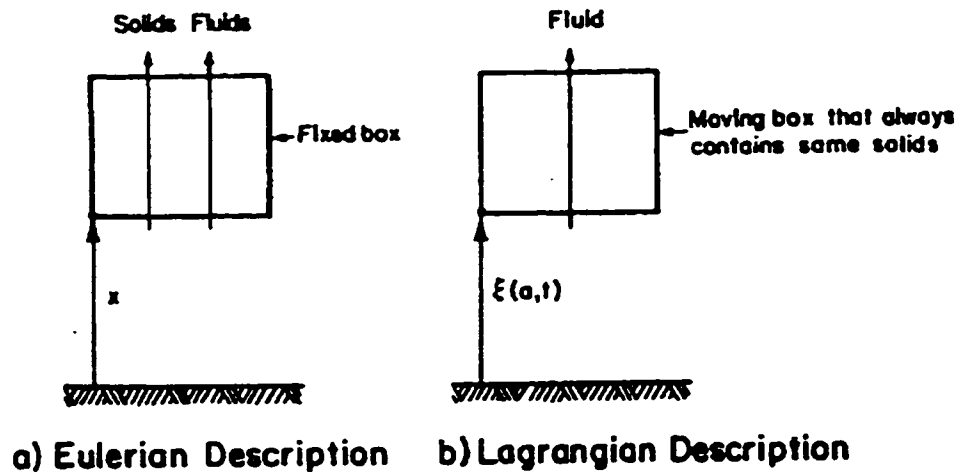


Figure 2.29 Eulerian and Lagrangian coordinates in consolidation (Schiffman, Vick and Gibson, 1984)

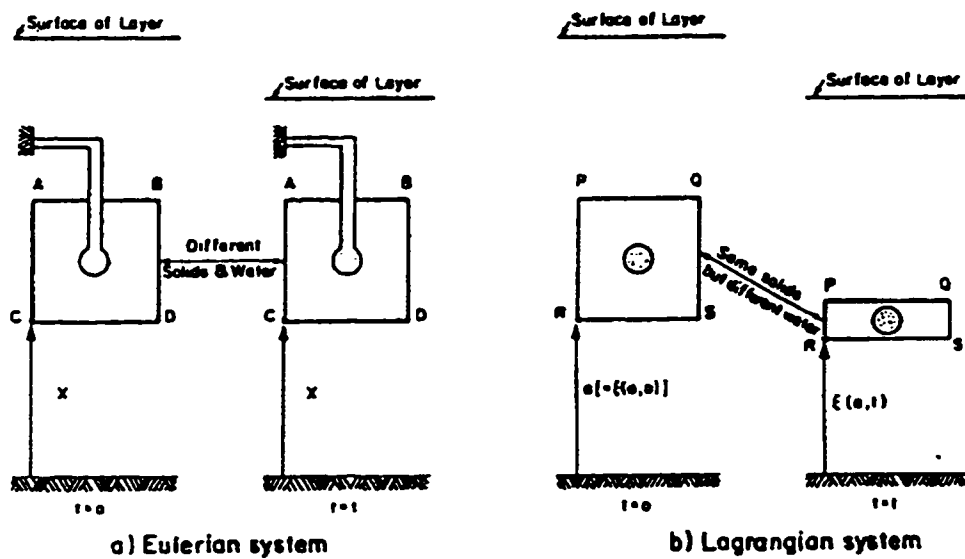


Figure 2.30 Eulerian and Lagrangian coordinates in consolidation - pore pressure measurement (Schiffman, Vick and Gibson, 1985)

*Linearized theory for a thin layer (Gibson, England and Hussey, 1967)*

The governing equation [2.19] may be simplified if the self-weight of solids and pore fluid is neglected:

$$\frac{\partial}{\partial a} \left( c_F \frac{\partial e}{\partial a} \right) = \frac{\partial e}{\partial t} \quad [2.20]$$

where the quantity  $c_F$  is given by the expression:

$$c_F(e, e_0) = - \frac{k(e)}{\rho_f} \cdot \frac{(1+e_0)^2}{(1+e)} \cdot \frac{d\sigma'}{de} \quad [2.21]$$

where  $e_0$  is the initial void ratio.

Linearized Gibson's theory assumes "as a first approximation" that  $c_F$  remains constant during the consolidation under a specific stress increment (experimental results in later references show that this assumption is often not reasonable). The main reason for this assumption is probably the mathematical in nature: it enables that the governing equation [2.20], which now reads simply:

$$c_F \frac{\partial^2 e}{\partial a^2} = \frac{\partial e}{\partial t} \quad [2.22]$$

can be analytically solved as a boundary value problem in Lagrangian coordinates.

A numerical scheme for a weakly nonlinear problem was also presented, assuming that  $c_F$  is a linear function of the void ratio  $e$ . It was solved by the finite difference method using the Runge-Kutta formula.

Linearized Gibson's solution gives higher consolidation rate in comparison with the classical theory of Terzaghi. An important feature of this solution is that it does not restrict the relationship between effective pressure and void ratio by a priori assuming any specific mathematical form.

*Theory for a thick layer - the self-weight included (Gibson, Schiffman and Cargill, 1981)*

This solution is the extension of the previous work from 1967. Consolidation of a thick layer, initially fully consolidated under its own weight, is considered. The governing equation is the equation [2.19]. Two parameters are distinguished:

$$\lambda(e) = - \frac{d}{de} \left( \frac{de}{d\sigma'} \right) \quad [2.23]$$

related to the compressibility, and

$$g(e) = - \frac{k(e)}{\rho_f} \cdot \frac{1}{1+e} \cdot \frac{d\sigma'}{de} \quad [2.24]$$

which plays the role of a "coefficient of consolidation". These parameters are assumed constant through the soil layer and equation [2.19] is transformed to:

$$\frac{\partial^2 e}{\partial z^2} - \lambda(\rho_s - \rho_f) \frac{\partial e}{\partial z} = \frac{1}{g} \frac{\partial e}{\partial t} \quad [2.25]$$

Equation [2.25], together with prescribed initial and boundary conditions in Lagrangian coordinates, was numerically solved for various combinations of drainage boundary conditions. Comparison with conventional small strain (Terzaghi) theory showed that nonlinear finite strain theory predicts the progress of settlement to be substantially swifter than indicated by small strain theory, although the dissipation of excess pore pressure may be slower. The consequence of this is that the conventional theory may seriously underestimate the excess pore pressure and thus overestimate the shear strength in a deposit, leading to a potentially unsafe design.

#### 2.4.2.3 Lee and Sills (1979)

Using the basic principles of the continuum mechanics: the continuity of solid and fluid phase, the generalized Darcy's law and the equilibrium equation, and referring to an Eulerian coordinate frame, Lee and Sills derive the governing equation for a finite strain nonlinear primary consolidation in terms of the porosity  $n$ :

$$\begin{aligned} \frac{\partial n}{\partial t} = & -\frac{\partial}{\partial x} \left\{ \left[ \frac{k}{\gamma_w} (1+e) \frac{d\sigma'}{de} \right] \frac{\partial n}{\partial x} \right\} - \left\{ (G_s - 1) \frac{d}{dn} [k(1-n)^2] - \frac{\partial q}{\partial x} \frac{d}{dn} \left[ \frac{k}{\gamma_w} (1-n) \right] \right\} \cdot \frac{\partial n}{\partial x} \\ & + \frac{k}{\gamma_w} \frac{\partial^2 q}{\partial x^2} (1-n) \end{aligned} \quad [2.26]$$

where:  $G_s = \frac{\rho_s}{\rho_w}$  is the specific gravity of solids,

$q$  a distributed body force within the soil layer,

$x$  a spatial (Eulerian) coordinate, and other variables the same as those used in Gibson's derivations.

It may be shown that this equation can be transformed into Gibson's equation when the distributed body force  $q$  is neglected. The apparent difference between the two expressions is in the use of alternative - Eulerian - frame of reference by Lee and Sills.

For a thin layer with the self weight of soil negligible, equation [2.26] reads:

$$\frac{\partial n}{\partial t} = \frac{\partial}{\partial x} \left[ -\frac{k}{\gamma_w} (1+e) \frac{d\sigma'}{de} \frac{\partial n}{\partial x} \right] \quad [2.27]$$

where the term  $C_v = -\frac{k}{\gamma_w}(1+e)\frac{d\sigma'}{de}$  seems related to the small strain coefficient of consolidation  $c_v$  and the whole expression gets the form of Terzaghi's equation. However, Lee and Sills point out two features of their derivation:

- firstly, the dependent variable is the porosity and variations of permeability and compressibility are included in the coefficient  $C_v$  and need not be restricted to any particular form;
- secondly, the equation has to be satisfied within moving boundaries (a consequence of the use of Eulerian frame), whose positions depend on the final deformation.

The simplified problem of a thin layer subjected to a step load (equation [2.27]) has been solved using a sophisticated (and complicated) finite difference scheme. The spatial grid is equidistant within the current thickness of the layer, but has to readjusted at the end of each time step, in order to account for the incremental deformation during that step. The functional values in new nodes are calculated from the old ones using polynomial interpolation within each segment. The solution is marched forward in time using the implicit Crank-Nicolson scheme. The positions of soil boundaries emerge as a part of the solution.

#### 2.4.2.4 Linked sedimentation and consolidation (Pane and Schiffman, 1985)

In his doctoral thesis, Been (1980) was the first to demonstrate that consolidation and hindered settling theories may be derived from the same basic principles, and that hindered settling can be deduced from consolidation theory by setting the effective stress to be zero. Experimental studies in sedimentation by Been and Sills (1981) have shown the existence of a transition zone between suspension and soil, which is characterized by large concentration gradients with depth.

These observations led Pane and Schiffman to reformulate Terzaghi's effective stress equation in a more general form:

$$\sigma = \beta(e)\sigma' + u_w \quad [2.28]$$

where the interaction coefficient  $\beta$  is a monotonic function of the void ratio. Reasonable forms of the  $\beta$  -  $e$  constitutive relationship are shown in Figure 2.31.

In the case *b* in this figure  $\beta$  is equal to zero for void ratios greater than  $e_m$  and the soil-water mixture behaves as a dispersion. For void ratios less than  $e_m$ , the coefficient  $\beta$  is equal to unity, the conventional effective stress principle fully applies and the mixture behaves as a soil. In the case *a* an abrupt change in  $\beta$  occurs at  $e_m$ .

Assuming the validity of equation [2.27], the governing equation of a linked theory of sedimentation and consolidation has been derived as:

$$\left(\frac{\gamma_s}{\gamma_w} - 1\right) \cdot \frac{d}{de} \left(\frac{k}{1+e}\right) \cdot \frac{\partial e}{\partial z} + \frac{\partial}{\partial z} \left[ \frac{k}{\gamma_w(1+e)} \beta \frac{d\sigma'}{de} \frac{\partial e}{\partial z} \right] + \frac{\partial}{\partial z} \left[ \frac{k}{\gamma_w(1+e)} \frac{d\beta}{de} \sigma' \frac{\partial e}{\partial z} \right] + \frac{\partial e}{\partial t} = 0 \quad [2.29]$$

It was then shown that for  $\beta = 0$  and  $e > e_m$  equation [2.29] reduces to:

$$\left(\frac{\gamma_s}{\gamma_w} - 1\right) \cdot \frac{d}{de} \left(\frac{k}{1+e}\right) \cdot \frac{\partial e}{\partial z} + \frac{\partial e}{\partial t} = 0 \quad [2.30]$$

which has the same form as Kynch's equation. For  $\beta = 1$  and  $e < e_s$  equation [2.29] reduces to Gibson's equation.

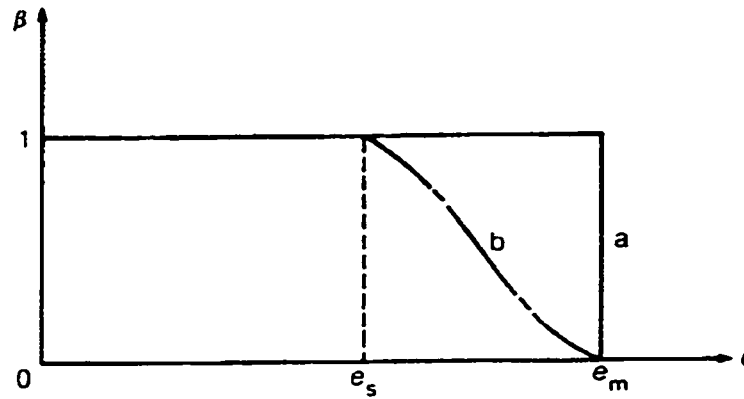


Figure 2.31 Modified effective stress principle after Pane and Schiffman (1985) – interaction coefficient  $\beta$  as a function of void ratio

Pane and Schiffman later show how to implement the proposed model in a practical situation, e.g. the sedimentation and simultaneous consolidation of an initially uniform suspension, using the method of characteristics and the reduced (material) coordinates. However, they do not apply the method to any real problem, but “leave the detailed numerical solutions and the laboratory verification to a later paper.”

It is not quite clear from their explanation whether they use the formulation of Kynch theory which postulates constant concentration in suspended region. Also, it seems that their solution is capable of handling only homogeneous initial conditions. The author of this text does not share their optimism with regard to “a variety of numerical techniques” available for “successful application in the solution.”

#### 2.4.2.5 Linked sedimentation and consolidation (Shodja and Feldkamp, 1993)

This paper is interesting because of the treatment of the transition between a liquid and a solid state of a sedimenting system, as well as the numerical method applied in the solution: the moving finite element method.

The model itself is rather “conventional” since it uses Gibson’s finite strain nonlinear theory of consolidation, in the form:

$$\frac{\partial e}{\partial t} = \frac{1}{\mu} \frac{\partial}{\partial m} \left[ \frac{k(e)}{\alpha(e)(1+e)^2} \frac{\partial e}{\partial m} \right] - \frac{(\rho_s - \rho_w)g}{\mu} \frac{\partial}{\partial m} \left[ \frac{k(e)}{1+e} \right] \quad [2.31]$$

by Feldkamp, where:  $m$  is the material coordinate ( $z$  in Gibson’s derivation),

$k(e)$  the intrinsic permeability,

$\mu$  the viscosity of liquid phase,

$g$  the acceleration of gravity,

$\alpha(e)$  the compressibility of soil skeleton, and the other symbols are the same as in earlier derivations.

The authors explicitly refuse Pane and Schiffman’s modification of Terzaghi’s concept of effective stress and offer an alternative approach through the modified constitutive model “which can differentiate between a collection of non-interacting particles (suspension) and interacting particles (soil)”. This is achieved “by allowing for the compressibility of the material to change abruptly from finite values to infinity in the so-called ‘transition region’ which delineates that portion of space where effective stress is zero from that where effective stress is non-zero.” Namely, the permeability and compressibility are assumed in the forms:

$$\begin{aligned} k(e) &= k_* \frac{e^b}{1+e} \\ \alpha(e) &= \alpha_* \frac{e^a}{1+e} \end{aligned} \quad [2.32]$$

where:  $e$  is the void ratio and  $k_*$  and  $\alpha_*$  are coefficients. The validity of the permeability function  $k(e)$  is assumed “regardless of the presence or absence of effective stress”, i.e. both for suspended and soil state. The same was certainly not possible for the compressibility  $\alpha(e)$ . It was assumed, instead, that the compressibility has a drastic increase at certain threshold void ratio  $e_i$ : below this value  $\alpha(e)$  has the form given by equation [2.32], but above that value becomes infinite. In this way, the first term in equation [2.31] becomes zero in the suspended region and the pure sedimentation equation is obtained. Since numerical reasons do not allow for infinite values, to include this behaviour in the model [2.31] the ratio

$$\frac{k(e)}{\alpha(e)} = \frac{k_*}{\alpha_*} \Phi(e) \quad [2.33]$$



was defined by the threshold function  $\Phi(e)$  which controls the rapidity with which  $\alpha(e)$  tends toward infinity, see Figure 2.32.

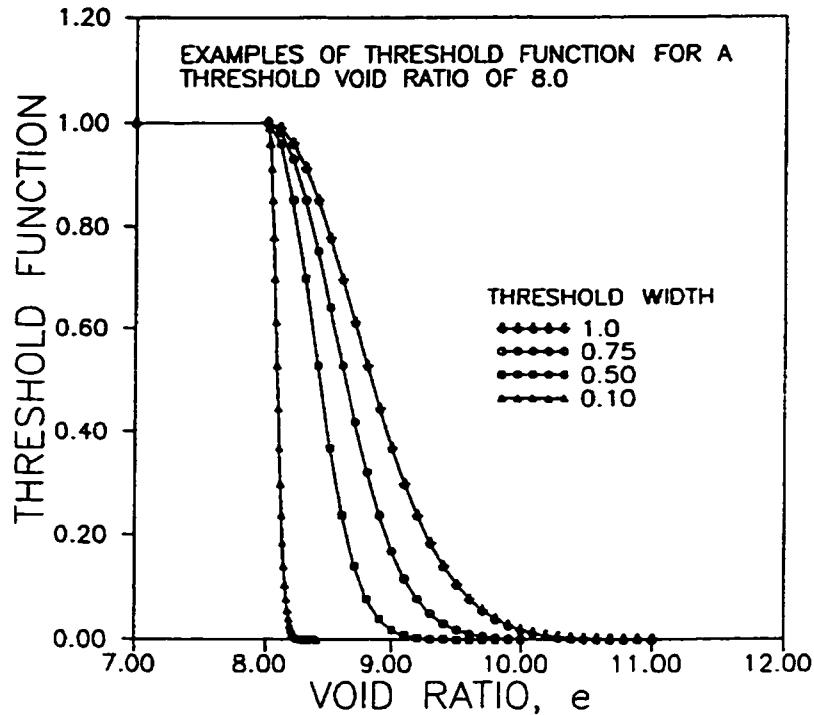


Figure 2.32 Linked sedimentation and consolidation after Shodja and Feldkamp (1993) – threshold function  $\Phi(e)$

The above procedure gives rise to serious difficulties when trying to solve the governing equation [2.31] numerically, because of the “abrupt, almost discontinuous, change in void ratio displayed in the transition region” (the suspension-sediment interface. This is because of coupling of two different types of PDE: nonlinear hyperbolic and nonlinear parabolic equations). A relatively new numerical technique known as the Moving Finite Element Method was used, “especially effective in solving problems which solutions exhibit a shock-like structure.”

This method differs from conventional finite element methodology in that the positions of the nodes are permitted to be time-dependent, i.e. they move in time. The basis functions are permitted to have discontinuities - jumps. The weighted residual method is applied in deriving the governing system of equations, in which both residual functions and positions of nodes are minimized. Actually, the procedure automatically readjusts the mesh so that the nodes are distributed in the most efficient manner possible (i.e., the grid is denser where the gradients are greater). An equation solver for stiff

PDE's was used and, in addition, a small linear second-order diffusion term had to be introduced in order to assure numerical stability of the solution.

The authors did not present any real example (this becoming a rule in recent papers) but rather an exercise in parameter variation. Judging from their graphs, it seems that their technique, although mathematically very complicated, is not so efficient in numerical sense as they claim. Also, a priori determined mathematical forms for the permeability and compressibility functions may be quite a severe restriction in real applications. And, finally, their "threshold function"  $\Phi(e)$  does not seem substantially different in its effect on the coupled sedimentation- consolidation problem from the interaction function  $\beta$  by Pane and Schiffman (Figure 2.31).

#### **2.4.2.6 Discrete element method in consolidation (Anandarajah, 1994)**

This reference is presented rather as a curiosity, to illustrate a variety of physical approaches and numerical methods applied in consolidation analysis in recent times.

The discrete element method has been applied in the past in the study of behaviour of granular materials. In this paper, the method is applied to cohesive soils where, in addition to mechanical forces, physicochemical forces between particles act, and significant bending of particles occurs.

In presented model, the double-layer repulsive forces were modelled approximately and the attractive forces were not considered at all. Bending of particles was simulated by dividing each particle into a number of interconnected discrete elements. It was possible to simulate the formation of new particle contacts, the deletion of existing contacts and the slip between particles.

The results were reasonable, although numerically somewhat rough. As an illustration, in Figure 2.33 an assembly of distinct elements at two stages during one-dimensional compression is shown, and in Figure 2.34 the histograms of particle orientations in the beginning and at the end of 1D consolidation.

It seems that the presented approach has an outstanding potential as a tool for fundamental research into the constitutive behaviour of cohesive soils.



Figure 2.33 Distinct element method in consolidation (Anandarajah 1994); Distinct element assembly at two stages during one-dimensional compression: (a) void ratio  $e = 1.868$ ; (b) void ratio  $e = 0.800$

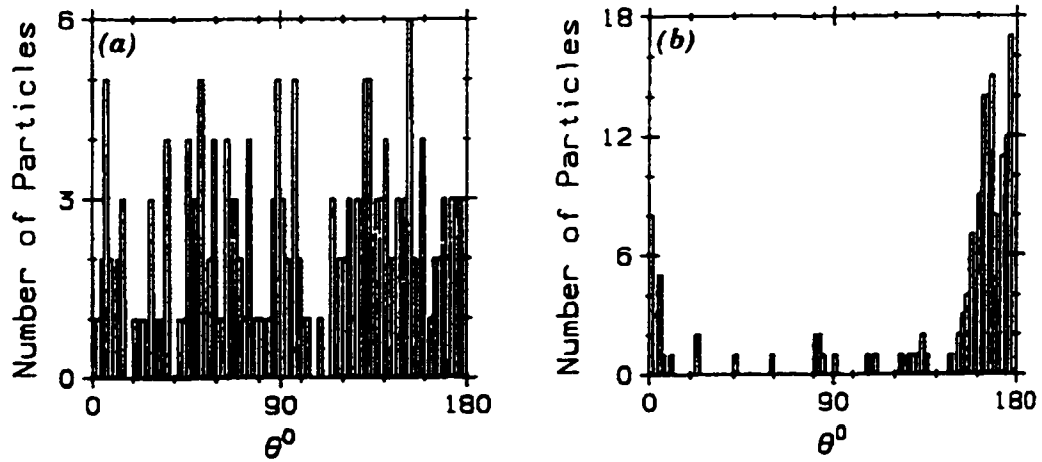


Figure 2.34 Distinct element method in consolidation (Anandarajah 1994); Histograms of particle orientation: (a) Computer generated initial assembly ( $e = 4.0$ ); (b) End of 1D consolidation ( $e = 0.8$ )

## 2.5 SUMMARY OF LITERATURE REVIEW

### 2.5.1 Sedimentation phenomenology

#### *(a) Modes of settling behaviour*

Experimentation has shown that an initially dilute suspension exhibits three modes of settling behaviour: free settling (Stokesian regime), hindered settling (or zone settling) and consolidation. These modes have their own characteristic regions on a batch settling curve (a diagram of interface heights versus time). Depending on the initial concentration, some of these modes may be absent.

The Stokesian regime appears in very dilute suspensions. It is characterized by the segregation of particles, which causes the blurring of the suspension surface and consequent difficulties in measuring its position. Segregation also changes the “initial conditions” for the hindered sedimentation stage, which follows. The boundary concentration (transition point) between the Stokesian and hindered settling regime is not distinct and is difficult to determine at all. The same is valid for the settling velocity, for grains fall at their own speeds. Segregation causes great problems in modelling too, because in the development of a model separate fractions should be traced and their mutual interaction accounted for.

Hindered (zone) settling is characterized by the sedimentation of a suspension as a whole, when the particles seem to be captured in a spatial network, but are likely to be without stable and systematic (regularly ordered) direct contacts. This phenomenon is called “hydrodynamic interaction”. The initial stage of zone settling is linear in the sedimentation diagram and is followed by a more or less pronounced non-linear stage. It seems that the non-linear section is characteristic of flocculated suspensions, while the stable suspensions (with particles of rigid spheres) show linear behaviour.

Consolidation under the self-weight is the terminal stage when the suspension layer in a settling system disappears. Boundary concentration, or a transition criterion between the suspended and the sedimentary state, is not unique and depends on a previous sedimentation regime. The main consequence is that there is no unique compressibility law (effective stress-void ratio relationship) in the small stress range for cohesive soils. Compressibility is affected by the sediment structure, which in turn depends on the way the sediment was formed, i.e. its sedimentation process. In general, stable suspensions (rigid spheres) result in less compressible sediments with a higher initial solids content.

#### *(b) Zonation within a settling system*

In an initially uniform suspension, certain zones (or layers) with varying concentrations appear over time: almost clear water at the top, a sediment layer at the bottom and a suspension zone between them. Further refinement is possible in the suspension zone dividing it into the upper zone of nearly constant (slowly changing) concentration and the lower zone with variable spatial concentration. The settling behaviour of solid particles in these zones in general corresponds to the sedimentation modes above.

Over time, changes in concentration in the suspension zone have been observed in experiments, but little importance has been attached to it, probably because of the relatively short duration of sedimentation experiments. However, the significance of the slow changes of the solids content in the suspension zone in a settling system can be seen through observation of the behaviour of tailings settling ponds in the mining industry.

*(c) Settling velocity of a suspension*

The settling velocity of a suspension in the Stokesian regime depends on the size, shape and specific weight of the particles and the viscosity of the fluid. The velocity is so varied that it is actually very difficult to determine experimentally.

In a hindered sedimentation regime, concentration is the main variable, but other parameters, such as the starting concentration, grain size distribution, mineral composition of grains, etc., affect the settling of particles in a quantitatively undetermined way, so that the settling velocity of the suspension has to be determined by sedimentation tests or back analysis of measured data. It is still not possible to assess the settling velocity curve only on the basis of certain properties of the particles and the fluid. It has, however, been shown that the free-settling velocity (in an infinitely long column) is equal to the fluidization velocity for the same concentration.

The shape of the settling curve determines the sedimentation behaviour, and further understanding of such behavior can be gained by using a parametric analysis of the existing models.

*(d) Effective stresses in a suspension*

The fact that seems determined beyond doubt (within the margins of experimental error) is the absence of effective stresses in a suspension. It is a “stress-free” environment, and this fact should be kept in mind during the analysis of sedimentation and self-weight consolidation.

*(e) Permeability and fluid-solid interaction*

It has become customary to measure the interaction between a solid and a fluid phase by the coefficient of permeability, extending thus the applicability of the concept of permeability to a suspended state of a soil. Problems with the experimental determination of permeability parameters are numerous, mainly due to seepage-induced sedimentation and consolidation. When an opposite direction of flow (upward) is applied, the internal mobility of fine particles causes a time-dependent liquid flow and, consequently, a time-dependent coefficient of permeability. Therefore, it seems that experimental setup (hydraulic gradient, seepage length, etc.) affects the results, but this influence has not been investigated in the available literature.

*(f) Specific properties of oil sands fine tailings*

Specific properties of oil sands fine tailings behaviour are:

- a time dependent increase of solids content in the suspension zone during sedimentation;
- the development of solids structure in the suspension and thixotropic strength gain in this zone;

- a relatively high creep in the sedimented material;
- difficulties in the laboratory determination of reliable permeability and compressibility parameters as input values for mathematical modelling;
- the presence of residual bitumen and its influence on the mechanical properties of the suspension;
- the appearance of an odd “perched consolidation zone” near the top of the suspension, with increased concentration probably caused by microbial activity and gas production; etc.

A particular problem with oil sands fine tailings is residual bitumen: it covers mineral grains, increasing repulsive interparticle forces and delaying sedimentation, and it slowly deforms during permeability testing, thus increasing the duration of the tests. It seems that it also accumulates in layers within the suspension, possibly decreasing the overall permeability.

## **2.5.2 Sedimentation modelling**

### *(a) Stokes' equation*

It has been experimentally proved that a Stokesian approach is inadequate in the simulation of hindered settling behaviour. It is possible, however, to obtain satisfactory results with a Stokesian approach using a correcting function which accounts for the concentration influence.

### *(b) Kynch's theory*

A dominant model for the hindered settling is Kynch's theory, which states that the settling velocity is a unique function of the suspension concentration, but it has no explicitly defined mathematical form and has parameters which have to be determined by experimentation.

It is common practice to postulate a constant concentration in the hindered settling region with time, although the original theory does not explicitly claim this.

### *(c) Discontinuities (shocks)*

Sedimentation behaviour is determined by the shape of a settling velocity curve (or solids flux curve) and the initial concentration in the suspension. A particular question arises regarding the appearance of additional shocks (sudden finite changes in concentration) within the suspension, besides the commonly known shock at the sediment-suspension interface. It has been proved that in the case of common “hump” flux curves, and when the initial concentration is very low or very high (the beginning and the ending part of a flux curve), the only permissible shock is the one at the sediment surface, and the settling rate is nearly constant. For moderate initial concentrations, shocks within the suspension region are possible, and are followed by the appearance of a variable concentration gradient zone. An understanding of such shocks is important in the choice of a numerical scheme. Another problem is that it is questionable whether these

shocks are observable in experiments, which makes experimental confirmation of the shock theory (Auzerais et al. 1988) difficult.

*(d) Chemical versus geotechnical approach*

There has recently been a highly pronounced convergence of two traditionally separate approaches to sedimentation and self-weight consolidation in geotechnics and chemical engineering. Both approaches tend to unify the whole process under one theory, or at least a computational scheme capable of tackling both processes.

In chemistry, which commonly neglects the consolidation stage, a standard approach nowadays is to apply Kynch's theory to a suspension and Gibson's theory to a sediment, satisfying internal boundary conditions at their interface.

In geomechanics, a more conservative approach prevails in which everything is considered as a soil: a suspension is treated as a solid body. This, however, causes problems with the concentration profile prediction. It seems that this approach proves inadequate at least for the long-term sedimentation of certain mine waste slurries.

### **2.5.3 Phenomenology of self-weight consolidation**

*(a) Non-uniqueness of the compressibility law*

Self-weight consolidation is a settling caused by the deformation of stable and permanent contacts among solid particles under their own weight, i.e. with finite effective stresses transmitted through the contact points. Boundary concentration between hindered settling and consolidation is not well defined and depends on the previous sedimentation regime. The main consequence is that the compressibility law in the small stress range (for high void ratios) is not unique, but depends on the initial concentration.

*(b) Permeability*

Permeability is one of the most varying parameters in geotechnics. There is still no general theory for permeability, and there is not even a well-defined methodology for experimental determination and interpretation of the permeability coefficient for very soft clays and clayey suspensions. Nevertheless, it is presently the most commonly used parameter for sedimentation and consolidation analyses. In sedimentation, it plays the role of a relative measure of fluid-solid (hydrodynamic) interaction. In consolidation, it defines the "permissible rate" of deformation caused by an increase of effective stresses, i.e. the rate of interaction among the solid particles themselves.

### **2.5.4 Modelling of self-weight consolidation**

*(a) Basic approaches*

The "micromechanics" of colloidal suspensions is still at a very early stage in its development of quantitative measurement and numerical computation, despite a vast amount of investigations into phase interaction in suspensions (and soils) and rare attempts at developing analyses which take into account the behaviour of solid particles

at the microscopic level (Anandarajah 1994). The engineering approach, based on continuum mechanics, dominates the theory and practical applications due to its simplicity (a minimum number of empirical parameters—compressibility and permeability only), easy calibration, sufficient accuracy and cost-effectiveness.

*(b) Coupled sedimentation and consolidation*

Current practice in chemical engineering in the modelling of coupled sedimentation and consolidation is physically correct: the suspension is considered as essentially a liquid, and Kynch's sedimentation theory is applied to it, while the sediment is considered as a solid body and Gibson's consolidation theory is used to study it. It has been shown that the Kynch theory is a special case of Gibson's theory for effective stresses assumed to be zero. This relationship between theories is consistent with the physical reality and experimental observations.

An undesirable extension of Gibson's theory to the suspension—assuming it is a solid body—is often encountered in geotechnical applications.

*(c) Numerical aspects*

Numerical problems in sedimentation analysis abound, starting from the choice of a coordinate frame (Eulerian and Lagrangian), then the method (finite differences or finite elements, etc.), the stability and convergence of calculation, shock handling, the proper selection of permeability and compressibility laws, etc. The available literature does not provide definite conclusions or guidelines for their solution.

In a coupled analysis the above problems multiply, because a mathematically difficult problem appears of simultaneous solution of two different types of partial differential equations: a hyperbolic equation for sedimentation and a parabolic equation for consolidation. The numerical stability of the solution method is critical, for numerical instability is associated with accuracy problems through numerical diffusion (magnitude change) and numerical dispersion (artificial oscillations in a solution). There is also an additional interface motion, even in Lagrangian formulation (the suspension-sediment boundary). These problems have recently been the subject of intensive mathematical research, but general and definite conclusions have not been found.



## **Chapter 3**

### ***FORMULATION OF A TIME DEPENDENT SEDIMENTATION MODEL***

#### **3.1 MATHEMATICAL DERIVATION OF THE MODEL**

##### **3.1.1. Introduction**

Consider a two-phase system presented in Figure 3.1 which consists of solid particles dispersed through a liquid. The dispersed solids tend to settle with time under the influence of gravity, due to a difference in the specific weights (densities) of the phases and the inability of the liquid to sustain long-term shear stresses on the surfaces of solid particles.

At the initial state, time  $t = 0$ , it is assumed that the distribution of particles is random and uniform throughout the suspension, as shown in Figure 3.1. Every point of a column of suspension of height  $H$  has the same concentration  $s^0$  and unit weight  $\gamma^0$ . The final state of the suspension, also shown in Figure 3.1, consists only of two phases: a layer of solid sediments at the bottom and a layer of clarified liquid at the top. The task is to define a model that can describe and calculate the important parameters of all the intermediate states.

The dashed lines in Figure 3.1 are imaginary lines. They are only used to indicate the movements of the internal boundaries of the three zones in the settling system:

- zone 1 - the bottom layer of solid sediments;
- zone 2 - the middle layer of suspension, and;
- zone 3 - the top layer of supernatant liquid.

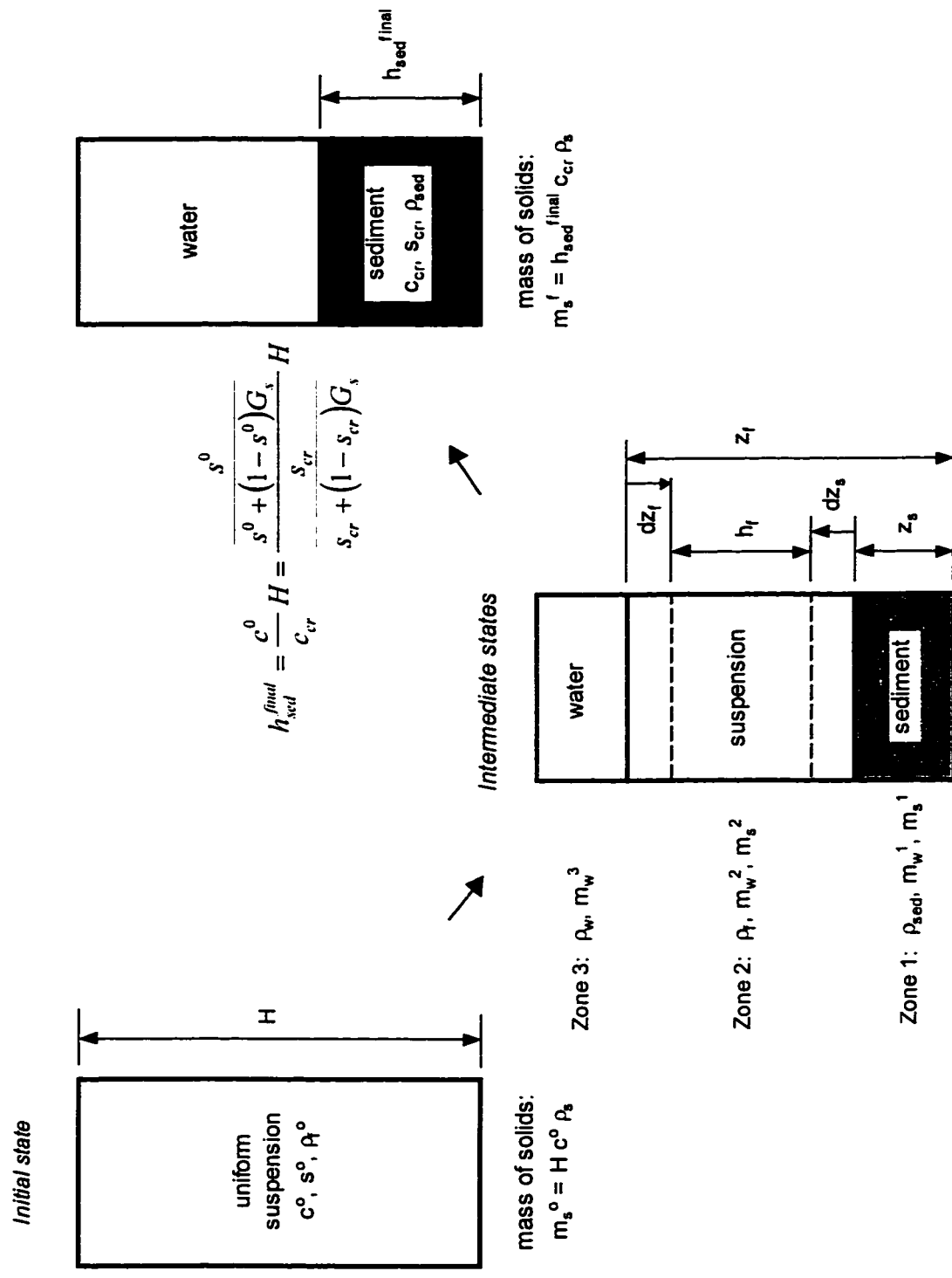


Figure 3.1 Sedimentation modelling - the initial, the final and intermediate states

### 3.1.2. Assumptions of the model

It should be noted that three distinct zones of sediment, suspension and water represent an idealization of a settling suspension. Such a division is common in a theoretical treatise on this problem. Each zone (sediment, suspension and water) is assumed to be homogeneous, which may not be true in reality. If unit weights were measured in a suspension at various depths, there would probably be a scattering of data. This scattering may be either a statistical dispersion or due to measurement error. The latter is not the subject of discussion here. Statistical scattering is neglected in the present consideration and each zone is assumed to be homogeneous. The present model therefore considers the averaged values of the parameters within each zone.

The problem is treated as one-dimensional and the only space coordinate is height. It is further assumed that the initial state of the suspension (height  $H$ , concentration  $s^0$  and density  $\rho^0$  or unit weight  $\gamma^0$ ) is known. The model then calculates subsequent states at later times. In the calibration of the model, measurements of the settlement characteristics, such as heights  $h_w$ ,  $h_f$  and  $h_s$  of the suspension, are required. These measurements are an essential ingredient of the empirical variant of the method (Chapter 3.1.3.1) and they are also necessary for the continuous check and adjustment of model parameters in the alternative method (Chapter 3.1.3.2).

The problem being considered here is the sedimentation process in a settling container. This means that the system is considered closed—there is no gain or loss of matter during the sedimentation process. Therefore, the total amounts of solids and water within the column of height  $H$  are constant, i.e. equal at the beginning of sedimentation (time  $t = 0$ ) and at any arbitrary moment of time  $t$ .

The next assumption is that solids and water are incompressible. This means that the total volume of the system is constant, i.e. the height  $H$  at time  $t = 0$  is equal to the sum of heights of three layers at any time  $t$ , i.e.

$$H = h_w + h_f + h_s \quad [3.1]$$

The *main assumption* in this model is that the *solids content in the suspension is constant with depth but it can vary with time*. This is the main novelty of the proposed method and may be considered as an extension of Kynch's theory of sedimentation, as described in Chapter 2.3.2.3.

It is also assumed that the solids concentration in the sediment layer is constant and equal to some prescribed value denoted as  $s_{cr}$ , "a critical concentration" designating the transition from a liquid state to a solid state. This is equivalent to assuming that the sediment layer is rigid and no consolidation takes place. This assumption has been discussed earlier (Chapter 2.3), but nevertheless deserves a little more attention. It seems at first that it is inadequate for materials that exhibit prolonged sedimentation and therefore undergo coupled sedimentation and consolidation. As a result, the assumption might be more suitable for fast-settling, coarser materials like fine sand and silt, rather than for clays. Notwithstanding, one may refer to experimental results (Been and Sills, 1981, silt material with 30 % clay) which show that, during the settling stage, variability in the density of sedimented material is not very high; for example, the density profile graph for experiment 7 of Been and Sills shows a range of sediment density from 11.1 to

11.8 kN/m<sup>3</sup>, less than 10 % of variation. The graph does not present data during further consolidation, and this range might be widened later. Nevertheless, it may be inferred that in the cases of coupled sedimentation and self-weight consolidation of suspensions (with no external loads), the sedimentation settlement is dominant with respect to the consolidation deformation since the effective stresses are small, and the assumption of constant sediment density may be justified as a good approximation in the analysis.

Therefore, the problem of sedimentation is reduced to a redistribution of phases: in the initial state they are homogeneously mixed and later on they separate. We will not discuss the causes of separation but will only show here how to calculate the concentrations of each phase in subsequent stages of the sedimentation process.

In the following derivation we will also exclude any effect of possible chemical changes in the suspension, as well as changes in physical environment such as temperature.

### 3.1.3 Mathematical derivation of the model

The first equation (which there is no need to derive) is one of the well-known equations for the calculation of the total density of a soil when the specific density of grains  $\rho_s$  and the void ratio (or water content, or porosity, etc.) are known:

$$\rho = \frac{\rho_w \rho_s}{(1-s)\rho_s + s\rho_w} \quad [3.2]$$

This equation may be applied to both the suspension and the sediment layer. Since both layers were considered homogeneous, their densities are only functions of time. In later derivations we will need the derivative of the suspension density  $\rho_f$  which can be expressed as:

$$\rho_f = \frac{\rho_w \rho_s}{(1-s_f)\rho_s + s_f \rho_w} \Rightarrow \dot{\rho}_f = \frac{\rho_w \rho_s (\rho_s - \rho_w)}{[s_f (\rho_w - \rho_s) + \rho_s]^2} \dot{s} = \frac{1}{K} \dot{s} \quad [3.3]$$

The second equation will be obtained using the total mass balance principle. Since this is a closed system, the total mass must be constant:

$$(m_s^1 + m_w^1) + (m_s^2 + m_w^2) + m_w^3 = \text{const.} \quad [3.4]$$

so that the derivatives are linked by:

$$(\dot{m}_s^2 + \dot{m}_w^2) = -(\dot{m}_s^1 + \dot{m}_w^1) - \dot{m}_w^3 \quad [3.5]$$

Now we will express the density of suspension as:

$$\rho_f = \frac{(m_s^2 + m_w^2)}{h_f} \quad [3.6]$$

and the time derivative as:

$$\dot{\rho}_f = \frac{(\dot{m}_s^2 + \dot{m}_w^2)h_f - (m_s^2 + m_w^2)\dot{h}_f}{h_f^2} \quad [3.7]$$

We can now make the following substitutions. First, based on the geometry of the problem:

$$(1) \quad h_f = z_f - z_s \quad \Rightarrow \quad \dot{h}_f = \dot{z}_f - \dot{z}_s \quad [3.8]$$

then considering the conditions at the water-suspension boundary:

$$(2) \quad \dot{m}_w^3 = -\dot{z}_f \rho_w \quad [3.9]$$

where the negative sign denotes that the mass of water  $m_w^3$  increases with decreasing  $z_f$  coordinate, and finally:

$$(3) \quad \dot{m}_s^1 + \dot{m}_w^1 = \dot{z}_s \rho_{sed} \quad [3.10]$$

which is obtained from the conditions at the sediment-suspension boundary, under the assumption of constant sediment solids content and density (rigid sediment, no consolidation).

In this way we obtain:

$$\dot{m}_s^2 + \dot{m}_w^2 = -\dot{z}_s \rho_{sed} + \dot{z}_f \rho_w \quad [3.11]$$

The equation for  $\dot{\rho}_f$  after substitution reads:

$$\dot{\rho}_f = \frac{(\dot{z}_f \rho_w - \dot{z}_s \rho_{sed})h_f - \frac{(m_s^2 + m_w^2)}{h_f} h_f (\dot{z}_f - \dot{z}_s)}{h_f^2} \quad [3.12]$$

Substituting  $\rho_f$  in the second term and canceling  $h_f$  we obtain:

$$\dot{\rho}_f = \frac{(\dot{z}_f \rho_w - \dot{z}_s \rho_{sed}) - \rho_f (\dot{z}_f - \dot{z}_s)}{h_f} \quad [3.13]$$

After rearrangement this equation reads:

$$\dot{\rho}_f = \frac{\dot{z}_s (\rho_f - \rho_{sed}) + \dot{z}_f (\rho_w - \rho_f)}{h_f} \quad [3.14]$$

Therefore, knowing the current state of the suspension ( $\rho_f$ ) and the internal boundary movements ( $z_f$  and  $z_s$ ), we are able to predict the rate of change of the suspension density and, using equation [3.13], the rate of change of solids content in the suspension. All the other variables (stresses, pore pressures) can easily be obtained from the above equations.

It is interesting to mention here that Kynch's solution may be obtained as a particular case of the described model by making the time rate of change of the suspension density in equation [3.14] equal to zero. Thus we obtain:

$$\dot{z}_s = -\dot{z}_f \frac{\rho_w - \rho_f}{\rho_f - \rho_{sed}} \quad [3.15]$$

Applying this equation to the proposed model reduces it to Kynch's solution. This may be useful for the verification of the method. Later in this thesis, examples are given in which the Kynch solution is obtained from the proposed model.

The remaining task is to find appropriate functions for  $z_f$  and  $z_s$ . There are two possible approaches.

### 3.1.3.1 Empirical procedure

The first approach is to find  $z_f$  and  $z_s$  empirically. This is possible only in the case where a real problem exists (an experimental container, tailings pond, sedimentation basin, etc.) which can provide observational data as input information for the model. Observations should be carried out continuously and interpolation curves should be adjusted based on updated information.

The following information is required for this empirical approach:

- both the top (clear water-suspension) interface and the bottom (sediment-suspension) interface should be measured;
- a solids concentration in the sediment  $s_{cr}$  must be assumed;  $s_{cr}$  may be estimated by measuring densities in the sediment layer, which need not necessarily be a constant at all times; otherwise  $s_{cr}$  can be treated as a model parameter which may be changed in order to obtain an optimum result (actually, changing  $s_{cr}$  with time may empirically introduce the effect of sediment consolidation and even enhance the model),
- the specific density of solids  $\rho_s$  must be known (for most materials  $\rho_s$  lies between 2.6 and 2.8),
- the initial conditions must be known: the initial suspension density  $s_f^0$  and the initial height  $H$ .

Usually, it is not easy to define the sediment boundary reliably. Sometimes this boundary is not measured, for example in tailings ponds, due to operational difficulties. In laboratory experiments, requirements of very sophisticated equipment (X-ray scanning or similar) may often be a limiting factor. As well, sometimes there is no distinct boundary at all—for instance, clayey materials, and colloidal suspensions in general, do not always show a sharp interface, but rather a zone of gradual density change. This is the main disadvantage of this model alternative.

Another disadvantage of the model is the uncertainty of determining the so-called “liquid-solid boundary” — the suspension density  $s_{cr}$  which designates the transition from a suspension to a soil. This is a problem in all the models proposed in this thesis as well as for other sedimentation models presented so far.

The advantages of this approach are its simplicity, the independence of material models (actually no material models need to be assumed *a priori*), and consequently, there is no need to determine the parameters experimentally. There are no special

requirements for interpolation functions  $z_f$  and  $z$ , either. Any interpolation polynomial may suit the need or any other function that can reasonably fit the measured data.

This approach is seen as an extrapolation of the curve fitting of the observed behaviour in an existing sedimenting pond. The time intervals of extrapolation depend on the particular problem and cannot be determined in advance. This empirical approach is not very “scientific” and will not be discussed in more detail in this thesis.

In the design of a settling pond, one often needs to predict its behaviour before it is actually built. The prediction should be based on material properties which can be determined using routine testing methods or should at least be based on existing observational data from comparative projects. In such cases it is desirable to be able to connect the interface movements  $z_f$  and  $z$ , with the material parameters of the suspension.

### 3.1.3.2 Alternative method with elements of suspension micromechanics

The second approach to solving the sedimentation problem requires an understanding of the material behaviour during this process. There is no straightforward way in this approach because the understanding of sedimentation micromechanics is still vague and relatively undeveloped (see Chapter 2.3.1). The field of sedimentation has rarely been studied in geomechanics, and most of the studies have been more interested in the later stages of consolidation of a previously sedimented suspension.

We shall now derive a set of governing equations for sedimentation that include elements of material modelling. We shall use Kynch’s theory of sedimentation which states that the settling velocity of solid particles in a suspension is a function of only one variable—the solids concentration  $c$  (by volume) or  $s$  (by weight). This theory is often used in sedimentation analyses in chemical engineering, but quite seldom in geomechanics, with the exception of McRoberts and Nixon (1976). This approach is very convenient here because it does not introduce new variables to the analysis ( $s$  has already been used in equations [3.1] and [3.2]).

It should be mentioned here that Kynch’s theory deals only with sedimentation in the suspension zone and that no consolidation effects in the sediment layer are considered.

The governing equations are derived by referring to Figure 3.2. The derivation consists of applying the mass balance principle in a differential form to the upper and the lower interface of the suspension layer. “Differential” here means that only small volumes of materials on both sides of an interface are involved. These volumes are determined by the velocities of solid particles or, actually, the lengths of the paths travelled by the particles within the time interval  $dt$ .

Figure 3.2.a shows the general layout of the problem. Both internal interfaces—the upper and the lower boundaries of the suspension layer—move in time.

Figure 3.2.b illustrates the application of the mass balance principle to the upper boundary of the suspension layer.

The solid particles in the suspension settle at the velocity  $v$ , which is a function of their concentration by weight (or solids content)  $s_f$ . During a time increment  $dt$ , the distance travelled by the particles is  $dh_f' = v_f dt$ . The mass of solids contained in this volume will

move into the suspension zone and “clean out” a volume of water above it. The increment of cap water height  $dh_w$  is determined by velocity  $v_s$  which is actually the velocity of motion of the water-suspension interface. It is obtained merely by making equal the amounts of water in the two zones  $dh_f'$  (“left” by solids) and  $dh_w$  (created above it).

Figure 3.2c illustrates the mass balance principle applied to the sediment-suspension interface (the lower boundary of the suspension zone). Compared with the upper interface (Figure 3.2b), the only difference here is that the mass of solids, instead of water, is used in the continuity equation. It is assumed here that the solids content in the sediment  $s_{cr}$  is constant (a rigid sediment, with no consolidation).

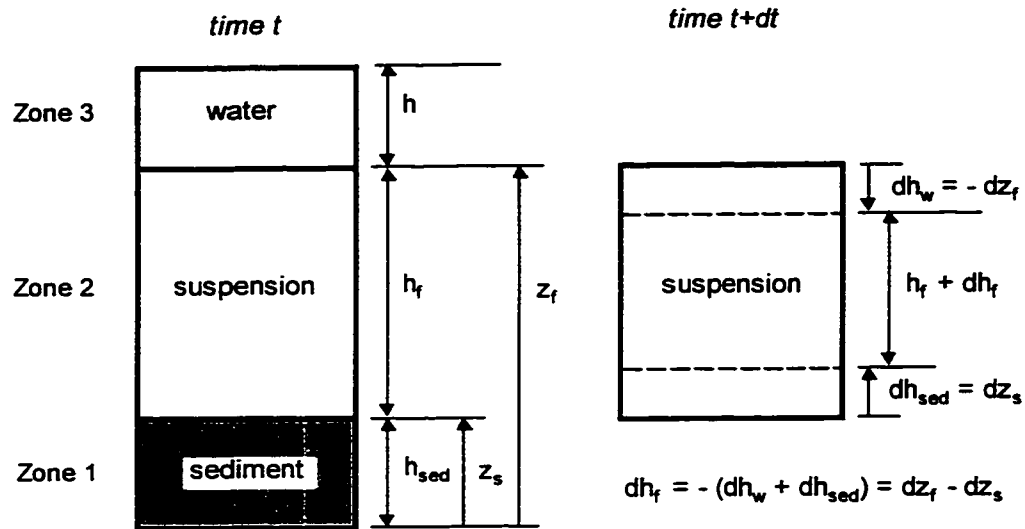
Following Kynch’s approach,  $v_s$  is only a function of the solids content in the suspension  $s_f$ . This approach requires no new variables in defining  $\dot{z}_f$ . The implicit assumption made here is that the change in the solids content in the suspension  $s_f$  during the time interval  $dt$  does not affect the settling velocity of the solid particles  $v_s$  during the same time interval. The function  $v_s$  is not restricted to a special class of functions. Any function which may reasonably fit the observational data may be used. The only condition is that it must be flexible enough to properly match some “actual” settling velocity function which will govern the real behaviour of the solid particles in a particular suspension. Furthermore, it is not necessary to choose a function that fits the “actual” velocity over the whole domain. The interval of interest is only between a concentration  $s_0$  in the initial liquid state and an adopted “critical concentration”  $s_{cr}$  in the solid state (i.e. from an initial suspension to a soil). This means that in the case of a relatively narrow concentration interval (or relatively flat “real” settling velocity function within the interval) even a simple linear function may fit well (see the example below—10 m standpipe test at the University of Alberta).

Possible mathematical forms for the  $v_s$  function were derived by Kynch (1951), Richardson and Zaki (1954), McRoberts and Nixon (1976), etc.

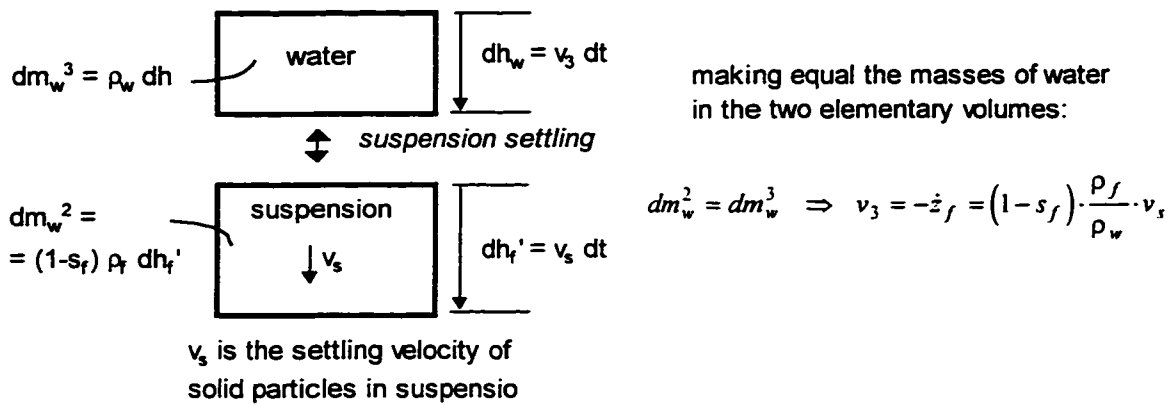
In conclusion, the following physical principles were used in the derivation:

- the volumetric relationship between the solids content and the density of the suspension (equation [3.2]);
- the mass balance equation for the total mass: solids + water (equation [3.14]); and
- the flux boundary conditions for the water-suspension and suspension-sediment interfaces.





*Upper boundary or water - suspension interface*



*Lower boundary or sediment - suspension interface*

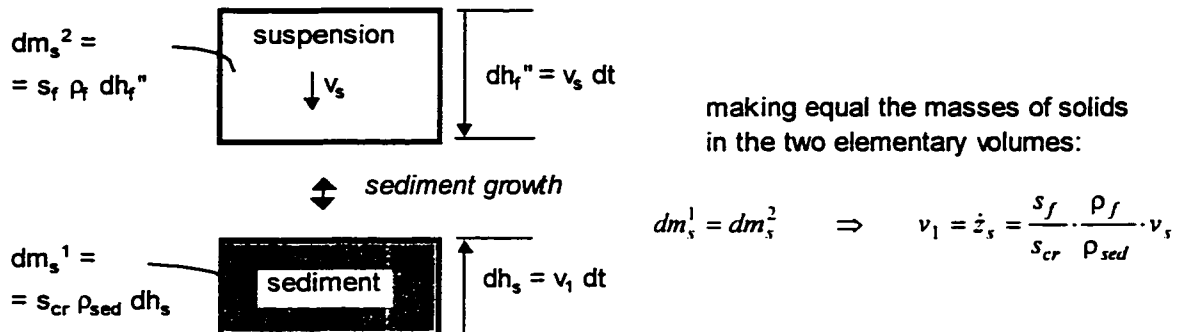


Figure 3.2 Sedimentation modelling—a general layout of the model and boundary conditions for the suspension layer

The complete set of equations used in this approach is given in Table 3.1.

The requirements for this approach are basically the same as those for the empirical approach, with the exception that instead of measuring the suspension boundaries, a set of sedimentation tests should be performed in order to determine the settling velocity law  $v_s = v_s(s)$  for the suspension. It should be noted that this law, determined in ideal experimental conditions, need not necessarily be a direct analogue of a “true” settling velocity governing the real problem. Deviations of the two may be due to many differences in settling and boundary conditions between laboratory tests and reality. Certain departures must be allowed and a variation of parameters should be accounted for in the analysis.

It should be remarked that, in cases when there is no experimentally determined settling velocity function,  $v_s$  can be merely taken as an optimization variable and the parameters of the chosen function are determined so as to minimize the differences between calculated and measured data (using the least squares method, for example). In a mathematical sense, this problem is simpler than the empirical approach above. However, a numerically independent adjustment of the functions for  $z_f$  and  $z_s$  may give better results due to the (possible) physical limitations of the theory of settling velocity applied in real situations.

Table 3.1 Governing equations for the sedimentation model with time-dependent density in suspension

<hr/>		
$v_s = v_s(s_f)$		
$\dot{h}_s = \dot{z}_s = \frac{s_f}{s_{cr}} \cdot \frac{\rho_f}{\rho_{sed}} \cdot v_s$		$z_s^{t+dt} = z_s' + \dot{z}_s dt$
$\dot{h}_w = -\dot{z}_f = \left(1 - s_f\right) \cdot \frac{\rho_f}{\rho_w} \cdot v_s$		$z_f^{t+dt} = z_f' + \dot{z}_f dt$
$\dot{h}_f = -(\dot{h}_w + \dot{h}_s) = \dot{z}_f - \dot{z}_s$		$h_f^{t+dt} = h_f' + \dot{h}_f dt$
$\dot{\rho}_f = \frac{\dot{z}_s(\rho_f - \rho_{sed}) + \dot{z}_f(\rho_w - \rho_f)}{h_f}$		$\rho_f^{t+dt} = \rho_f' + \dot{\rho}_f dt$
$\dot{s}_f = K \cdot \dot{\rho}_f$	$K = \frac{[s_f(\rho_w - \rho_s) + \rho_s]^2}{\rho_w \rho_s (\rho_s - \rho_w)}$	$s_f^{t+dt} = s_f' + \dot{s}_f dt$
<hr/>		

## 3.2 SOLVED EXAMPLES

### 3.2.1 Checking the method by simplification to the Kynch theory

As it was shown in Chapter 3.1.3, it is possible to reduce the present theory to Kynch's theory, assuming a constant concentration in the suspension region. Several examples were found in the literature in which a typical Kynch behaviour was observed or calculated. Unfortunately, the necessary data for checking the model were not generally provided, as a rule, so that only one complete example could be found. This example will be solved using the proposed method in order to demonstrate its validity.

#### 3.2.1.1 Toorman (1998)

The example is taken from Toorman's reply to Gudehus' discussion (1998). Toorman has simulated the settling of spherical glass beads, and the result presented in his paper is reproduced here as Figure 3.3.a. The density profile was computed using the finite element method on a fixed Eulerian grid with 1000 nodes. Particles were  $67\text{ }\mu\text{m}$  in diameter with a specific gravity of  $\rho_s = 2450\text{ kg/m}^3$ , and the initial solids concentration was  $c^o = 0.15$ ; i.e. the initial solids content (by weight)  $s^o = 0.302$  and initial height  $H_o = 31.2\text{ cm}$ .

The positions of the phase boundaries were graphically read from Figure 3.3.a and entered as input data in a simplified variant of the proposed method. The constant volumetric concentration in the sediment was also determined from the picture as  $c_{cr} = 0.64$ , and the corresponding solids content (needed by the program) was calculated as  $s_{cr} = 0.81$ . Since the particle settling velocity function was not known in advance, the solution was obtained by optimizing the numerical response. The least squares method was applied to the suspension settlement data only.

The settlement diagram for this problem is plotted in Figure 3.3.b. Measured data are shown by points and the calculated response by lines. An almost perfect matching was obtained.

The settling velocity of particles falls within the typical range for silts and it matches well the actual grain size of  $0.067\text{ mm}$ . Assuming that the Stokesian regime is valid, an "equivalent grain size" of  $0.050\text{ mm}$  was determined from the calculated settling velocity  $v_s$ . Comparing this value with the real diameter of the glass spheres ( $0.067\text{ mm}$ ), it may be concluded that the effect of hindered sedimentation is an apparent decrease of the particle size, if the problem were thought of as Stokesian.

It seems that Toorman's problem is very similar to the problem considered by Auzeais et al. (1988); see Chapter 2.3.

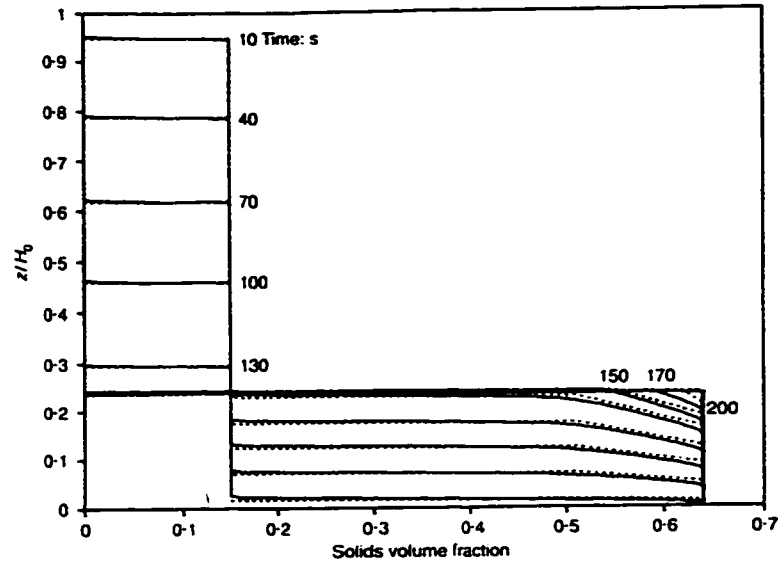


Fig. 1. Computed density profiles for 67- $\mu\text{m}$  spherical glass beads ( $\rho_s = 2450 \text{ kg/m}^3$ ): (---) analytical solution (Kynch's sedimentation theory); (—) finite element solution on a fixed Eulerian grid (1001 nodes). Initial height  $H_0 = 0.312 \text{ m}$ ; initial solids concentration  $\phi_0 = 0.15$

Figure 3.3.a Test example - simulation of glass beads settling (Toorman, 1998)

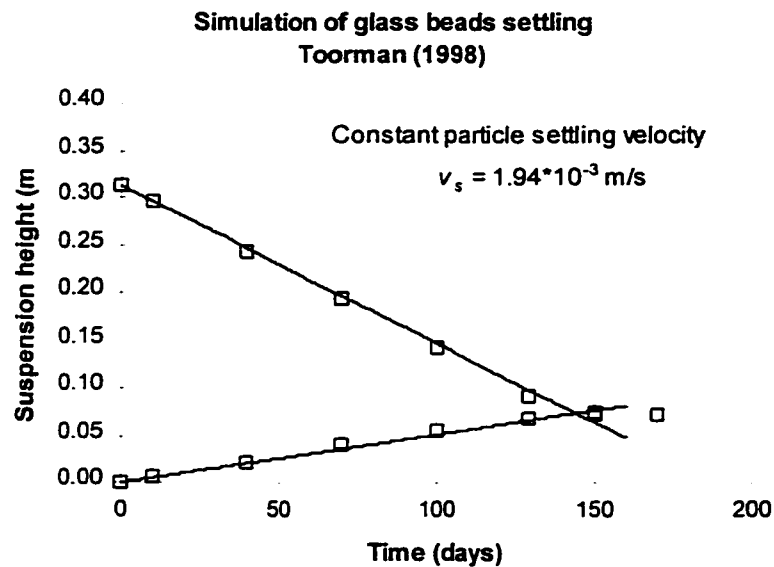


Figure 3.3.b Settlement diagram for Toorman's problem, obtained by the proposed method (squares = Toorman's data, lines = calculated)

### **3.2.2 University of Alberta large scale sedimentation tests on oil sands fine tailings**

#### **3.2.2.1 Material properties and behaviour**

The next two examples are related to the waste material produced in the process of bitumen extraction from oil sands at the Syncrude plant in Alberta. These are actually large scale sedimentation tests that have been performed (and are still being carried out) at the University of Alberta, the so-called 10 metre and 2 metre standpipe tests (Scott et al, 1986; Suthaker, 1995; Suthaker, Scott and Miller, 1997). Experimental setups for these tests are shown in Figures 3.4.a and 3.4.b.

The material for the 10 m standpipe test is an “average mature fine tailings” (MFT) with a solids content of about 30 %, reached after 3 years in a settling pond. The fine tailings is dominantly kaolinite (55% to 65%) and illite (30% to 40%) with traces of other clay minerals. The average grain size curve is shown in Figure 3.5.a (Suthaker, Scott and Miller, 1997). In the oil sands industry sand is defined as material coarser than 45 mm, so that the fine tailings is about 10% fine sand, 40% silt and 50% clay-sized. The position of the MFT in a plasticity diagram, relative to other mine wastes, is shown in Figure 3.5.b.

The material for the series of 2 m tests was the same tailings with a solids content ranging from 21% to 32% and a varying percentage of coarser material (sand). Figure 3.6.a reproduces a table with material properties from Suthaker (1995) and Figure 3.6.b presents the grain size distributions.

The bitumen content is around 2%, based on the total mass, or 6.5%, as a percent of the minerals. The bitumen was found to be responsible for many strange aspects of the tailings behaviour, particularly for the hydraulic gradient dependent permeability, which was attributed to viscous deformation of the bitumen (Suthaker, 1995). The material also exhibits high thixotropic strength, due to development of a particle structure - gel network (Tang et al. 1997), and a large creep with values similar to those of organic soils. Very unusual sedimentation behaviour, as described earlier in Chapter 2.3.1.7, has been observed for 15 years (Suthaker, Scott and Miller, 1997).

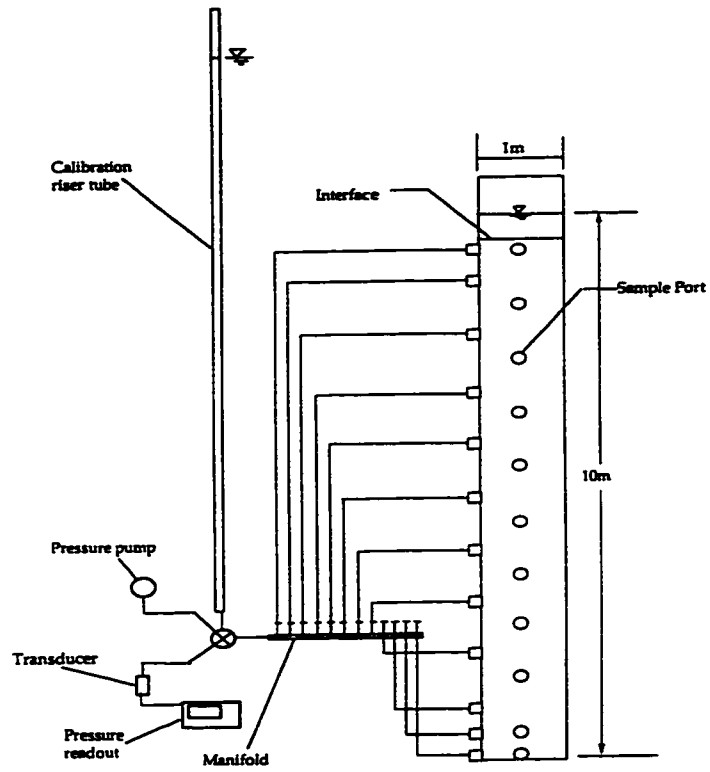


Figure 3.4.a 10 m standpipe test setup

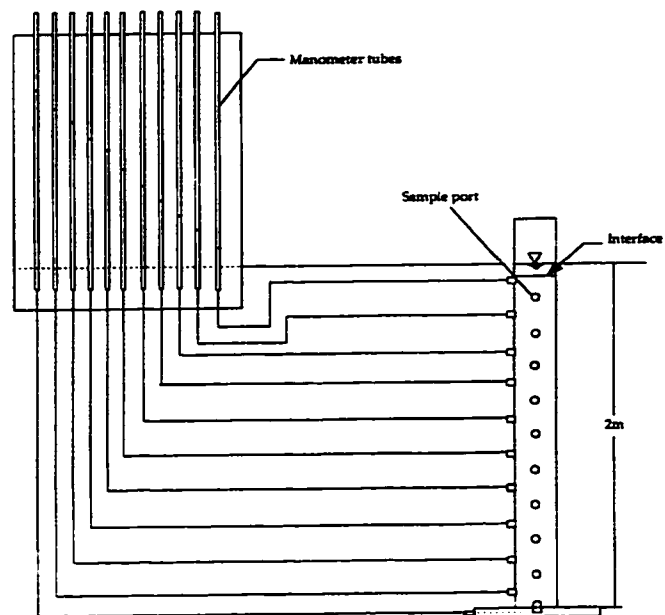


Figure 3.4.b 2 m standpipe test setup

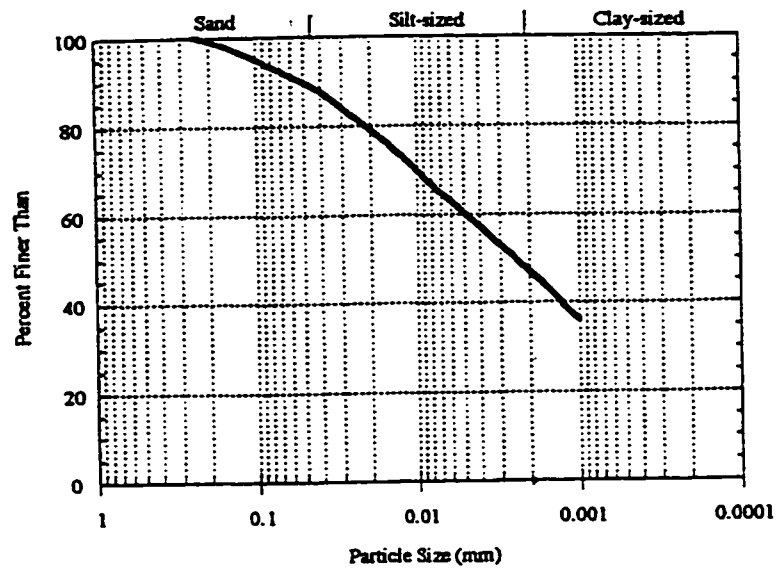


Figure 3.5.a Grain size distribution diagram for 10 m standpipe material

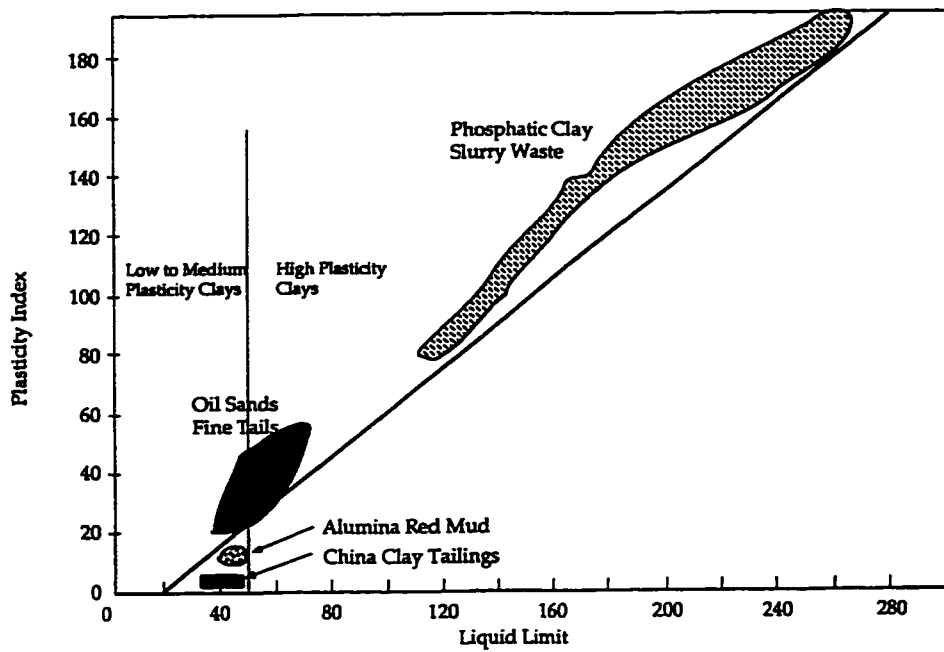


Figure 3.5.b Plasticity of the 10 m standpipe material

Standpipe No.	Initial Height (m)	Initial Solids Content (%)	Fines Content (%)	Origin	Duration (days)
A	2	31.9	90	Syncrude	1200
1	1.993	25.67	96	Syncrude	840
2	1.996	21.38	96	Syncrude	835
3	1.995	24.88	90	Syncrude	830
4	1.985	26.4	89	Syncrude	580
5	1.997	23	86	Syncrude	580
6	1.8	27.95	89	Suncor	330

Figure 3.6.a Material properties in 2m standpipe tests

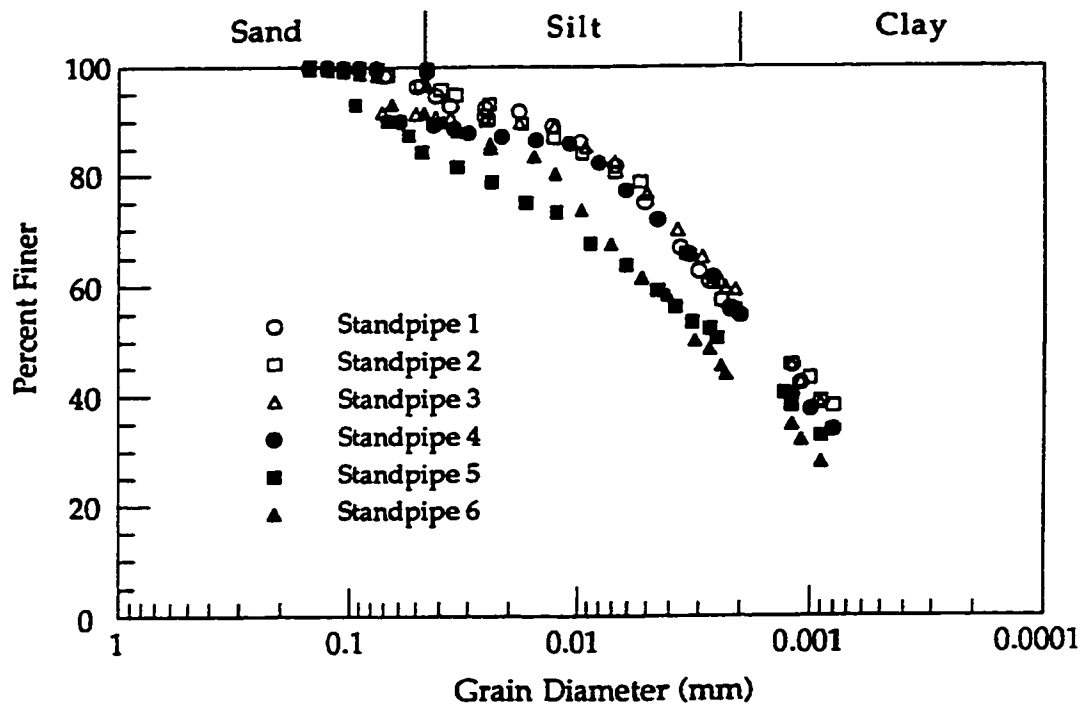


Figure 3.6.b Grain size distribution of 2m standpipe test material



### 3.2.2.2 Possibilities of presently used methods of analysis

Presently there are basically two techniques for predicting the sedimentation and consolidation behaviour of the oil sands fine tailings. Pollock's model (1988) is based on Gibson's finite strain consolidation theory and allows for non-linearity in the permeability and deformability parameters, expressed in the power law form (straight lines in semi-logarithmic scales). The original program did not incorporate creep in the sediment layer, but its modification does (Skopek and McRoberts, 1997). This model is able to calculate the settlement rate and pore pressures in the sediment layer, but fails to predict the concentration profile and the sedimentation stage in general—the existence of a hindered zone and all related phenomena. This limitation is obviously due to the inherent assumptions in the theory and *a priori* treatment of the suspension as a “soil”.

The hindered settling model by Eckert et al. (1996) combines sedimentation and consolidation using fluid dynamics concepts. This model can predict the sedimentation stage accurately and fit the settlement rate and the sediment growth rate. It does not provide any pore pressure information (although it seems that some algebraic manipulations can provide such results). Moreover, assuming a constant solid concentration in the hindered sedimentation zone, as was done in this model, contradicts experimental observations.

It was shown by the authors that this model reduces to Gibson's finite strain theory (1967) in a consolidating sediment. According to Skopek and McRoberts (1997), this model gives similar results to Pollock's consolidation model with the same input data. Skopek and McRoberts (1997) used Pollock's modified method with creep to simulate the 10 m standpipe test. Their results are chosen for comparison with the method proposed in this study.

### 3.2.2.3 Comparison of the results for 10 m standpipe with the consolidation theory

Before examining the results of the analysis, it should be mentioned that the oil sands fine tailings is not a very good material for validating a sedimentation theory due to its long lasting sedimentation and, consequently, pronounced consolidation effects that simultaneously occur. However, 10 m and 2 m standpipe tests are the most detailed and comprehensive ones that could be found in the literature, and they are simply the best source of data for checking and comparing the results of calculation.

In discussing the results for the tailings examples, it must be understood that the method derived here is a sedimentation theory and the effects of consolidation are not included in the analysis.

Figure 3.7 shows the suspension settlement with time, together with the complete set of input data for the calculation. This is actually the input data sheet in the spreadsheet program MS Excel in which the procedure has been programmed. The settling function was deliberately formulated in its simplest possible form, which is a linear function  $v_s = A \cdot s + B$ . It was mentioned earlier in Chapter 3.1.3.2 that even such a simple function can fit the data well if the range of concentration variability is not very wide and the “true” settling velocity function is not excessively curved. Since there was no

predefined settling velocity function for the tested materials, the parameters A and B were determined as the best fit values using the least squares procedure applied to the measured data of the suspension settlement.

Figures 3.8 to 3.14 present the calculated results and the laboratory measurements of density profiles and excess pore pressure distributions with depth, at various times. The calculation for the same problem, using a consolidation theory (Skopek and McRoberts, 1997) in which the suspension layer is treated as a consolidating soil, is also shown in these diagrams (the dashed lines). These data were obtained using non-linear permeability and compressibility laws and creep, with the relevant parameters increased or decreased from the measured values in order to obtain the best possible matching with experimental data. Although some of these parameters are far beyond measured ranges or even logically acceptable limits, they were adopted “as they are” since in this case they represent the optimum attainable values using the consolidation approach.

Comparing the results of the sedimentation approach and the consolidation approach, it can be seen that both methods are equally good at the beginning stages of the test, but that the sedimentation method gives better results as time progresses, particularly for the density profile. The density profile derived from the consolidation theory is inherently a curved line which cannot be adjusted to match the apparently constant trend of the measured data in the suspension zone. On the other hand, the step change in density obtained by the sedimentation method does not properly fit the density curve in the lower portion of the settling column, where gradual change occurs due to mixed thickening of the suspension and consolidation of already sedimented layer (“soil” layer). It was mentioned earlier that a sedimentation theory is not capable of encompassing consolidation phenomena.

Both theories fail to predict the variation of solids content with depth, which has an interesting profile whose shape evolves in time due to changing settling velocity within the test column.

**Material data:**

Water density $\gamma_w =$	9.81 kN/m <sup>3</sup>
Solids relative density $G_s =$	2.28
Specific solids density $\gamma_s =$	22.37 kN/m <sup>3</sup>
Critical solids content $s_{cr} =$	0.42
Critical sediment density $\gamma_{sed} =$	12.837 kN/m <sup>3</sup>
Initial height $H =$	10.00 m

**Parameters of solids velocity function:**

Linear function $v = A s + B$	
$A =$	-8.00E-03 m/day
$B =$	3.36E-03 m/day

**Initial state:**

Solids content $s_0 =$	0.306
Suspension density $\gamma_i =$	11.845 kN/m <sup>3</sup>
Concentration $c_0 =$	0.162

**Calculation:**

$\Delta T =$	10 days
--------------	---------

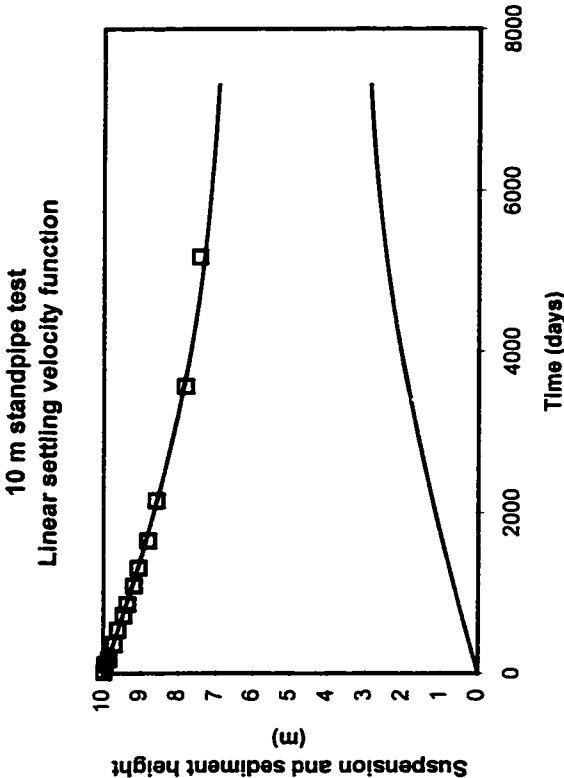


Figure 3.7 10 m standpipe test - the input data sheet for interactive optimization of the proposed sedimentation model with the diagram of measured and calculated settlement of the suspension surface; the linear settling velocity function

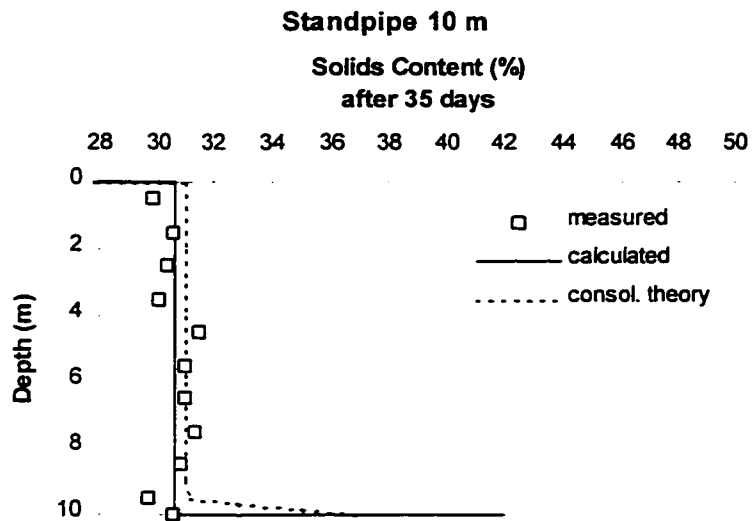
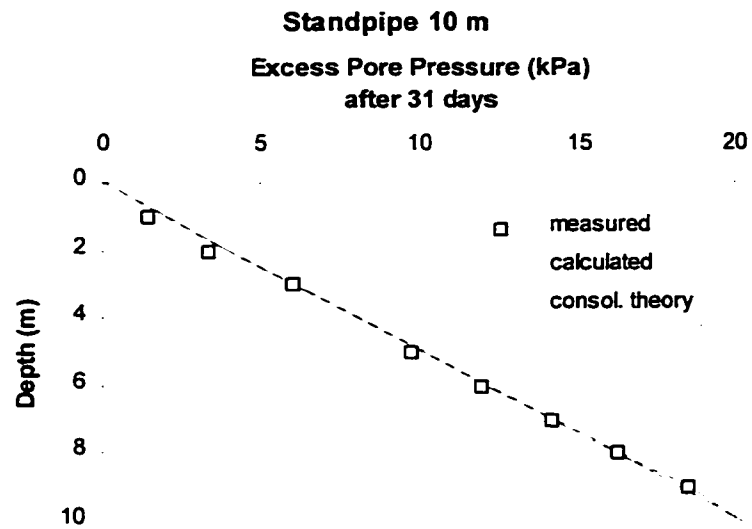


Figure 3.8 10 m standpipe test;  
excess pore pressure and solids content distributions  
after 31 days

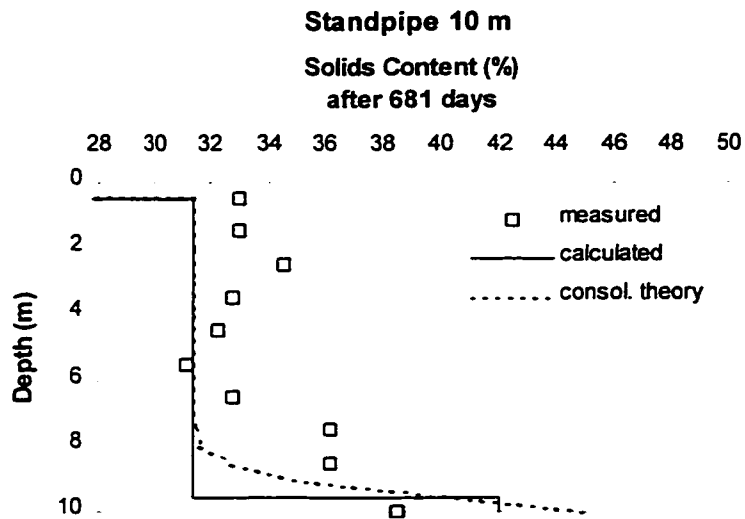
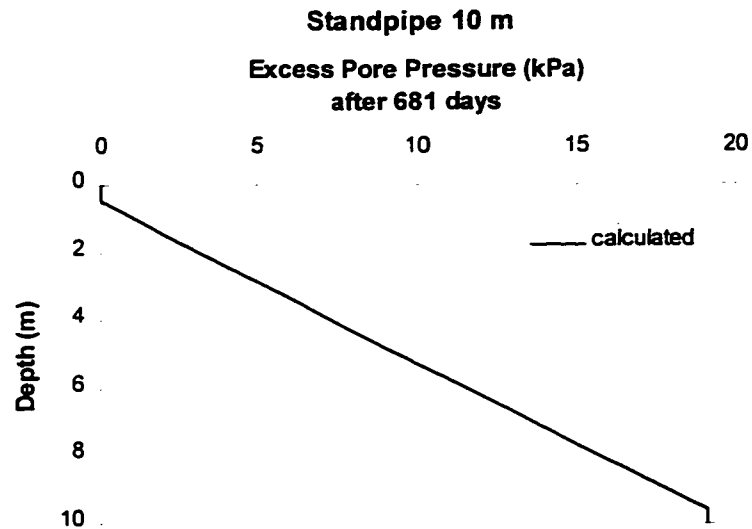


Figure 3.9 10 m standpipe test;  
excess pore pressure and solids content distributions  
after 681 days

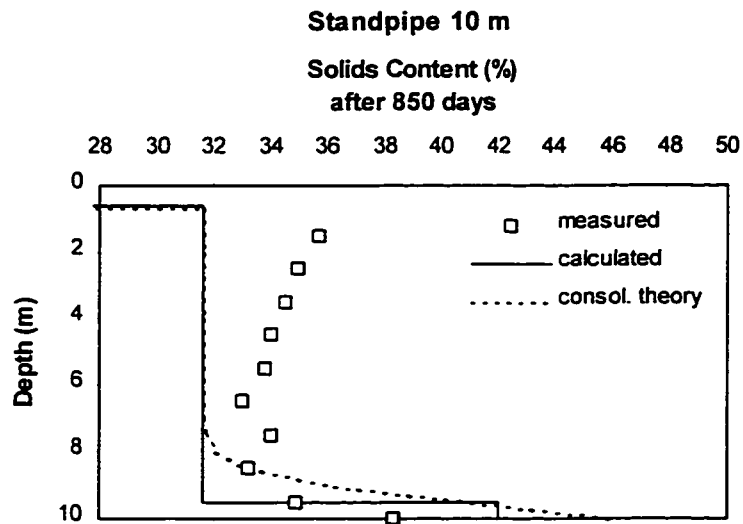
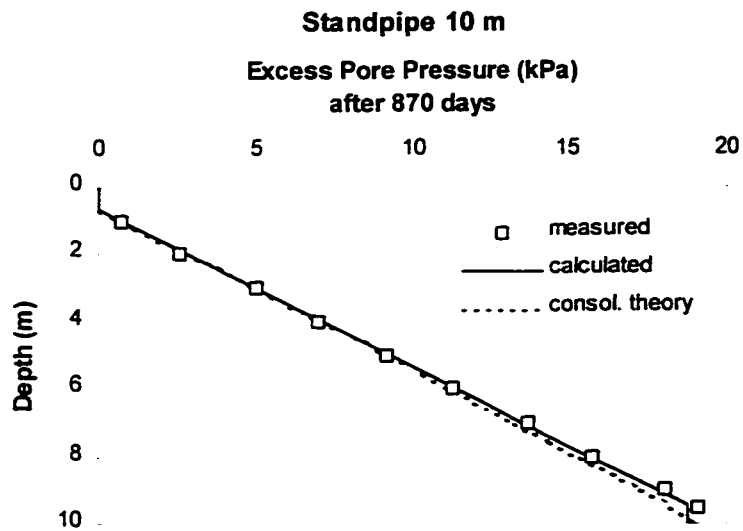


Figure 3.10 10 m standpipe test;  
excess pore pressure and solids content distributions  
after 870 and 850 days, respectively

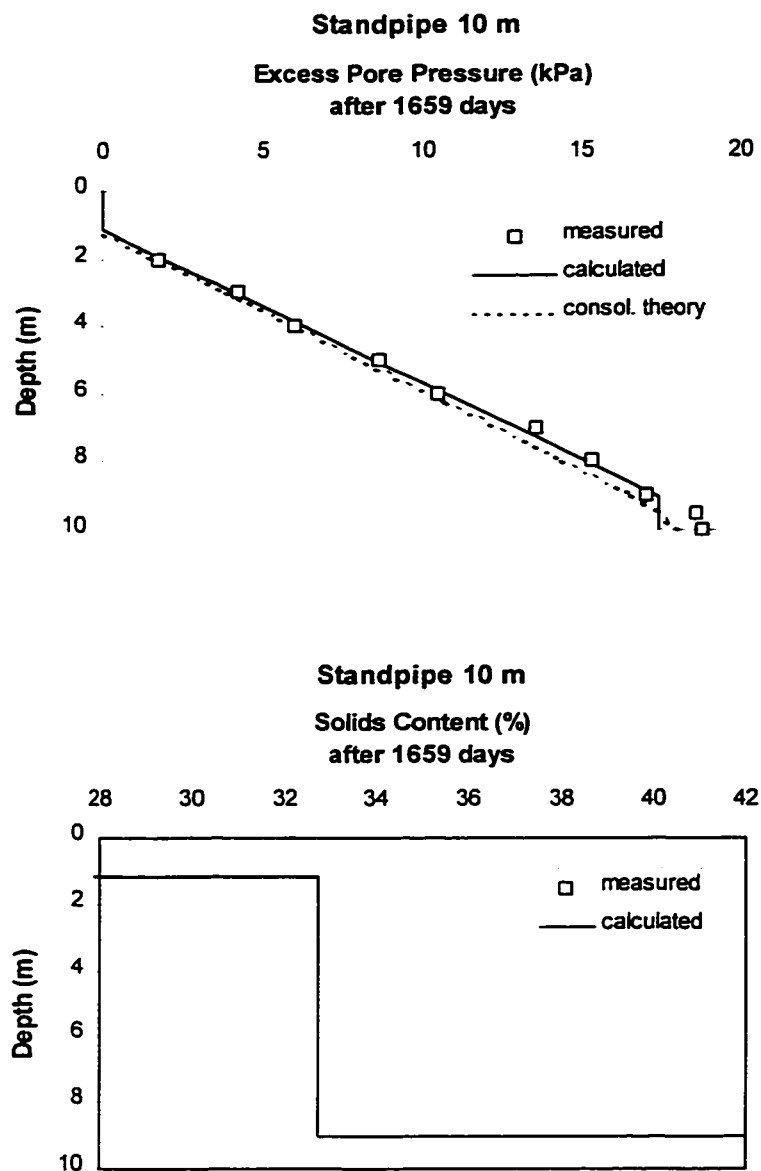


Figure 3.11 10 m standpipe test;  
excess pore pressure and solids content distributions  
after 1659 days

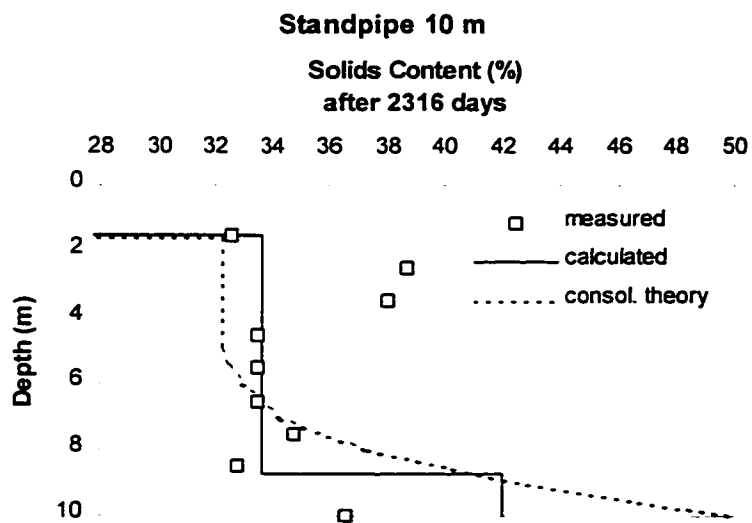
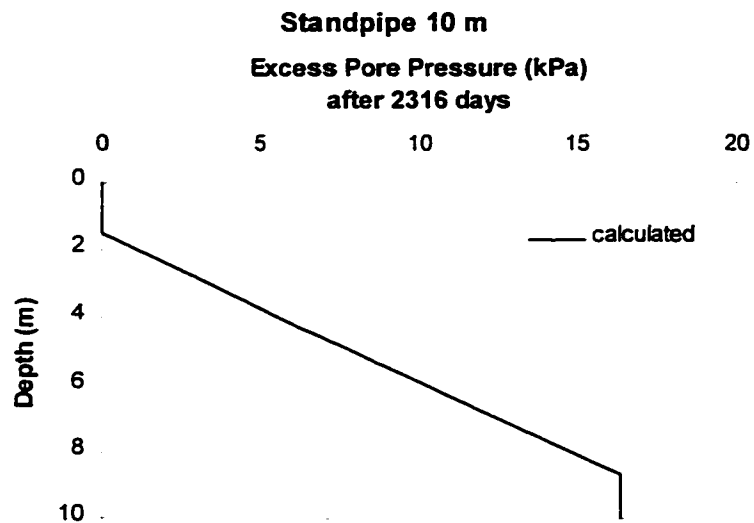


Figure 3.12 10 m standpipe test;  
excess pore pressure and solids content distributions  
after 2316 days



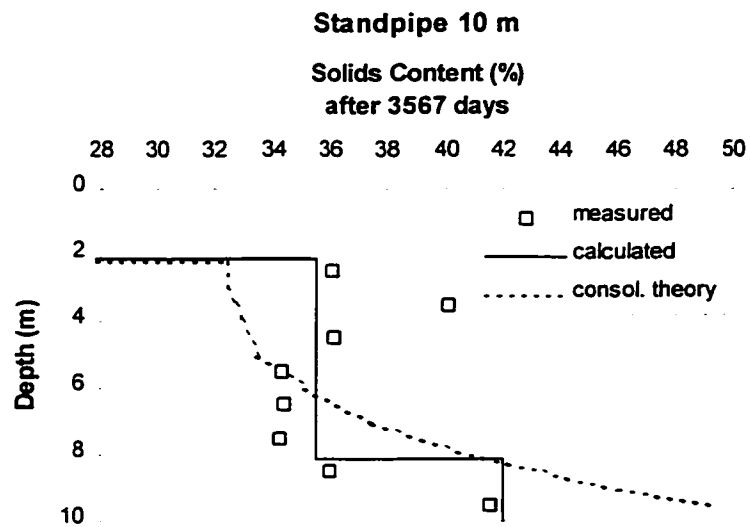
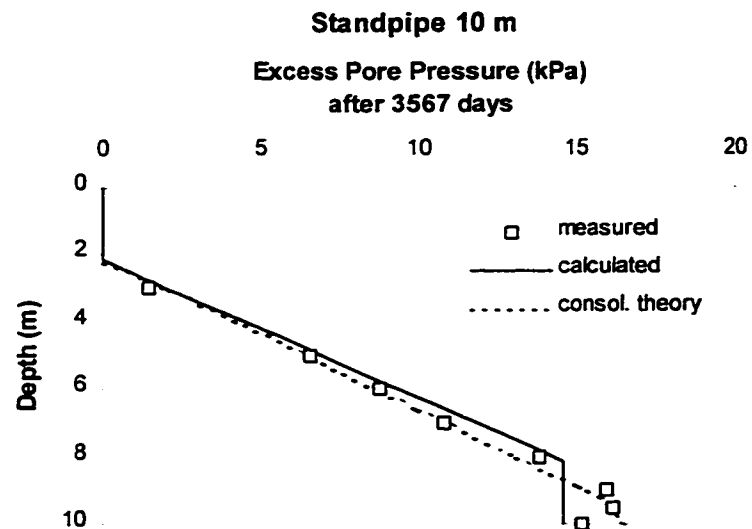


Figure 3.13 10 m standpipe test;  
excess pore pressure and solids content distributions  
after 3567 days

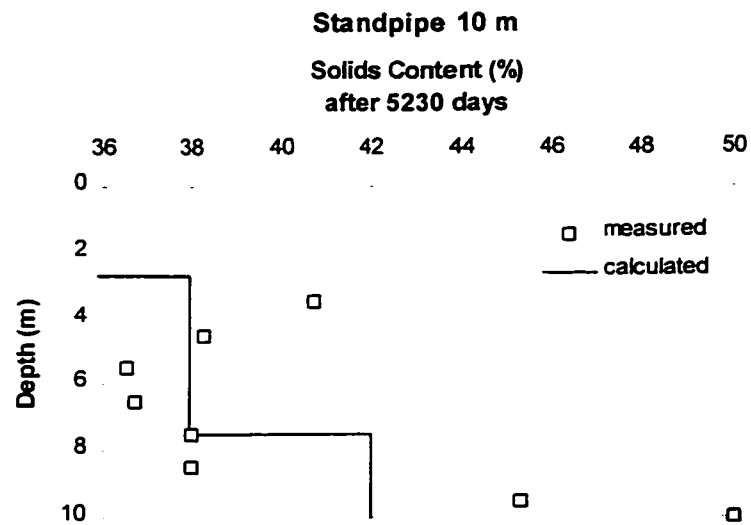
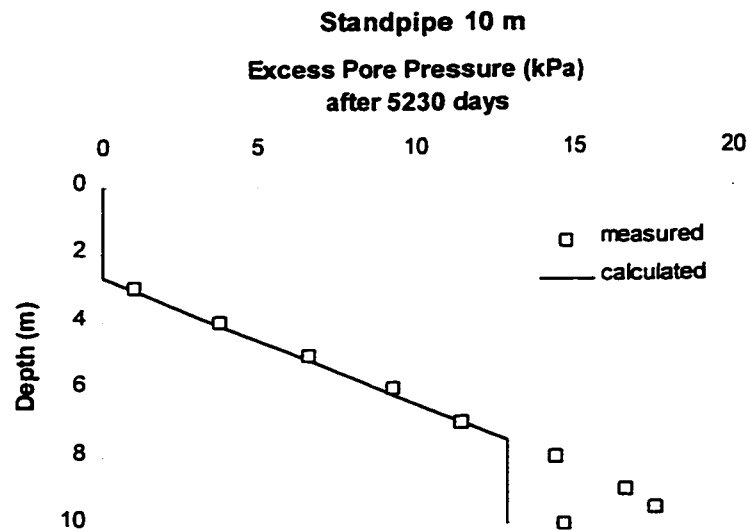


Figure 3.14 10 m standpipe test;  
excess pore pressure and solids content distributions  
after 5230 days

### *The influence of different mathematical forms of the settling velocity function*

Three mathematical functions were used to represent the particle settling velocity in the proposed sedimentation model. They are: a linear function (a straight line, the simplest possible form), a polynomial (the Richardson and Zaki function) and a mixed rational-power function (i.e. a power law permeability function is used to express the initial settling velocity in a suspension, Pane and Schiffman 1997; this will be explained in more detail in the following text). All three functions gave the results practically coincident with those shown in Figures 3.7 to 3.14. The explanation of this effect is found in Figure 3.15, where all the velocity functions are plotted against solids content. For solid contents between the initial state  $s_0 = 0.306$  and the critical value  $s_{cr} = 0.42$  in the sedimented layer, all three functions provide approximately the same settling velocities (but this is not true for higher or lower solid contents). The velocity curves actually bend themselves in an attempt to adapt their shape to a certain “real” settling velocity function which is unknown to us, but which actually governs the behaviour of the real suspension. The success of this “self reshaping” is measured by the magnitude of the variance of the error function (the sum of the squares of the errors) in an optimization procedure which reveals the best-fit parameters.

The fact that the results of the analysis using the proposed sedimentation model are not sensitive to the mathematical form of the settling velocity function provides some comfort in applying the model in real problems.

### *Using the coefficient of permeability to define the settling velocity function*

The settling velocity of the solid particles  $v_s$  to be used in an analysis can be determined from sedimentation tests on a given material. This method appears sound when such a material is available before the analysis stage, a representative sample can be taken and a testing can be finished within a reasonable interval of time. In the case of clayey materials in colloidal suspensions, particularly for tailings and similar by-products of modern mineral processing, artificially generated electrochemical forces between suspended solid particles may have a dominant influence on their overall behaviour and prolong sedimentation time. It is desirable, therefore, to have some preliminary data that enable one to make predictions of the settling behaviour before a real problem itself is brought to life.

In such a case the settling velocity  $v_s$  can be assessed from the permeability tests on a given suspension. Even though such tests are still questionable with regard to the underlying physical processes and interpretation (internal movement of particles, segregation, difficulties in experimental setup, ambiguities in data processing, etc.) the data obtained are undoubtedly very useful in practical analyses.

In the following section will be presented a method proposed by Pane and Schiffman (1997) for estimating the settling velocity  $v_s$  using the permeability tests.

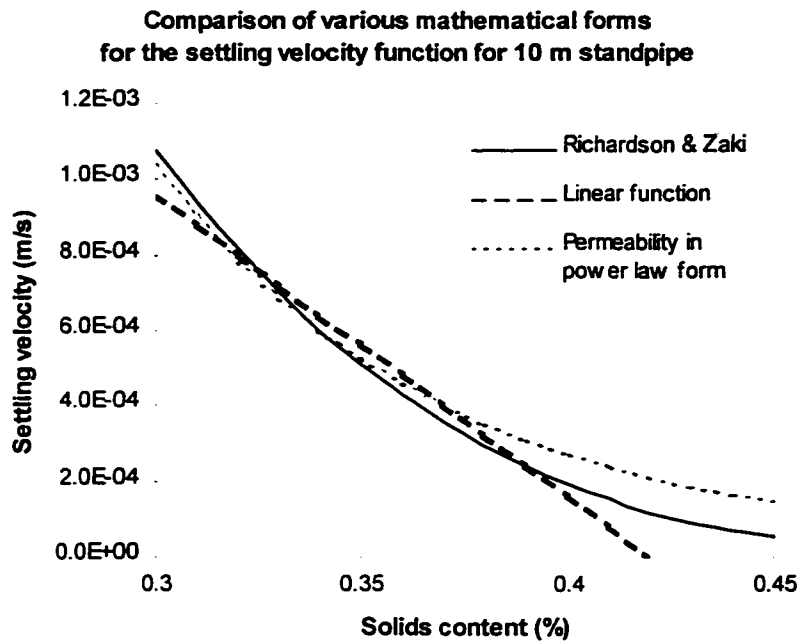


Figure 3.15 10 m standpipe test; comparison of various mathematical forms for the settling velocity function:

Richardson and Zaki  $v_s = A(1 - Bc)^D$

Linear  $v_s = Es + F$

Power law permeability  $v_s = \frac{G_s - 1}{1 + e} \cdot Ge^H$

where:  $c$  is volumetric concentration,

$s$  is solids content (by weight), and

$e$  is void ratio

Pane and Schiffman (1997) state that their experiments in sedimentation and fluidization indicate that the coefficient of permeability varies continuously over a wide range of porosities, encompassing both soil and suspended conditions, and they express the permeability as a two-constant power function of the void ratio. Following the works of Richardson and Zaki (1954) and Been (1980), they determine  $k(e)$  from a sedimentation test on a uniform suspension of void ratio  $e$  as:

$$k(e) = \frac{v_{si}(1+e)}{\frac{\gamma_s - \gamma_w}{\gamma_w}} \quad [3.16]$$

where:  $v_{si}$  is the initial settling velocity of the solids and  $\gamma_s$  and  $\gamma_w$  are the unit weights of solids and water, respectively. Following the same idea and actually extending the  $k - v_{si}$  relationship to the whole sedimentation process, it is possible to express the settling velocity function in the proposed model in the form:

$$v_s = \frac{G_s - 1}{1 + e} A e^B \quad [3.17]$$

where  $G_s$  is the specific gravity of solids and  $A$  and  $B$  are the parameters of the permeability function in a power law form.

The parameters  $A$  and  $B$  may be either:

- known values, defined by a previous permeability testing or simply assessed, or
- optimization variables that have to be defined in the solution process.

Both approaches were used in this example. Firstly, the two permeability functions of Pollock and Suthaker, see Chapter 2.4.1.4, were employed, and then  $A$  and  $B$  were adopted as free variables in the solution process, according to the second option. The results are presented in Figure 3.16.

The settlement versus time diagram in Figure 3.16a shows that the two experimental functions by Pollock and Suthaker bound the real solution within a relatively narrow region. This fact is very important since it provides a link between the settling velocity of a suspension and a soil property that can be determined independently. Therefore, the applicability of the proposed method can be extended to the situations when there is no real, existing pond or settling tank, etc. but its future behaviour has to be predicted on the basis of a general knowledge of the material properties (a common situation in the stage of a preliminary design). The settling velocity function can be reasonably estimated from the known permeability-void ratio relationship in such cases.

Figure 3.16b shows the positions of these three permeability functions in the  $\log k - \log e$  diagram. The relevant range of void ratios is roughly between 3 and 6. It appears at first that the functions do not differ significantly, especially when compared to the ranges of permeability that were used in certain consolidation analyses of this problem (Suthaker, 1995, and Skopek and McRoberts, 1997). At this point, a logical question arises about the sensitivity of the proposed model to the variation of input parameters.

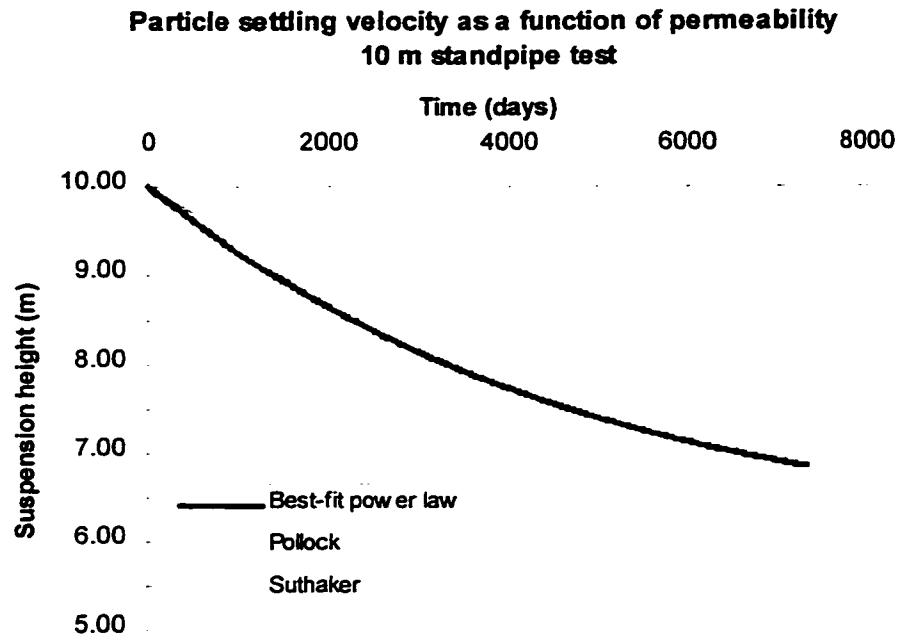


Figure 3.16.a The settling velocity as a function of the permeability;  
the settlement diagram for three different permeability laws

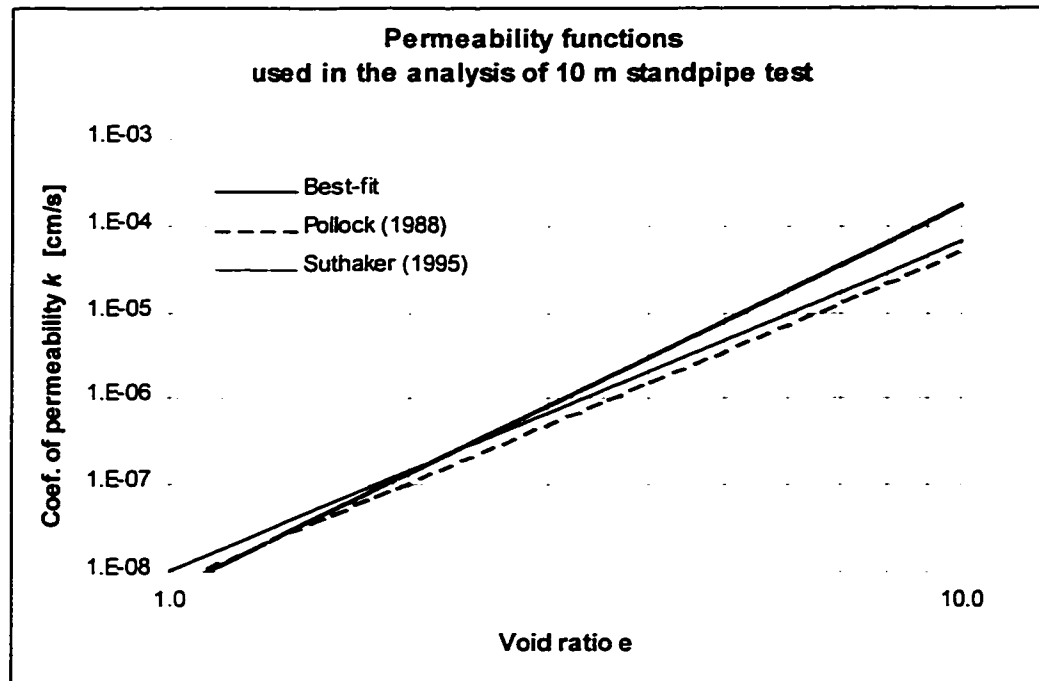


Figure 3.16.b The settling velocity as a function of the permeability;  
the three permeability laws used in the analysis

### *Sensitivity analysis of the proposed model*

The following parameters were chosen:

- the critical solids content  $s_{cr}$  in the sediment, i.e. the liquid-solid transition point,
- the initial solids content  $s_0$  in the suspension,
- the parameters  $A$  and  $B$  of the linear settling velocity function,
- the parameters  $A$  and  $B$  of the settling velocity function which uses the power form permeability law (discussed above).

The influence of the variation of  $s_{cr}$  and  $s_0$  on the results is shown in Figures 3.17 and 3.18, respectively. Both concentrations vary within the range of approximately  $\pm 50\%$  from the optimum values given in Figures 3.7 to 3.14. Only the linear settling velocity function was considered. The solids content in the sediment  $s_{cr}$  has a very limited influence on the initial portion of the solution. The initial concentration  $s_0$ , however, has pronounced influence on the shape of the settlement curve from the very beginning. This could have been predicted by considering the effect of the initial conditions in solving a partial differential equation.

The effect of varying parameters  $A$  and  $B$  of the linear velocity function is shown in Figures 3.19a and 3.19b. The parameters are varied within  $\pm 20\%$  from the optimum values given in Figures 3.7-3.14. It is apparent that both parameters have an equal influence on the result. This could have been expected from the previous discussion on the different mathematical forms of the velocity function as shown in Figure 3.15. A linear function has a “fixed” form and is relatively “stiff” in a geometrical sense. In order to accommodate to the shape of a real settling velocity function which governs the sedimentation behavior, a linear function must change both its “altitude” (vertical position) and slope, therefore both parameters  $A$  and  $B$  must change. A linear function is, more precisely, an interpolation polynomial of the first order applied to the actual settling velocity.

The effect of parameters  $A$  and  $B$  on the power law permeability function (used to define the settling velocity after Pane and Schiffman) is presented in Figures 3.20a and 3.20b. It is obvious that the parameter  $B$ , which is a measure of the slope of a  $k$ - $e$  relationship in a logarithmic scale, has a much greater effect than the parameter  $A$ , which only shifts the  $k$  -  $e$  function, parallel to itself, in the same diagram. This simple analysis indicates that properly estimating the rate of change of the permeability in a suspension is probably much more important in a sedimentation analysis than accurately determining the permeability function itself.

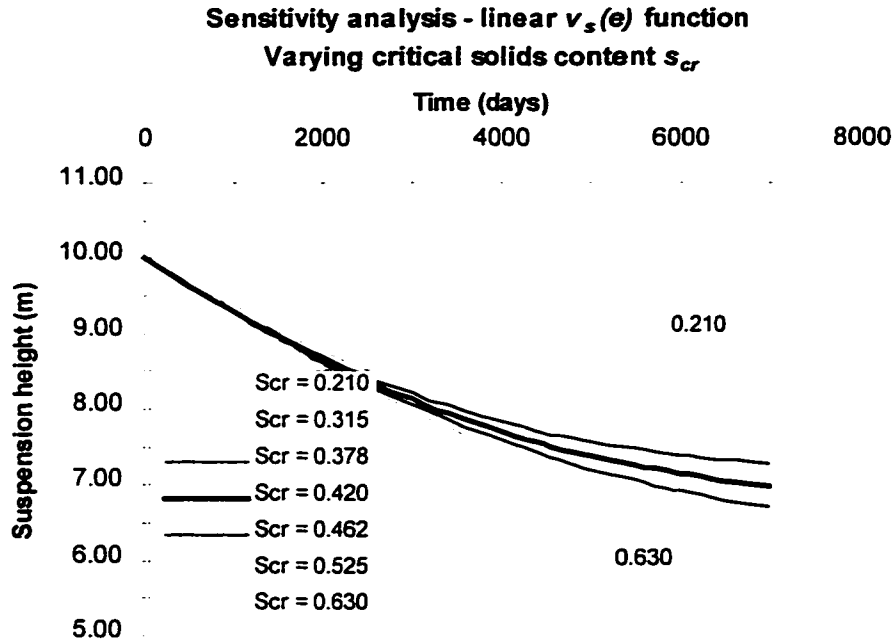


Figure 3.17 Sensitivity analysis of the proposed sedimentation model; the critical solids content varied within the range of  $\pm 50\%$  of the optimum value  $s_{cr} = 0.42$

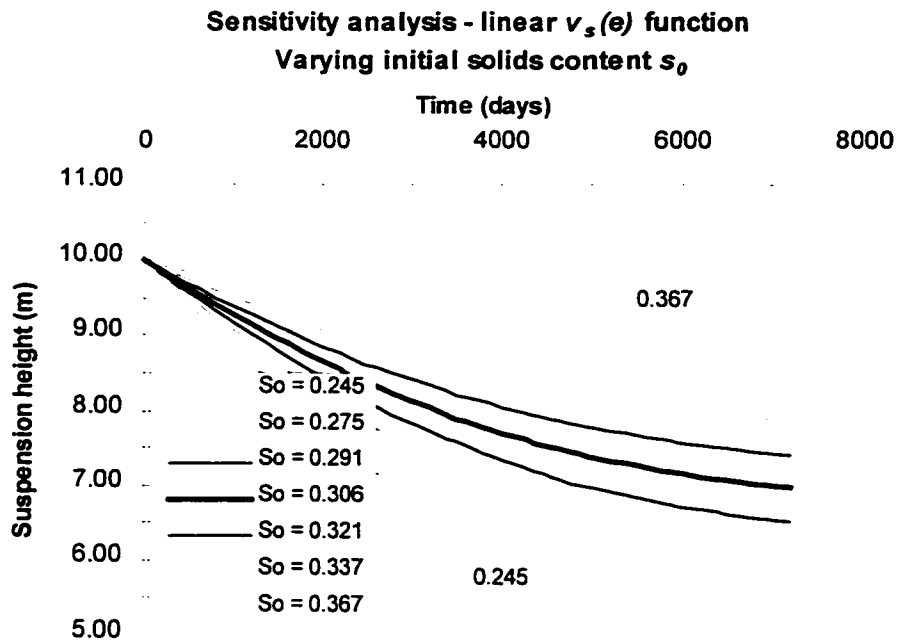


Figure 3.18 Sensitivity analysis of the proposed sedimentation model; the initial solids content varied within the range of  $\pm 50\%$  of the optimum value  $s_0 = 0.306$



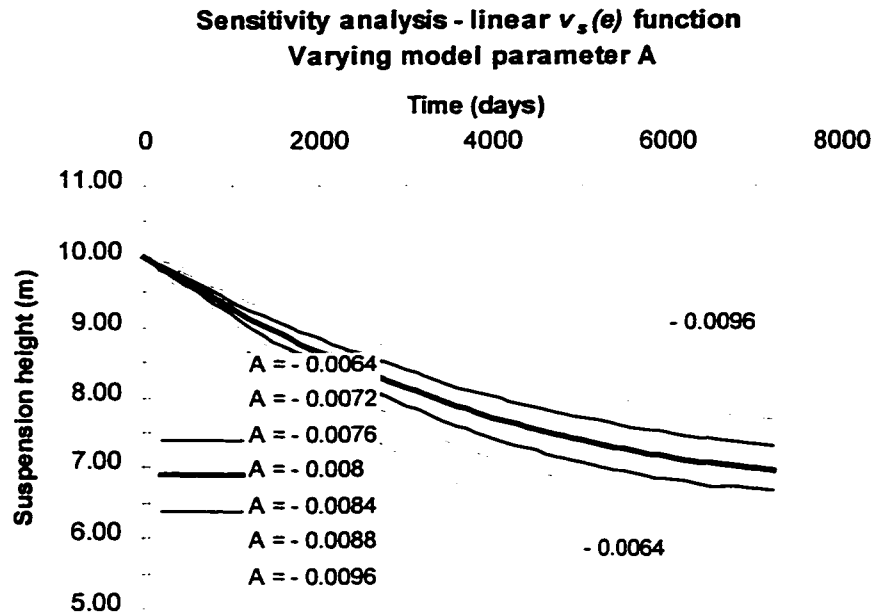


Figure 3.19.a Sensitivity analysis of the proposed sedimentation model; the linear settling velocity; the parameter  $A$  varied within the range of  $\pm 20\%$  of the optimum value

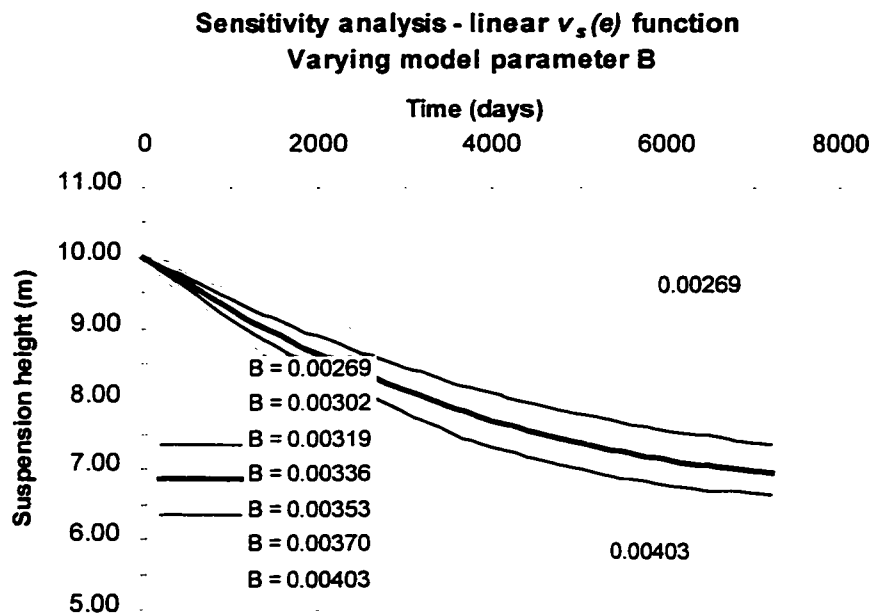


Figure 3.19.b Sensitivity analysis of the proposed sedimentation model; the linear settling velocity; the parameter  $B$  varied within the range of  $\pm 20\%$  of the optimum value

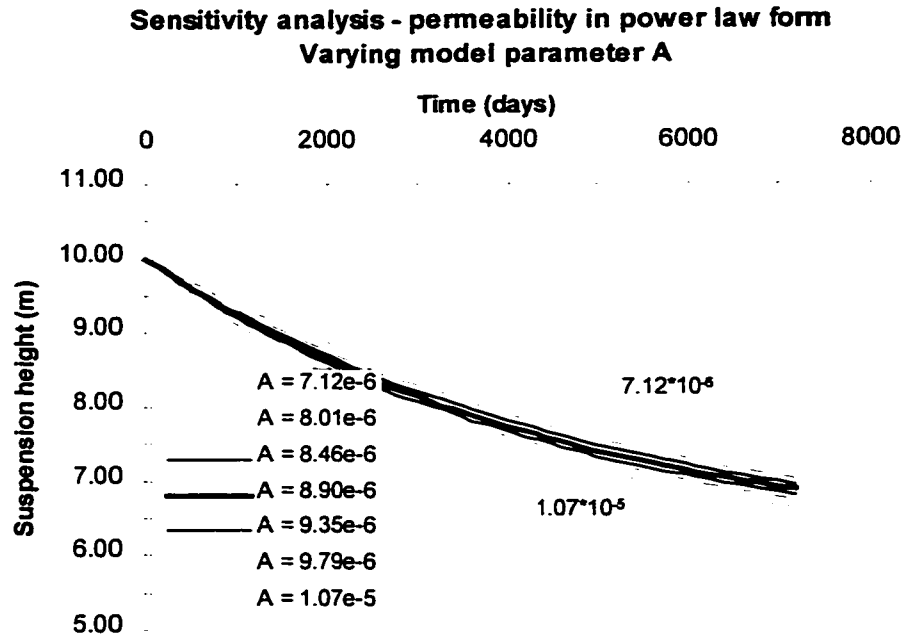


Figure 3.20.a Sensitivity analysis of the proposed sedimentation model; the settling velocity as a function of the permeability; the parameter  $A$  varied within  $\pm 20\%$  of the optimum value

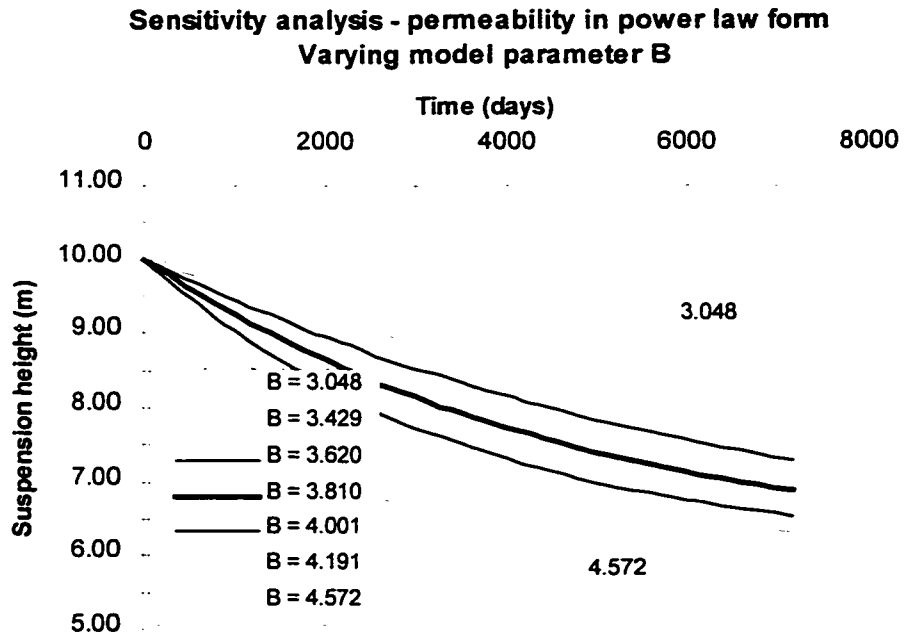


Figure 3.20.b Sensitivity analysis of the proposed sedimentation model; the settling velocity as a function of the permeability; the parameter  $B$  varied within  $\pm 20\%$  of the optimum value

#### **3.2.2.4 Simulation of the 2 m standpipe tests**

Seven 2 m high standpipe tests were performed at the University of Alberta (Suthaker 1995). The material data were given in Chapter 3.2.2.1. The standpipes were continuously monitored for settlement of the water-suspension interface. Pore pressure changes were measured at 20 cm height intervals by small diameter manometers. Samples to determine the density and solids content were obtained using three methods, syringe, port and scoop, each giving rather consistent results. It may be seen from the enclosed diagram in Figures 3.22 to 3.27 that the syringe samples always show a slightly lower concentration than the port samples. A probable cause may be the sampling velocity of the syringe method, which may have been faster than needed, causing more water than solids to enter a syringe.

It should be noted that the measured data are fairly irregular (the causes are not provided in the original reference), a phenomenon which will prevent one from arriving at a definite conclusion when evaluating the proposed model.

The first prediction was made using Pollock's finite strain consolidation model and the program described in Chapter 3.2.2.2, without creep being incorporated (Suthaker 1995). A summary of the input data for this method is given in Figure 3.21. Several sets of input data with different permeabilities were used. The results of the input data sets—"cases" 1, 5 and 6 in this Figure—were presented by Suthaker (1995). They were graphically read from the original paper and reproduced here as dashed lines in Figures 3.22 to 3.27. The choice of these data sets by Suthaker indicates that the coefficient of permeability may have been overestimated in her consolidation analyses.

These tests were also simulated using the proposed sedimentation model, and the results are plotted in Figures 3.22 to 3.27.

It is difficult to estimate the differences quantitatively, but it seems that the proposed model has at least an equal amount of prediction power as the consolidation model, which means neither are very good, since both fail in certain tests (standpipes 1 and 4) particularly in pore pressure and solids content calculations. The possible causes of such discrepancies may include pronounced sedimentation effects (standpipes 1 and 4), a relatively long time of flocculation in the beginning of almost all tests, and possible segregation in the tests with a higher percentage of sand fraction, etc.

Case	Compressibility Model			Permeability Model		
	Compressibility	A	B	Permeability	C	D
1	30 % solids	29.04	-0.3118	Lab. measured	6.16e-11	4.468
2	25 % solids	40.29	-0.3169	Lab. measured	6.16e-11	4.468
3	20 % solids	54.12	-0.3224	Lab. measured	6.16e-11	4.468
4	30 % solids	29.04	-0.3118	Upper limit	6.16e-11	5.361
5	30 % solids	29.04	-0.3118	Lower limit	6.16e-11	4.021
6	30 % solids	29.04	-0.3118	Conservative	6.16e-11	3.574

Figure 3.21 Summary of input data for analysis of 2 m standpipe tests using nonlinear large-strain self-weight consolidation model (Suthaker 1995)

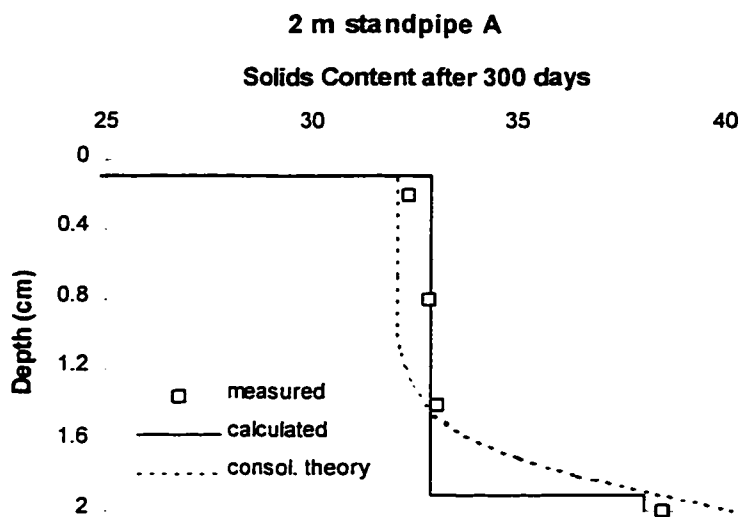
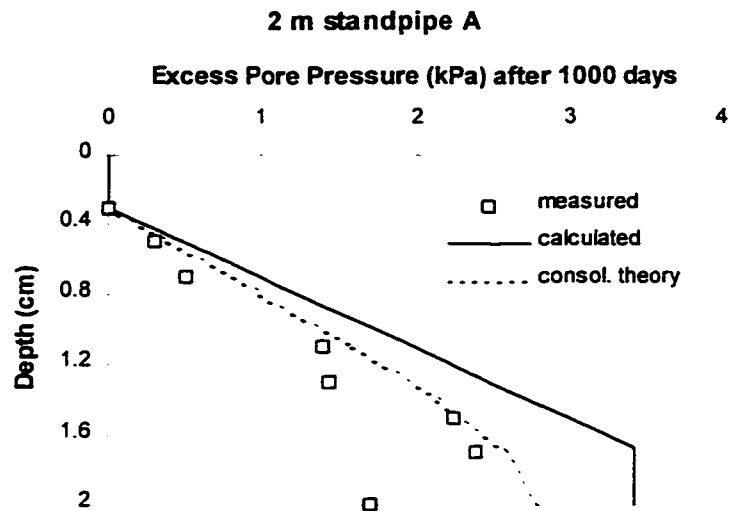
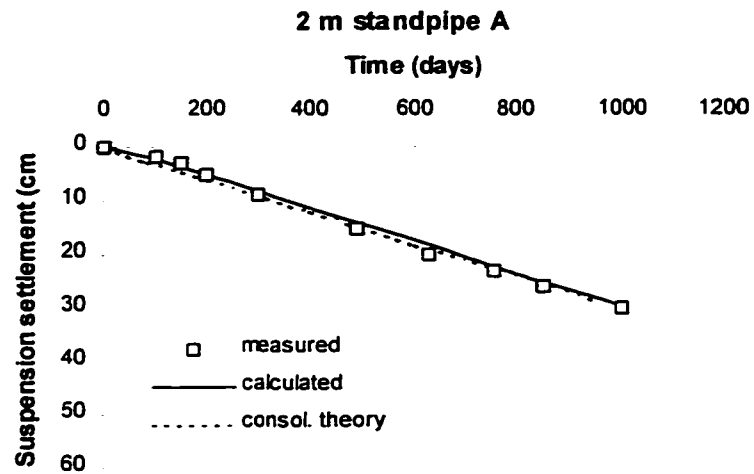


Figure 3.22 2 m standpipe test A

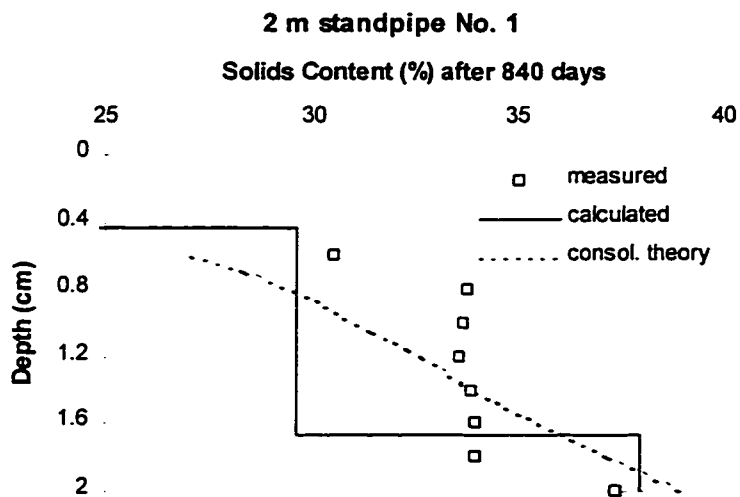
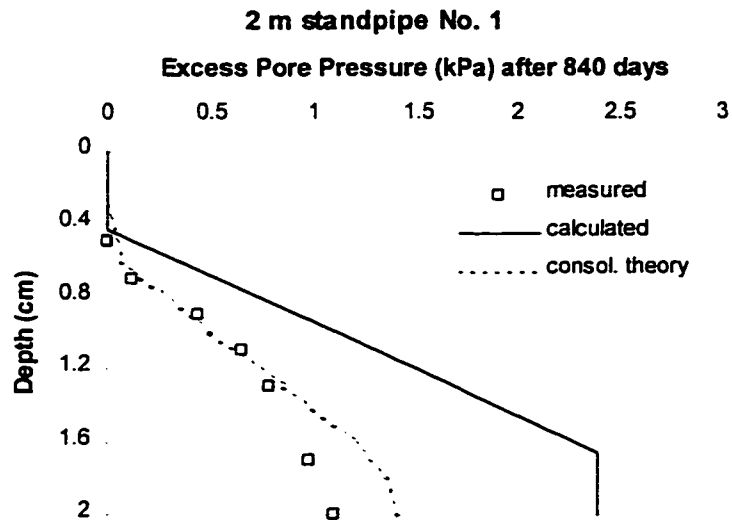
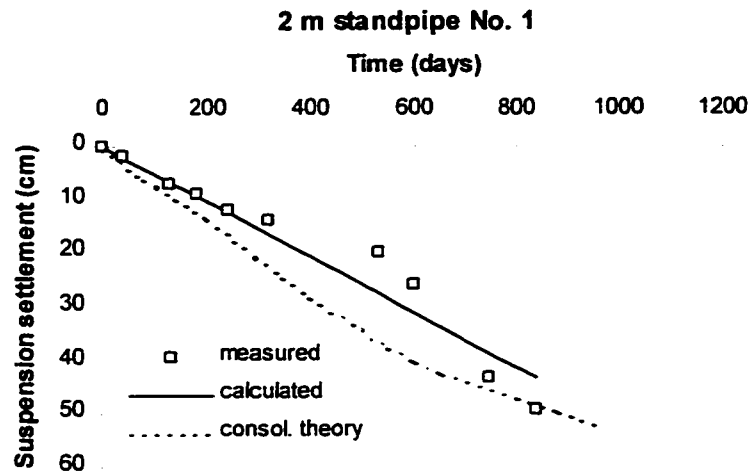


Figure 3.23 2 m standpipe test 1

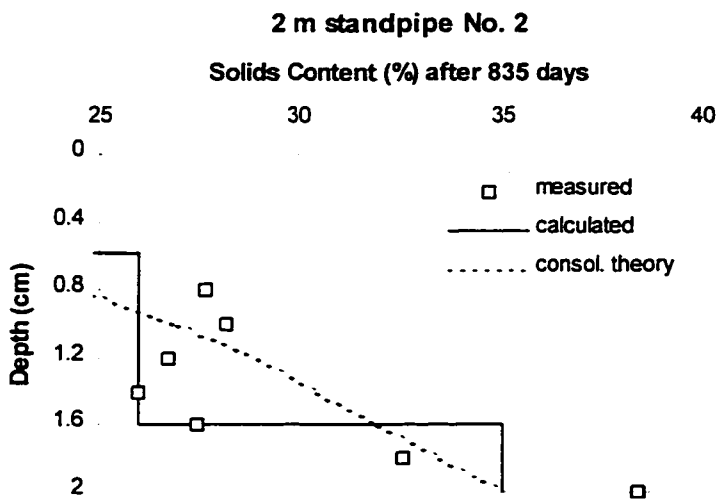
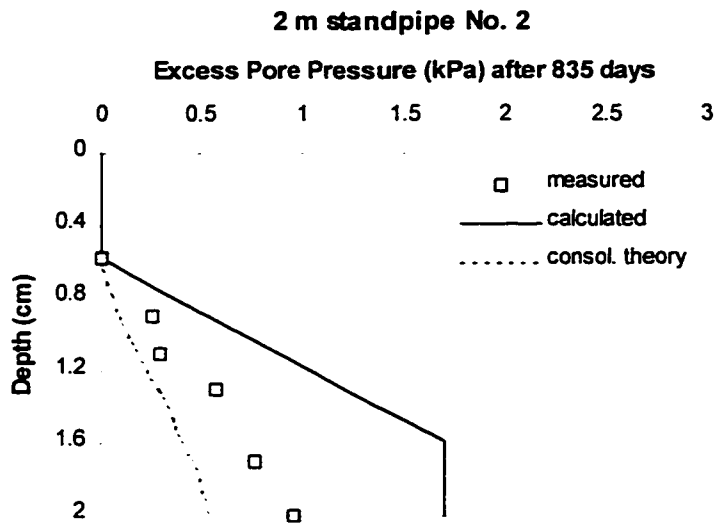
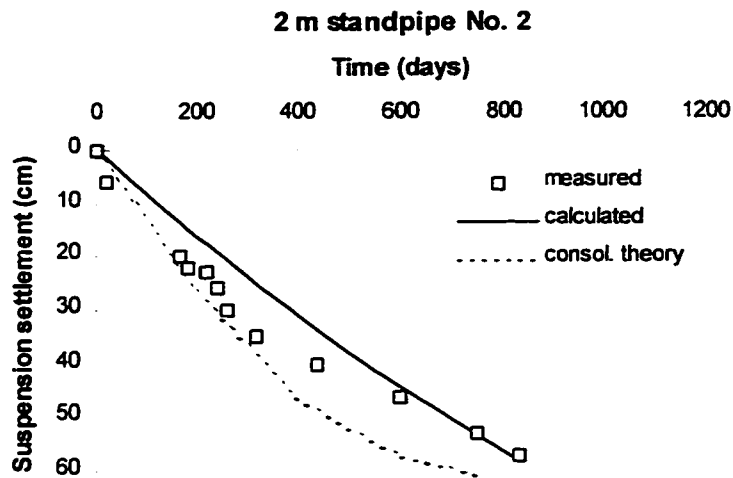


Figure 3.24 2 m standpipe test 2

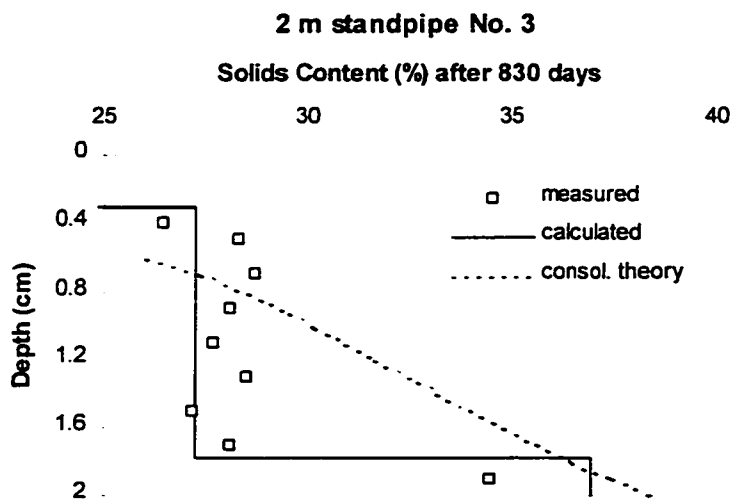
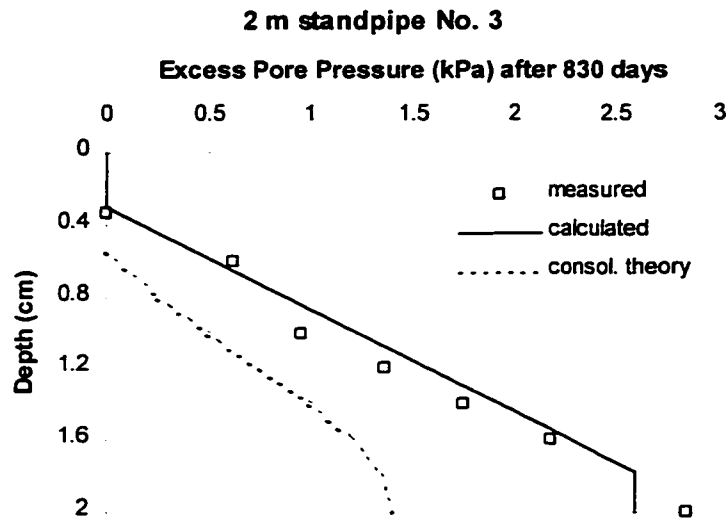
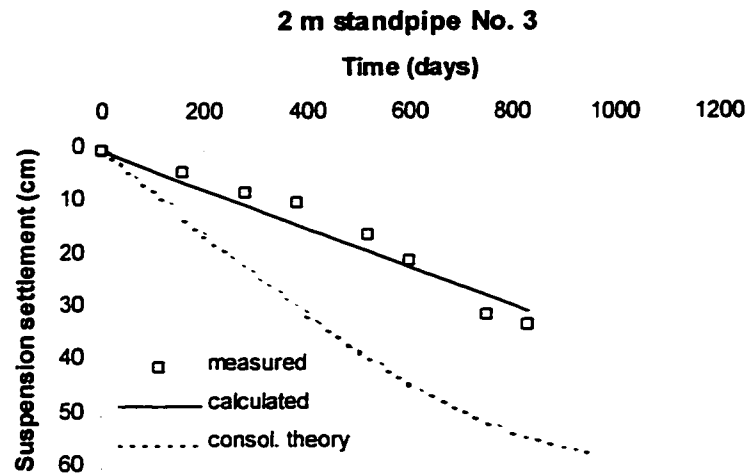


Figure 3.25 2 m standpipe test 3



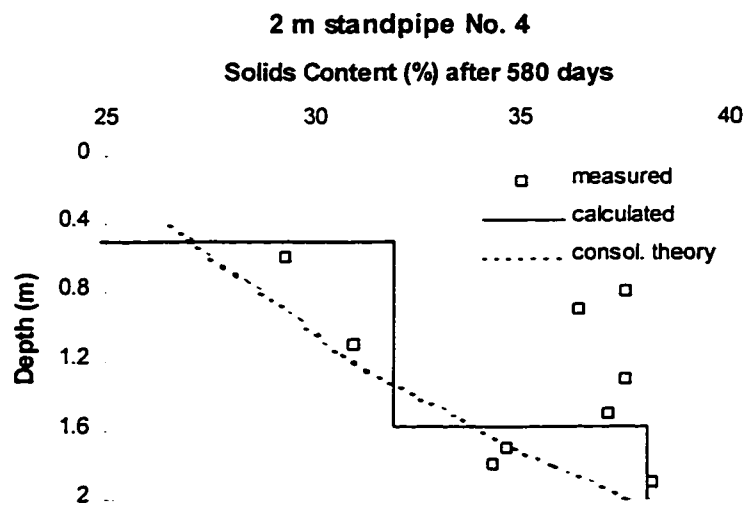
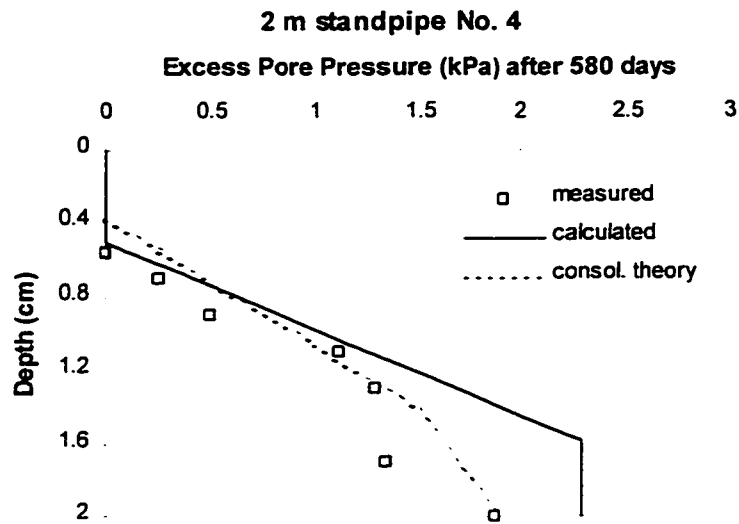
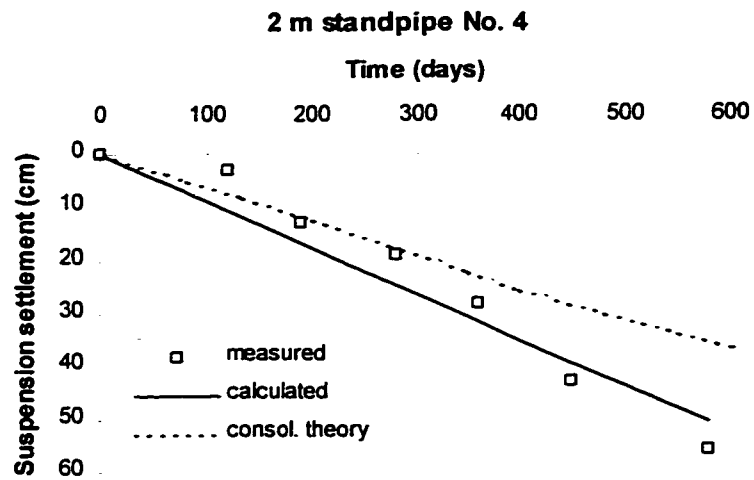


Figure 3.26 2 m standpipe test 4

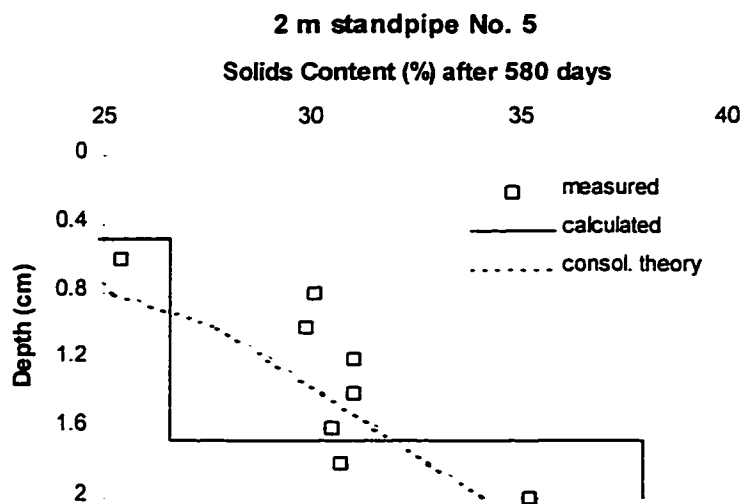
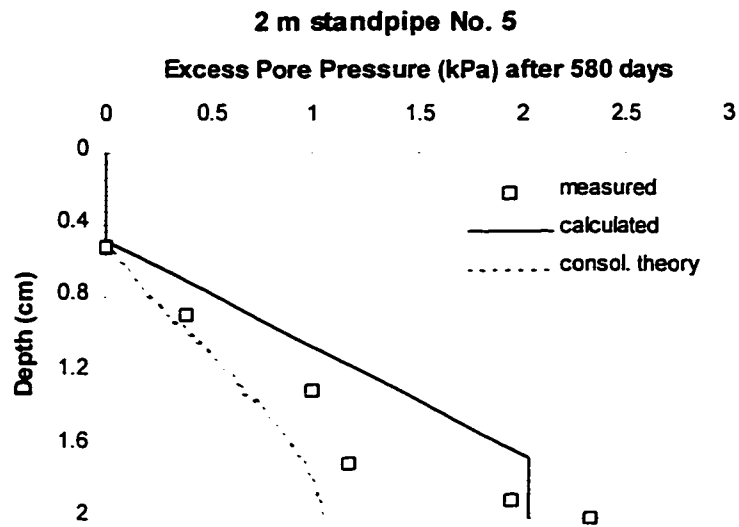
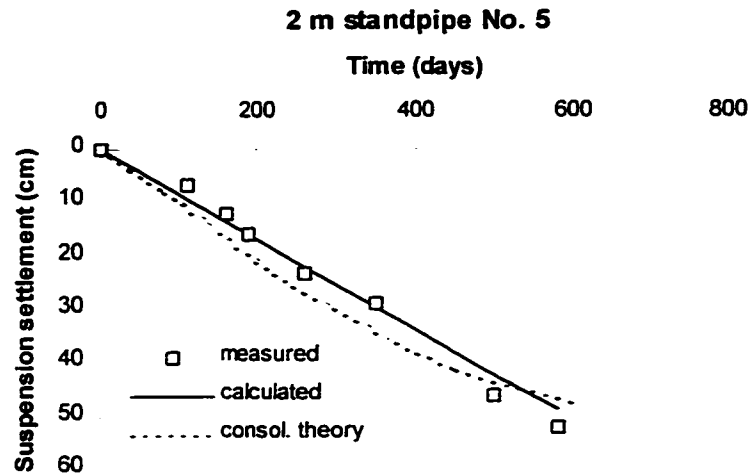


Figure 3.27 2 m standpipe test 5

## ***Chapter 4***

### ***A MODEL FOR COUPLED SEDIMENTATION AND CONSOLIDATION***

#### **4.1 A MODEL FOR SEDIMENTATION**

##### **4.1.1. Introduction**

In this chapter the governing differential equation for one-dimensional sedimentation is derived in Eulerian coordinates. The derivation is based on two fundamental laws of continuum mechanics: the law of conservation of mass and the principle of linear momentum.

The concept of permeability is extended to a suspended state of solids; in other words, it is assumed that the expression for the coefficient of permeability applies smoothly over a range of void ratios which encompasses both soil and suspension, regardless of whether effective stresses are present or absent. Permeability thus appears as a measure of hydrodynamic interaction between solid and liquid in a suspension. In a very general sense, it may be understood as a “constitutive law” for the solid-fluid interaction in suspensions.

The main assumption, which is supported by extensive experimental evidence, is that effective stress does not exist in a suspended state, i.e. that suspension behaves as a fluid, with the fluid pressure equal to the total stress.

The governing equation is expressed in terms of the volumetric solids concentration  $c$  as the dependent variable. The use of the solids concentration is preferred over the void ratio because of its mathematical convenience: in the sedimentation stage  $e$  becomes infinite when the concentration decreases to zero, i.e. when all particles settle down. Besides, the mathematical form of the governing equation is the most concise when expressed using the volumetric concentration.

It is shown in section 4.2 that the governing equation for sedimentation may be simply obtained from the governing equation for consolidation by setting  $\sigma' = 0$ . Nevertheless,

this derivation is presented here to show that there are various approaches in sedimentation analysis. The present approach is based mainly on the mass balance principle, and the equilibrium equation is invoked towards the end of the derivation.

The final governing equation is a hyperbolic partial differential equation. It has the mathematical form of Kynch's solution for the hindered settling of a suspension. Referring to the previous paragraph, this shows that the concept of permeability offers a base for unification of theories of sedimentation and consolidation.

#### **4.1.2 Derivation**

##### **4.1.2.1 The conservation of mass (continuity) equation**

The law of conservation of mass states that the mass of a specific portion of the continuum remains constant with time. In Lagrangian coordinates this condition is automatically satisfied through the use of deformation gradients (Jacobian) to determine the deformed elemental volume in time. In Eulerian formulation, in which the control volume is stationary and fixed in space, a separate equation must be written to express the mass conservation relation.

In the case of a mixture of two or more materials, the continuity equation should be written separately for each component, together with a certain relation between their concentrations within an elemental volume. Even with only two components, these equations become very complicated if the components are assumed to be deformable, i.e. if they are allowed to change their densities. To simplify the problem, the assumption of incompressibility of both components of the mixture is introduced.

In this way, the change in the total density of a mixture is completely convective—a plain result of the change in the proportion of the components within a control volume due to various fluxes over its boundaries. It should be remarked that as a rule, this assumption is made in the development of consolidation theories. It is therefore natural to adopt it in the case of a suspension where effective stresses are assumed to vanish. Possible deviations may be imagined in those problems where highly flocculated suspensions of some organic substances are considered (the problem of mass exchange between components, see Chapter 2.2.1).

The mass balance equations for the two phases of a solid-liquid suspension are more easily understood with the help of the graphical presentation in Figure 4.1.

$$\begin{aligned} \frac{\partial c}{\partial t} + \frac{\partial \phi_s}{\partial x} &= 0 & \text{where } \phi_s &= c \cdot v_s, \text{ and } c = \frac{dV_s}{dV} \\ \frac{\partial c}{\partial t} + \frac{\partial \phi_w}{\partial x} &= 0 & \text{where } \phi_w &= n \cdot v_w, \text{ and } n = \frac{dV_w}{dV} \end{aligned} \quad [4.1]$$

Here  $c$  and  $n$  denote volumetric concentrations of solid and liquid particles in an elementary volume, and  $\phi_s$  and  $\phi_w$  are corresponding fluxes. In soil mechanics  $n$  is the

porosity and  $v_w$  is the true (or seepage) velocity.

This type of equation is usually encountered in continuum mechanics, as well as in science in general, and it is called the “law of conservation”. The temporal rate of change is governed by the spatial rate of change. i.e. the change in time of a certain variable is determined by the fluxes of that variable across the boundaries of a control volume.

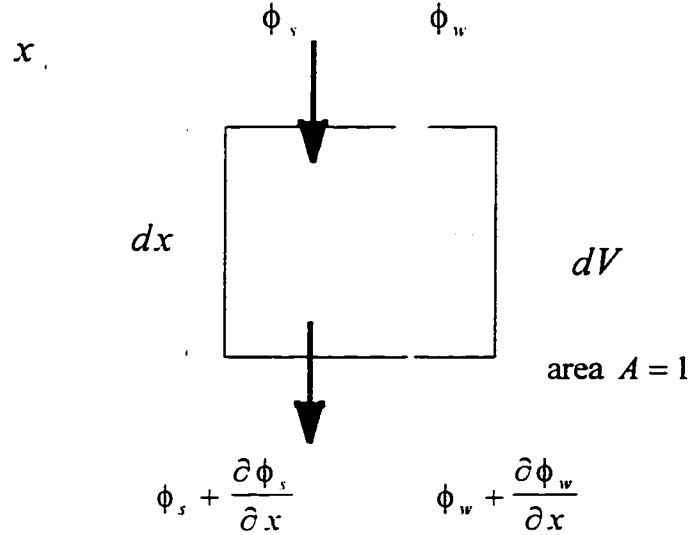


Figure 4.1 The mass balance principle for a solid-liquid mixture

It should be noted here that an implicit assumption of an isotropic porosity  $n$  (and concentration  $c$ ) was made in equation [4.1]. This means that the porosity is assumed to be independent of direction. in other words that from the expression for the volumetric porosity:

$$n = \frac{V_w}{V} \quad (\text{or } c = \frac{V_s}{V}) \quad [4.2]$$

naturally follows for an arbitrary cross section and the corresponding planar porosity:

$$n = \frac{A_w}{A} \quad \text{and} \quad c = \frac{A_s}{A} \quad [4.3]$$

where  $A = A_s + A_w$  is the total area. In reality, the porosity usually depends on the direction of a cutting plane and it could be a result of the orientation of such elements as flocs or plate-like clay particles. But, since we are dealing with a one-dimensional problem, the anisotropic porosity is beyond the capabilities of the model.

The condition that connects the variables in the equation [4.1] is that of a constant control volume  $dV$ :

$$c + n = 1 \quad \Leftrightarrow \quad \frac{\partial c}{\partial t} + \frac{\partial n}{\partial t} = 0 \quad \Leftrightarrow \quad \frac{\partial}{\partial t}(dV) = 0 \quad \Leftrightarrow \quad dV = \text{const.} \quad [4.4]$$

Substituting equation [4.4] in the second of the equations [4.1] gives:

$$\frac{\partial}{\partial t}(1 - c) + \frac{\partial \phi_w}{\partial x} = -\frac{\partial c}{\partial t} + \frac{\partial \phi_w}{\partial x} = 0 \quad [4.5]$$

and then adding equation [4.5] to the first of the equations [4.1], we obtain:

$$\begin{aligned} \frac{\partial \phi_s}{\partial x} + \frac{\partial \phi_w}{\partial x} &= 0 \\ \frac{\partial}{\partial x}(\phi_s + \phi_w) &= 0 \quad \Rightarrow \quad \phi_s + \phi_w = f(t) \end{aligned} \quad [4.6]$$

where the integration constant  $f(t)$  is a function of time. If we substitute for the fluxes from equation [4.1] we will get:

$$f(t) = c \cdot v_s + n \cdot v_w = c \cdot v_s + (1 - c) \cdot v_w \quad [4.7]$$

It can be seen that  $f(t)$  may be thought of as an "average suspension velocity", where  $c$  and  $n = 1 - c$  are the weighting functions. Since equation [4.6] must be valid throughout the domain at any time,  $f(t)$  can be determined from the known initial and boundary conditions: for example, at an impermeable boundary both the solid and the liquid flux must be zero at any time instant, and this causes the  $f(t) = 0$ . Therefore, in a tank settling there is no motion of a suspension "on average"—there is only a redistribution of phases.

It may be valuable here to point out the difference between the meaning of "incompressibility" in a sedimentation problem and its meaning in a common deformation problem in soil mechanics. In soil mechanics, incompressibility is often associated with an "undrained" deformation which occurs at constant volume and thus, constant density. In sedimentation, even though both components of a mixture are incompressible, the total density of a suspension is not constant and variations occur as a result of a net mass (solids and water) flux.

Equation [4.6] in its differential form reads:

$$\begin{aligned} \frac{\partial}{\partial x}(\phi_s + \phi_w) &= \frac{\partial}{\partial x}(c \cdot v_s + n \cdot v_w) = \frac{\partial}{\partial x}[c \cdot v_s + (1 - c) \cdot v_w] = \frac{\partial}{\partial x}[c \cdot (v_s - v_w) + v_w] = 0 \\ \frac{\partial c}{\partial x} \cdot (v_s - v_w) + c \cdot \frac{\partial}{\partial x}(v_s - v_w) + \frac{\partial v_w}{\partial x} &= 0 \end{aligned} \quad [4.8]$$

So far, we have 1 equation with 3 unknowns:  $c$ ,  $v_s$  and  $v_w$ . Therefore it is necessary to introduce more physics into the problem to obtain the additional needed equations.

#### 4.1.2.2 Equilibrium equation

The principle of linear momentum, which is based upon Newton's second law, states that the rate of change of motion of a portion of a continuum is equal to the resultant force acting upon it. It is mathematically expressed as the equation of motion in continuum mechanics. In the case of static equilibrium, this is reduced to:

$$\sigma_{ij,j} + \rho b_i = 0 \quad [4.9]$$

It is assumed in this derivation that the acceleration terms in the equations of motion vanish. This makes all derivations much simpler and the solution of the resulting equation easier to carry out. As a consequence, the application of the method is restricted to "slowly settling" suspensions ("non-segregating" dispersions, colloidal suspensions, etc.). Because the term "slowly" is not clearly defined, it should be estimated for each particular case.

The derivation of the equilibrium equation in a one-dimensional case is elementary and is clearly illustrated in Figure 4.2. Since lateral stresses are equal and have only normal components, they do not make any contribution to the equilibrium condition in the axial direction. The following equation is written in terms of total axial stress:

$$\frac{\partial \sigma_x}{\partial x} = \rho g \quad [4.10]$$

where  $g$  is the acceleration of gravity and  $\rho$  is the total density of the mixture. In further derivation the subscript "x" for the axial stress will be omitted for simplicity.

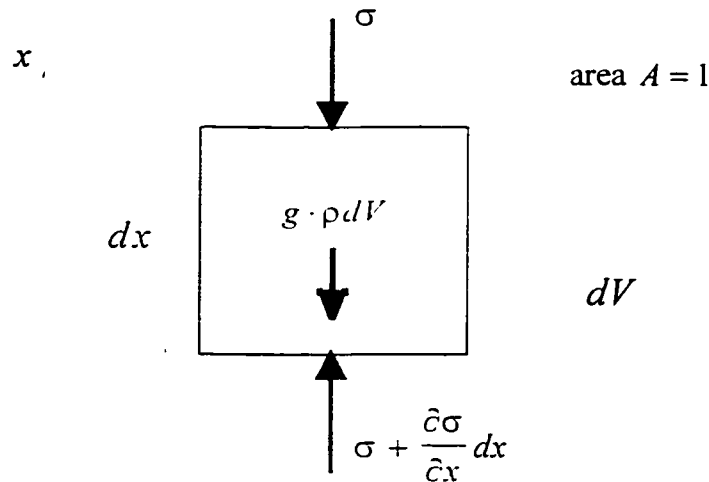


Figure 4.2 The equilibrium of an elemental volume

The total density of a mixture may be easily expressed through the densities of its constituents, in this case:

$$\rho = \rho_s \cdot c + \rho_w \cdot n \quad [4.11]$$

where  $\rho_s$  and  $\rho_w$  are related to the solid and the liquid phase, respectively. Substituting it into equation [4.10] gives:

$$\frac{\partial \sigma}{\partial x} = g(\rho_s \cdot c + \rho_w \cdot n) \quad [4.12]$$

It is common in geotechnics to define a liquid state as the one in which the effective stress  $\sigma'$  becomes zero. The effective stress, which is taken to be transmitted through soil grains, determines the shear strength of a soil and is therefore “responsible” for deformation. Except in the case of physically cemented materials with real cohesion, it is widely accepted that a saturated soil has no shear strength at zero effective stress. Therefore, the soil will undergo large distortional deformations, since it cannot sustain shear stresses and begins to deform infinitely under small static deviatoric loading. This is another common concept used to distinguish between solids and liquids in mechanics.

We shall therefore assume that the effective stress in a suspension is zero so that:

$$\frac{\partial u}{\partial x} = g(\rho_s \cdot c + \rho_w \cdot n) \quad [4.13]$$

The total stress is equal to the fluid (pore) pressure, and the fluid pressure is determined for the suspension as a whole—a “heavy” liquid.

Therefore, considering the equilibrium of a differential element provides one additional equation but also introduces a new variable  $u$ .

#### 4.1.2.3 Connecting continuity and equilibrium

The equilibrium equation in the previous chapter was written for total stresses, i.e. for the suspension as a whole. It can be written for the solid and the liquid phase separately, provided that the force of their mutual mechanical interaction can be defined. It has been assessed that this approach would have involved enormous difficulties when evaluating numerous influential factors, such as the structure of solids in a suspension, the nature of flow through pore spaces, constitutive laws for the components of a suspension, physico-chemical origins of interaction forces, etc. Even if it were theoretically possible to establish such relations, it would be impossible to determine the numerical values of the parameters in practical problems.

It seems that permeability is a parameter which offers a shortcut to quantify the interaction force of a solid-liquid mixture. For practical applications, it is important that there be well established procedures and equipment specially developed to determine the magnitude and variability of this parameter for various materials and states of matter.



There is still no general theory of permeability, but in practice it is widely used and reasonably well understood.

In the following derivation we shall introduce permeability as a measure of the mutual relationship between solid and liquid particles, and we shall derive from Darcy's law the equation connecting velocities of deformation  $v_s$  and  $v_w$ .

In its original form Darcy's law reads:

$$\bar{v}_w = n \cdot v_w = k \cdot i = -k \cdot \frac{\partial h}{\partial s} \quad [4.14]$$

The discharge velocity on the left hand side is actually the flux of a liquid through a unit of cross-sectional area. In a one-dimensional case, the length along a streamline  $s$  is equal to the spatial dimension  $x$ , and the hydraulic gradient is:

$$\frac{\partial h}{\partial s} = \frac{\partial h}{\partial x} \quad [4.15]$$

The hydraulic head  $h$  is determined assuming low velocities of water flow (the kinetic energy term is neglected):

$$h = \frac{u}{\gamma_w} + z \quad [4.16]$$

where  $u$  is the pore pressure and  $z$  is the geometric head. Since  $h$  is measured from a certain datum,  $z$  is equal to  $\pm x$  (the sign indicates whether or not both axes point in the same direction) shifted for a certain constant value. Assuming that  $z$  is measured upward, and substituting equation [4.16] into [4.15]:

$$\frac{\partial h}{\partial s} = \frac{\partial h}{\partial x} = \frac{1}{\gamma_w} \frac{\partial u}{\partial x} + \frac{\partial z}{\partial x} = \frac{1}{\gamma_w} \frac{\partial u}{\partial x} - 1 \quad [4.17]$$

We may now express the pore pressure  $u$  as the sum of the hydrostatic pressure and a "beyond hydrostatic—excess" pressure (excess pore pressure may thus include the seepage effect in a general sense), as it is commonly done in consolidation analyses:

$$u = u_h + \bar{u} \quad [4.18]$$

remembering that both hydrostatic pressure and  $x$  increase with depth:

$$\frac{\partial u_h}{\partial x} = \gamma_w \quad [4.19]$$

substituting for  $u$  from equation [4.18] into [4.17], and using [4.19]:

$$\frac{\partial h}{\partial s} = \frac{1}{\gamma_w} \frac{\partial}{\partial x} (u_h + \bar{u}) - 1 = \frac{1}{\gamma_w} \frac{\partial \bar{u}}{\partial x} \quad [4.20]$$

and further into equation [4.14]:

$$\begin{aligned}\bar{v}_w &= n \cdot v_w = -k \cdot \frac{1}{\gamma_w} \frac{\partial \bar{u}}{\partial x} \\ v_w &= -\frac{k}{n} \cdot \frac{1}{\gamma_w} \frac{\partial \bar{u}}{\partial x}\end{aligned}\tag{4.21}$$

It was assumed so far that the liquid percolates through a non-deformable, rigid solid structure. If the solid structure is deformable and changes its shape due to the pressure exerted by the flowing water (or due to any other reason), then the extension of Darcy's law after Gersevanov has to be applied:

$$v_w - v_s = -\frac{k}{n} \cdot \frac{1}{\gamma_w} \frac{\partial \bar{u}}{\partial x}\tag{4.22}$$

In this way, we can obtain a link between the local velocities of the two components of the suspension, which will enable us to derive the governing equation for sedimentation.

#### 4.1.2.4 Differential governing equation for sedimentation

Substituting the Darcy-Gersevanov law [4.22] into the continuity equation [4.8] we obtain:

$$\begin{aligned}\frac{\partial c}{\partial x} \cdot \left( \frac{k}{n} \cdot \frac{1}{\gamma_w} \frac{\partial \bar{u}}{\partial x} \right) + c \cdot \frac{\partial}{\partial x} \cdot \left( \frac{k}{n} \cdot \frac{1}{\gamma_w} \frac{\partial \bar{u}}{\partial x} \right) + \frac{\partial}{\partial x} \cdot \left( v_s - \frac{k}{n} \cdot \frac{1}{\gamma_w} \frac{\partial \bar{u}}{\partial x} \right) &= 0 \\ \frac{\partial c}{\partial x} \cdot \left( \frac{k}{n} \cdot \frac{1}{\gamma_w} \frac{\partial \bar{u}}{\partial x} \right) + (c-1) \cdot \frac{\partial}{\partial x} \cdot \left( \frac{k}{n} \cdot \frac{1}{\gamma_w} \frac{\partial \bar{u}}{\partial x} \right) + \frac{\partial v_s}{\partial x} &= 0\end{aligned}\tag{4.23}$$

Substituting now  $c = 1-n$ :

$$\begin{aligned}-\frac{\partial n}{\partial x} \cdot \left( \frac{k}{n} \cdot \frac{1}{\gamma_w} \frac{\partial \bar{u}}{\partial x} \right) - n \cdot \frac{\partial}{\partial x} \cdot \left( \frac{k}{n} \cdot \frac{1}{\gamma_w} \frac{\partial \bar{u}}{\partial x} \right) + \frac{\partial v_s}{\partial x} &= 0 \\ -\frac{\partial}{\partial x} \left( n \cdot \frac{k}{n} \cdot \frac{1}{\gamma_w} \frac{\partial \bar{u}}{\partial x} \right) + \frac{\partial v_s}{\partial x} &= 0 \\ -\frac{\partial}{\partial x} \left( v_s - k \cdot \frac{1}{\gamma_w} \frac{\partial \bar{u}}{\partial x} \right) &= 0 \\ v_s &= k \cdot \frac{1}{\gamma_w} \frac{\partial \bar{u}}{\partial x} + V(t)\end{aligned}\tag{4.24}$$

where  $V(t)$  is an integration constant, which is a function of time. It is assumed to be zero, since it was adopted that the motion of solid particles must be entirely driven by

mechanical causes.

Turning our attention back to the equilibrium equation [4.13], and using [4.18], we obtain:

$$\begin{aligned}\frac{\partial u}{\partial x} &= \frac{\partial}{\partial x}(u_h + \bar{u}) = g(\rho_s \cdot c + \rho_w \cdot n) = \gamma_s \cdot c + \gamma_w \cdot n \\ \frac{\partial u}{\partial x} &= \frac{\partial}{\partial x}(\bar{u} + u_h) = \frac{\partial \bar{u}}{\partial x} + \gamma_w\end{aligned}\quad [4.25]$$

We can express the excess pore pressure as:

$$\frac{\partial \bar{u}}{\partial x} = \frac{\partial u}{\partial x} - \gamma_w = \gamma_s \cdot c + \gamma_w \cdot n - \gamma_w \quad [4.26]$$

Substituting the last formula into [4.24] we have the expression that:

$$\begin{aligned}v_s &= k \cdot \frac{1}{\gamma_w}(\gamma_s c + \gamma_w n - \gamma_w) = \\ &= k \cdot \left( \frac{\gamma_s}{\gamma_w} c + (n - 1) \right) = k \cdot \left( \frac{\gamma_s}{\gamma_w} c - c \right) = k c \cdot \left( \frac{\gamma_s}{\gamma_w} - 1 \right) = \\ &= k c \cdot (G_s - 1)\end{aligned}\quad [4.27]$$

where  $G_s$  is the specific weight of solids. In this equation  $k$  is a known function which can be determined by testing. It is usually expressed as a function of the void ratio:  $k = k(e)$ .

Finally, the governing equation for sedimentation has the form of a conservation law, only the flux term  $F$  is specified as a function of the permeability coefficient  $k$ :

$$\frac{\partial c}{\partial t} + \frac{\partial F}{\partial x} = 0 \quad \text{where} \quad F = F[c, k(c)] = k \cdot c^2 \cdot (G_s - 1) \quad [4.28]$$

The state variable is the concentration of the solid phase  $c$ , but it may be converted to some other parameter—the porosity or the void ratio, if needed. The process is entirely defined by permeability as the only parameter included in the governing equation.

The earliest continuity equation above [4.1] may be transformed into a form identical to that derived first by Kynch (1952): see Chapter 2.3.2.3:

$$\frac{\partial c}{\partial t} + \frac{\partial \phi_s}{\partial x} = \frac{\partial c}{\partial t} + \frac{\partial}{\partial x}(c \cdot v_s) = \frac{\partial c}{\partial t} + \frac{\partial c}{\partial x} v_s + c \frac{dv_s}{dc} \frac{\partial c}{\partial x} = \frac{\partial c}{\partial t} + \frac{\partial c}{\partial x} \left( v_s + c \frac{dv_s}{dc} \right) \quad [4.29]$$

having in mind that  $v_s$  is a function of the concentration  $c$  as a single variable.

It is now easy to substitute the solids velocity from equation [4.27] into [4.29]:

$$\begin{aligned}
\frac{\partial c}{\partial t} + \frac{\partial \phi_s}{\partial x} &= \frac{\partial c}{\partial t} + \frac{\partial c}{\partial x} \left( k c \cdot (G, -1) + c \cdot (G, -1) \cdot \left( \frac{dk}{dc} c + k \right) \right) = \\
&= \frac{\partial c}{\partial t} + \frac{\partial c}{\partial x} \left( (G, -1) \left[ k c + \frac{dk}{dc} c^2 + k c \right] \right) = \\
&= \frac{\partial c}{\partial t} + \frac{\partial c}{\partial x} \left( (G, -1) \cdot c \cdot \left( 2k + c \frac{dk}{dc} \right) \right)
\end{aligned} \tag{4.30}$$

The governing equation may be specialized to suit specific forms of the permeability function. As an example, we adopt here a power law, as it is usually done in the testing of oil sands tailings at the University of Alberta. The letter  $e$  in the following derivation designates void ratio.

$$\begin{aligned}
k &= A e^B = A \left( \frac{n}{1-n} \right)^B = A \left( \frac{1-c}{c} \right)^B \\
\frac{dk}{dc} &= AB \left( \frac{1-c}{c} \right)^{B-1} \left( -\frac{1}{c^2} \right) = B \cdot k \cdot \frac{c}{1-c} \left( -\frac{1}{c^2} \right) = -B \cdot k \cdot \frac{1}{c(1-c)} \\
2k + c \frac{dk}{dc} &= 2k - B \cdot k \cdot \frac{1}{1-c} = k \cdot \left( 2 - \frac{B}{1-c} \right) \\
\frac{\partial c}{\partial t} + \frac{\partial c}{\partial x} \cdot \left[ (G, -1) \cdot k \cdot c \cdot \left( 2 - \frac{B}{1-c} \right) \right] &= 0
\end{aligned} \tag{4.31}$$

## 4.2 A MODEL FOR CONSOLIDATION

### 4.2.1. Introduction

In this chapter a governing differential equation for one-dimensional finite strain consolidation is derived in Eulerian coordinates. The derivation is based on two fundamental laws of continuum mechanics: the conservation of mass and the principle of linear momentum. Mutual interaction of the two interpenetrating phases of a sedimenting material is taken into account, as is usually done in consolidation problems, using permeability as the governing property and making use of Darcy's law (assuming thus the implicitly laminar flow of the fluid). It was further assumed that the constitutive relationships between permeability and void ratio, and those between void ratio and effective stress (compressibility), are known in advance.

The resulting equation is a partial differential equation of the second order of the parabolic type. The equation may be derived in terms of various state variables: void ratio (as usual), excess pore pressure (again in the form usually encountered), effective stress, porosity and volumetric solids concentration. The forms that involve void ratio, porosity and concentration are easily derived from each other in a rather direct way. The same is true when dealing with excess pore pressure and effective stress variants.

This derivation is probably most similar to the one by Lee and Sills (1979), up to the point of a thin layer assumption. Actually, all derivations of finite strain consolidation theories are just various forms of the same formula (first derived by Gibson et al. (1967) in Lagrangian coordinates) because they are all based on the same fundamental laws of continuum mechanics. Differences appear in the definitions of constitutive laws (regarding permeability and compressibility) and eventual simplifications made in order to meet the requirements of the chosen numerical method. The latter are either:

- assumptions of the constancy of certain complex parameters.

These are, in fact, the constraints imposed upon mutual relations among the parameters. For example, the coefficients of permeability and compressibility are related by the coefficient of consolidation, which when assumed constant, becomes a constraining equation for these two parameters. A similar assumption was made for the  $C_F$  coefficient by Gibson et al (1967) and by Lee and Sills (1979) for their  $C_I$ .

- simplifications of initial conditions and boundary conditions in order to obtain an analytical solution.

The initial concentration profile is usually adopted as uniform, and the pore pressures are assumed to be initially absent. It is common procedure to adopt either impermeable or completely free drainage boundaries as limiting cases; or

- omissions of certain components of the model:

For instance, omission of the self-weight (a thin layer is assumed), the inertial forces during motion (the static equilibrium equation is therefore used instead of the equation of motion), the creep deformation of solids (which enables a unique relationship between effective stress and soil density), etc.

Some of the above simplifications are simply not acceptable here because the derivation must be kept as inclusive as possible. For example, in the absence of external forces on the surface of a settling mud, the self-weight is the only driving force which causes sedimented material to further consolidate. Furthermore, a constant total stress assumption, usually adopted for consolidation under the self-weight, is not feasible in the case of coupled sedimentation and consolidation because of continually accreting material from the suspension at the top of the consolidating layer. Also, neither an impermeable nor a free draining boundary may be assumed at the top of the consolidating layer, since this is an interface between two materials, and drainage from the sediment is defined by the properties of the suspension (its permeability, i.e. concentration).

## 4.2.2 Derivation

### 4.2.2.1 Equilibrium equation

This has been chosen as the starting point for consolidation analysis, since the existence of finite effective stress is what differs a sediment from a suspended state of what is initially one and the same material during the settling process.

Without repeating what has been presented previously in the derivation of the governing equation for sedimentation, the equilibrium equation in terms of total stresses (equation [4.12], see also Figure 4.2), reads:

$$\frac{\partial \sigma}{\partial x} = g(\rho_s \cdot c + \rho_w \cdot n) \quad [4.32]$$

Adopting the validity of Terzaghi's original effective stress principle:

$$\sigma = \sigma' + u \quad [4.33]$$

equation [4.32] becomes:

$$\frac{\partial \sigma'}{\partial x} + \frac{\partial u}{\partial x} = g(\rho_s \cdot c + \rho_w \cdot n) \quad [4.34]$$

### 4.2.2.2 Continuity equation

The same continuity equation as the one derived for the sedimentation problem is used here, with the same underlying assumptions of the incompressibility of both phases and

the isotropy of porosity:

$$\begin{aligned}\frac{\partial \phi_s}{\partial x} + \frac{\partial \phi_w}{\partial x} &= 0 \\ \frac{\partial}{\partial x}(\phi_s + \phi_w) &= 0 \quad \Rightarrow \quad \phi_s + \phi_w = f(t)\end{aligned}\quad [4.35]$$

The integration constant  $f(t)$  has already been discussed in Chapter 4.1.2.1: if one of the boundaries is completely impervious, both fluxes are identically zero throughout the entire time and, therefore,  $f(t) = 0$ . If both boundaries are drainage free and the flux of the liquid is known at either of them, then  $f(t)$  is equal to that flux. So, the function  $f(t)$  can always be determined from the boundary conditions—see for example Lee and Sills (1979).

#### 4.2.2.3 Connection between continuity and equilibrium

For this purpose the Darcy-Gersevanov law is used, as it was done in the sedimentation analysis:

$$n(v_w - v_s) = -\frac{k}{\gamma_w} \frac{\partial \bar{u}}{\partial x} \quad [4.36]$$

Now, using equation [4.35] we obtain:

$$\begin{aligned}\phi_w &= n \cdot v_w = f(t) - \phi_s = f(t) - c \cdot v_s \\ n(v_w - v_s) &= n \cdot v_w - n \cdot v_s = f(t) - c \cdot v_s - (1-c) \cdot v_s = f(t) - v_s = -\frac{k}{\gamma_w} \frac{\partial \bar{u}}{\partial x} \\ v_s &= f(t) + \frac{k}{\gamma_w} \frac{\partial \bar{u}}{\partial x}\end{aligned}\quad [4.37]$$

At this moment, we have concluded that the distribution of solids' velocity within the consolidation domain will be a function of the excess ("over hydrostatic") pore pressure and the boundary conditions  $f(t)$ .

#### 4.2.2.3 Differential governing equation for consolidation

Equation [4.37] can be further transformed using the flux of solids:

$$\begin{aligned}\phi_s &= c \cdot v_s \\ \phi_s &= c \cdot (\phi_s + \phi_w) + c \cdot \frac{k}{\gamma_w} \frac{\partial \bar{u}}{\partial x}\end{aligned}\quad [4.38]$$

Now, differentiating with respect to  $x$ :

$$\frac{\partial \phi_s}{\partial x} = \frac{\partial c}{\partial x} \cdot (\phi_s + \phi_w) + \frac{\partial}{\partial x} \left( c \frac{k}{\gamma_w} \frac{\partial \bar{u}}{\partial x} \right) \quad [4.39]$$

$$\text{where } \frac{\partial}{\partial x} (\phi_s + \phi_w) = \frac{\partial}{\partial x} [f(t)] = 0$$

and, using the continuity equation for the solid phase, substitute the time derivative of  $c$  for the spatial derivative of the solids' flux:

$$-\frac{\partial c}{\partial t} = \frac{\partial c}{\partial x} \cdot (\phi_s + \phi_w) + \frac{\partial}{\partial x} \left( c \frac{k}{\gamma_w} \frac{\partial \bar{u}}{\partial x} \right) \quad [4.40]$$

This equation may be alternatively expressed in terms of the porosity  $n$ :

$$\frac{\partial n}{\partial t} + \frac{\partial n}{\partial x} \cdot (\phi_s + \phi_w) = \frac{\partial}{\partial x} \left( (1-n) \frac{k}{\gamma_w} \frac{\partial \bar{u}}{\partial x} \right) \quad [4.41]$$

or in terms of the void ratio  $e$ :

$$\begin{aligned} \frac{\partial}{\partial t} \left( \frac{e}{1+e} \right) + \frac{\partial}{\partial x} \left( \frac{e}{1+e} \right) \cdot (\phi_s + \phi_w) &= \frac{\partial}{\partial x} \left( (1+e) \frac{k}{\gamma_w} \frac{\partial \bar{u}}{\partial x} \right) \\ \text{and simplified by } \frac{\partial}{\partial t} \left( \frac{e}{1+e} \right) &= \frac{1}{(1+e)^2} \frac{\partial e}{\partial t} \\ \frac{\partial}{\partial x} \left( \frac{e}{1+e} \right) &= \frac{1}{(1+e)^2} \frac{\partial e}{\partial x} \end{aligned} \quad [4.42]$$

$$\frac{\partial e}{\partial t} + \frac{\partial e}{\partial x} \cdot (\phi_s + \phi_w) = (1+e)^2 \cdot \frac{\partial}{\partial x} \left( (1+e) \frac{k}{\gamma_w} \frac{\partial \bar{u}}{\partial x} \right)$$

It is now possible to derive the governing equation in terms of either of the  $c$ ,  $n$ , or  $e$ , substituting for the excess pore pressure derivative from equation [4.34]:

$$\begin{aligned} \frac{\partial \bar{u}}{\partial x} &= \frac{\partial \sigma}{\partial x} - \frac{\partial \sigma'}{\partial x} - \frac{\partial u_h}{\partial x} \\ \frac{\partial \sigma}{\partial x} = g(c\rho_s + n\rho_w) &= \begin{cases} g[(\rho_s - \rho_w)c + \rho_w] = \gamma_w[(G_s - 1)c + 1] \\ g[\rho_s - (\rho_s - \rho_w)n] = \gamma_w[G_s - (G_s - 1)n] \\ g\left[\rho_s - (\rho_s - \rho_w)\frac{e}{1+e}\right] = \gamma_w\left[\frac{G_s + e}{1+e}\right] \end{cases} \end{aligned} \quad [4.43]$$

$$\frac{\partial u_h}{\partial x} = g\rho_w = \gamma_w$$

obtaining finally :



$$\frac{\partial \bar{u}}{\partial x} = \begin{cases} \gamma_w (G, -1) c - \frac{\partial \sigma'}{\partial x} \\ \gamma_w (G, -1) (1-n) - \frac{\partial \sigma'}{\partial x} \\ \gamma_w \left( \frac{G, -1}{1+e} \right) - \frac{\partial \sigma'}{\partial x} \end{cases} \quad [4.44]$$

Since the effective stress is usually expressed as a function of the void ratio, the substitution of equation [4.44] into equations [4.43] will give three equivalent governing equations:

$$-\frac{\partial c}{\partial t} = \frac{\partial c}{\partial x} \cdot (\phi_s + \phi_w) + \frac{\partial}{\partial x} \left\{ c \frac{k}{\gamma_w} \left[ \gamma_w (G, -1) c - \frac{\partial \sigma'}{\partial x} \right] \right\} \quad [4.45]$$

$$\frac{\partial n}{\partial t} + \frac{\partial n}{\partial x} \cdot (\phi_s + \phi_w) = \frac{\partial}{\partial x} \left\{ (1-n) \frac{k}{\gamma_w} \left[ \gamma_w (G, -1) (1-n) - \frac{\partial \sigma'}{\partial x} \right] \right\} \quad [4.46]$$

$$\frac{\partial e}{\partial t} + \frac{\partial e}{\partial x} \cdot (\phi_s + \phi_w) = (1+e)^2 \cdot \frac{\partial}{\partial x} \left\{ (1+e) \frac{k}{\gamma_w} \left[ \gamma_w \frac{G, -1}{1+e} - \frac{\partial \sigma'}{\partial x} \right] \right\} \quad [4.47]$$

These are non-linear parabolic partial differential equations of the second order, with a convective term in the case of permeable boundaries, when the sum of fluxes ( $\phi_s + \phi_w$ ) does not vanish.

In a typical case of a settling tank with an impervious bottom boundary, equations [4.45] to [4.47] lose the convective term and become simpler:

$$-\frac{\partial c}{\partial t} = \frac{\partial}{\partial x} \left\{ c^2 k (G, -1) - c \frac{k}{\gamma_w} \frac{\partial \sigma'}{\partial x} \right\} \quad [4.48]$$

$$\frac{\partial n}{\partial t} = \frac{\partial}{\partial x} \left\{ (1-n)^2 k (G, -1) - (1-n) \frac{k}{\gamma_w} \frac{\partial \sigma'}{\partial x} \right\} \quad [4.49]$$

$$\frac{\partial e}{\partial t} = (1+e)^2 \cdot \frac{\partial}{\partial x} \left\{ k (G, -1) - (1+e) \frac{k}{\gamma_w} \frac{\partial \sigma'}{\partial x} \right\} \quad [4.50]$$

It can be seen that the governing sedimentation equation [4.28] is a simplified case of equations [4.48] introducing the assumption of zero effective stresses.

Since the effective stress cannot be directly expressed as an explicit function of the spatial coordinate  $x$ , an intermediate step has to be introduced: the derivative  $\frac{\partial \sigma'}{\partial x}$  should

be written as a chain derivative of the compressive constitutive relation  $\sigma'(c)$  and the spatial derivative of the concentration  $\frac{\partial c}{\partial x}$ . Taking equation [4.48] for example, one obtains:

$$-\frac{\partial c}{\partial t} = \frac{\partial}{\partial x} \left\{ c^2 k(G, -1) - c \frac{k}{\gamma_w} \frac{\partial \sigma'}{\partial c} \frac{\partial c}{\partial x} \right\} \quad [4.51]$$

A similar expression is obtained from equations [4.49] and [4.50].

Consolidation equations [4.48] to [4.50] have been derived in the conservation law form, which is more commonly done for sedimentation problems. This again gives evidence for the fact that both processes have the same underlying physics. It is also convenient, from a mathematical point of view, to indicate that the same numerical procedure can be used in solving the coupled problem.

## 4.3 SOLUTION

### 4.3.1 Introduction

Solution of the coupled sedimentation and consolidation problem requires solving the system of partial differential equations (PDE) [4.28] and [4.51], if one chooses the concentration as the state variable.

$$\frac{\partial c}{\partial t} + \frac{\partial}{\partial x} [k \cdot c^2 \cdot (G, -1)] = 0 \quad [4.28_1]$$

$$\frac{\partial c}{\partial t} + \frac{\partial}{\partial x} \left\{ c^2 k(G, -1) - c \frac{k}{\gamma_w} \frac{\partial \sigma'}{\partial c} \frac{\partial c}{\partial x} \right\} = 0 \quad [4.51_1]$$

The solution is not possible in an analytical form without oversimplifications of the problem which can invalidate the model: see Chapter 4.2.1.

The finite difference method (FDM) was selected as the numerical solution scheme. Although the equations were derived in Eulerian coordinates, the particular numerical procedure in fact makes use of the Lagrangian coordinate frame. The principal factor for such a discrepancy is the incapability of the methods based on Eulerian description to properly handle discontinuities—the water-suspension and the suspension-sediment interfaces—that normally appear in a solution of the problem. In the solution presented, the water-suspension discontinuity is dealt with explicitly, while the suspension-sediment interface is actually “smeared off” between the two consecutive nodes of a grid which bound a temporary position of this discontinuity.

### 4.3.2 Mathematical aspects

The system of equations [4.28] and [4.51] couples a hyperbolic PDE (the sedimentation equation [4.28]) and a parabolic PDE (the consolidation equation [4.51]), each defined in its own domain, with their internal boundary moving in time. It is not possible at all to solve such a system using an analytical procedure, so a numerical method has to be chosen. The available literature offers numerous methods and approaches, but without definite conclusions and guidelines.

The main considerations that arise in choosing a method are:

- a numerical procedure (FDM or FEM),
- a coordinate frame (Eulerian or Lagrangian),
- a particular solution scheme (an element type and an interpolation function in FEM or a stencil in FDM), and
- a choice of adequate parameters for the scheme chosen, to assure the stability and accuracy of the result.

The “weak link” in the governing system is the sedimentation equation as a hyperbolic PDE. The solution of such equations may have discontinuities which originate from the discontinuities in the initial and boundary data or, in the case of a non-linear PDE such as [4.28], which may be developed even from smooth initial data at some later time (for more details see Appendix 2). One discontinuity point in the initial data for a sedimentation problem is the top surface of a suspension: at time  $t = 0$  the concentration is a finite value, while at any further moment it becomes zero. The discontinuities propagate along characteristic lines: in any particular sedimentation problem the upper boundary of the suspension layer is a characteristic line. The sediment-suspension interface is not a discontinuity in its original meaning in PDE theory, but rather a consequence of the “redundant” boundary conditions at the bottom boundary (Appendix 2). Nevertheless, it behaves as a discontinuity in a numerical scheme.

#### *Choice between FEM and FDM*

After consulting the available literature (Ames 1969, Lapidus and Pinder 1982, Oran and Boris 1987, Strikwerda 1989, Ganzha and Vorozhtsov 1996) it was concluded that there are no particular advantages of the finite element method over the finite difference method when solving a 1-D hyperbolic PDE problem; see for example Lee and Sills (1979) and Shodja and Feldkamp (1993), chapters 2.4.2.3 and 2.4.2.5. Even the use of new sophisticated finite element methods (the Moving FEM in the latter reference) did not seem to offer significant advantages with respect to the stability and accuracy of the solution, despite enormous additional numerical work. Therefore, the FDM was chosen as the procedure to be used in solving the coupled sedimentation and consolidation problem as defined here.

#### *Choice of coordinate system frame*

In this research project it was first attempted to apply the FDM schemes that were developed in the Eulerian coordinate frame, which means on a fixed grid. There are two basic options: an explicit scheme or an implicit scheme. An explicit FDM scheme uses

the forward difference procedure in time, namely it “projects” the solution forward in time based on the knowledge of the system state at the present moment. An implicit scheme uses the backward difference procedure in time, i.e. it optimizes the state of the system at the next time instant based on the knowledge of the system at the previous moment. An implicit scheme is in general not bounded by the conditions of the maximum permitted time step  $\Delta t$ , which is an unavoidable problem with explicit schemes, but it requires much more computational effort since one must solve a linear algebraic system of equations at each time step.

The results were discouraging with both types of schemes. Even those procedures which have been claimed to behave well in the presence of discontinuities, particularly the recently developed ones—the “total variation diminishing” schemes (TVD) and the “essentially nonoscillatory” schemes (ENO), Gantzha and Vorozhtsov (1996), were not capable of handling the discontinuities. Without going into too many details here, it should be pointed out that two phenomena are responsible for deviations of particular numerical solutions from an actual solution: numerical dispersion and numerical diffusion (dissipation). They are illustrated in Figures 4.3 and 4.4 (Gantzha and Vorozhtsov, 1996).

Both figures present the results of solving the simplest hyperbolic PDE, the so called “travelling wave” equation:

$$\frac{\partial u}{\partial t} + a \frac{\partial u}{\partial x} = 0$$

where  $u$  is a state function and  $a$  is a constant. The wave has a form of a semi-elliptical pulse. The analytical solution shows that the wave simply passes from the left to the right, preserving the same shape and magnitude. Two different Eulerian FDM schemes were used.

A scheme exhibiting numerical dispersion gives the solution in Figure 4.3, which is characterized by artificial oscillations, starting at the discontinuity points at the ends of the wave. The magnitude of these oscillations increases with time and finally completely destroys the shape of the solution. In a sedimentation problem oscillations appear at the suspension boundaries, and after a very short time it is not possible to give even a rough estimate of their positions. Besides, the solution itself becomes merely one wildly vibrating wave.

A scheme showing numerical dissipation produces no oscillations near the corners, but the height of the numerically computed pulse decreases as the amount of time increases, as can be seen in Figure 4.4. The corners of the pulse, which are present in the exact solution profiles, are strongly rounded. This is also unacceptable in a solution of the sedimentation problem, since the positions of the internal boundaries are an essential part of the solution.

The problem with these two numerical phenomena is that they are compatible: one cannot avoid them, but can only attempt to determine the amounts of their relative effect on the solution. These phenomena appear even in Lagrangian formulation, but it is easier

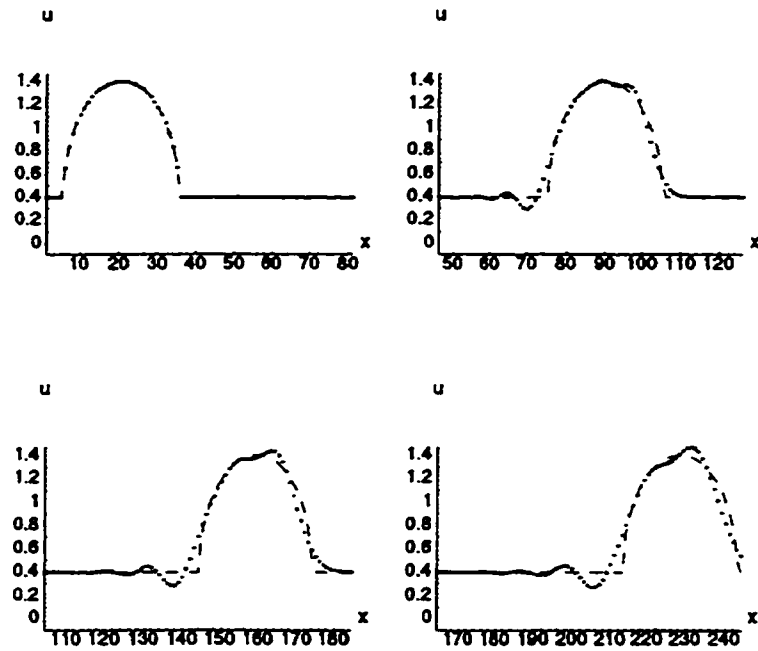


Figure 4.3 Numerical dispersion in the solution of a "travelling wave" equation (Ganzha and Vorozhtsov, 1996)

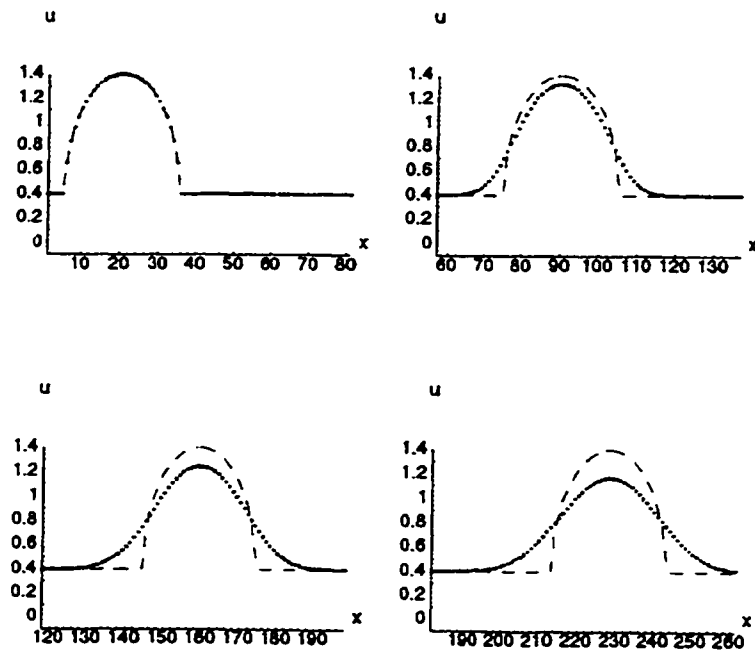


Figure 4.4 Numerical dissipation in the solution of a "travelling wave" equation (Ganzha and Vorozhtsov, 1996)

to handle some of the phenomena (this is, at least, the author's experience with the problem described here), especially considering the position of the water-suspension interface, i.e. the settlement of the system, which is automatically satisfied in Lagrangian coordinates. This was the reason for selecting this coordinate frame to solve the problem.

Instead of any further comment on the problems with solving a PDE, the concluding paragraph from a relevant chapter in Lapidus and Pinder's book (1982) will provide a vivid illustration of the situation:

"Recapitulating the material of this section, we state the following. The solution of first-order hyperbolic problems is schizophrenic. One can achieve a sharp front with associated spurious oscillations or a smooth solution that is smeared due to numerical diffusion. The trade-off between these two deleterious effects is elucidated through an analysis of phase and amplitude error attributable to the numerical scheme. Although all the numerical schemes considered here suffer from these limitations, some methods exhibit behaviour superior to others."

#### *Choice of a numerical scheme and its parameters*

The selected concrete FDM scheme is described in the next chapter. The idea was actually borrowed from the "moving mesh" methods, see Chapter 2.4.2.5. An initially uniform grid deforms with time and the nodal points move relative to each other to try to adapt their spatial distribution to the requirements of an optimal description of the deformation process. When each nodal point remains connected to the same material point to which it has been connected in the initial state, then one says that the grid is a Lagrangian one. The grid used in the solution of the coupled sedimentation and consolidation problem in this chapter behaved in just this way, following the motion of the material.

The simplest Eulerian time-forward marching scheme was chosen for advancing the solution in time. Although it is not very sophisticated by itself, it behaved well for limited time intervals in the examples calculated. The problem of numerical dispersion (oscillations) which sometimes appeared was simply removed by reducing the time step. This worked well for relatively smooth initial conditions, but not, for example, a very thinly laminated suspension in the initial state, with high differences in concentrations among layers. Although such problems are not likely to occur in practice, a more advanced scheme than the Eulerian one would be needed if one intends to extend the applicability of the model.

It should be noted that the model is presently available to deal with closed systems only (e.g. tank settling) without percolation of a fluid (seepage) through the system.

### **4.3.3 Description of the solution method**

Discretization of the initial settling column is shown in Figure 4.5a. The sedimenting system is divided into an array of equal cells (actually, intervals along the x-axis) and the nodal points are situated at the centres of the cells. The origin of the spatial coordinate  $x$  is placed at the surface of the suspension.

The state variable is the volumetric concentration  $c(x,t)$ . It is assumed that the initial state is known, i.e. that  $c(x,0) = c_0(x)$ , where the latter is a given function of  $x$ . In other words, the volumetric concentrations  $c_i^n$  at the nodal points are determined at the beginning of the calculation. Here the subscript  $i$  denotes the spatial position (node), while the superscript  $n$  denotes the time instant.

The cell  $i$  is shown in Figure 4.5b. The solids fluxes over the cell boundaries are denoted by a fraction in the subscript, for example  $(\phi_s)_{i+\frac{1}{2}}$  denotes the solids flux between the cells  $i$  and  $i+1$ .

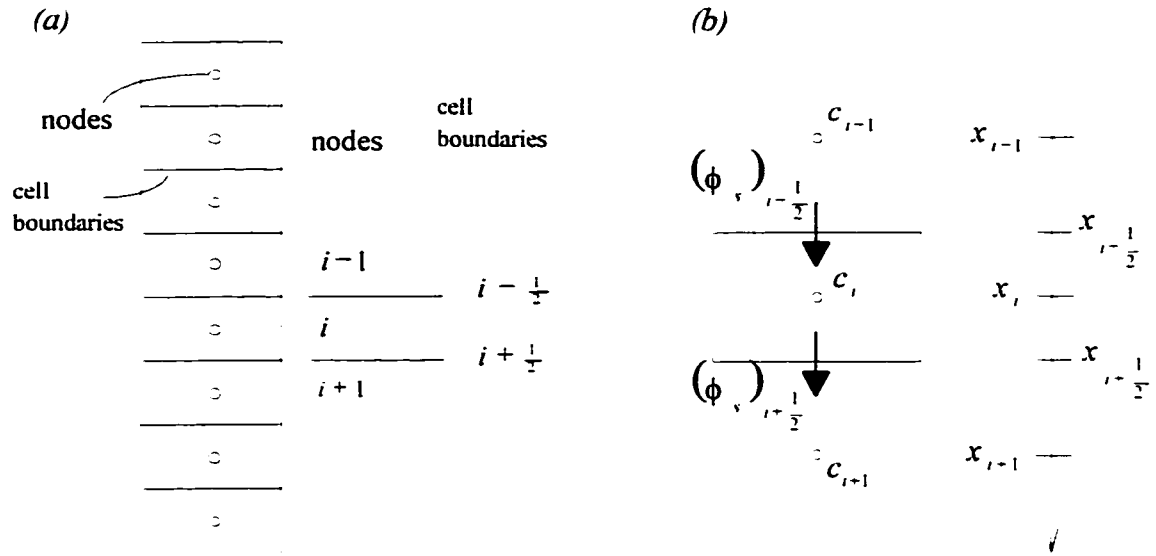


Figure 4.5 Numerical scheme in coupled sedimentation and consolidation analysis  
(a) discretization (b) principal variables—concentrations and fluxes

The system of governing equations is expressed in the form of a conservation law for both regions of sedimentation (the suspension) and consolidation (the sediment):

$$\begin{aligned} \frac{\partial c}{\partial t} + \frac{\partial (\phi_s)_{sed}}{\partial x} &= 0 & \text{where } (\phi_s)_{sed} &= c \cdot (v_s)_{sed} \\ \frac{\partial c}{\partial t} + \frac{\partial (\phi_s)_{cons}}{\partial x} &= 0 & \text{where } (\phi_s)_{cons} &= c \cdot (v_s)_{cons} \end{aligned} \quad [4.52]$$

where  $v_s$  is the settling velocity of solid particles. Its value is calculated according to two different expressions, depending on the region:

$$\begin{aligned}
(v_s)_{red} &= (G_s - 1) \cdot c \cdot k \\
(v_s)_{conv} &= (G_s - 1) \cdot c \cdot k - \frac{k}{\gamma_w} \frac{d\sigma'}{dc} \frac{\partial c}{\partial x}
\end{aligned} \tag{4.53}$$

noting again that the average flux  $(\phi_s + \phi_w) = f(t)$  is zero for a closed system assumed here.

The scheme is mathematically defined as “forward in time—centered in space” because of the use of the following finite difference approximations:

$$\begin{aligned}
\frac{\partial c}{\partial t} &\approx \frac{c_i^{n+1} - c_i^n}{\Delta t} & \Delta t &= t_n - t_{n-1} \\
\frac{\partial \phi_s}{\partial x} &\approx \frac{(\phi_s)_{i+\frac{1}{2}}^n - (\phi_s)_{i-\frac{1}{2}}^n}{\Delta x_i^n} & \Delta x_i^n &= x_{i+\frac{1}{2}}^n - x_{i-\frac{1}{2}}^n
\end{aligned} \tag{4.54}$$

where the solids flux at the element boundary is calculated as a sole function of the concentration at that boundary:

$$(\phi_s)_{i+\frac{1}{2}}^n = c_{i+\frac{1}{2}}^n \cdot v_s \left( c_{i+\frac{1}{2}}^n \right) \tag{4.55}$$

The “moving mesh” approach consists of the following steps:

(1) calculate concentrations at cell boundaries as averages of concentrations in adjacent nodes:

$$\begin{aligned}
c_{i+\frac{1}{2}}^n &= \frac{1}{2} (c_{i+1}^n + c_i^n) \\
c_{i-\frac{1}{2}}^n &= \frac{1}{2} (c_i^n + c_{i-1}^n)
\end{aligned} \tag{4.56}$$

(2) calculate boundary velocities and solids fluxes:

$$\begin{aligned}
(v_s)_{i+\frac{1}{2}}^n &= v_s \left( c_{i+\frac{1}{2}}^n \right) \\
(\phi_s)_{i+\frac{1}{2}}^n &= c_{i+\frac{1}{2}}^n \cdot v_s \left( c_{i+\frac{1}{2}}^n \right)
\end{aligned} \tag{4.57}$$

(3) calculate net (differential) solids fluxes:

$$(\Delta \phi_s)_i^n = (\phi_s)_{i+\frac{1}{2}}^n - (\phi_s)_{i-\frac{1}{2}}^n \tag{4.58}$$

(4) calculate the total volume of solids in the cell  $i$  at  $t + \Delta t$  (the next time step  $n+1$ ):



$$(V_s)_i^{n+1} = (V_s)_i^n - (\Delta\phi_s)_i^n \cdot \Delta t \quad \text{with} \quad (V_s)_i^n = c_i^n \cdot \Delta x_i^n \quad [4.59]$$

(5) update geometry:

$$\begin{aligned} x_{i+\frac{1}{2}}^{n+1} &= x_{i+\frac{1}{2}}^n + (v_s)_{i+\frac{1}{2}}^n \cdot \Delta t \\ \Delta x_i^{n+1} &= x_{i+\frac{1}{2}}^{n+1} - x_{i-\frac{1}{2}}^{n+1} \end{aligned} \quad [4.60]$$

(6) update concentrations (the state variable):

$$c_i^{n+1} = \frac{(V_s)_i^{n+1}}{\Delta x_i^{n+1}} \quad \text{or better} \quad c_i^{n+1} = \frac{(V_s)_i^0}{\Delta x_i^0} \quad [4.61]$$

where the second option is only valid for Lagrangian grid, and preferred then, because it eliminates the possibility of accumulation of computational errors.

Ideally, if the grid is really Lagrangian, the net solids fluxes are zero and steps 4 and 5 can be skipped. Practically, there is a possibility that the computational accuracy influences these values, giving a small but finite value to the net flux, and thus creating an error which may progressively increase with time. Certain trial calculations indicated that this type of error is negligible in the analyses conducted. Therefore, steps 4 and 5 were simply neglected in further analyses. The calculation of a current concentration from the initial one in the cell (the second option in step 6) eliminated another kind of progressively spreading computational error.

The boundary conditions for the whole settling column consisted of prescribed zero solids fluxes at the outer boundaries of the first and the last cell. This was transformed into the prescribed concentrations in two imaginary cells before the first and after the last cell, and two additional imaginary nodes in these cells, denoted as nodes (0) and (N+1). The concentrations in these imaginary cells was always set equal to the concentration values at adjacent nodes 1 and N, respectively:

$$\begin{aligned} c_0^n = -c_1^n &\Rightarrow (\phi_s)_{\frac{1}{2}}^n \equiv 0 \\ c_N^n = -c_{N+1}^n &\Rightarrow (\phi_s)_{N+\frac{1}{2}}^n \equiv 0 \end{aligned} \quad [4.62]$$

thus keeping the boundary fluxes at the ends of the settling column identically equal to zero.

Since the  $x$ -coordinate origin was set at the suspension surface, the settlement of the water-suspension interface was merely the displacement of the left boundary of cell 1. The internal boundary between suspended and sedimented material in the settling column was determined in each step by comparing the nodal concentrations with the critical concentration  $c_{cr}$ .

This procedure was simple to program and modify for the various variants tested. The main output was in the form of the suspension surface settlement versus time, as well as

the concentration profiles at chosen time instants. Other variables (stresses, pore pressures) were easily computed using simple algebraic expressions.

## **4.4 EXAMPLE**

The example chosen to illustrate the model for simultaneous sedimentation and consolidation derived in this chapter is again the 10 m standpipe test on the oil sands fine tailings. The geotechnical properties of this material have already been described in Chapter 3.2.2.

### **4.4.1 Result of simulation of 10 m standpipe test**

#### **4.4.1.1 Checking parameters from the sedimentation analysis in Chapter 3**

The analysis began with the parameters used earlier in the time-dependent sedimentation model from Chapter 3. The main parameters were:

- three permeability laws  $k(e)$  after Pollock (1988), Suthaker (1995) and the best-fit power function determined in Chapter 3;
- the critical concentration  $c_{cr} = 0.241$  (the suspension-sediment transition point), and the corresponding critical solids content  $s_{cr} = 0.42$ ; and
- the compressibility law according to Pollock (1988), see Chapter 2.4.1.4.

The spatial domain was discretized into 100 elements (intervals) and the time step was fixed at 0.005 years, giving thus resolution of 0.10 m spatially and about 2 days temporally. A few trial analyses were run with varying computation parameters to ensure that this choice was satisfactory. Therefore, all further analyses were carried out with these spatial and time steps.

The results are shown in Figures 4.6 and 4.7. It can be seen that this time the best results are obtained using Pollock's permeability data: there is almost perfect matching between the calculated settlement and the measured data in the first 5 years, as shown in Figure 4.7. This fact seems to support the findings of Pane and Schiffman (1997), see Chapters 2.3.1.5 and 3.2.2.3., that the initial velocity of particles falling in a suspension can be quite accurately predicted from the permeability measurements. However, the later deviation of the calculated line from the observational data also indicates that either the permeability law used is not the "real" one or that there are other factors of influence which were neglected in this analysis.

It may be noticed that the shapes of the suspension settlement lines and the sediment growth lines highly resemble the experimental results from Chapter 2. The initial straight portion of the settlement curve apparently corresponds to the "constant settling rate

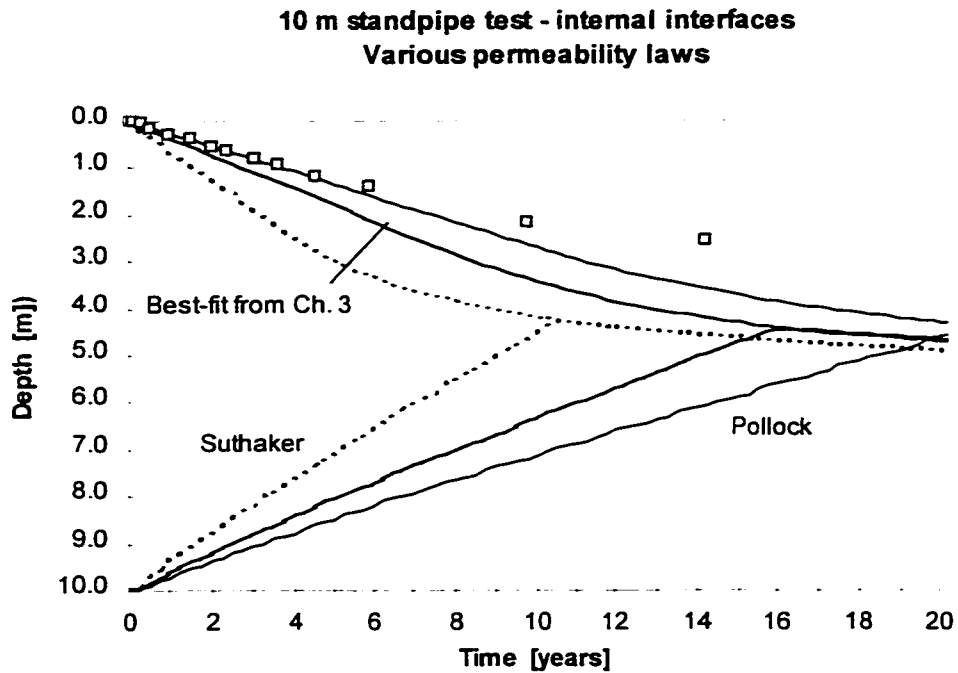


Figure 4.6 10 m standpipe test - motion of internal interfaces in time for various permeability laws in the power function form  $k(e) = Ae^B$

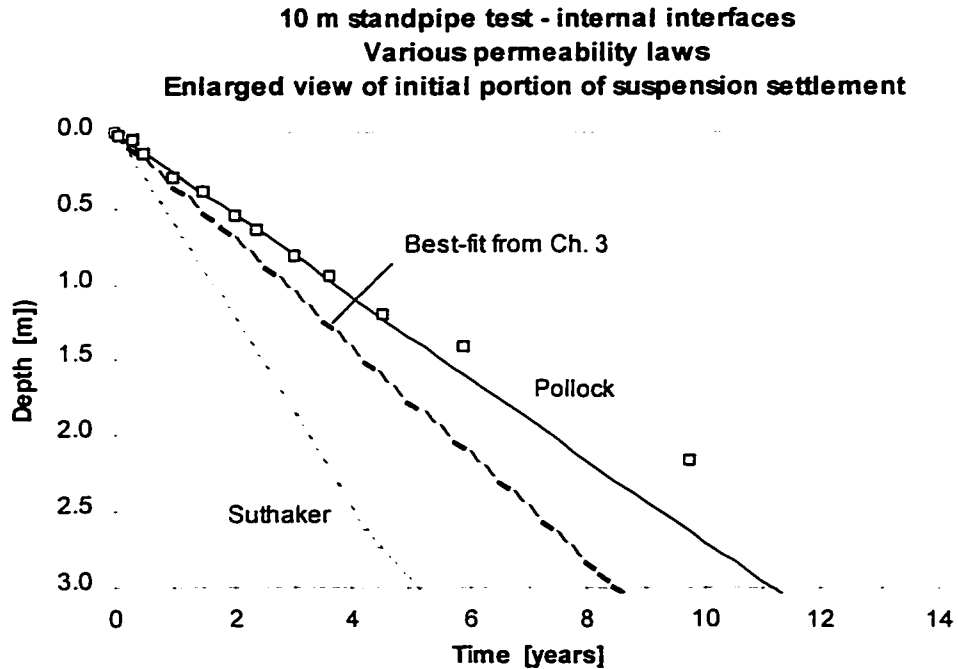


Figure 4.7 10 m standpipe test—motion of internal interfaces in time for various permeability laws—enlarged view of initial portion of settlement curves

region” from Tiller and Khatib (1984), see Chapter 2.3.1.2. The later bending of these lines and non-linear behaviour occurs when the first “density wave” from the bottom meets the suspension surface, as described by Kynch (1952); see Chapters 2.3.2.3 and 2.3.2.4. According to Pollock’s data it happens after about 10 years.

It is seen in Figure 4.6 that the sedimentation growth line merely merges with the suspension settlement line and that the latter appears continuous and smooth during the whole process. This is because the same permeability law  $k(e)$  is assumed to be valid in both the sedimentation and the consolidation stage. It also indicates that the permeability is the principal parameter in this model and possibly for the physical phenomenon itself. This agrees well with relevant experimental and observational facts gathered so far (see Chapter 2).

It may be concluded that the basic phenomenology is common to the sedimentation models in Chapters 3 and 4, although the parameters that optimize the results of comparative analyses of one and the same problem will probably never be identical. This is because the time-dependent sedimentation model in Chapter 3 deals with the average values of the parameters and assumes a rigid sediment, while the coupled model in this chapter considers differential changes and explicitly accounts for the sediment deformation.

From a practical point of view, it is important to recognize that accurate permeability measurements can lead to successful prediction of at least the beginning stages of the process of sedimentation and self-weight consolidation of a suspension.

#### **4.4.1.2 Best-fit permeability function for this model**

The best fit permeability function expressed in a power law form was determined by matching calculated with the measured data for the suspension settlement only; the other data (concentrations, pore pressures) were not considered. The model parameters are as given in the previous chapter.

Figure 4.8 shows that an almost perfect fit with measurements was reached. The permeability parameters  $A$  and  $B$  are written into the Figure. The position of this new permeability function is shown in a logarithmic  $e$ - $k$  diagram in Figure 4.9. It can be seen that this function is much steeper than the best fit  $k(e)$  from Chapter 3 (see Figure 3.16.b). It also differs in slope from other experimentally determined permeability laws—it almost crosses them at the ends of the void ratio axis. However, if one considers only the area of this graph which was of actual interest in the analysis (the dashed box in the Figure—void ratios in the range of approximately  $e \approx 2.5 - 5$ ) it can be seen that the best fit function is still within the boundaries of the measured permeability data, which gives credibility to the model. This is very important for practical applications because it reaffirms permeability testing and experimentally determined parameters. There is no need to artificially modify the permeability law or look for arguable influences in order to bring the analytical data of inadequate models closer to measurements (see Chapter 3.2.2.2).

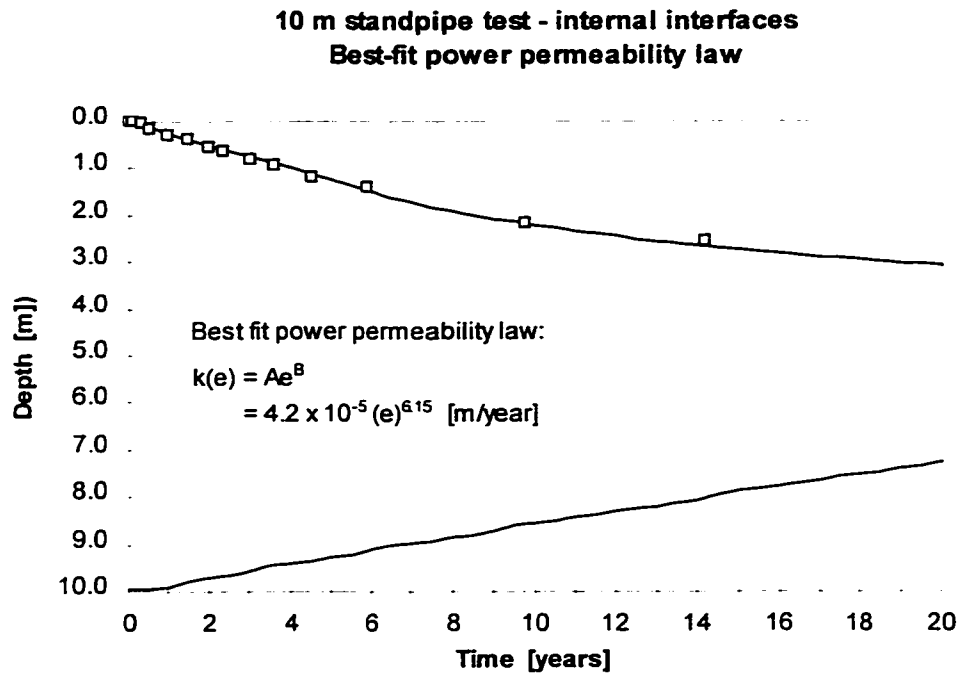


Figure 4.8 10 m standpipe test—best-fit power law permeability function (obtained considering settlement data only)

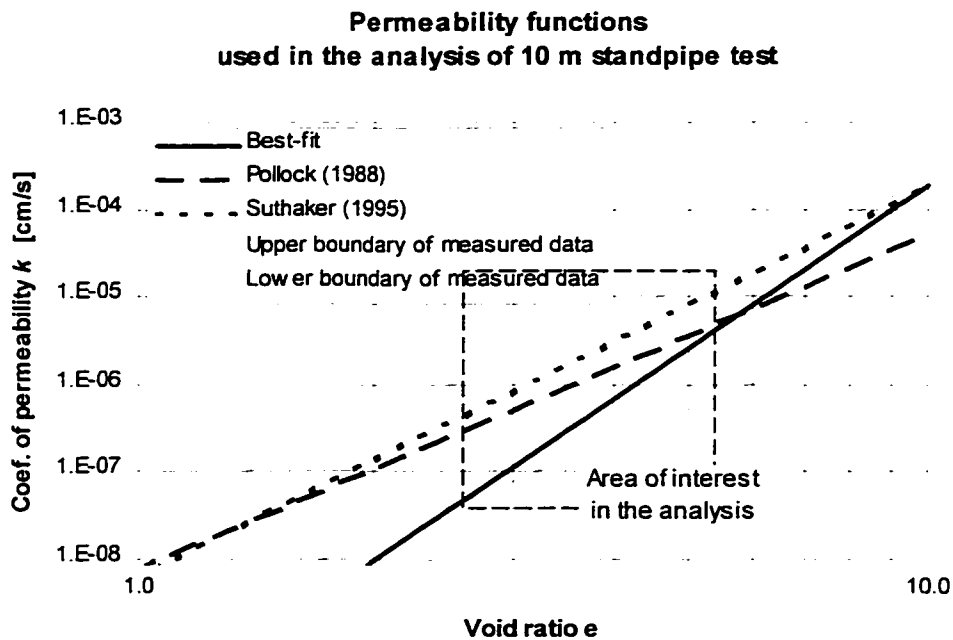


Figure 4.9 10 m standpipe test—the three power law permeability functions used in the analysis presented in Figures 4.6 - 4.8

On the other hand, if it is possible to have several differing interpretations of the same database of measurements, it indicates high sensitivity of a model response to the measured variable (the coefficient of permeability here). This interpretative ambiguity points out the need to develop both experimental procedures and interpretation tools to narrow the range of variability of the test results.

#### 4.4.1.3 Sensitivity analysis of the model

The following parameters were varied in the same way as it was done in Chapter 3:

- the parameters  $A$  and  $B$  of the permeability function  $k(e)$ ,
- the critical concentration  $c_{cr}$  (the suspension-sediment transition);
- the initial concentration  $c_0$  in the suspension;
- the parameters  $C$  and  $D$  of the compressibility function  $e(\sigma')$ ,
- the initial concentration distribution in the suspension.

##### *Parameters of the permeability function*

The effects of varying parameters  $A$  and  $B$  of the permeability function are shown in Figures 4.10 and 4.11. It is here confirmed what was already noted in Chapter 3: a proper estimate of the rate of change of permeability function  $k$  (parameter  $B$ ) is much more important in a sedimentation analysis than the relative magnitude of the function at a certain void ratio (parameter  $A$ ).

##### *Critical concentration $c_{cr}$*

The influence of the variation of  $c_{cr}$  on the results is shown in Figure 4.12. The influence is negligible during the sedimentation stage but becomes visible with the advance of consolidation. This means that the deformation of the consolidating layer in a simultaneous sedimentation and consolidation problem is of secondary importance compared with the settlement of the suspension layer. The latter is a dominant part of the vertical settlement (“deformation”) of the settling system as a whole.

A practical consequence of the above observation is that  $c_{cr}$  may be roughly estimated in an analysis without having significant effects on the settlement of the suspension surface. The same cannot be immediately concluded for other variables (concentrations and pore pressures).

To clarify this point, the solids content profiles after 14.33 years were plotted in Figure 4.16 for various critical concentrations  $c_{cr}$  from Figure 4.12. It is apparent that there are large differences in the sedimented layer at the bottom, where the solids content distribution (and the pore pressure distribution too) depends on the value of  $c_{cr}$ .

The relative insignificance of the exact moment when a suspension becomes a sediment (a soil) may be a fact in favour of Pane and Schiffman’s modification of the

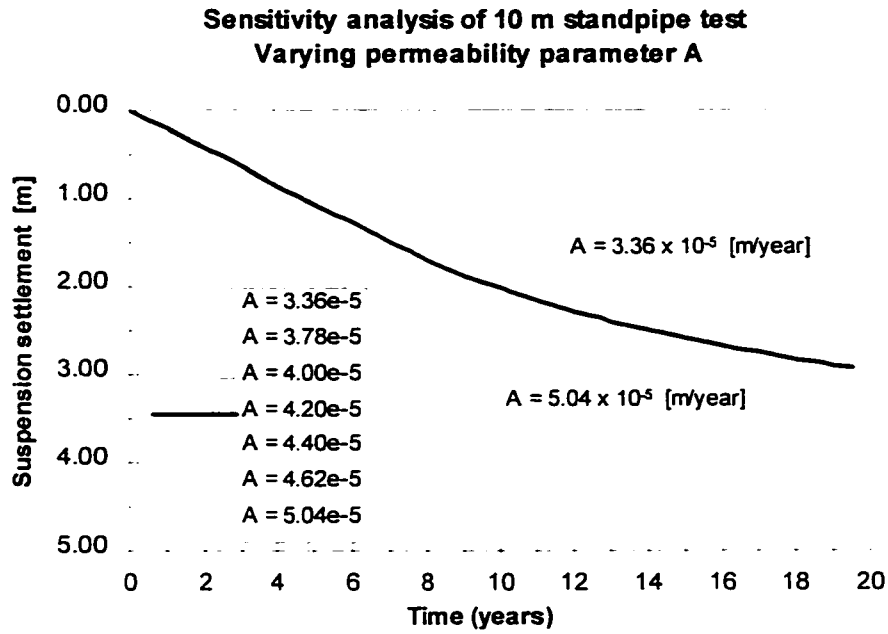


Figure 4.10 10 m standpipe test—sensitivity analysis of the proposed model; permeability parameter  $A$  varied  $\pm 20\%$  of the optimum value

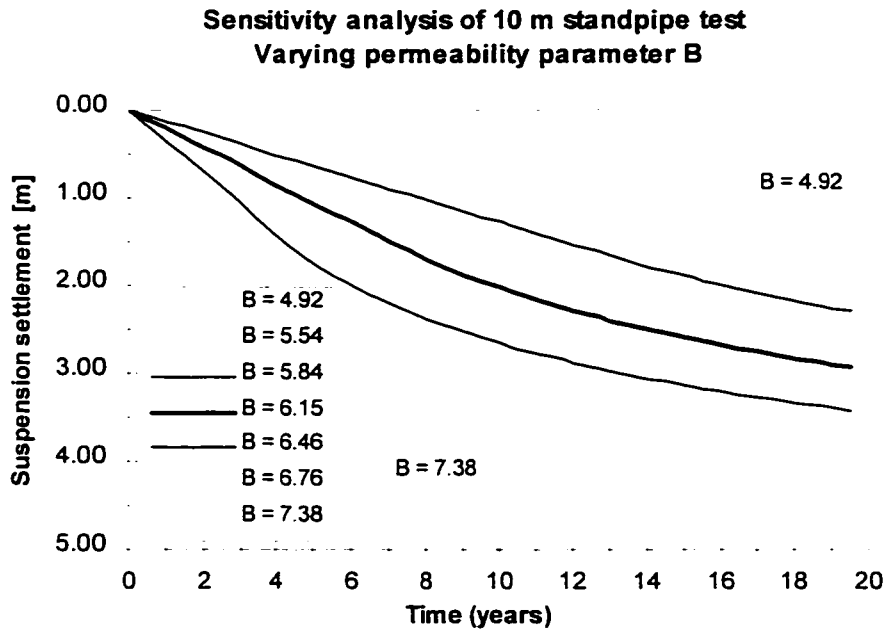


Figure 4.11 10 m standpipe test—sensitivity analysis of the proposed model; permeability parameter  $B$  varied  $\pm 20\%$  of the optimum value

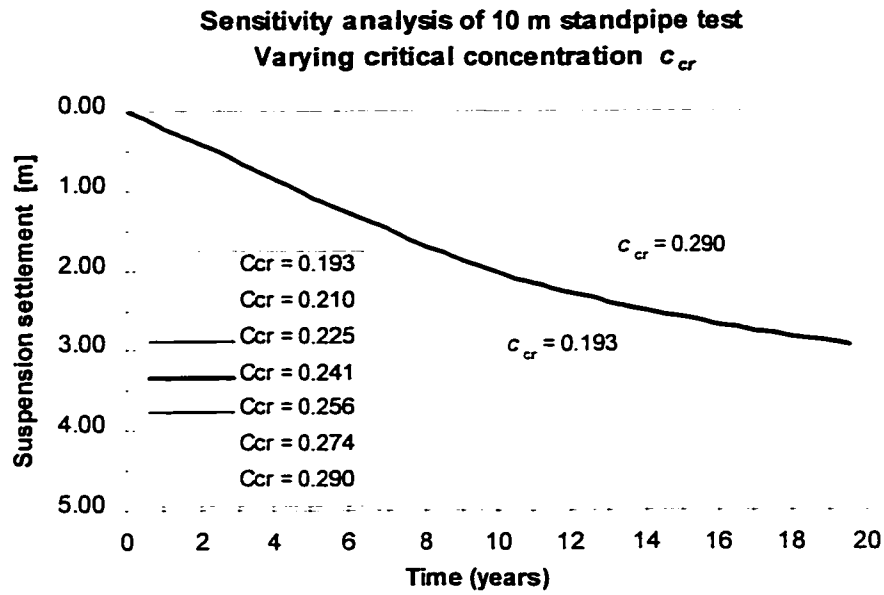


Figure 4.12 10 m standpipe test—sensitivity analysis of the proposed model:  
critical concentration  $c_{cr}$  varied  $\pm 20\%$  of the optimum value

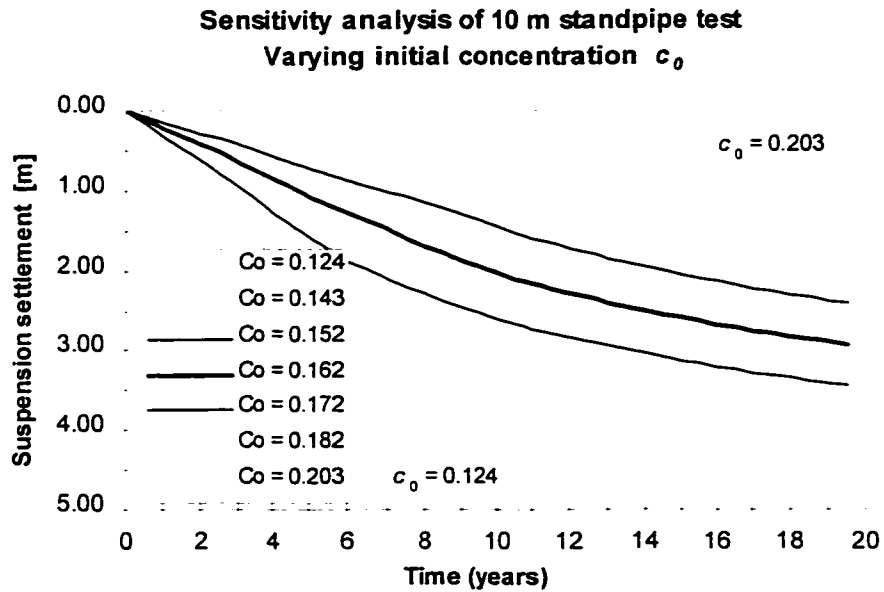


Figure 4.13 10 m standpipe test—sensitivity analysis of the proposed model:  
initial concentration  $c_0$  varied  $\pm 20\%$  of the optimum value



effective stress theory (the  $b$  coefficient, see Chapter 2.4.2.4) and Yong's observations on a zone, one between a suspension and a sediment, for which both sedimentation and consolidation theories may be concurrently applied (see Chapter 2.3.1.3). However, any further discussion on this subject would not be justified without some "true", convincing experimental data as a physical background. Otherwise, it might be reduced to an undesirable discussion about the theoretical possibilities of the proposed model.

#### *Initial concentration $c_0$*

The effect of  $c_0$  is shown in Figure 4.13. It can be seen that the initial concentration has a huge effect on the shape of the settlement curve, as already concluded in Chapter 3. If the initial concentration (the initial boundary condition) in a sedimentation problem is not accurately determined, a simulation may give erroneous results with otherwise correct input data.

#### *Parameters of the compressibility function*

The effect of varying parameters  $C$  and  $D$  of the compressibility function  $e(\sigma')$  is shown in Figures 4.14 and 4.15. There is no effect (within computational accuracy) of sediment compressibility on the settlement curve in this model.

The solids content profiles after 14.33 years are plotted in order to clarify other possible effects of compressibility on the response of our model; see Figure 4.17. As in the case of  $c_{cr}$ , there are large differences in the sedimented layer at the bottom, where the compressibility function dominantly influences the solids content distribution (and the pore pressure distribution as well).

#### *Effect of the type of initial solids content distribution*

Several types of likely initial concentration profiles in the suspension are shown in the settlement diagram in Figure 4.20. Besides a uniform profile, the so called "normal" profiles, with concentration increasing with depth, and the "inverted" profiles, with concentration decreasing with depth, were analysed. The maximum range of variation from the top to the bottom ( $T/B$  or  $B/T = 0.14/0.18$ ) is  $\pm 10\%$  of the initial value in the uniform suspension, a percentage that seems sensible (see Chapter 2). The reason for using an "inverted" concentration profile is that there is possible segregation when the coarse fraction settles "immediately" leaving the fine fraction in the suspension.

It can be seen that the type of initial solids content distribution is of limited effect in time: all the lines converge to the same curve after some time. "Mature" suspensions behave as if the initial concentration profile were uniform. This means that the detailed solids content profile in time  $t = 0$  is not as important as the average value of  $s_0$  at the beginning of the process (see the chapter on  $c_0$  above).

#### *General remarks about fitting the measured data in the 10 m standpipe test*

It is difficult to accurately fit the rather erratic data of this test even when only the settlement curve is considered. It is especially complicated when other variables are taken into account, for example the concentration profiles shown in Figure 4.21. It is

particularly hard to simulate the so called “perched consolidation” in the upper half of the suspension, which is attributed to the microbial activity and gas production within the suspension and the consequent decrease of permeability in that zone. These processes are obviously beyond the scope of this model.

On the other hand, it can be seen that in the lower part of the standpipe the trends in solids content profile development resemble the model response, despite the scarcity of data. For that purpose, the evolutionary processes of an initially uniform suspension and an initially “normal concentration” profile (with density increasing with depth) are plotted in Figures 4.22 and 4.23, respectively.

It may be noted that both profiles reach similar states after about 5 years and then continue to behave in a similar manner. One can easily recognize the process of time-dependent increase in concentration in the suspension zone, with almost parallel shifting of the concentration curve, indicating uniform “densification” over the whole height of the suspension zone. This phenomenon is present from the very beginning in the case of an initially “normal” density profile, as in Figure 4.23. In an initially uniform suspension, a certain period of time must elapse for the process to start (this may probably be connected to the motion of “density waves” within the suspension, according to Kynch’s theory). It should be emphasized that the cause of this time-dependent change in the suspension zone is a completely natural consequence of the sedimentation process and that there is no need to invoke other phenomena such as creep or thixotropy. This does not mean that these other phenomena do not exist or contribute to the process, but simply that a possible explanation of the observations does not necessarily need to include them.

Moreover, it was realized during the work that it is very difficult to optimize the model manually in the presence of numerous influential factors. It is possible to change:

- firstly, the permeability parameters within a very wide region of the measured data, in order to obtain a good matching of the settlement curve,
- secondly, the critical concentration and the compressibility parameters, to fit the spatial distributions of other measured variables (of solids contents and pore pressures) in selected time instants,
- then it is advisable to check that the parameters obtained are still within the acceptable limits, and to repeat the first step again in a recursive manner. This procedure may become very tedious, especially when measured data are not very regular and accurate. An automated procedure has to be developed which will account for all the important features of the physical phenomena and the simulation model.

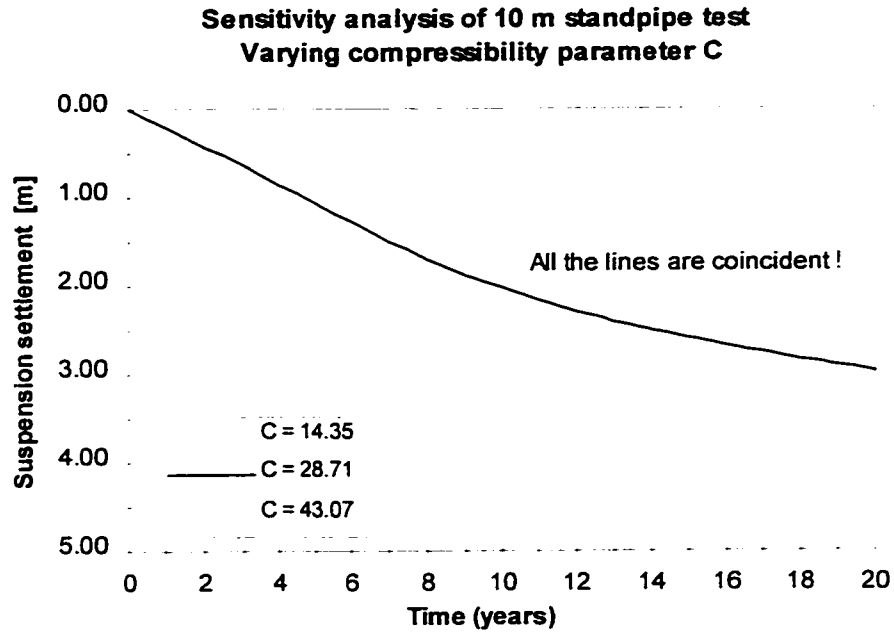


Figure 4.14 10 m standpipe test—sensitivity analysis of the proposed model; compressibility parameter  $C$  varied  $\pm 50\%$  of the optimum value

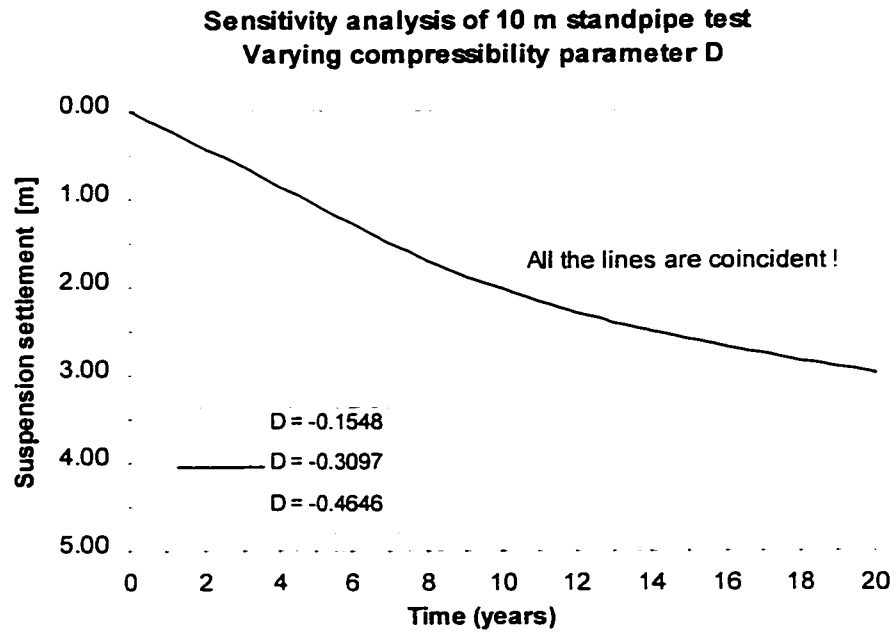


Figure 4.15 10 m standpipe test—sensitivity analysis of the proposed model; compressibility parameter  $D$  varied  $\pm 50\%$  of the optimum value

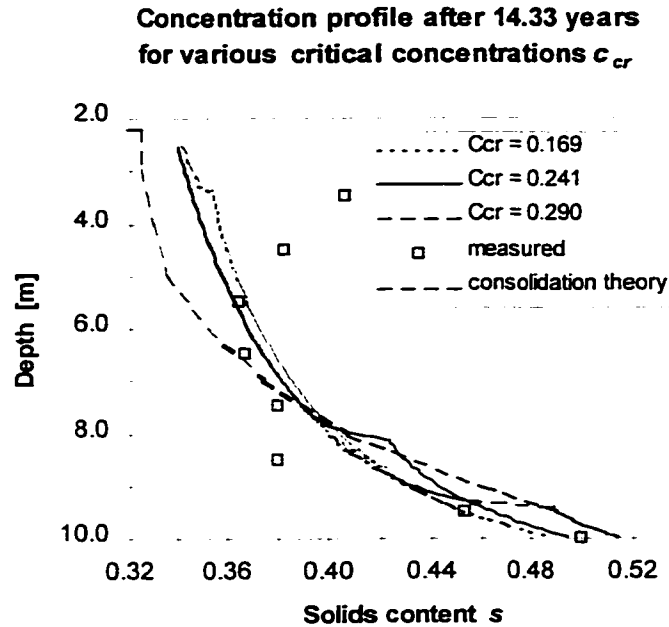


Figure 4.16 10 m standpipe test—sensitivity analysis of the proposed model: solids content profiles after 14.33 years for various critical concentrations  $c_{cr}$  from Figure 4.12

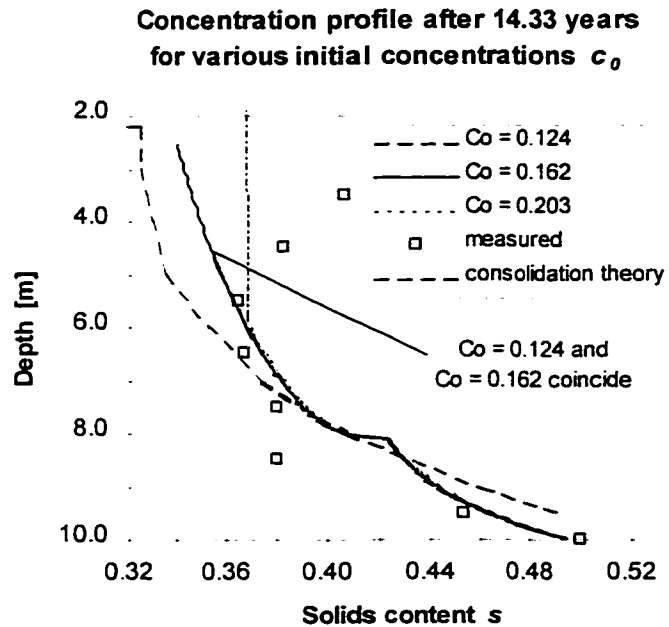


Figure 4.17 10 m standpipe test—sensitivity analysis of the proposed model: solids content profiles after 14.33 years for various initial concentrations  $c_0$  from Figure 4.13

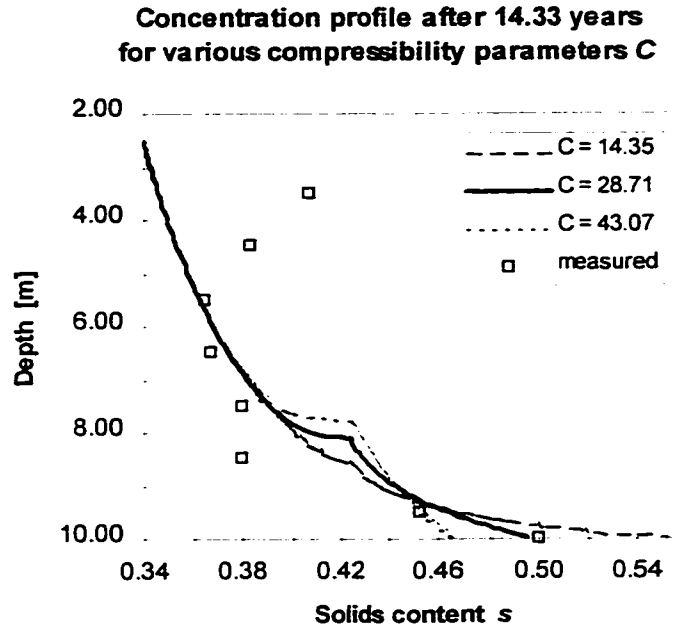


Figure 4.18 10 m standpipe test—sensitivity analysis of the proposed model; solids content profiles after 14.33 years for various compressibility parameters  $C$  from Figure 4.14

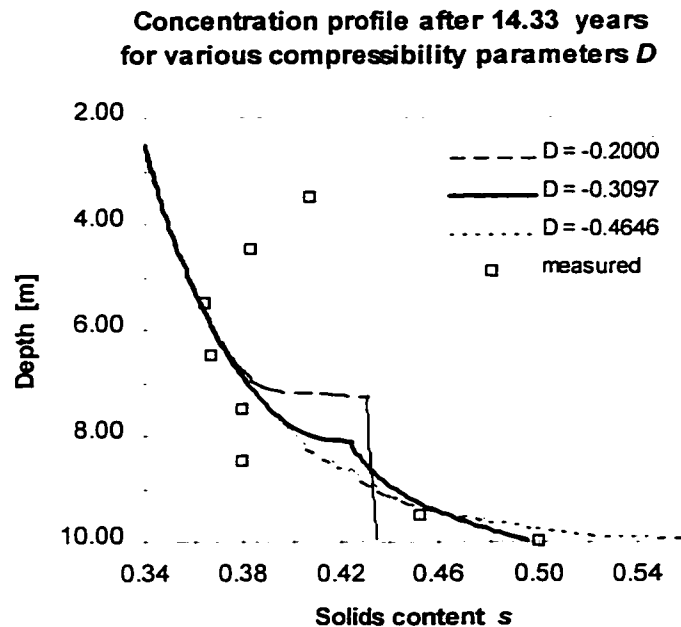


Figure 4.19 10 m standpipe test—sensitivity analysis of the proposed model; solids content profiles after 14.33 years for various compressibility parameters  $D$  from Figure 4.15

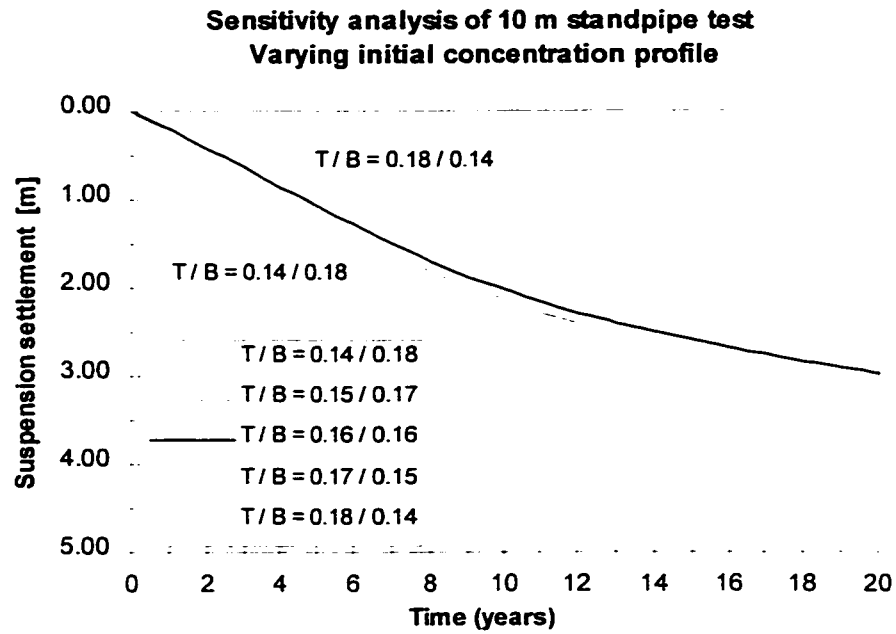


Figure 4.20 10 m standpipe test—sensitivity analysis of the proposed model; various initial concentration profiles (T , B - concentrations at the top and the bottom of the initial suspension)

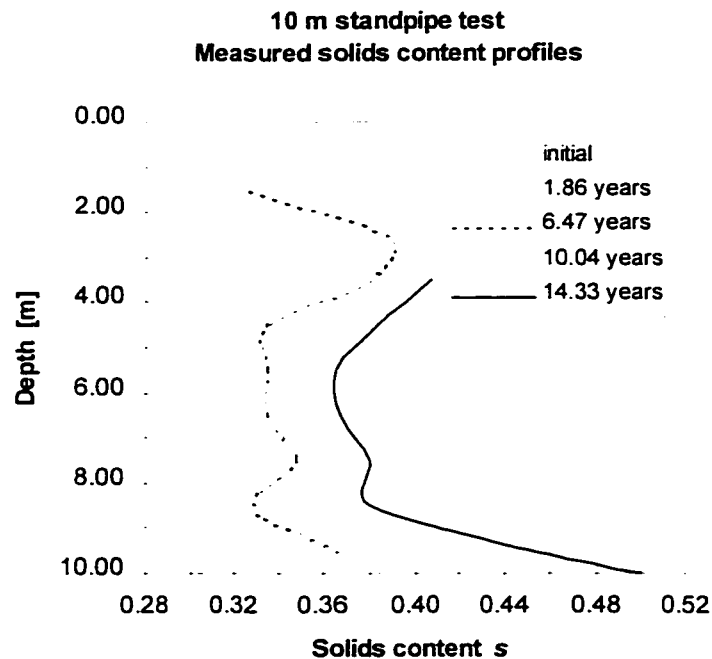


Figure 4.21 10 m standpipe test—sensitivity analysis of the proposed model; measured solids content profiles

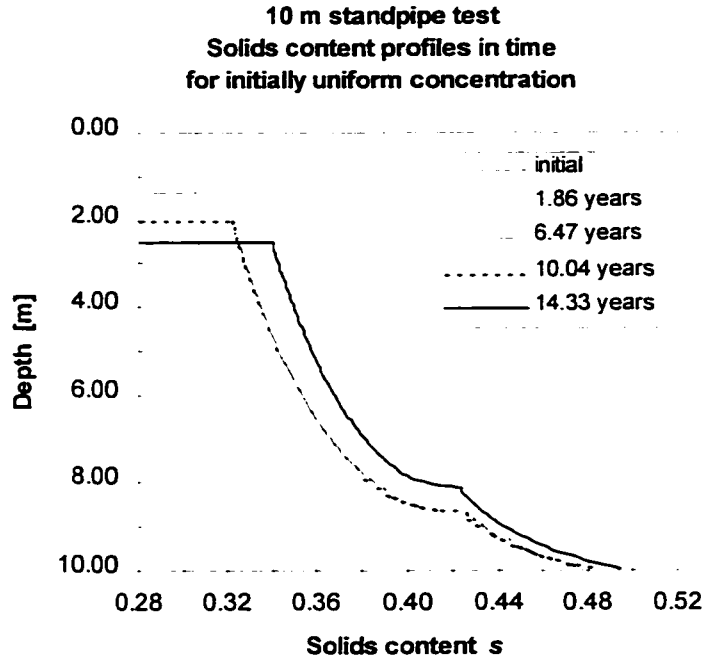


Figure 4.22 10 m standpipe test—sensitivity analysis of the proposed model: solids content profiles for an initially uniform suspension

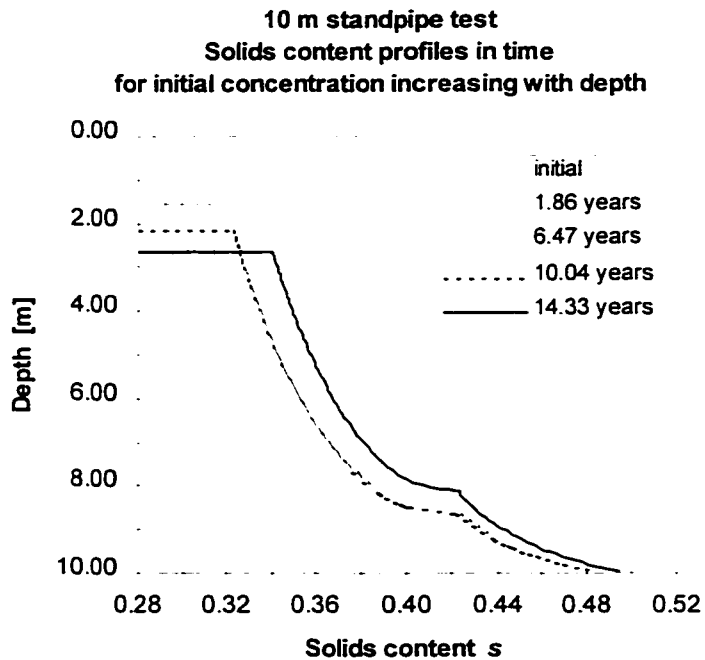


Figure 4.23 10 m standpipe test—sensitivity analysis of the proposed model: solids content profiles for an initial profile with concentration increasing with depth (top / bottom concentration = 0.15 / 0.17)

## 4.5 CONCLUSIONS

(a) A theory for coupled sedimentation and consolidation analysis has been derived from a common theoretical base consisting of fundamental laws of continuum mechanics.

The governing equation for sedimentation is expressed as a hyperbolic partial differential equation in the form of a conservation law. It is basically a non-linear form of the Kynch solution for hindered settling of a suspension.

The governing equation for consolidation is a parabolic partial differential equation expressed again in the form of a conservation law. It may be shown that it actually reduces to Gibson's general non-linear finite strain consolidation theory, as well as other finite strain consolidation theories. It may be further shown that Kynch's sedimentation theory is a special case of Gibson's consolidation theory for effective stresses set at zero.

The theory neglects any time-dependent phenomena in the system; specifically, thixotropy in the suspension and creep in the sediment are not considered.

(b) The concept of permeability offers a base for unification of the theories of sedimentation and consolidation. It may be assumed that the expression for the coefficient of permeability is applicable in both soil and suspended conditions of matter, regardless of the presence or absence of effective stress.

In the proposed model the permeability is modelled using a power law form, namely a straight line in a logarithmic  $k$ - $e$  diagram.

(c) Simultaneously solving the equations of sedimentation and consolidation is a very difficult mathematical problem because of the appearance of discontinuities in a typical solution. The procedure used in this instance is a finite difference scheme in a Lagrangian coordinate frame, with an Euler forward-marching time scheme. This procedure is presently capable of solving only a "closed system" with one impermeable boundary; i.e. it is confined to problems without percolation of the fluid through the system.

(d) Application of the theory to the simulation of the large-scale sedimentation and self-weight consolidation test on the oil sands fine tailings—the so called 10 m standpipe test at the University of Alberta—shows that it is possible to obtain a good match of the settlement observations and reasonable agreement with the concentration distribution in the lower part of the system. "Perched consolidation" in the upper part is probably caused by factors which are beyond this model.

(e) In the simulation of the 10 m standpipe test, the parameters of the model were varied within the limits of the measured data. No artificial adjustment of parameters was allowed, in order to reach better agreement of the calculation results with observations. Regardless of the variations, the correspondence was considered to be satisfactory.

(f) The calculated behaviour of the simulated system highly resembles general experimental and observational data in the reviewed literature, although the desired numerical accuracy was not achieved. It was realized that it is difficult to optimize the



model manually in the presence of numerous influential factors. An automated procedure which will account for all the important features of the physical phenomena and the simulation model has to be developed.

(g) Sensitivity analysis of the model shows that the principal parameters for settlement behaviour are permeability and initial concentration, while compressibility and critical concentration are insignificant.

Compressibility and critical concentration are of dominant importance for the calculation of solids content distribution in the sediment.

The process has a “smoothing” effect on irregularities in the initial concentration profile. After a certain amount of time passes, the system behaves almost as if it were an initially uniform suspension.

## ***Chapter 5***

### ***CONCLUSIONS AND RECOMMENDATIONS***

#### **5.1 CONCLUSIONS**

##### **5.1.1 Phenomenology of sedimentation and consolidation**

(a) It has been experimentally determined that a suspension passes through three settling regimes, or modes, in its lifetime: free settling, hindered (or zone) settling and consolidation. Depending on the initial concentration of the suspension, some of these modes may be absent.

The free settling regime appears in very dilute suspensions and is characterized by segregation of particles. This settling mode is not of great importance in geotechnics since the suspensions usually dealt with in practice are much more concentrated. The transition between free and hindered settling is not distinct. Hindered (zone) settling has best been described as the sedimentation of a suspension as a whole, with the particles seemingly captured in a spatial network. This phenomenon occurs without systematic and stable direct contacts between solid particles and, consequently, without definite effective stress. It is usually called a “hydrodynamic interaction”.

Consolidation is the settling caused by the “yielding” of stable and permanent particle contacts under self-weight, i.e. with finite effective stresses transmitted through the contact points. The boundary concentration between the hindered settling mode and the consolidation mode is not well defined and depends on the previous sedimentation regime. The main consequence is that the compressibility law in the small stress range is not unique, but depends on the initial concentration.

(b) Three well defined zones with varying concentrations appear in a still suspension over time: almost clear water at the top, a suspension zone in the middle and a sediment layer at the bottom. The settling behaviour of solid particles in these zones in general corresponds to the sedimentation modes above.

Experiments have determined the absence of effective stresses in the suspension zone. Consequently, physically correct models should treat the suspension zone as a “heavy liquid” and not as a solid body.

A refinement in the zonation of a settling system is possible by dividing the

suspension zone into an upper zone of nearly constant (or more precisely, slowly changing) concentration and a lower zone with variable spatial concentration. Some authors suggest that the lower suspension zone may exhibit features of both the suspension and the sediment. This is closely related to the problem of defining the boundary concentration between a suspension and a sediment.

(c) There is no agreement in the literature about the existence of a distinct value of solids concentration at the boundary between a suspended and a solid state of a particle assembly. Experimentation has not indicated any distinct physical transition, or a state transformation, or a sudden change in measurable quantities which may suggest a sharp boundary between the two states. Some authors (Been and Sills, 1981) intuitively understand this as a gradual transition depending not only on the concentration, but on many other parameters in play during the complete history of the sedimentation stage. Others (Yong 1984) have presented theoretical foundations and experimental methods to determine the boundary concentration explicitly, and have also proposed other factors of influence to this value.

Connected with this boundary issue is the question of discontinuities, or “shocks”, in the solutions of sedimentation problems. There are studies (Auzerais et al. 1988) that present very detailed theoretical discussions on this subject, but with limited practical value, because these features are difficult to observe and to measure experimentally.

The problem described above is directly related to the validity and applicability of Terzaghi’s effective stress principle. If a sharp boundary exists, then the region of applicability for this principle can be clearly defined. If not, the relevance of the laws that govern the behaviour of the system in these intermediate states remains questionable. Some authors (Pane and Schiffman, 1985) propose modifications to the effective stress principle, but without explanations of the physical background and without practical methods of estimating the influential factors. Others (Shodja and Feldkamp, 1993) invent rather artificial numerical ways to avoid this problem. Unfortunately, the available literature does not offer any definitive answer to this question.

This author decided to accept Terzaghi’s original concept of effective stress and to postulate the existence of the critical concentration  $c_{cr}$  as the boundary between the suspension and the sediment in his model. This determination was made only because of its practical convenience in the computational procedure. The value of  $c_{cr}$  itself was not *a priori* fixed, but rather considered as an optimization variable and determined as a part of the solution process. There is nothing to prevent one from including in a model a region of gradually changing parameters from a suspended state to a solid state. However, in the absence of the necessary experimental data which would more closely set boundaries for this transition zone, these parameters simply remain new optimization variables, and unnecessarily burden the calculation.

(d) The “micromechanics” of colloidal suspensions is still at an insufficiently high quantitative level for numerical computations, despite a vast amount of investigations on phase interaction in suspensions (and soils), and rare attempts of analyses which take into account the behaviour of solid particles at the microscopic level (Anandarajah 1994). The engineering approach, based on continuum mechanics, dominates the theory and practical applications due to its simplicity (there is a minimum number of empirical

parameters—only compressibility and permeability), its easy calibration, sufficient accuracy and cost-effectiveness.

(e) Permeability is one of the most varying parameters in geotechnics. There is still no general theory for permeability and neither is there yet a well defined methodology for experimental determination and interpretation of the permeability coefficient for very soft clays and clayey suspensions. Nevertheless, permeability is presently the most commonly used parameter in sedimentation and consolidation analyses. In sedimentation, it plays the role of a relative measure of the fluid-solid (hydrodynamic) interaction. In consolidation, it defines the “permissible rate” of deformation caused by an increase of effective stresses, i.e. the rate of interaction among the solid particles themselves. As such, permeability appears as a logical unifying property linking the suspended and the solid state of a soil.

(f) Specific properties of oil sands fine tailings behaviour are: (1) time dependent increase of solids content in the suspension zone during sedimentation; (2) development of solids structure in the suspension and thixotropic strength gain in this zone; (3) relatively high creep in the sedimented material; (4) difficulties in laboratory determination of reliable permeability and compressibility parameters as input values for mathematical modelling; (4) presence of residual bitumen and its influence on the mechanical properties of the suspension; (5) the appearance of an odd “perched consolidation zone” near the top of the suspension, with increased concentration probably caused by microbial activity and gas production; etc. All these peculiarities indicate difficulties encountered in the simulation of real behaviour of this material.

Permeability and compressibility of fine tailings are experimentally determined as unique functions of a void ratio, although other factors may have significant influence (such as thixotropy, creep, etc., which are practical consequences of the changes in particle interaction without a change in porosity). Since these effects have not been defined in a mathematically precise way, they were not introduced into this developed model. Nevertheless, in concrete computations, the parameters were carefully chosen so as to reflect the behaviour of the real material.

### **5.1.2 Modelling sedimentation and consolidation**

(g) Current practice in modelling these processes in chemical engineering is physically correct: the suspension is considered essentially as a liquid and Kynch’s sedimentation theory is applied, while the sediment is considered as a solid body and Gibson’s consolidation theory is used. It has been shown that the Kynch theory is a special case of Gibson’s theory for effective stresses assumed to be zero. These theories are thus consistent with physical reality and experimental observation.

An undesirable extension of Gibson’s theory to the suspension, assuming it is a solid body, is usually encountered in geotechnical applications. It may be practically useful in certain situations where it gives approximate solutions to the problems considered, but is surely not a reliable enough approach for deeper understanding of the phenomenon and the future development of its modelling.

(h) A pure sedimentation model is here derived which considers the suspension as a

uniform zone with time-dependent concentration, and which assumes a rigid, non-deformable sediment. The only two parameters are the velocity of particles settling in the suspension and the fixed concentration in the sediment. This model was applied to the simulation of large-scale sedimentation tests on the oil sands fine tailings and showed improved agreement with experimental observations in comparison with the results of a purely consolidation model.

The fact that an essentially simple sedimentation model gives results of at least equal quality as a sophisticated consolidation model (with nonlinear material properties, incorporated creep, etc.) witnesses to the importance of physical consistency in the analysis. If the model correctly represents reality, there is no need to use complicated theories and adjust the parameters artificially. Then the phenomenon may be simulated with a minimum number of parameters, and their values can be reliably determined by simple experiments.

(i) A model for simultaneous sedimentation and consolidation was derived based on the laws of continuum mechanics and the theory of solid-liquid mixtures. It uses the concept of permeability as a unifying principle at the level of theory. Namely, the coefficient of permeability is the main factor in determining the particle velocity in the suspension and the rate of deformation of the sediment in corresponding governing equations. The same permeability law is assumed to be valid continuously over the range of void ratios covering both sedimentation and consolidation.

The assumption of existence of the critical concentration  $c_{cr}$  as a distinct boundary between the suspension and the sediment is introduced in this model because of its practical convenience in the computational procedure.

This theory neglects any purely time-dependent phenomena in the system: specifically, thixotropy in the suspension and creep in the sediment are not considered.

The model was tested again on the example of a 10 m standpipe sedimentation test on oil sands fine tailings with reasonable agreement between calculation and measured data.

The calculated behaviour of the selected example highly resembles the general experimental and observational data in the published literature (Tiller and Khatib 1984, Been and Sills 1981). Sensitivity analysis shows reasonable agreement between the effects of model parameters and their physical counterparts. The model also possesses the versatility needed for practical applications. Nevertheless, detailed checks and further verification on more diverse examples are needed in order to: (1) verify the validity of fundamental assumption that permeability is the principal factor in the process, and (b) to properly estimate the area of applicability.

(j) It is the author's opinion that the main obstacle in further development of coupled sedimentation-consolidation models are mathematical difficulties in solving the system of governing equations. This difficulty is especially related to the sedimentation equation which introduces discontinuities into the solution. Discontinuities are very difficult to deal with in Eulerian coordinate frame.

The author solved the governing equations by actually abandoning the problem of discontinuities through a combination of convenient theoretical assumptions and the use of Lagrangian coordinates. Namely, determination of the position of the water-

suspension interface was eliminated by the use of Lagrangian coordinates which are connected to material points and move with them. Determination of the suspension-sediment interface was avoided: (1) by assuming the continuous validity of the permeability law  $k(e)$  in both sedimentation and consolidation regions, and (2) by adopting the fluid nature of the suspension zone with effective stress  $\sigma' = 0$ , and the gradual increase of effective stress in the sediment from zero value at the suspension-sediment interface. Therefore, discontinuities do not exist in the model in a mathematical sense, although it may not seem so when one looks at the concentration profiles.

The author does not claim that this is an efficient approach for similar problems. It was just a convenient simplification, in the sense of the assumption of a constant coefficient of consolidation in some theories, which enabled one to obtain the analytical solution. Further improvement of the numerical procedure is one of the main tasks ahead.

(*k*) Parametric analysis of the possibilities of the model shows that the principal factors for settlement behaviour are the permeability and the initial concentration of the suspension, while the compressibility and the critical concentration of solids (the solid-liquid transition) are of dominant importance only in the sediment. This seems consistent with previous knowledge.

The process has a “smoothing” effect on irregularities in the initial concentration profile. After a certain amount of time passes, the system behaves almost as if it were an initially uniform suspension.

(*l*) Application of the theory to the simulation of the large scale sedimentation and self-weight consolidation test on the oil sand fine tailings—the so-called 10 m standpipe test at the University of Alberta—shows that it is possible to obtain very good matching of the settlement observations and reasonable agreement with the concentration distributions in the lower part of the system. So-called “perched consolidation” in the upper part is probably caused by other factors which are beyond this model.

It may be worth repeating that in this simulation the parameters of the model were varied within the limits of experimentally measured values. No artificial adjustment of parameters was allowed in order to reach better agreement of the calculation results with the observations.

(*m*) It was realized that it is difficult to optimize the model manually in the presence of numerous influential factors. An automated procedure which will account for all the important features of the physical phenomena and the corresponding measured data has to be developed and incorporated into the model.

## 5.2 RECOMMENDATIONS

(a) Further advance in understanding, and possibly expanding, the capabilities of the model for simultaneous sedimentation and consolidation requires verification of the concept of permeability as the unifying property of both processes. One of the possible ways is to apply the concept to a set of selected examples which cover reasonable ranges of the model parameters, although it is doubtful that such examples may be found in the available literature.

Another more direct way is to improve the features of the solution procedure and allow for the fluid percolation through the system in the analysis, in order to be able to simulate permeability testing as a process which yields the principal input data. In this way, a discrepancy between the test and its interpretation will be avoided—the model will be used to back-calculate the properties of the material which it simulates. On the other hand, it might be necessary to investigate the effects of the test setup (the slurry consolidometer) on the values of permeability coefficients obtained as the results of the test.

(b) It may be useful to incorporate into the model the “missing parts”: the time-dependent deformation (creep) in the sediment and the thixotropic strength gain in the suspension. The physical basis for the latter is not clear, nor the way in which the parameters may be affected (namely, the permeability of the suspension as the only one). Nevertheless, this inclusion may enhance the versatility of the model in various applications.

(c) With regard to the behaviour of oil sands fine tailings, further analyses of the ways in which the hydraulic gradient and the bitumen content influence permeability, and the ways in which the initial void ratio (actually, the “ageing” and the solids structure development in the suspension) affects compressibility, may be useful. In computational terms, both parameters may be defined as functions not only of void ratio, but of the other parameters as well, and then the sensitivity analysis may be performed.

(d) The model itself should be improved by:

- substituting the Eulerian time-marching scheme with a more robust procedure,
- enabling more arbitrary mathematical forms for permeability and compressibility functions than it is allowed by a power law, and
- incorporating the model into an optimization procedure which can enable automatic adjustment of the parameters to a set of complete measured data (settlements, concentrations and pore pressures).

## BIBLIOGRAPHY

- Anandarajah, A. 1994. Discrete-Element Method for Simulating Behaviour of Cohesive Soil. *Journal of Geotechnical Engineering*, **120**:1593-1613.
- Ames, W.F. 1969. *Numerical Methods for Partial Differential Equations*. Thomas Nelson and Sons, London.
- Auzerais, F.M., Jackson, R., and Russel, W.B. 1988. The resolution of shocks and the effect of compressible sediments in transient settling. *Journal of Fluid Mechanics*, **195**: 437-462.
- Been, K., and Sills, G.C. 1981. Self-weight consolidation of soft soils: an experimental and theoretical study. *Geotechnique*, **31**: 519-535.
- Bourgeois, E., and Dormieux, L. 1996. Consolidation of a nonlinear poroelastic layer in finite deformations. *European Journal of Mechanics, A/Solids*, **15**: 575-598.
- Burland, J.B., and Roscoe, K.H. 1969. Local strains and pore pressures in a normally consolidated clay layer during one-dimensional consolidation. *Geotechnique*, **19**: 335-356.
- Cheng, N-S. 1997. Effect of Concentration on Settling Velocity of Sediment Particles. *ASCE Journal of Hydraulic Engineering*, **123**: 728-731.
- Diplas, P., and Papanicolaou, A.N. 1997. Batch Analysis of Slurries in Zone Settling Regime. *ASCE Journal of Environmental Engineering*, **123**: 659-667.
- Dixon, D.C. 1977. Momentum balance aspects of free settling theory. I: Batch thickening. *Separation Science*, **12**: 171-191.
- DuChateau, P., and Zachmann, D.W. 1983. *Partial Differential Equations*. McGraw Hill, New York, N.Y.
- Eckert, W., Masliyah, J.H., Gray, M.R., and Fedorak, P.M. 1996. Prediction of sedimentation and consolidation of fine tails. *AIChE Journal*, **42**: 960-972.
- Font, R., Perez, M., and Pastor, C. 1994. Permeability Values from Batch Tests of Sedimentation. *Industrial Engineering Chemistry Research*, **33**: 2859-2867.
- Fox, P.J., and Berles, J.D. 1997. CS2: A piecewise-linear model for large strain consolidation. *International Journal for Numerical and Analytical Methods in Geomechanics*, **21**: 453-475.
- Ganzha, V.G., and Vorozhtsov, E.V. 1996. *Numerical Solutions for Partial Differential Equations: Problem Solving Using Mathematica*. CRC Press, Boca Raton, Florida.
- Garlanger, J.E. 1972. The consolidation of soils exhibiting creep under constant effective stress. *Geotechnique*, **22**: 71-78.



- Gibson, R.E., England, G.L., and Hussey, M.J.L. 1967. The theory of one-dimensional consolidation of saturated clays, I. Finite non-linear consolidation of thin homogeneous layers. *Geotechnique*, **17**: 261-273.
- Gibson, R.E., Schiffman, R.L., and Cargill, K.W. 1981. The theory of one-dimensional consolidation of saturated clays, II. Finite non-linear consolidation of thick homogeneous layers. *Canadian Geotechnical Journal*, **18**: 280-293.
- Harr, M.E. 1977. *Mechanics of Particulate Media: A Probabilistic Approach*. McGraw-Hill, New York, N.Y.
- Howells, I., et al. 1990. Time-dependent batch settling of flocculated suspensions. *Applied Mathematical Modelling*, **14**: 77-86.
- Kynch, G.J. 1952. A Theory of Sedimentation. *Transactions of Faraday Society*, **48**: 166-176.
- Lapidus, L., and Pinder, G. 1982. *Numerical Solution of Partial Differential Equations in Science and Engineering*. John Wiley and Sons, Inc., New York.
- Lee, K., and Sills, G.C. 1979. A moving boundary approach to large strain compression of a thin soil layer. *Proceedings, 3<sup>rd</sup> International Conference on Numerical Methods in Geomechanics*, Rotterdam, Netherlands, 1979. pp. 163-173.
- Lee, K., and Sills, G.C. 1981. The consolidation of a soil stratum, including self-weight effects and large strains. *International Journal for Numerical and Analytical Methods in Geomechanics*, **5**: 405-428.
- Leroueil, S. 1997. Critical state soil mechanics and the behaviour of real soils. *Symposium on Recent Developments in Soil and Pavements Mechanics*, Rio de Janeiro, Brazil.
- Li, Y., and Mehta, A.J. 1998. Assessment of Hindered Settling of Fluid Mudlike Suspensions. *ASCE Journal of Hydraulic Engineering*, **124**: 176-178.
- Lin, T.W., and Lohnes, R.A. Sedimentation and Self Weight Consolidation of Dredge Spoil. *Proceedings, Sedimentation/Consolidation - Prediction and Validation*, San Francisco, California, October 1, 1984. pp. 464-480.
- Mase, G.E. 1970. *Theory and Problems in Continuum Mechanics*. Mc-Graw Hill, New York, N.Y.
- McRoberts, E.C., and Nixon, J.F. 1976. A theory of soil sedimentation. *Canadian Geotechnical Journal*, **13**: 294-310.
- McVay, M.C., Townsend, F.C., and Bloomquist, D.G. 1986. Quiescent Consolidation of Phosphatic Waste Clays. *ASCE Journal of Geotechnical Engineering*, **112**: 1033-1049.
- McVay, M.C., Townsend, F.C., and Bloomquist, D.G. 1989. One-Dimensional Lagrangian Consolidation. *ASCE Journal of Geotechnical Engineering*, **115**: 893-898.
- Mesri, G., and Rokhsar, A. 1974. Theory of consolidation for clays. *ASCE Journal of the Geotechnical Engineering Division*, **100**: 889-904.

- Mitchell, J.K. 1993. Fundamentals of soil behaviour. 2<sup>nd</sup> edition. John Wiley and Sons, Inc., New York.
- Monte, J.L., and Krizek, R.J. 1976. One-dimensional mathematical model for large-strain consolidation. *Geotechnique*, **26**: 495-510.
- Olson, R.E., and Ladd, C.C. 1979. One-dimensional consolidation problems. *ASCE Journal of the Geotechnical Engineering Division*, **105**: 11-30.
- Olson, R.E. 1986. State of the art: Consolidation testing. Consolidation of soils: Testing and evaluation. ASTM STP 892, American Society for Testing and Materials, Philadelphia, pp. 7-70.
- Oran, E.S., and Boris, J.P. 1987. Numerical Simulation of Reactive Flow. Elsevier. New York, N.Y.
- Pane, V., and Schiffman, R.L. 1985. A note on sedimentation and consolidation. *Geotechnique*, **35**: 69-72.
- Pane, V., and Schiffman, R.L. 1997. The permeability of clay suspensions. *Geotechnique*, **47**: 273-288.
- Pollock, G.W. 1988. Large strain consolidation of oil sands tailing sludge. M.Sc. thesis. University of Alberta, Edmonton, Alberta.
- Prevost, J.H. 1980. Mechanics of Continuous Porous Media. *International Journal of Engineering Science*, **18**: 787-800.
- Richardson, J.F., and Zaki, W.N. 1954. Sedimentation and fluidisation: part 1. *Transactions of Institution of Chemical Engineers*, **32**: 35-53.
- Schiffman, R.L., Vick, S.G., and Gibson, R.E. Behaviour and properties of hydraulic fills. Proceedings, Hydraulic Fill Structures, Fort Collins, Colorado, August 15-18, 1988.
- Schofield, A.N., and Wroth, C.P. 1968. Critical State Soil Mechanics. McGraw-Hill, London.
- Skopek, P. and McRoberts, E.C. 1997. Report to Syncrude Canada Ltd.. Edmonton Research Centre, Progress on MFT Modelling. AGRA Earth & Environmental Ltd., Edmonton, Alberta, Edmonton.
- Scott, J.D., and Cymerman, G.J. 1984. Prediction of viable tailings disposal methods. Proceedings, Sedimentation/Consolidation Models-Predictions and Validation, San Francisco, California, October 1, 1984. pp. 522-544.
- Scott, J.D., Dusseault M.B., and Carrier III, W.D. 1986. Large-scale self weight consolidation testing. Consolidation of Soils: Testing and Evaluation. ASTM SPT 892, pp. 500-515.
- Shen, C., Russel, W.B., and Auzeais, F.M. 1994. Colloidal Gel Filtration: Experiment and Theory. *AIChE Journal*, **40**: 1876-1891.

- Shodja, H.M., and Feldkamp, J.R. 1993. Numerical analysis of sedimentation and consolidation by the moving finite element method. *International Journal for Numerical and Analytical Methods in Geomechanics*, **17**: 753-769.
- Song, T., and Chiew, Y-M. 1997. Settling Characteristics of Sediments in Moving Bingham Fluid. *ASCE Journal of Hydraulic Engineering*, **123**: 812-815.
- Strikwerda, J.C. 1989. *Finite Difference Schemes and Partial Differential Equations*. Wadsworth & Brooks/Cole Advanced Books & Software, Pacific Grove, California.
- Suthaker, N. 1995. Geotechnics of oil sands fine tailings. Ph.D. thesis. University of Alberta, Edmonton, Alberta.
- Suthaker, N.N., and Scott, J.D. 1995a. Creep behaviour of oil sand fine tails. *Proceedings, International Symposium on Compression and Consolidation of Clayey Soils, Hiroshima, May 10-12, 1995*. pp. 195-200.
- Suthaker, N.N., and Scott, J.D. 1995b. Thixotropic strength measurements of oil sand fine tails. *Canadian Geotechnical Journal*, **34**: 974-984.
- Suthaker N., Scott, J.D. and Miller, W.G. 1997. The first fifteen years of a large scale consolidation testing.
- Tang, J., Biggar, K.W., Scott, J.D., and Sego, D.C. 1997. Examination of Mature Fine Tailings Using a Scanning Electron Microscope. *Proceedings, Canadian Geotechnical Conference, October 1997, Ottawa, Ontario*.
- Terzaghi, K. 1943. *Theoretical soil mechanics*. John Wiley and Sons. Inc., New York.
- Tiller, F.M. 1981. Revision of Kynch Sedimentation Theory. *AIChE Journal*, **27**: 823-828.
- Tiller, F.M., and Khatib, Z. 1984. The theory of sediment volumes of compressible, particulate structures. *Journal of Colloid and Interface Science*, **100**: 55-67.
- Toorman, E.A. 1996. Sedimentation and self-weight consolidation: general unifying theory. *Geotechnique*, **46**: 103-113.
- Toorman, E.A. and Gudehus, G. 1998. Sedimentation and self-weight consolidation: general unifying theory, Discussion. *Geotechnique*, **48**: 295-298.
- van Olphen, H. 1977. *An Introduction to Clay Colloid Chemistry*. John Wiley & Sons, New York, N.Y.
- Yong, R.N. 1984. Particle Interaction and Stability of Suspended Solids. *Proceedings, Sedimentation/Consolidation - Prediction and Validation, San Francisco, California, October 1, 1984*. pp. 30-59.

## ***Appendix 1***

### ***VOLUMETRIC AND WEIGHT RELATIONS***

#### **A.1.1 Notation**

The following symbols are used in this Appendix (see Figure A.1.1 for graphical illustration):

$W_t$	total weight of an element
$W_s$	total weight of solids in an element
$W_w$	total weight of water in an element
$V_t$	total volume of an element
$V_s$	total volume of solids in an element
$V_w$	total volume of water in an element
$s$	solids content
$w$	water content
$c$	concentration
$n$	porosity
$e$	void ratio
$\gamma$	total unit weight
$\gamma_s$	unit weight of solids
$\gamma_w$	unit weight of water
$G_s$	specific weight of solids

Subscripts:

$t$	total
$s$	solids
$w$	water

### A.1.2 Basic definitions

These definitions are valid for a completely saturated material only.

Solids content (or solids concentration by weight):

$$s = \frac{W_s}{W_t} = \frac{W_s}{W_s + W_w} \quad [\text{A.1.1}]$$

Water content:

$$w = \frac{W_w}{W_s} = \frac{W_t - W_s}{W_s} = \frac{1-s}{s} \quad \text{and} \quad s = \frac{1}{1+w} \quad [\text{A.1.2}]$$

Concentration (or solids concentration by volume):

$$c = 1 - n = \frac{V_s}{V_t} = \frac{V_s}{V_s + V_w} \quad [\text{A.1.3}]$$

Porosity:

$$n = 1 - c = \frac{V_v}{V_t} = \frac{V_w}{V_s + V_w} \quad [\text{A.1.4}]$$

Void ratio:

$$e = \frac{V_v}{V_s} = \frac{V_w}{V_s} \quad [\text{A.1.5}]$$

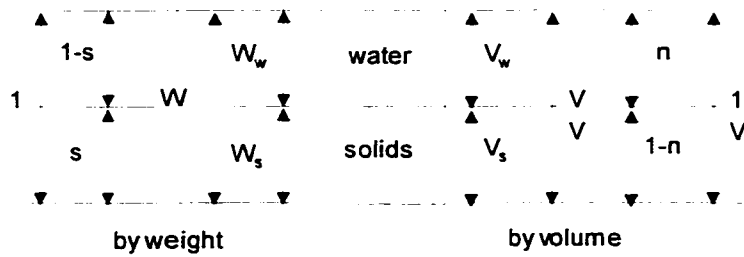


Figure A.1.1 Weights and volumes

Specific weight of solids:

$$G_s = \frac{\gamma_s}{\gamma_w} \quad [\text{A.1.6}]$$

### A.1.3 Mutual relations

Total unit weight may be expressed in many different ways:

(a) using  $s$  and  $\gamma_s = G_s \gamma_w$

$$\gamma = \frac{W_t}{V_t} = \frac{W_s + W_w}{V_t} = \frac{W_s(1+w)}{V_t} = \frac{W_s}{sV_t}$$

$$\text{using } V_t = V_s + V_w = \frac{W_s}{\gamma_s} + \frac{W_w}{\gamma_w} = \frac{W_s \gamma_w + W_w \gamma_s}{\gamma_s \gamma_w} = W_s \frac{\gamma_w + w \gamma_s}{\gamma_s \gamma_w}$$

$$\gamma = \frac{1}{s \frac{\gamma_w + w \gamma_s}{\gamma_s \gamma_w}} = \frac{\gamma_s \gamma_w}{s \gamma_w + s \frac{1-s}{s} \gamma_s} = \frac{\gamma_s \gamma_w}{s \gamma_w + (1-s) \gamma_s}$$

$$\gamma = \frac{G_s}{s + (1-s)G_s} \gamma_w \quad [\text{A.1.7}]$$

(b) using  $w$  and  $\gamma_s$

$$\gamma = \frac{G_s}{s + (1-s)G_s} \gamma_w = \frac{1}{s} \cdot \frac{G_s}{1 + \frac{1-s}{s} G_s} \gamma_w = \frac{1+w}{1+wG_s} \gamma_w = \frac{1+w}{\gamma_w + wG_s} \gamma_s \gamma_w \quad [\text{A.1.8}]$$

or in a more elegant form:

$$\gamma = \frac{\gamma_s}{s + (1-s) \frac{\gamma_s}{\gamma_w}} \gamma_w = \frac{\gamma_s \gamma_w}{s \gamma_w + (1-s) \gamma_s}$$

$$\frac{1}{\gamma} = \frac{s}{\gamma_s} + \frac{1-s}{\gamma_w} \quad [\text{A.1.9}]$$

Relations among concentration, porosity  $n$  and void ratio  $e$ :

$$c = 1 - n = \frac{1}{1+e} \quad [\text{A.1.10}]$$

$$n = 1 - c = \frac{e}{1+e} \quad [\text{A.1.11}]$$

$$e = \frac{1-c}{c} = \frac{n}{1-n} \quad [\text{A.1.12}]$$

Relations among void ratio  $e$ , solids content  $s$  and water content  $w$ :

$$e = \frac{V_w}{V_s} = \frac{\frac{W_w}{\gamma_w}}{\frac{W_s}{\gamma_s}} = \frac{\frac{W_w}{\gamma_w}}{\frac{1}{\gamma_s} \frac{s}{1-s} W_w} = \frac{1-s}{s} \cdot \frac{\gamma_s}{\gamma_w} = \frac{1-s}{s} G_s = w G_s, \quad [\text{A.1.13}]$$

Relations between concentration  $c$  and solids content:

$$c = \frac{1}{1 + \frac{1-s}{s} G_s} = \frac{s}{s + (1-s) G_s}, \quad [\text{A.1.14}]$$

$$s = \frac{c G_s}{1 - (1 - G_s) c} \quad [\text{A.1.15}]$$

## ***Appendix 2***

### ***ELEMENTS OF THE THEORY OF HYPERBOLIC AND PARABOLIC PARTIAL DIFFERENTIAL EQUATIONS AND FINITE DIFFERENCE METHODS FOR SOLVING THESE EQUATIONS***

#### **A.2.1 ELEMENTS OF THE THEORY OF HYPERBOLIC AND PARABOLIC PARTIAL DIFFERENTIAL EQUATIONS**

This Appendix consists of selected topics from the introductory part of the book on partial differential equations by Du Chateau and Zachmann (1986). It is assumed in this chapter that a general 2<sup>nd</sup> order partial differential equation in the form of expression [A.2.4] is considered, unless specified otherwise.

##### **A.2.1.1 Auxiliary conditions and well-posed problems**

To select a single solution for a physical problem among an infinite number of them offered by a general mathematical solution, certain auxiliary conditions must be imposed that further characterize the physical system being modelled. There are two categories of auxiliary conditions.

*Initial conditions* are those which must be satisfied through the spatial domain  $\Theta$  at the moment when analysis begins. Typical initial conditions prescribe values of the function at time  $t = 0$  in the case of a spatially one-dimensional problem, or values of the function together with its time derivatives in the case of a multidimensional problem. If the PDE contains time derivatives up to order  $k$ , then the initial state can be specified using time derivatives of the unknown function up to order  $k-1$ .

*Boundary conditions* must be satisfied at the boundary  $S$  of the spatial domain  $\Theta$  of definition of the PDE. There are three possible forms of boundary conditions:

$$\text{Dirichlet condition} \quad u = \varphi$$

$$\text{Neumann (or flux) condition} \quad \frac{\partial u}{\partial n} = \varphi \quad [\text{A.2.1}]$$

$$\text{Robin (or mixed) condition} \quad \alpha u + \beta \frac{\partial u}{\partial n} = \varphi$$

where  $\varphi$ ,  $\alpha$  and  $\beta$  are functions prescribed on  $S$  (DuChateau and Zachmann, 1986).



The prescribed initial and boundary conditions, together with possible non-homogeneous terms in the PDE equation, are said to comprise the data on the modelled problem. The solution is said to depend continuously on the data if small changes in the data result in correspondingly small changes in the solution. The problem is then said to be well-posed if a solution to the problem exists, if the solution is unique and if it depends continuously on the data. If the converse is true, the problem is said to be ill-posed.

Since the physical problem creates its own initial and boundary conditions, independently of the mathematical nature of corresponding governing PDE, these auxiliary conditions must not be too many (in a well-posed problem) or the problem will have no solution. On the other hand, if there are not enough auxiliary conditions, the solution will not be unique.

We shall here consider the heat equation as the prototype of parabolic equations. It may be shown that a well-posed initial value problem requires that the solution be bounded at infinity, regardless of the number of spatial dimensions:

$$\begin{aligned} u_t &= k \nabla^2 u(\underline{x}, t) & \underline{x} \in R^n, t > 0 \\ u(\underline{x}, 0) &= f(\underline{x}) & \underline{x} \in R^n \\ |u(\underline{x}, t)| &< M & \underline{x} \in R^n, t > 0 \end{aligned} \quad [\text{A.2.2}]$$

In the case of an initial-boundary value problem, in addition to the above requirements, the boundary conditions must be specified over the finite portion of the domain in which the solution is searched for.

It may also be shown that the initial conditions must not be replaced by conditions at some time  $T$  other than the initial one; otherwise the problem will become ill-posed, even in the case where nothing else has been changed. That is, the problem has no solution for an arbitrary function describing the state at time  $T$ . Even when the solution exists, it may not depend continuously on the data—it is unstable. This means that there are no possibilities for back-calculation in problems described by the heat equation.

In the case of a wave equation as an example of hyperbolic equations:

$$\begin{aligned} u_{tt} &= k^2 \nabla^2 u(x, t) & x \in R^n, t > 0 \\ u(x, 0) &= f(x), u_t(x, 0) = g(x) & x \in R^n \\ u(0, t) &= u(l, t) = 0 & t > 0 \end{aligned} \quad [\text{A.2.3}]$$

it can be shown that for a well-posed initial problem there are no requirements imposed on its behaviour at infinity. The same is valid for an initial-boundary value problem for hyperbolic equations.

### **A.2.1.2 Characteristics**

If the second order linear PDE in two dimensions (DuChateau & Zachmann, 1986)

$$au_{xx} + 2bu_{xy} + cu_{yy} + du_x + eu_y + fu = g \quad [\text{A.2.4}]$$

is subjected to a change of independent variables

$$\xi = \phi(x, y) \quad \eta = \psi(x, y) \quad (\phi_x \psi_y - \phi_y \psi_x \neq 0) \quad [\text{A.2.5}]$$

then the following transformation occurs:

$$au_{xx} + 2bu_{xy} + cu_{yy} \Rightarrow Au_{\xi\xi} + 2Bu_{\xi\eta} + Cu_{\eta\eta} + \text{lower order terms} \quad [\text{A.2.6}]$$

The transformed equation takes a particularly simple form (only a mixed derivative term remains) if new variables are chosen in such a way that  $A = C = 0$ , which is the case when both  $\xi$  and  $\eta$  are solutions of

$$az_x^2 + 2bz_xz_y + cz_y^2 = 0 \quad [\text{A.2.7}]$$

This equation is called the characteristic equation of the PDE; curves  $z(x, y) = \text{const.}$  which are solutions of the above equation are called characteristic curves of the PDE. These curves are also solutions of the following equation

$$a dy^2 - 2b dx dy + c dx^2 = 0 \quad [\text{A.2.8}]$$

which may be considered as a simpler form of the characteristic equation.

The most important property of a characteristics is that the second order derivatives  $u_{xx}, u_{xy}, u_{yy}$  are not uniquely determined along this curve, although the function  $u$  itself, with first-order derivatives  $u_x$  and  $u_y$ , is determined uniquely along the characteristics. The physical significance of this property lies in the fact that discontinuities (singularities) of the PDE solution can propagate only along characteristics.

The number of characteristic curves is determined by the sign of the discriminant:

$$b^2(x, y) - a(x, y) \cdot c(x, y) \quad [\text{A.2.9}]$$

Therefore, hyperbolic equations have two families of characteristics passing through an arbitrary point  $(x, y)$ , parabolic equations have one family of characteristics, and elliptic equations have none. The characteristics of hyperbolic equations are straight lines, if coefficients in corresponding PDE are constant; otherwise they are curved in general.

The characteristic curve may be initiated by any discontinuity in the initial or boundary data. The point of discontinuity is the starting point of the characteristics along which a singularity is propagated through time.

In case of a nonlinear PDE, it is possible, even for smooth initial data, to develop a discontinuity at some distance (in time) from the initial moment. This happens when two curved characteristics intersect, each "transmitting" its own information, and these two pieces of information are incompatible. A generated curve, across which the function itself or some of its derivatives have discontinuity, is called a shock. An example of a shock is the well known hydraulic jump in open channel flow problems. The position of a shock and jump conditions (magnitudes) across the shock may be determined using conservation principles; for example, in the case of hydraulic jump, the mass and linear momentum must be preserved across the shock.

### **A.2.1.3 Qualitative behaviour of solutions of hyperbolic and parabolic equations—peculiarities of time evolution processes defined by them**

While elliptic equations describe a steady state, parabolic and hyperbolic equations depict processes that are developing—evolving—in time. The "evolution operator" is the one which transforms the initial state  $u(x, 0)$  into the evolved state  $u(x, t)$ .

Two mutually opposing properties characterize the evolution operators of parabolic and hyperbolic PDE (DuChateau & Zachmann, 1986).

#### *Parabolic equations*

First, the solution propagates with infinite speed. This means that at any time  $t > 0$ , even if it is infinitely small, the solution of a parabolic PDE depends on all of the initial data, regardless of the spatial location  $x$ . The consequence has been cited earlier: namely, that for a well-posed problem, the behaviour at infinity must be determined (bounded).

The second property is the smoothening action of the operator. This means that the solution is infinitely differentiable within the domain with regard to both time and spatial coordinates. It is not possible to obtain a non-smooth solution from smooth "initial data", for example by going backward in time. A very important consequence is that the processes modelled by these equations are irreversible in a physical sense.

The parabolic PDE operator is said to describe diffusion-like evolution.

#### *Hyperbolic equations*

The following two properties of the hyperbolic PDE operator directly contrast those of the diffusion-like operator.

The first property is the finite speed of propagation. This means that the solution will be defined in a bounded spatial region (defined by the initial conditions at  $t = 0$ ) that expands with time or, in other words, the solution at an arbitrary point  $(x, y)$  at any time  $t$  will depend on clearly defined portion of the initial data (so called "domain of dependency", determined by characteristics). The rate at which the mentioned region expands with time is explained as the speed of propagation (of finite value) of the effect modelled by the PDE. The consequence of finite speed was cited in a previous chapter: there is no need to impose any conditions on the infinite time behaviour of the solution.

The hyperbolic PDE operator does not possess the smoothening action property. Thus the solution is not smoother than the initial data—it may be even less smooth, as it was explained in a previous chapter. The irregularities (singularities, discontinuities) in the solution persist with time and propagate along characteristics.

In a physical sense, the lack of smoothening in parabolic PDE operators is the result of thermodynamic reversibility of the processes described by this model. Mathematically, this further means that it is possible to go backward in time to find the evolution process which generated the evolved state at time  $t$ . Therefore, back-calculation is possible in the processes described by hyperbolic equations.

It should be noticed here that this possibility is not available in a coupled analysis of

sedimentation and consolidation because of simultaneous solving of a parabolic and a hyperbolic equation ("mixed" conditions).

#### **A.2.1.4 Illustrative examples of hyperbolic differential equations and the influence of boundary conditions**

##### **A.2.1.4.1 Travelling wave equation**

The textbook prototype for all hyperbolic partial differential equations is the "travelling wave" equation in 1-D:

$$\begin{aligned} u_t + au_x &= 0, & u(x,t)|_{t=0} &= u(x,0) = u_0(x) \\ u_t &= \frac{\partial u}{\partial t}, & u_x &= \frac{\partial u}{\partial x} \end{aligned} \quad [\text{A.2.10}]$$

where  $a$  is a constant,  $t$  represents time and  $x$  is the spatial variable. This is called an initial value or Cauchy problem, since the solution is required to be equal to a certain given function  $u_0(x)$  for  $t = 0$ . It can be shown that the solution is:

$$u(x,t) = u_0(x - at) \quad [\text{A.2.11}]$$

The following can be concluded from this simple expression. First, the solution  $u(x,t)$  at any time  $t^*$  is a copy of the original function  $u_0(x)$ , but shifted to the right for  $a > 0$ , or to the left for  $a < 0$ , by the amount  $|a| t^*$ . The solution at a point  $(x,t)$  depends only on the value of the parameter  $\xi = x - at$  which represents a set of straight lines in the  $(x,t)$  coordinate space called "characteristics" (see Chapter A.2.12). The parameter  $a$  is called the speed of propagation along the characteristics. Thus the solution may be regarded as a wave that propagates with speed  $a$  without change of shape and magnitude, as illustrated in Figure A.2.1 (Strikwerda 1989). These properties are very useful in testing various FDM and FEM schemes for solving hyperbolic equations.

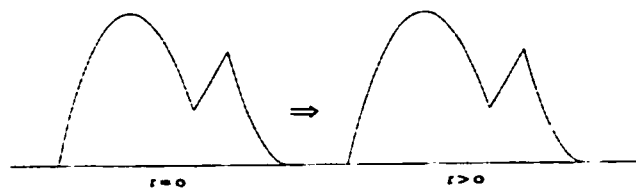


Figure A.2.1 Travelling wave in 1-D

Secondly, it may be noted that there are no requirements for the continuity, and differentiability, of the initial function  $u_0$ . Therefore, discontinuous solutions are allowed even in the simplest hyperbolic equations. A further example of a discontinuous solution is a shock wave, which is a feature of solutions of non-linear hyperbolic equations.

The concept of characteristics may be further expanded to a method of solution which uses transformation of basic independent variables in the equation. It can be shown that the solution depends only on the values of initial condition  $u_0$  at the characteristics through a given point; it is said that it propagates along characteristics.

#### A.2.1.4.2 Nonlinear “conservation law” equation

Consider the equation

$$u_t + a(x,t)u_x = 0 \quad , \quad u(x,0) = u_0(x) \quad [\text{A.2.12}]$$

for which the characteristic speed  $a(x,t)$  is a function of  $t$  and  $x$ . It can be shown that characteristics are given by:

$$\frac{dx}{dt} = a(t, x) \quad [\text{A.2.13}]$$

so that the characteristics need not be a straight line. This means that characteristics (characteristic curves) of non-linear equations may intersect, which further complicates the behaviour of the solution. It also means that special care is required in numerical methods of solving such equations.

This type of equation is often encountered in science and is called a “balance or conservation law” equation since it usually appears in problems of convective transport of a certain variable. It should be noticed that the governing equation of Kynch’s theory of sedimentation has this form.

#### A.2.1.4.3 Boundary conditions

So far the equations considered were defined along a whole real  $x$ -axis. Many physical problems are, however, defined on finite spatial intervals. There are either known (experimental) data on the ends of that spatial interval, or it is possible to define certain conditions there with which the solution must comply. In cases of definition domains with boundaries, it is important to properly define conditions at those locations—boundary conditions. The problem with both initial and boundary data is called an “initial-boundary value problem”.

Boundary conditions are closely connected to the characteristics. In 1-D equations they determine the side for which the boundary conditions must be defined for a so-called “well posed” problem. Simple illustration for this is again provided by the travelling wave equation. Consider the following problem:

$$u_t + a u_x = 0 \quad 0 \leq x \leq 1 \quad , \quad t \geq 0 \quad [\text{A.2.14}]$$

The characteristics for this problem are shown in Figure A.2.2. Consider for example the case with  $a > 0$ . It is obvious that the triangular zone between  $x = 0$  and the first characteristics, originating from the point  $(x,t) = (0,0)$ , would be undefined if only initial conditions existed. So, boundary conditions for  $x = 0$  provide the uniqueness of the

solution—the characteristics from the left boundary convey information to the definition domain (actually the mentioned triangular zone) through time. If we specify, in addition to initial data  $u(x, 0) = u_0(x)$ , boundary data  $u(0, t) = g(t)$ , the solution will be given with:

$$u(x, t) = \begin{cases} u_0(x - at) & \text{if } x - at > 0 \\ g(t - a^{-1}x) & \text{if } x - at < 0 \end{cases} \quad [\text{A.2.15}]$$

If  $u_0(0)$  is not equal to  $g(0)$  then there will be a jump—a discontinuity in the solution along the characteristics  $x - at = 0$  (originating from the left corner).

It is also clear that no data are needed for the right boundary. Moreover, if there are certain boundary conditions there in reality, they may introduce mathematical incompatibility—the problem may be over-determined.

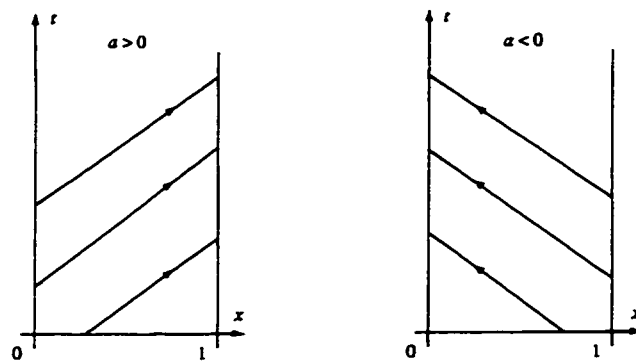


Figure A.2.2 Characteristics for the travelling wave equation

In the theory of hyperbolic equations, an initial-boundary value problem is well posed (see Chapter A.2.1.1) if the number of boundary conditions is equal to the number of incoming characteristics (characteristics entering the domain).

Boundary conditions are a particular problem in numerical solutions (for example, in the finite difference method) because they are always "mathematically" present, despite the physical nature of the problem, and thus they require proper treatment.

## A.2.2 FINITE DIFFERENCE SCHEMES FOR HYPERBOLIC PDE

### A.2.2.1 Introduction

The basic idea of finite difference schemes for solving differential equations is to replace derivatives by finite differences, for example:

$$\begin{aligned}\frac{\partial u(x,t)}{\partial t} &\approx \frac{u(x,t+\varepsilon) - u(x,t)}{\varepsilon} \\ \frac{\partial u(x,t)}{\partial x} &\approx \frac{u(x+\varepsilon,t) - u(x-\varepsilon,t)}{2\varepsilon}\end{aligned}\tag{A.2.16}$$

These expressions are then substituted into the differential equation to transform it into an algebraic equation. Writing these equations for all points on a grid defined in the domain of the ODE or PDE provides a matrix equation whose solution is an approximate solution of the original differential equation.

It is possible to write many difference schemes using various definitions of finite difference expressions. Deriving such schemes is very simple, but determining if they are good approximations to a differential equation is very complicated. Moreover, developing an efficient and accurate scheme for a given problem requires powerful mathematical tools, intuition and, sometimes, even luck.

In the following text a regular grid of points in the rectangular  $(x,t)$  domain is considered, with spacing  $dx$  in the  $x$ -direction and  $dt$  in time. Then the grid point is defined by  $(x_m, t_n) = (m \, dx, n \, dt)$ . The value of the continuous function  $u(x,t)$  at a grid point will be designated as:

$$u_m^n = u(x_m, t_n)\tag{A.2.17}$$

### A.2.2.2 Basic concepts

The most basic property for a difference scheme is that its solution must approximate the true solution of corresponding PDE and that the approximation must improve as the grid spacings  $dx$  and  $dt$  diminish, or tend to zero. It is said that such a scheme is *convergent*.

The proof for convergence is related to two easier concepts in a mathematical sense: *consistency and stability*.

The definition of *consistency* is based on the pointwise convergence (at each grid point) of the finite difference scheme to any smooth function which satisfies the partial differential equation (Strikwerda, 1989). Thus, consistency implies that the solution of the PDE, if it is smooth, is an approximate solution of the finite difference scheme. But, consistency is not sufficient for a scheme to be convergent.

Without quoting its strict mathematical definition, the stability of a finite difference scheme means that the norm of the solution at any time  $t$  is limited in the amount of growth that can occur. The proof is obtained using sophisticated methods from Fourier

analysis, but a relatively simple procedure, von Neumann analysis, may be applied to determine the stability of difference schemes.

The concept of stability for FD schemes is closely related to the concept of well-posedness for initial value problems for PDE's (see Chapter A.2.1.1)

These two concepts are connected and interrelated by the Lax-Richtmyer Equivalence Theorem, which states that a consistent FD scheme for a well posed initial value problem is convergent if and only if it is stable. It is therefore easy to prove the convergence of a particular FD scheme using two simpler concepts which are easily verifiable by essentially algebraic operations.

This is further worked out into a relatively simple criterion which will be widely used in this thesis, namely the Courant-Friedrichs-Lewy Condition. It is related to so-called "explicit" schemes—those in which the forward-time scheme is employed. The CFL condition says that for a stable (and convergent) FD scheme there must be:

$$\left| a \cdot \frac{dt}{dx} \right| = |a\lambda| \leq 1 \quad [\text{A.2.18}]$$

This is actually a criterion to limit the time step  $dt$ , since other parameters are either defined (i.e.  $a$  is fixed value) or determined *a priori* (the spatial step  $dx$ ).

There is another theorem proved by Courant, Friedrichs and Lewy which states that there is no explicit, unconditionally stable, consistent (and therefore convergent) FD scheme for hyperbolic PDE; i.e. there is no stable FD scheme for all values of  $\lambda$  (for  $\lambda$  constant as  $dx, dt \rightarrow 0$ ). This finding is important for the non-linear class of hyperbolic PDE.

This theorem does not extend to implicit schemes—those with backward-time interpolation. They may be stable for any value of CFL number. But this does not mean that an arbitrarily large time step may be used in calculation. The accuracy of solution now requires restrictions on the magnitude of time step  $dt$ .

### **A.2.2.3 Review of the schemes investigated**

Relevant literature on the methods for solving the problems governed by hyperbolic equations has been thoroughly reviewed, and it was found that there was no "best method" established for a certain type of equations, even for the simplest case of a spatially one-dimensional problem. The "conservation law" type of equations is particularly difficult, and the main problem appears to be how to handle discontinuities (shocks). There is no "ready to use" method of handling such an equation.

The following methods are recommended in the available literature for use with hyperbolic PDE of the conservation law type. They are sorted according to the method of solution (explicit, implicit) and further sorted according to the order of finite difference approximation (first, second, higher) and characteristic property, or author.



Explicit schemes:	1 <sup>st</sup> order:	Upwind differentiation
	2 <sup>nd</sup> order:	Lax-Wendroff MacCormack
TVD ("total variation diminishing") schemes:		
Chakravarthy and Osher Runge-Kutta of the 2 <sup>nd</sup> and 3 <sup>rd</sup> order		
Implicit schemes:	2 <sup>nd</sup> order:	Wendroff Crank-Nicolson

In the following text a very brief description of the listed schemes is presented, together with mathematical expressions for a "calculation molecule". The behaviour of these schemes in solving several simple test problems with known analytical solutions is described in the following section.

Perhaps it is worth repeating that the following PDE equation is to be approximated by finite differences:

$$u_t + [F(x, t, u)]_x = 0 \quad [\text{A.2.19}]$$

or in simplified form, when  $F(x, t, u) = F(u)$  only:

$$u_t + a(u) \cdot u_x = 0 \quad [\text{A.2.20}]$$

This equation is a prototype of the sedimentation equation of the Kynch type.

#### A.2.2.3.1 Upwind differencing scheme

This is the simplest scheme recommended, based on "biased" differentiation in one spatial direction. Its advantage is its capability to handle sharp differences in the solution. Its disadvantage is the need to know in advance the sign of the coefficient  $a(u)$ , to adjust the direction of differentiation. In the case of a linear equation with constant coefficients, this is not a problem. But in the case of a non-linear equation, where the sign of  $a(u)$  may vary in time or even within the spatial domain in a certain time instance, this is a serious deficiency.

In the case of a linear equation and positive  $a$ , the FD expression is simply:

$$\frac{u_j^{n+1} - u_j^n}{\Delta t} + a \cdot \frac{u_j^n - u_{j-1}^n}{\Delta x} = 0 \quad [\text{A.2.21}]$$

For negative  $a$  the direction of differentiation is merely reversed.

The only unknown  $u_j^{n+1}$  is directly calculated from the above equation.

It was noticed that this scheme gradually diminishes the solution with elapsed time—it possesses the property of *dissipation*.

### A.2.2.3.2 Lax-Wendroff explicit scheme

This scheme is considered one of the best general FD schemes for hyperbolic equations. It may be presented in either of two essentially equal forms: the one-step or the two-step method. The two-step method is quoted here because of its relative simplicity. This scheme may be abbreviated as “FTCS” in the notation customary in the related literature, meaning approximation by forward difference in time and central difference in space.

$$\begin{aligned}\frac{u_j^{n+1} - u_j^n}{\Delta t} + \frac{F_{j+\frac{1}{2}}^n - F_{j-\frac{1}{2}}^n}{\Delta x} &= 0 \\ F_{j+\frac{1}{2}}^n &= a \frac{u_j^n + u_{j+1}^n}{2} - \frac{a^2 \Delta t}{2\Delta x} (u_{j+1}^n - u_j^n) \\ F_{j-\frac{1}{2}}^n &= a \frac{u_{j-1}^n + u_j^n}{2} - \frac{a^2 \Delta t}{2\Delta x} (u_j^n - u_{j-1}^n)\end{aligned}\quad [\text{A.2.22}]$$

or directly, as used in this work:

$$\frac{u_j^{n+1} - u_j^n}{\Delta t} + a \frac{u_{j+1}^n - u_{j-1}^n}{2\Delta x} = \frac{a^2 \Delta t}{2} \frac{u_{j+1}^n - 2u_j^n + u_{j-1}^n}{(\Delta x)^2} \quad [\text{A.2.23}]$$

It is obvious that the solution is straightforward for the only unknown  $u_j^{n+1}$ .

It should be remarked that this scheme introduces *diffusion* into the solution, which appears as oscillations emanating from discontinuity points in initial and boundary conditions (the “corner points”).

### A.2.2.3.3 MacCormack scheme

It is defined by the following calculation molecule:

$$\begin{aligned}u_j^{n+1} &= \frac{1}{2} \left( u_j^n + \bar{u}_j - a\Delta t \frac{\bar{u}_j - \bar{u}_{j-1}}{\Delta x} \right) \\ \bar{u}_j &= u_j^n - a\Delta t \frac{u_{j+1}^n - u_j^n}{\Delta x} \\ \bar{u}_{j-1} &= u_{j-1}^n - a\Delta t \frac{u_j^n - u_{j-1}^n}{\Delta x}\end{aligned}\quad [\text{A.2.24}]$$

It can be easily shown that MacCormack's scheme reduces to Lax-Wendroff in the case of an equation with constant coefficients.

This scheme was generally rated better than the Lax-Wendroff scheme in solving problems involving discontinuities.

#### A.2.2.3.4 Chakravarthy and Osher

The basic expressions are:

$$\begin{aligned}
 \frac{u_j^{n+1} - u_j^n}{\Delta t} + a \frac{\hat{u}_{j+\frac{1}{2}}^n - \hat{u}_{j-\frac{1}{2}}^n}{\Delta x} &= 0 \\
 \hat{u}_{j+\frac{1}{2}}^n &= u_j^n + \frac{1+\beta}{4} \cdot \overline{\Delta_{j+\frac{1}{2}} u^n} + \frac{1-\beta}{4} \cdot \overline{\overline{\Delta_{j-\frac{1}{2}} u^n}} \\
 \hat{u}_{j-\frac{1}{2}}^n &= u_{j-1}^n + \frac{1+\beta}{4} \cdot \overline{\Delta_{j-\frac{1}{2}} u^n} + \frac{1-\beta}{4} \cdot \overline{\overline{\Delta_{j+\frac{1}{2}} u^n}} \\
 \overline{\Delta_{j+\frac{1}{2}} u^n} &= \min \text{mod} \left[ \Delta_{j+\frac{1}{2}} u^n, b \cdot \Delta_{j-\frac{1}{2}} u^n \right] \\
 \overline{\overline{\Delta_{j-\frac{1}{2}} u^n}} &= \min \text{mod} \left[ \Delta_{j-\frac{1}{2}} u^n, b \cdot \Delta_{j+\frac{1}{2}} u^n \right] \\
 \Delta_{j+\frac{1}{2}} u^n &= u_{j+1}^n - u_j^n \\
 \Delta_{j-\frac{1}{2}} u^n &= u_j^n - u_{j-1}^n \\
 \min \text{mod} [r, m] &= \text{sign}(r) \cdot \max \{0, \min [|r|, m \cdot \text{sign}(r)]\}
 \end{aligned} \tag{A.2.25}$$

This numerically rather complicated scheme is a so-called “total variation diminishing” (TVD) scheme if the following conditions are satisfied:

$$\begin{aligned}
 \kappa &= \frac{a\Delta t}{\Delta x} \leq \frac{4}{5 - \beta + b(1 + \beta)} \\
 1 &\leq b \leq \frac{3 - \beta}{1 - \beta} \\
 -1 &\leq \beta \leq 1
 \end{aligned} \tag{A.2.26}$$

The TVD schemes have recently gained wide acceptance because of the property of the non-increasing total variation. This means that they are able to reduce the amplitude of parasitic oscillations in numerical solutions of PDEs, i.e. to suppress the dispersion.

#### A.2.2.4 Author's experience

The finite difference schemes in the previous chapter were tested on a simple example—the traveling wave equation (with constant coefficients); see Chapter A.2.1.4. An initially rectangular pulse with the magnitude of 1.0 was given (on the left in the figures), which should have travelled to the right without any change in shape or magnitude. Typical results are presented in Figures A.2.3 to A.2.6.

The upwind differencing scheme shows the appearance of numerical dissipation, while the Lax-Wendroff explicit scheme and MacCormack's scheme show numerical dispersion.

It seems that the scheme of Chakravarthy and Osher does not allow the pulse to move at all, deforming it at the same time—decreasing both the magnitude and the shape. It

seems that there is an error in the formulas in the original reference, since almost all possible combinations of the parameters were tested. The presented graph appeared to be one of the best obtained.

A few additional trials with a non-linear equation of the type described in Chapter A.2.1.4.2 were attempted without any relative improvement of the results. Since all these schemes were developed for a fixed spatial grid, it was concluded that it would not be possible to use Eulerian formulation in the solution of the sedimentation equation derived in Chapter 4.1, and one should turn to the Lagrangian formulation instead.

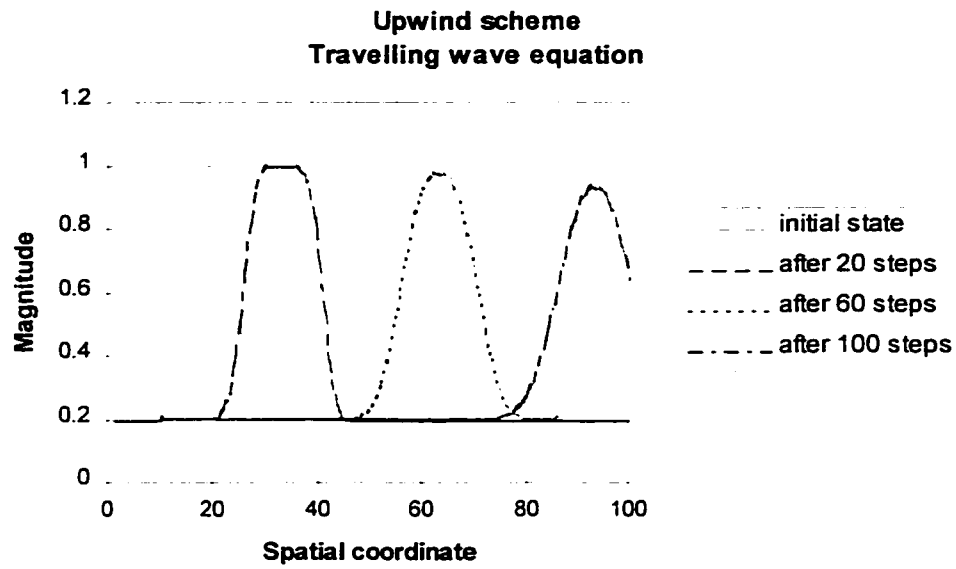


Figure A.2.3 Testing FD schemes using the travelling wave equation  
Upwind differencing scheme

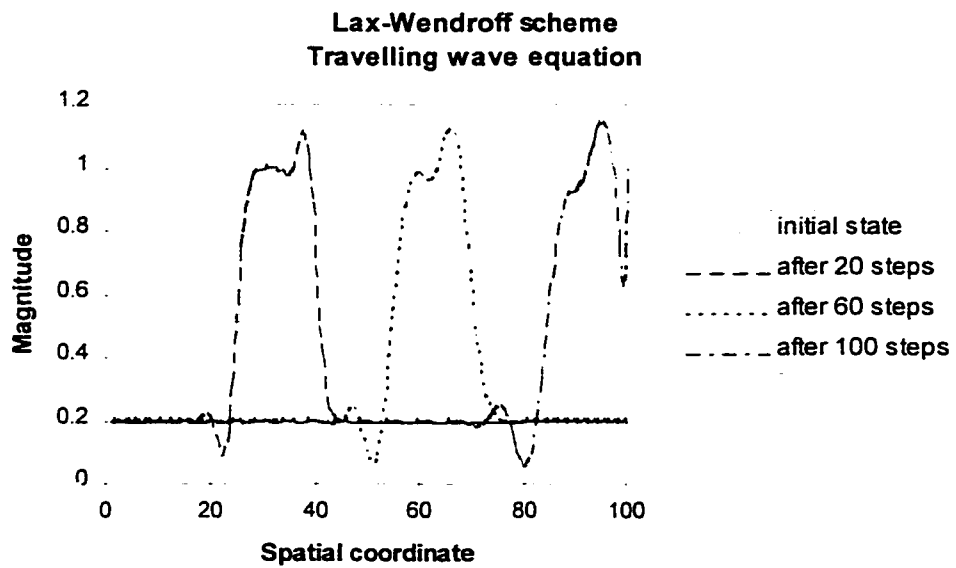


Figure A.2.4 Testing FD schemes using the travelling wave equation  
Lax-Wendroff explicit scheme

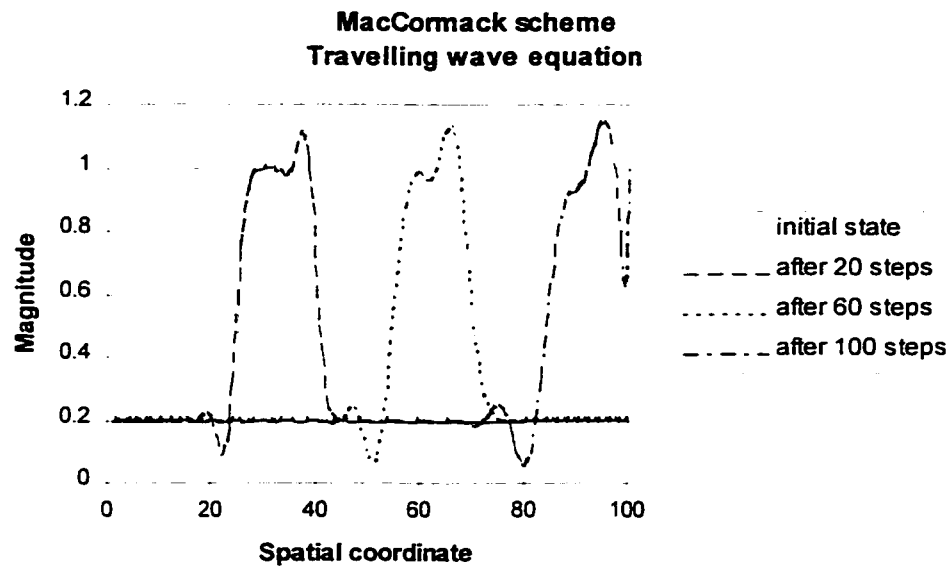


Figure A.2.5 Testing FD schemes using the travelling wave equation  
MacCormack scheme

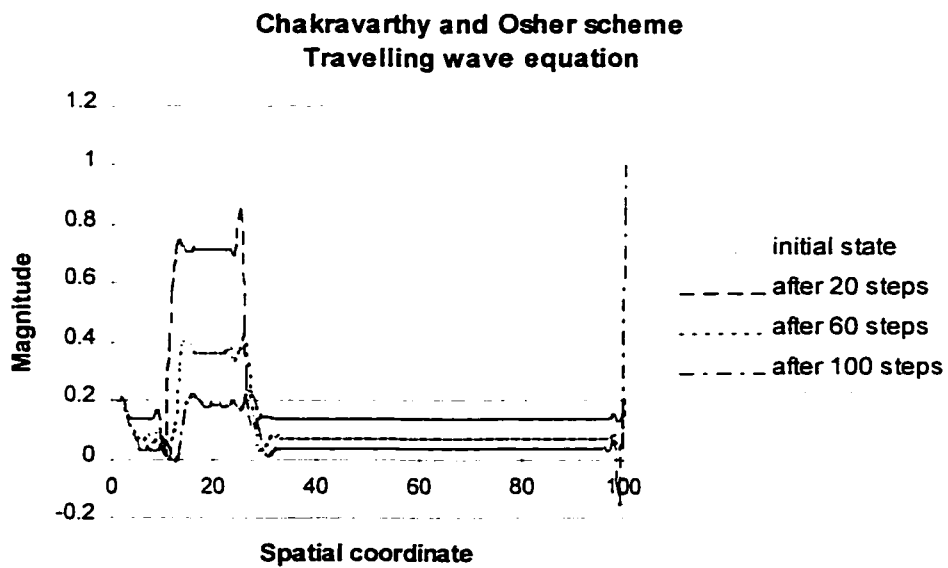
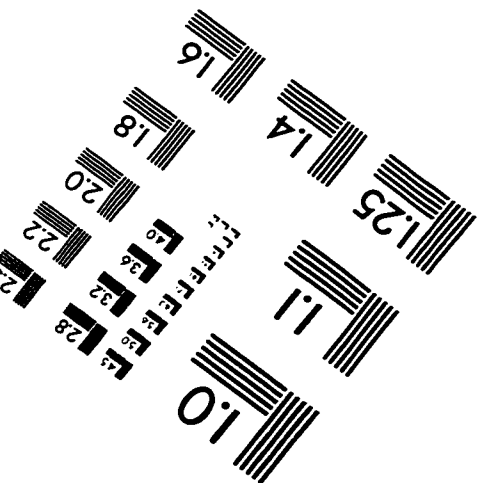
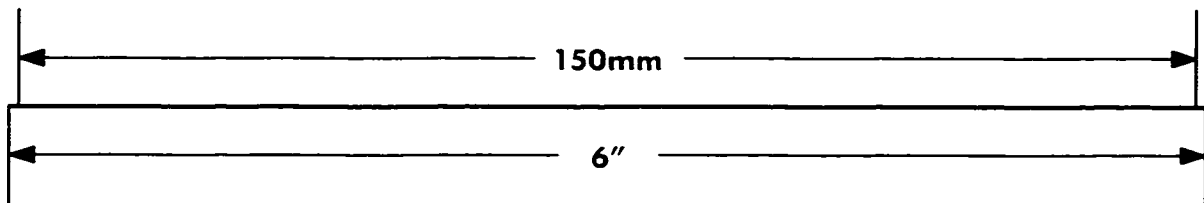
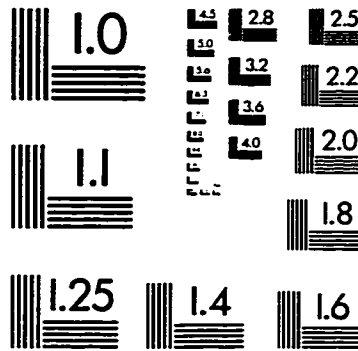
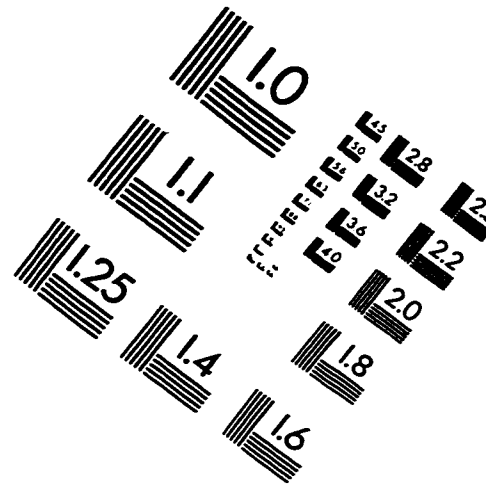
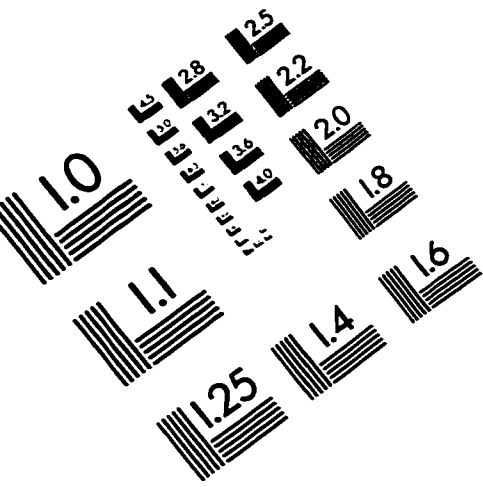


Figure A.2.6 Testing FD schemes using the travelling wave equation  
Chakravarthy and Osher scheme

# IMAGE EVALUATION TEST TARGET (QA-3)



APPLIED IMAGE, Inc  
1653 East Main Street  
Rochester, NY 14609 USA  
Phone: 716/482-0300  
Fax: 716/288-5989

© 1993, Applied Image, Inc.. All Rights Reserved

